NASA-CR-54646

MATERIALS FOR POTASSIUM LUBRICATED JOURNAL BEARINGS

Quarterly Progress Report No. 8
Quarter Ending April 22, 1965

EDITED BY R. G. FRANK

prepared for
NATIONAL AERONAUTICS AND SPACE ADMINISTRATION
CONTRACT NAS 3-2534

SPACE POWER AND PROPULSION SECTION
MISSILE AND SPACE DIVISION
GENERAL ELECTRIC
CINCINNATI, OHIO 45215

NASA-CR-54646

MATERIALS FOR POTASSIUM LUBRICATED JOURNAL BEARINGS

Quarterly Progress Report No. 8

Covering the Period

January 22, 1965 to April 22, 1965

Edited by

R. G. Frank
Program Manager

Approved by

J. W. Semmel, Jr.
Manager, Materials and Processes

Prepared for

NATIONAL AERONAUTICS AND SPACE ADMINISTRATION

Contract NAS 3-2534

Technical Management
NASA - Lewis Research Center
Space Power Systems Division
Mr. R. L. Davies

SPACE POWER AND PROPULSION SECTION
MISSILE AND SPACE DIVISION
GENERAL ELECTRIC COMPANY
CINCINNATI, OHIO 45215

FOREWORD

The work described herein is being performed by the General Electric Company under the sponsorship of the National Aeronautics and Space Administration under Contract NAS 3-2534. Its purpose, as outlined in the contract, is to evaluate materials suitable for potassium lubricated journal bearing and shaft combinations for use in space system turbogenerators and, ultimately, to recommend those materials most appropriate for such employment.

R. G. Frank, Manager, Physical Metallurgy, Materials and Processes, is administering the program for the General Electric Company. L. B. Engel, Jr., D. N. Miketta, T. F. Lyon, W. H. Hendrixson and B. L. Moor are directing the program investigations. The design for the friction and wear testers was executed by H. H. Ernst and B. L. Moor.

R. L. Davies of the National Aeronautics and Space Administration is the Technical Manager for this study.

CONTENTS

CONTENTS (Cont'd)

ILLUSTRATIONS

ILLUSTRATIONS (Cont'd)

ILLUSTRATIONS (Cont'd)

ILLUSTRATIONS (Cont'd)

ILLUSTRATIONS (Cont'd)

TABLES

TABLES (Cont'd)

TABLES (Cont'd)

I. INTRODUCTION

The program reviewed in this eighth quarterly report, covering activities from January 22, 1965 to April 22, 1965, is performed under the sponsorship of the National Aeronautics and Space Administration. Its purpose is to evaluate materials suitable for potassium lubricated journal bearing and shaft applications in space system turbogenerators operating over a 400° to 1600°F temperature range. The critical role of bearings in such systems demands the maximum reliability attainable within today's state-of-the-art. Achieving this reliability requires an interdisciplinary approach employing the best mechanical designs of journal bearings combined with the selection of the optimum materials to serve as the structural members. Satisfying this latter requirement constitutes the aim of this program.

A number of investigators have conducted studies in this field and their contributions have advanced the state-of-the-art considerably (Section VIII, Ref. 1). Although their work is significant, there are no common criteria for a comparison of the existing data. Therefore, establishing a unified approach to the development and evaluation of materials for potassium lubricated bearing application is deemed essential. The program involves a comprehensive investigation of material properties adjudged requisite to reliable journal bearing operation in the proposed environment. This includes: 1) corrosion testing of individual materials and potential bearing couples in potassium liquid and vapor, 2) determination of hot hardness, hot compressive strength, modulus of elasticity, thermal expansion and dimensional stability characteristics, 3) wetting tests by potassium and 4) friction and wear measurements of selected bearing couples in high vacuum and in liquid potassium.

In cooperation with the cognizant NASA Technical Manager, 14 candidate materials were selected (Table I) from a compilation of existing data on available materials. The materials reviewed fall into four broad categories:

- Superalloys and refractory alloys with and without surface treatment
- Commerical metal bonded carbides
- Refractory compounds such as stable oxides, carbides, borides and nitrides
- Cermets based on the refractory metals and stable carbides

Each material is procured from appropriate suppliers to mutually acceptable specifications and subsequently is subjected to chemical, physical and metallurgical analyses to document its characteristics before utilization in the program. After the documentation of processes and properties, the candidate materials undergo corrosion, dimensional stability, thermal expansion,

TABLE I. CANDIDATE BEARING MATERIALS

Material Class	Candidate Material
A. Nonrefractory Metals and Alloys	Star J (17%W-32%Cr-2.5%Ni-3%Fe-2.5%C-Bal. Co)
B. Refractory Metals and Alloys	Mo-TZM (0.5%Ti-0.08%Zr-Bal. Mo) Tungsten
C. Fe-Ni-Co Bonded Carbides	Carboloy 907 (74%WC-20%TaC-6%Co) Carboloy 999 (97%WC-3%Co) K601 (84.5%W-10%Ta-5.5%C)
D. Carbides	TiC (94%)
E. Oxides	Lucalox (99.8% Al_2O_3) Zircoa 1027 (95.5% ZrO_2)
F. Bordies	TiB_2 (98%)
G. Refractory Metal Bonded Carbides	TiC+5%W TiC+10%Mo TiC+10%Cb Grade 7178

compression and hot hardness testing. Considering the bearing material requirements and the information obtained on the candidate bearing materials which were subject to both potassium and non-potassium testing, seven materials combinations were selected in cooperation with the NASA Technical Manager. Potassium corrosion and wetting tests and friction and wear measurements in high vacuum and liquid potassium will proceed with these combinations.

The ultimate product of this program will be a recommendation, substantiated with complete documentation, of the material or materials which have the greatest potential for use in alkali metal journal bearings in high speed, high temperature, rotating machinery for space applications. Hopefully, the results will indicate the future course of alloy or material development specifically designed for alkali metal lubricated journal bearing and shaft combinations.

II. SUMMARY

During the eighth quarter of this program, the topics abstracted below were covered and the results are interpretively presented in this report.

A review of the available data from the corrosion, dimensional stability, thermal expansion and hot hardness test programs were made for the purpose of selecting material combinations for friction and wear testing in high vacuum and in liquid potassium. Seven material combinations were selected for testing in high vacuum and three material combinations were selected for testing in liquid potassium. The combinations are:

	Rider	Disc
*1.	Mo-TZM	Grade 7178
2.	Grade 7178	Mo-TZM
*3.	Grade 7178	Grade 7178
4.	Mo-TZM	Carboloy 907
5.	Carboloy 907	Carboloy 907
6.	Mo-TZM	TiC+10%Cb
*7.	TiC+10%Cb	TiC+10%Cb

Those combinations marked with an (*) are to be tested in both high vacuum and liquid potassium. All the friction and wear test specimens for Mo-TZM alloy and Carboloy 907 have been received.

Evaluation of the corrosion test specimens that were exposed to potassium for 1,000 hours at 1600°F essentially is completed. Preparation of metallographic specimens, x-ray diffraction patterns and chemical analyses for carbon, oxygen, nitrogen and hydrogen have been completed and the results are being analyzed. Chemical analyses of the inner 0.020 inch layer of the Cb-1Zr alloy capsule wall which also was exposed to potassium for 1,000 hours at 1600°F showed that a considerable amount of carbon had transferred from the Star J and the WC containing cermet specimens (except K601) to the capsule wall. The lack of transfer of carbon from the K601 material is attributed to its processing history. From weight change data, significantly less carbon was transferred during the 1,000-hour exposure at 1200°F. All the corrosion capsules that were tested for 1,000 hours at 800° and 1200°F have been opened and evaluation of the test specimens has been initiated.

A second series of hot hardness tests from room temperature to 1600°F were completed under vacuum (10^{-5} to 10^{-6} torr) for all the 14 candidate bearing materials. Considerably less scatter was observed in the test data in this test series which incorporated a 150-gram load as compared to the previous test series in which a 100-gram load was used. Room temperature compression tests were conducted on duplicate test specimens of 13 candidate materials. Compressive strength values ranged from 103 ksi (0.2% yield strength) for Mo-TZM alloy to

over 600 ksi (fracture strength) for WC containing materials. The fracture strength of Lucalox, TiB_2, TiC and refractory metal bonded TiC materials varied between 304 and 424 ksi.

Checkout tests for the high vacuum friction and wear tester were continued. Procedures for taring out the loading arm were established, the temperature distribution achieved from the bakeout heaters was determined and the vacuum capability of the system was established. An ultimate vacuum of 4.5×10^{-10} torr was reached with the system cold. The liquid potassium friction and wear tester was received from the vendor and installation of the supporting facilities is nearing completion. Three Cb-1Zr alloy sheathed, BN insulated potassium immersion heating elements of the type intended for use in the liquid potassium friction tester were received and tested in vacuum for 123 hours at surface temperatures of 1600°-1680°F.

All components for the potassium wetting facility were received and final assembly is nearing completion.

III. MATERIALS PROCUREMENT

A. Compression Test Specimens

Ten compression specimens of arc cast and extruded unalloyed tungsten were received March 3, 1965. With the exception of the K601 compression specimens, the receipt of the tungsten compression specimens marks the completion of the procurement of all the test specimens ordered for the first series of test programs (corrosion, dimensional stability, thermal expansion, hot hardness and compression). A total of 628 specimens have been received. Continued problems in the finish grinding operation have prevented the delivery of the K601 compression specimens.

B. Selection and Procurement of Candidate Journal Bearing Material Combinations

A review of the data available from the test programs was made early in the reporting period for the purpose of selecting material combinations for further evaluation. Material combinations selected will be subject to isothermal corrosion testing in potassium and friction and wear testing in high vacuum and liquid potassium. Also, the temperature at which the selected materials are wetted by potassium will be determined. The test data reviewed included:

1. Visual[2], dimensional[2], weight[2] and microstructural changes of specimens exposed to potassium liquid and vapor for 1,000 hours at 1600°F.

2. Spectrographic analyses of the potassium after the 1600°F test exposure[2].

3. Chemical analyses of the inner surface of Cb-1Zr alloy capsule wall for oxygen, nitrogen, hydrogen and carbon (see page 80 of this report).

4. Dimensional and weight changes of specimens exposed to vacuum for 1,000 hours at 800°[2], 1200°[3] and 1600°F[3].

5. Mean coefficients of thermal expansion between room temperature and 1600°F[2,3].

6. Hot hardness between room temperature and 1600°F[2].

In addition to the review of the test data obtained under this program, the remaining criteria that were considered in the selection of the 14 candidate materials also were applied in the selection of possible bearing material combinations. These criteria were discussed in detail in Quarterly Progress Report No. 1[1] and are listed on the following page:

1. Alloying tendency
2. Resistance to corrosion by potassium/formation of protective films in potassium
3. Stability in Cb/K system
4. Dimensional stability
5. Strength
6. Hardness
7. Conformability or ability to "wear-in"
8. Thermal expansion match
9. Thermal conductivity
10. Producibility/low porosity/surface finish
11. Resistance to thermal and mechanical shock

Based on the above considerations, the following candidate journal bearing material combinations were selected and were approved by the NASA Technical Manager for friction and wear testing in high vacuum:

	Disc	Rider
*1.	Grade 7178	Mo-TZM
2.	Mo-TZM	Grade 7178
*3.	Grade 7178	Grade 7178
4.	Carboloy 907	Mo-TZM
5.	Carboloy 907	Carboloy 907
6.	TiC+10%Cb	Mo-TZM
*7.	TiC+10%Cb	TiC+10%Cb

Those materials combinations marked with an asterick (*) also were selected for friction and wear testing in liquid potassium. Where significant differences in hardness exist, the softer material, i.e., Mo-TZM alloy, was selected as the rider material (stationary specimen) to facilitate wear-in during testing in liquid potassium. Couple No. 2 was selected to determine what affect a hard rider material would have on the wear pattern of a soft disc material in comparison with the reverse combination.

A summary of the technical justifications for the selection of each combination is given in Table II. It is worthy to note that many of the ten materials eliminated from further evaluation were eliminated primarily because of the limited number of combinations that can be tested under the provisions of the program rather than for any anticipated poor performance.

The decision to place considerable emphasis on the refractory metal bonded carbides was based on their excellent stability at the higher temperatures. Also, it was elected to test the hard carbide materials against themselves in order to obtain a direct comparison of the friction and wear behavior of hard/hard combinations vs hard/soft combinations where Mo-TZM alloy is one material in a pair. From investigations conducted by Coffin (4,5), it was concluded that generally it is desirable to have one of the materials harder than the other in order to facilitate wear-in of the couple. If both materials are hard and brittle, the surface asperities on the weaker material can fracture and the resultant debris could cause severe surface damage by abrasion. However, recent friction and wear tests and full scale bearing tests conducted elsewhere (6), using liquid potassium as a lubricant, have indicated superior performance of hard/hard combinations over hard/soft combinations because of the tendency of wear debris from the hard material to become imbedded in the soft material of hard/soft combinations and possibly resulting in a cutting action.

Inquiries were sent to the vendors for the procurement of corrosion and friction and wear specimens, quotations were received, orders were placed and all specimens for Mo-TZM alloy and Carboloy 907 were received. The procurement status of the test specimens is shown in Table III.

TABLE II. SELECTION OF BEARING
MATERIAL COMBINATIONS FOR FRICTION AND WEAR TESTS

	Materials		
	Disc	Rider	Justification
1.	Grade 7178	Mo-TZM	• Good thermal expansion match. • Conformability potential (wear-in) is good, i.e., hard-soft combination. • Good producibility. Grade 7178 is liquid phase sintered. Excellent surface finish of Grade 7178. • Both materials are dimensionally stable and are resistant to corrosion by potassium at temperatures to 1600°F under the conditions tested. • Mo-TZM is a possible shaft material. • Moderate temperature capability in a Cb/K system, i.e., no Co or Ni present. • Mo-TZM has high thermal conductivity and can dissipate heat rapidly.
2.	Mo-TZM	Grade 7178	• See advantages listed for 1 above. • Provides comparison of friction and wear behavior of hard-soft combination with the soft material as the rotating member.
3.	Grade 7178	Grade 7178	• Good thermal expansion match. • Hard/hard combination. • Good producibility. Liquid phase sintered. Excellent surface finish. • Dimensionally stable and resistant to corrosion by potassium at temperatures to 1600°F under conditions tested. • Moderate temperature capability in a Cb/K system.
4.	Carboloy 907	Mo-TZM	• Good thermal expansion match. • Conformability potential (wear-in) good, i.e., hard-soft combination. • Good producibility. Low porosity of Carboloy 907 (liquid phase sintered). Excellent surface finish.

TABLE II (Cont'd)

	Materials		
	Disc	Rider	Justification
			• Both materials are dimensionally stable and resistant to corrosion at temperatures to 1200°F under the conditions tested. • Mo-TZM is a possible shaft material. • Low-moderate temperature capability in a Cb/K system. • Mo-TZM has high thermal conductivity and can dissipate heat rapidly. • Both materials are resistant to thermal shock.
5.	Carboloy 907	Carboloy 907	• Good thermal expansion match. • Hard/hard combination. • Good producibility. Low porosity (liquid phase sintered). Excellent surface finish. • Dimensionally stable and resistant to corrosion at temperature to 1200°F under the conditions tested. • Low-moderate temperature capability in a Cb/K system. • Resistant to thermal shock.
6.	TiC+10%Cb	Mo-TZM	• TiC has low solubility in Mo-TZM at 1600°F; little tendency for "alloying". • Conformability potential (wear-in is good, i.e., hard-soft combination. • Good producibility. Low porosity of TiC+10%Cb. • Both materials are dimensionally stable and resistant to corrosion by potassium at temperature to 1600°F under the conditions tested. • Mo-TZM is a possible shaft material. • High temperature capability in a Cb/K system . • Mo-TZM has high thermal conductivity and can dissipate heat rapidly.

TABLE II (Cont'd)

	Materials		
	Disc	Rider	Justification
7.	TiC+10%Cb	TiC+10%Cb	• Good thermal expansion match. • Hard/hard combination. • Good producibility. Low porosity. • Dimensionally stable and resistant to corrosion by potassium at temperatures to 1600°F under the conditions tested. • High temperature cability in a Cb/K system.

TABLE III. PROCUREMENT STATUS OF CANDIDATE BEARING MATERIALS TEST SPECIMENS

Material	Spec.	Vendors	Test Specimen Identity: Corrosion Qty.	Corrosion Promise/ Delivery Date	Disc Qty.	Disc Promise/ Delivery Date	Rider Qty.	Rider Promise/ Delivery Date	MCN Series
Mo-TZM (raw stock)	SPPS-15	American Metal Climax	0.437" ø x 36"	3-23-65	10-each 0.187" thk x 4.375" x 4.375"	3-25-65	0.250" ø x 36"	3-23-65	1084 1085 1086
Mo-TZM (machining)	--	Dawson Carbide	15	4-10-65	10	5-3-65	74	5-18-65	1037
Carboloy 907	SPPS-23T	GE-MPD	--(1)	--	17	5-3-65	18	5-3-65	1036
Grade 7178	SPPS-36T	Kennametal, Inc.	--(1)	--	36	7-23-65	54	7-15-65	1046
TiC+10%Cb	SPPS-35T	Kennametal, Inc.	--(1)	--	27	7-23-65	35	6-30-65	1046

(1) Corrosion Test Specimens are on Hand at General Electric.

IV. TEST FACILITIES

A. Friction and Wear

Friction and Wear in High Vacuum

During the reporting interim, major emphasis was directed toward the check-out of the high vacuum friction and wear tester. The tare-weight tests of the loading arms, the vacuum capability test and the heat distribution tests of the bakeout heaters were completed.

Tare-Weight Tests

Three different phases of tare-weight testing were accomplished:

Vertical loading balanced by outer dead weight

Vector loading balanced by outer dead weight

Vector loading balanced by force pickup

The four loading arms to be used on the high vacuum friction test (HVFT) and two loading arms to be used on the liquid potassium friction test (KFT) were submitted to the same tests. The method of testing is listed in detail in Appendix A.

Vertical Tare-Weight Tests - The loading arms and supports were disassembled, cleaned in acetone and all arm bearings lubricated with a suspension of light machine oil and MoS_2. Subsequently, the loading arm assemblies were reassembled carefully to assure that the locations of the sleeves supporting the outer weight trays were recorded, the load-transmitting arms of the sleeves were truly vertical and the center of the loading arms and the center of the force pickups were horizontally aligned. The thermocouples were installed in loading arm No. 1 and the free ends of the thermocouples and the force pickup cables were suspended so that they would not load the arms. The weights of all components used in either the tare-weight tests or that were required for the specimen tests were carefully measured and recorded.

With the arm to be tested assembled in the No. 1 arm position, weights were placed in the inner tray. Then, the friction tester main chamber was bolted to the base assembly, openings for loading arms No. 2, 3 and 4 were sealed with blank flanges, the arm stop-mechanism was installed in the lower bearing position and the diaphragm and viewing port were installed. No other components were inside the tester.

The loading arm balance point was defined as the condition where the outer weights were of just sufficient magnitude to bring the point above the hemispherical specimen location into contact with the stop-mechanism as shown by Figure 1. The location of the stop-mechanism caused the gimbal center-line and the center-line of the inner end of the loading arm to be at equal vertical distances from a common reference point on the vacuum chamber.

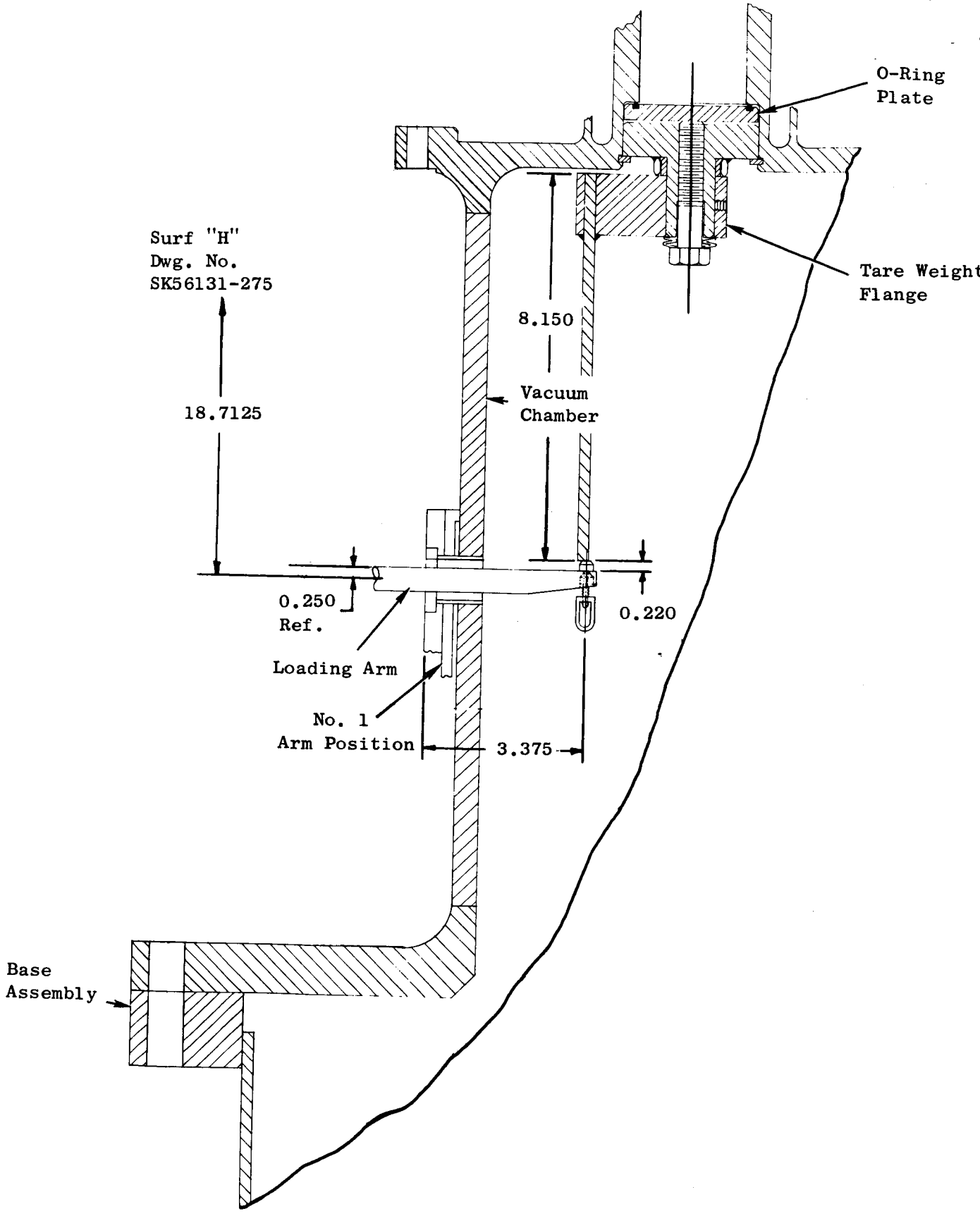

Figure 1. Vertical Tare-Weight Flange Assembly for the Calibration of the Loading Arms for the Friction and Wear Testers.

The original test plan of verifying the balance point was to visually observe contact with the stop-mechanism, verified by manually sensing to determine whether more or less loading was required to produce contact with the stop. However, it was found that a more precise measurement could be made by setting a dial indicator on the arm support and plotting arm deflection versus outer load. One characteristic load line was obtained for the unbalanced region and another characteristic load line was obtained after contact was made with the stop due to bending of the arm as a result of further loading. A typical curve is shown in Figure 2. The balance point was obtained from the intersection of the characteristic load lines. Three or more readings were made for each condition of pressure and inner load for a given loading arm and the readings averaged and reported as one reading. A spread of more than 0.5 ounce between these three readings was considered unacceptable. The loading arm was tapped very gently after each new outer weight was applied so that equilibrium was achieved in as nearly friction-free state as possible. The balance points thus achieved were repeatable and verified by the visual observation of contact. The arms were not removed during testing, nor were the inner weights disturbed; the sequence of operations were repeated for a vacuum of approximately 0.05 torr for arms 1, 2, 3, and 4; for pressures of 0 psig and 15 psig for all arms; and for 30 psig for arms 5 and 6 (to be used in the liquid potassium friction tester). The measured outer weights, W_o, are tabulated for all arms in Table IV. Figure 3 shows the variation of outer weight, W_o, with inner weight, W_i, and chamber pressure. From these data, it can be seen that the deviation of W_o with pressure is very small. However, a dimensionless plot, Figures 4, 5 and 6, shows this relationship more clearly; each loading arm has its own characteristic variation of W_o with W_i.

In constructing the dimensionless form, a constant is subtracted from each function f (W_o), which corresponds approximately to the value of W_o at $W_i = 0$, to move the measured W_o curve close to the expected balance line curves. That value then is divided by 0.8676 W_i so that a ratio of measured values need not be used. With this method a direct percentage change may be read. Compared to the tare weights obtained at 0 psig, the averaged tare weights for all the loading arms in vacuum (-14.7 psig) were 1.0% less, at 15 psig were 0.5% less, and at 30 psig were 1.1% less (neglecting only the 2 pound reading for loading arm 5). The slope of the curves shows the pressure trend and the deviation of the curves from the ratio 1.0 line indicates the parallelism of the data with the "expected blanace lines to be shown later in Figures 8 thru 13.

The purpose of the vertical tare-weight tests was to provide a means for the determination of the exact outer weight, W_o, which must be placed in the outer loading arm tray to produce the desired compressive force C between the hemispherical rider specimens and the disc specimens. To do so, all of the moments due to known and unknown forces in the loading train, shown in Figure 7, must be taken into consideration.

The general equilibrium equation for the loading arms under tare-weight or specimen testing conditions is:

$$\Sigma M_g = 0 \text{ (about gimbal)}$$

$$M_{to} + M_p + M_{ss} + M_{ao} + M_d + M_{ftc} + M_g = M_b + M_{ai} + M_{wtc} + M_{ti} + M_s + M_c \qquad (1)$$

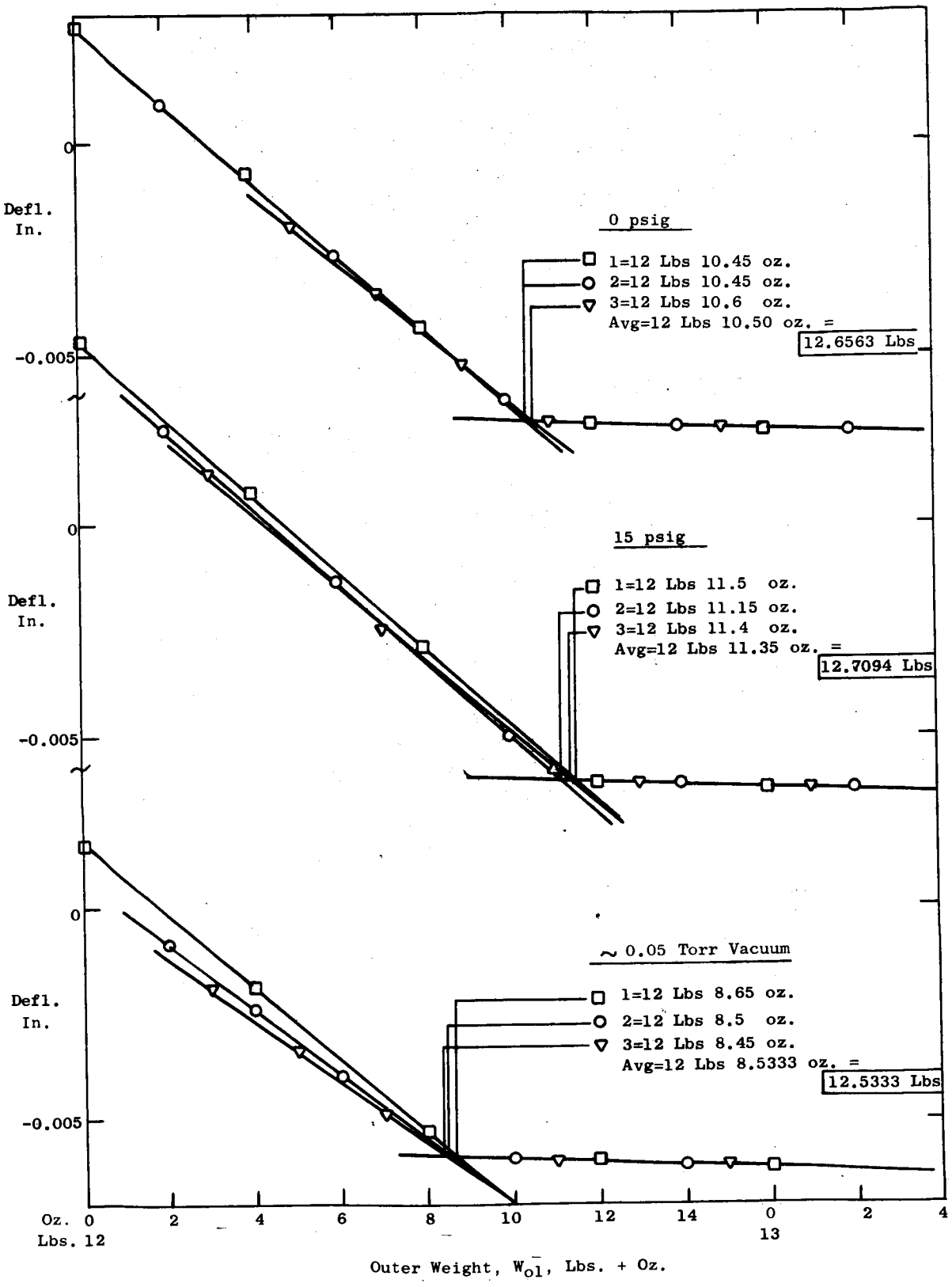

Figure 2. Deflection of Loading Arm No. 1 of High Vacuum Friction and Wear Tester as a Function of Applied Load, W_{o1}, on the Outer Tare-Weight Tray. Load, W_{i1}, on Internal Tray is 15 Pounds.

TABLE IV. VERTICAL TARE TEST -
UNCORRECT MEASURED VALUES OF W_o (OUTER WEIGHTS) VERSUS
W_i (INNER WEIGHTS) FOR THE LOADING ARMS OF THE FRICTION AND WEAR TESTERS

		Outer Weight, W_o, lbs.						
Inner Weight, W_i, lbs. →		1	2	3	5	8	11	15
Loading Arm No. 1 (HVFT)	Vacuum 0.05 Torr	0.2575	--	2.0250	3.8297	6.2917	--	12.5333
	0 psig	0.3219	--	2.0156	3.8261	6.4615	--	12.6563
	15 psig	0.3489	--	2.1875	3.8125	6.5063	--	12.7094
Loading Arm No. 2 (HVFT)	Vacuum 0.05 Torr	--	2.2711	--	4.8563	7.4844	10.1177	13.5323
	0 psig	--	2.2865	3.8698	4.8833	7.4531	10.1112	13.5959
	15 psig	--	2.3115	--	--	7.4989	--	13.6198
Loading Arm No. 3 (HVFT)	Vacuum 0.05 Torr	--	2.9438	--	5.8448	--	11.3990	--
	0 psig	--	2.9188	--	5.8406	8.6115	11.3250	--
	15 psig	--	2.8875	--	5.7917	8.5771	11.2865	--
Loading Arm No. 4 (HVFT)	Vacuum 0.05 Torr	--	3.4958	--	6.2219	8.8913	11.5469	--
	0 psig	--	3.5557	--	6.1677	8.8417	11.4530	--
	15 psig	--	3.4500	--	6.1011	--	--	--
Loading Arm No. 5 (KFT)	0 psig	--	2.4802	--	5.2438	8.0500	10.8250	--
	15 psig	--	2.4602	--	5.2063	8.0427	10.7802	--
	30 psig	--	2.4219	--	5.1844	8.0042	10.7427	--
Loading Arm No. 6 (KFT)	0 psig	--	3.6292	--	6.2520	8.8750	11.5000	--
	15 psig	--	3.5740	--	6.1865	8.8177	11.4281	--
	30 psig	--	3.5218	--	6.1320	8.7521	11.3896	--

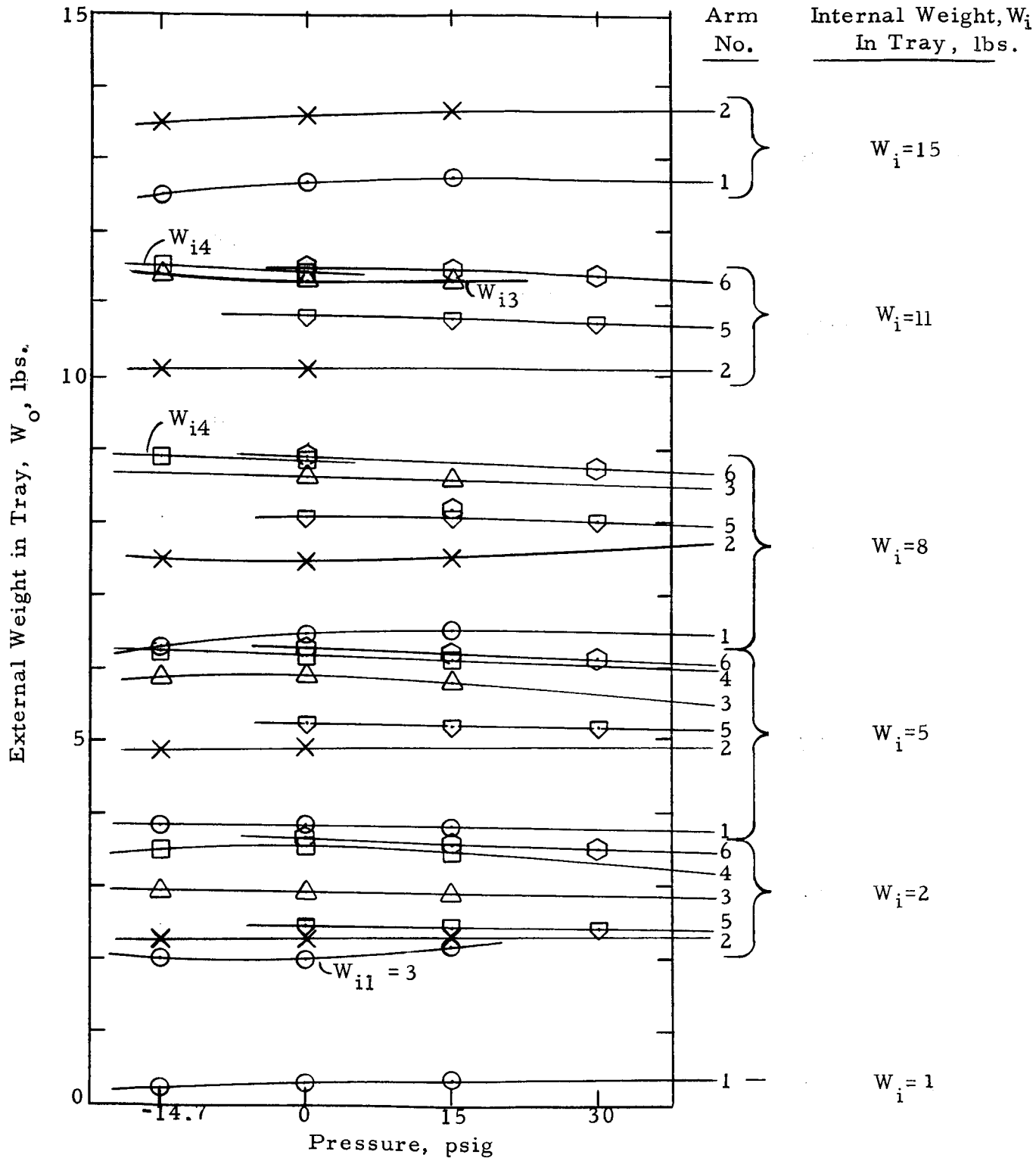

Figure 3. Variation of Vertical Tare-Weight with Pressure for the Loading Arms of the High Vacuum Friction and Wear Tester.

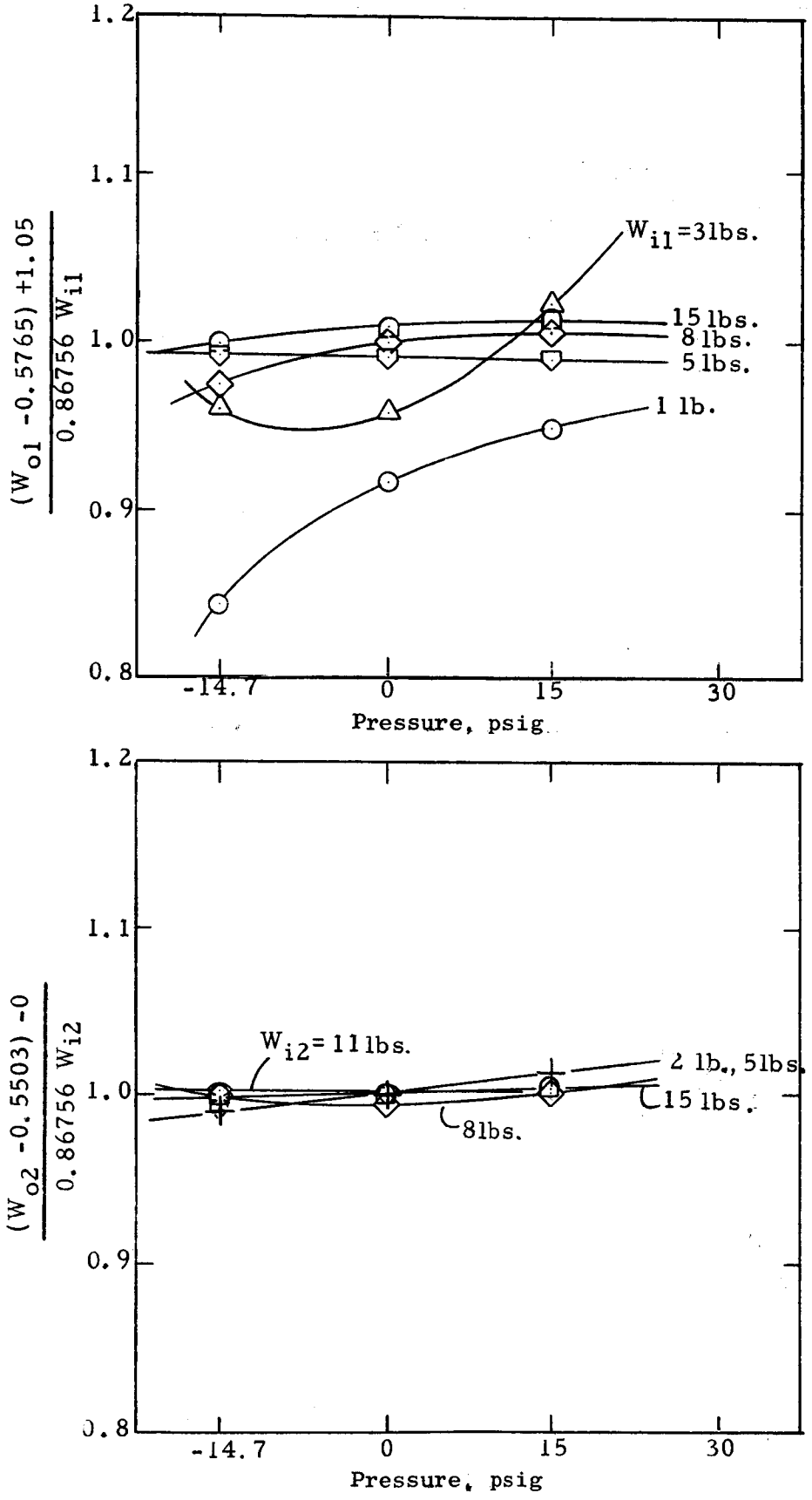

Figure 4. Effect of Pressure on the Tare-Weight of Loading Arms No. 1 & No. 2.

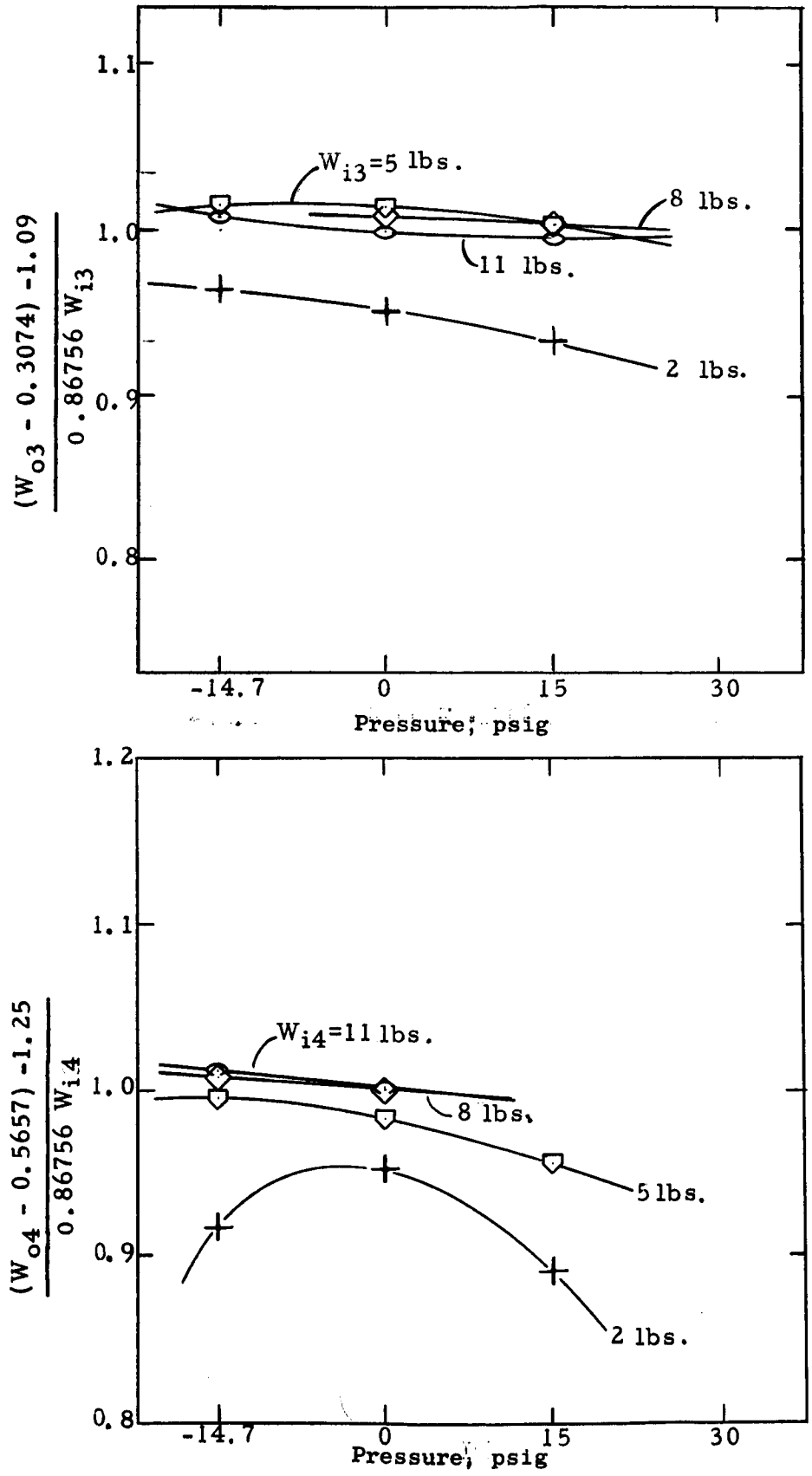

Figure 5. Effect of Pressure on the Tare-Weight of Loading Arms No. 3 & No. 4.

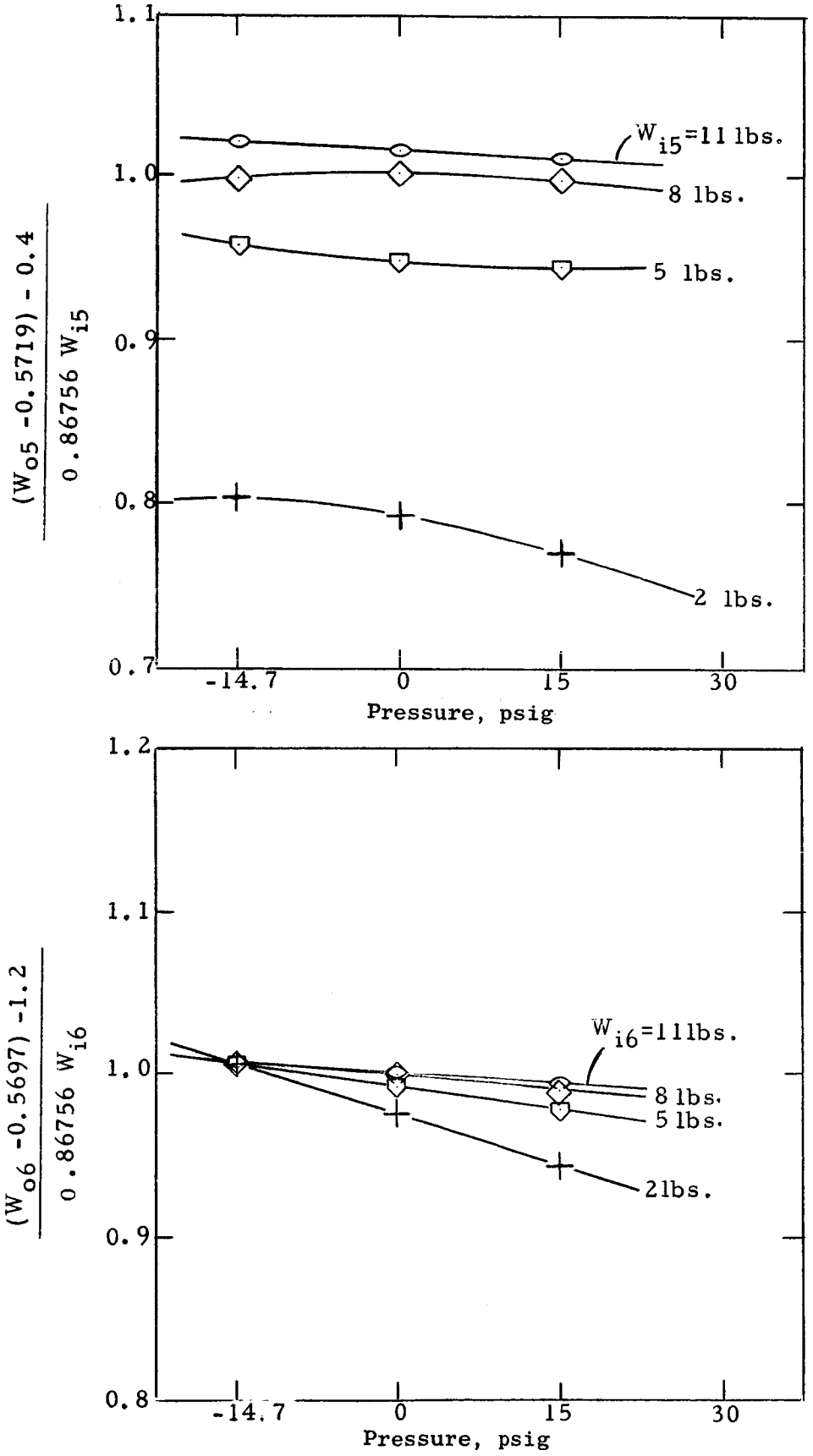

Figure 6. Effect of Pressure on the Tare-Weight of Loading Arms No. 5 and No. 6.

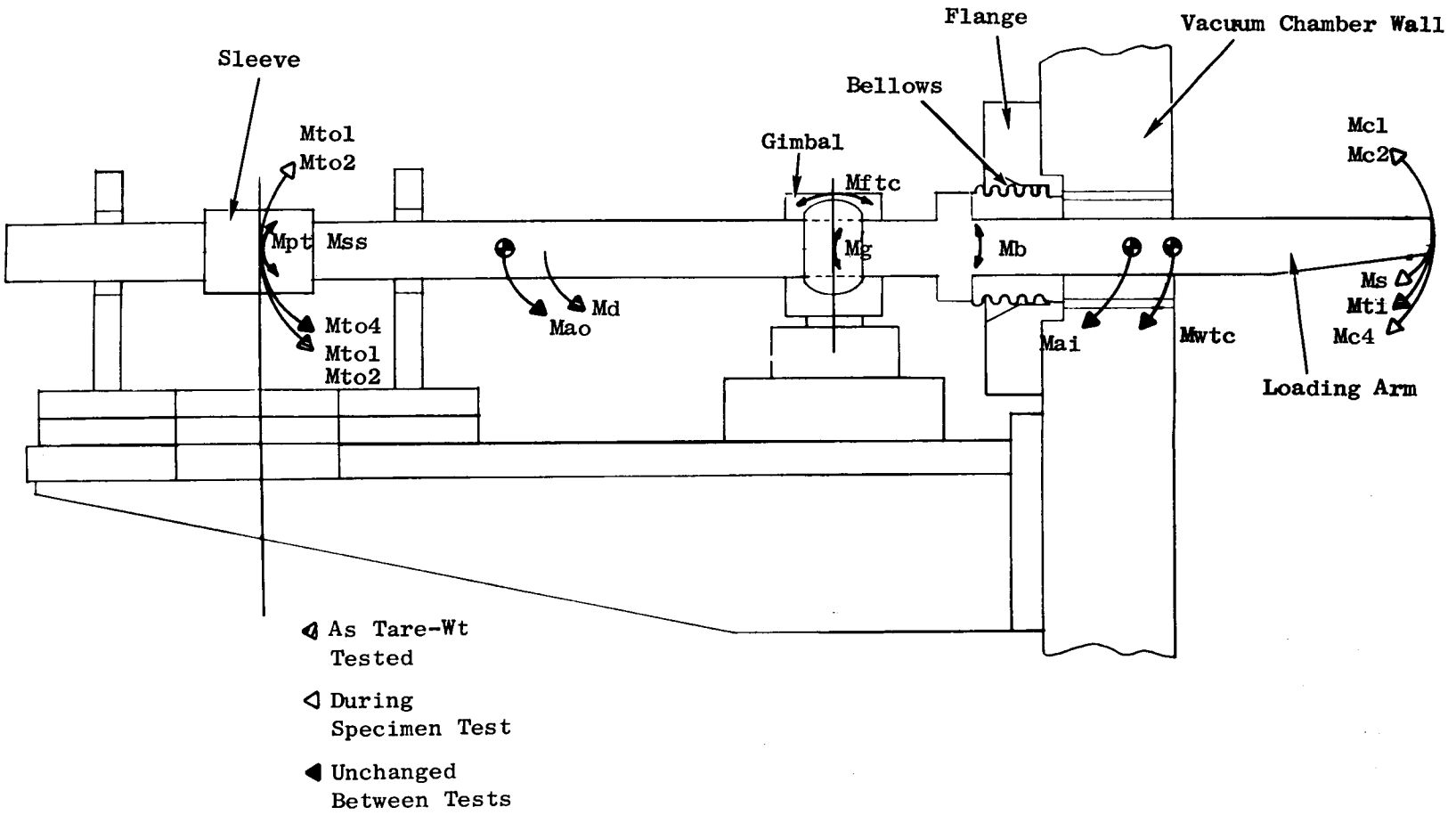

Figure 7. Moments Used to Derive General Equilibrium Equation for the Loading Arms in the Friction and Wear Testers.

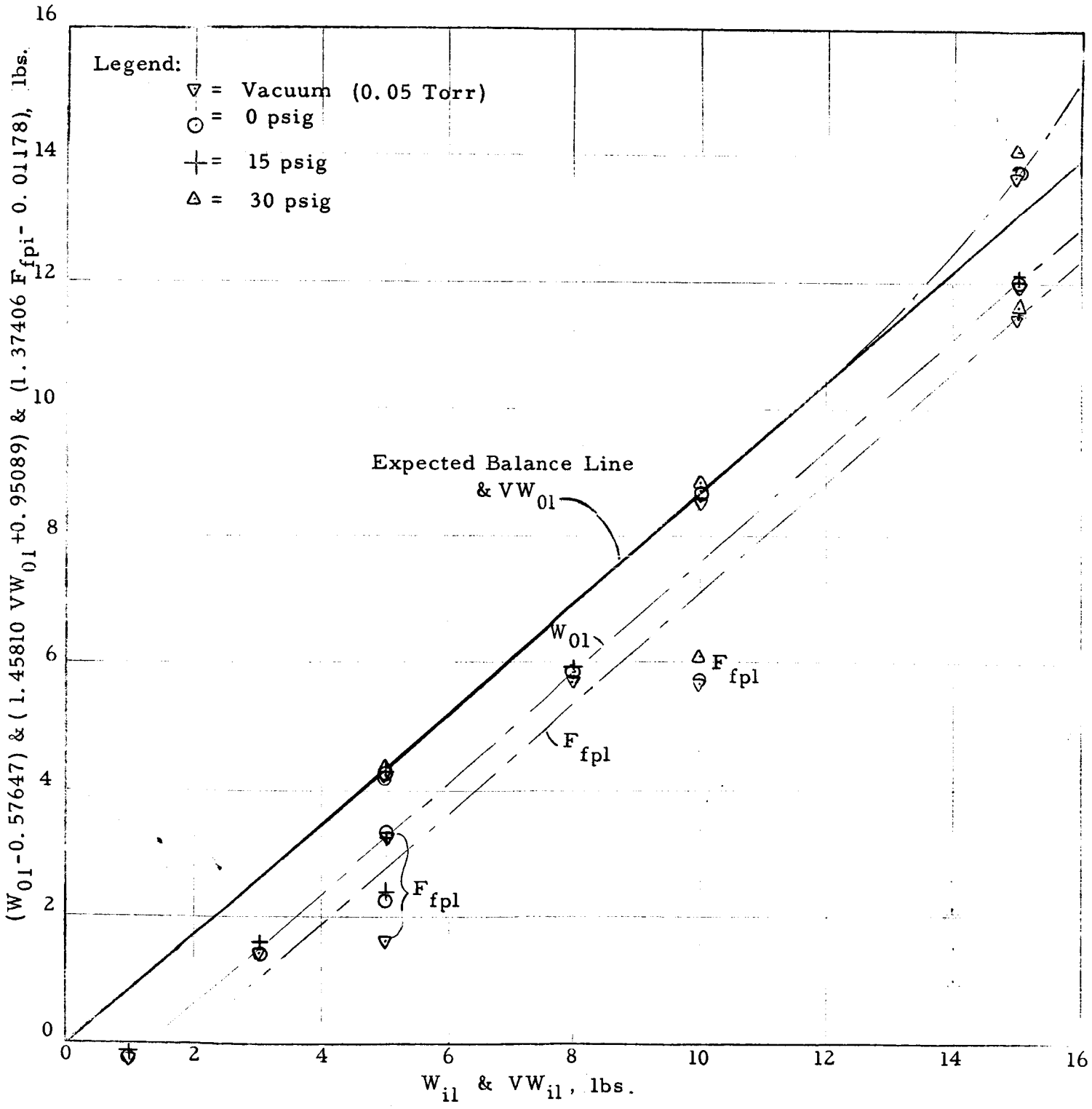

Figure 8. Tare-Weight Performance of High Vacuum Friction Tester Loading Arm No. 1.

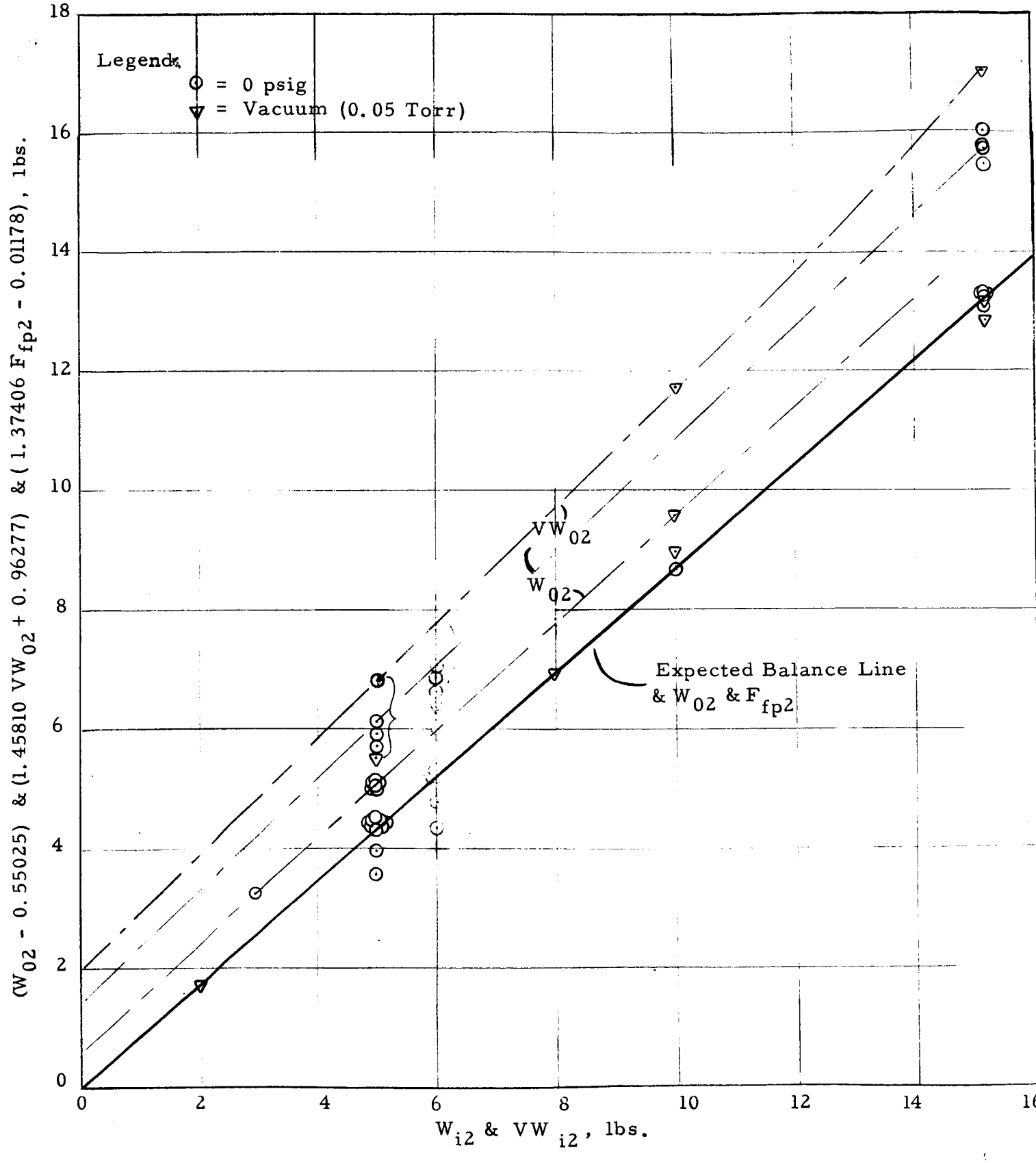

Figure 9. Tare-Weight Performance of High Vacuum Friction Tester Loading Arm No. 2.

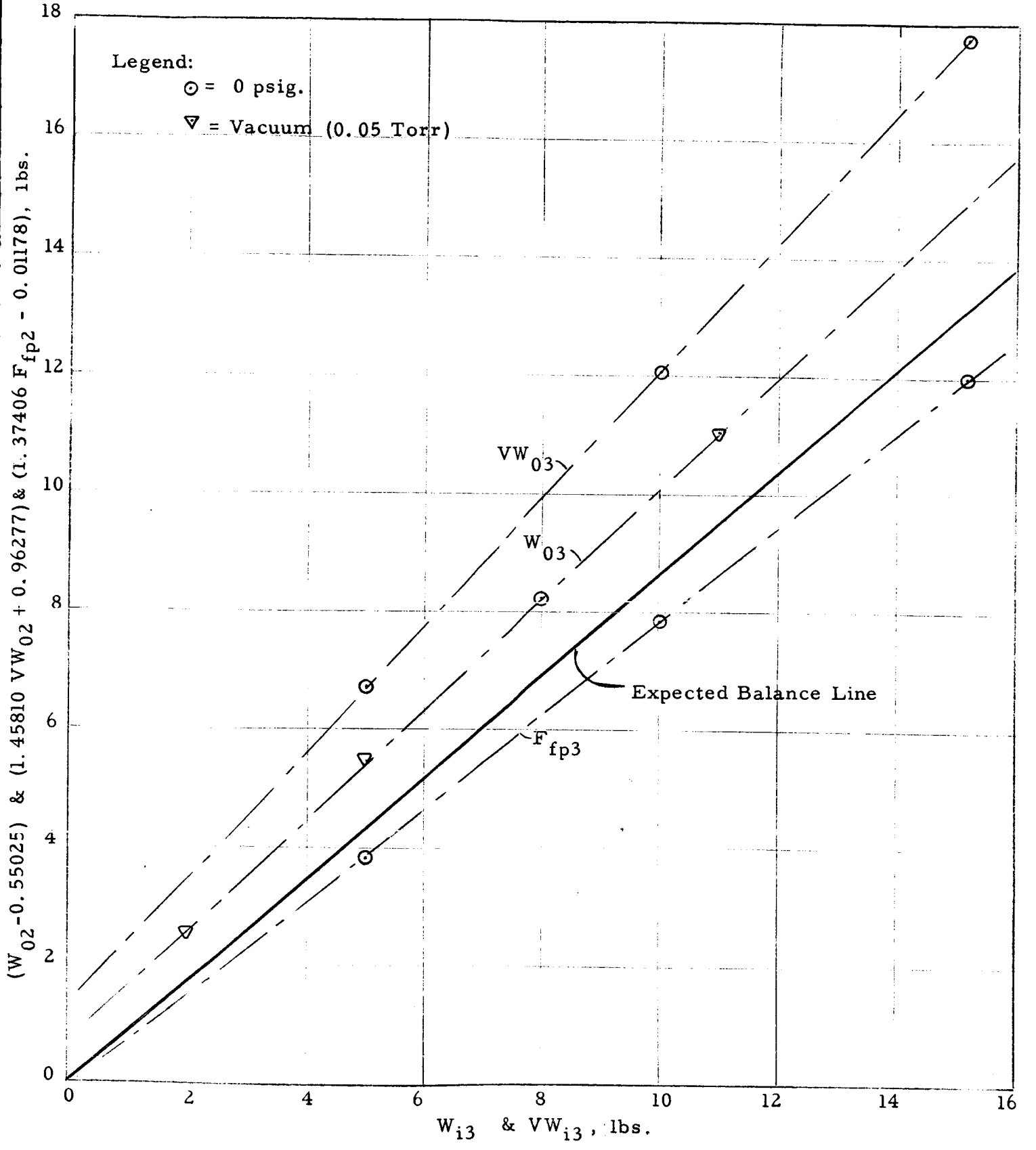

Figure 10. Tare-Weight Performance of High Vacuum Friction Tester Loading Arm No. 3.

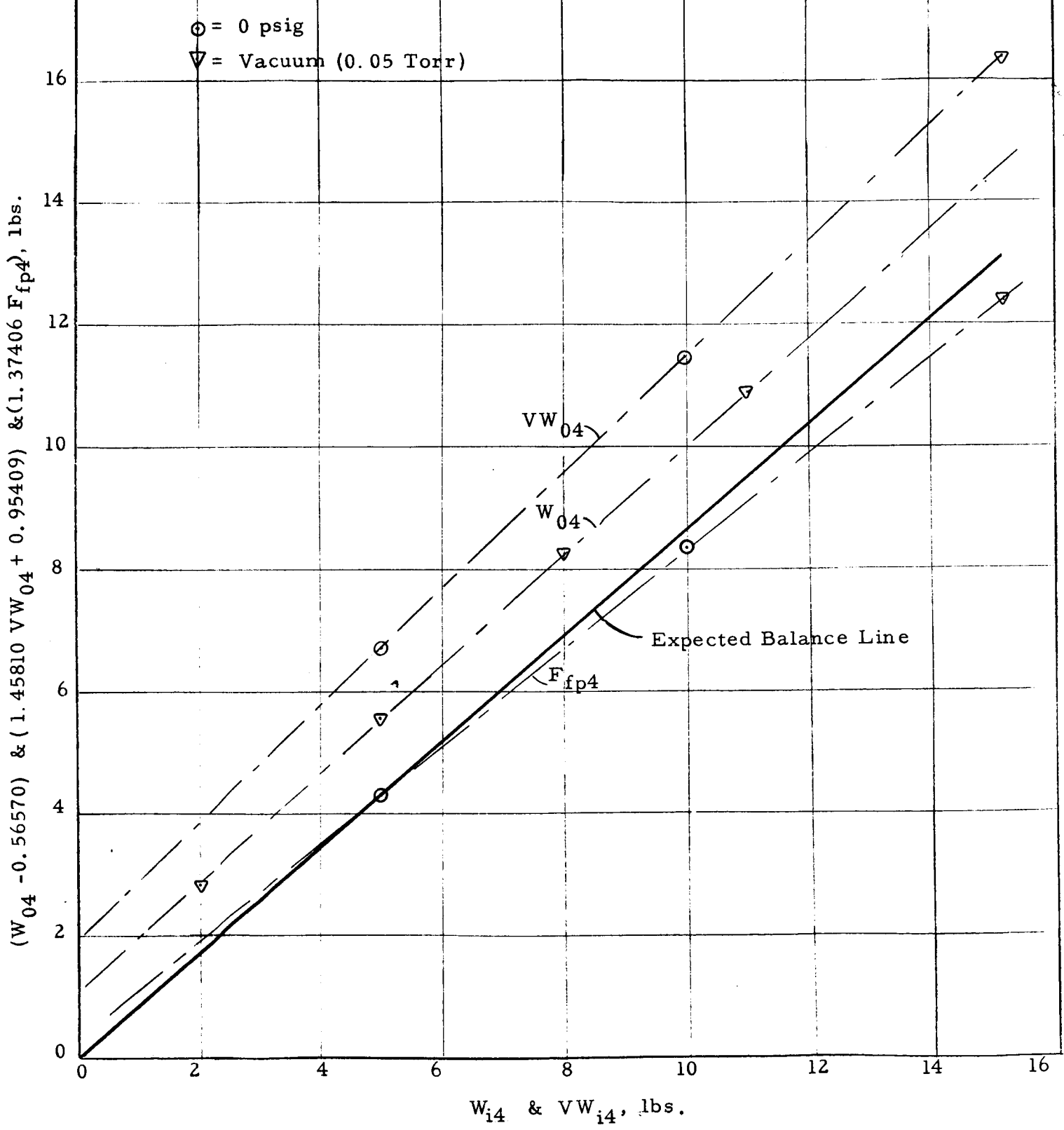

Figure 11. Tare-Weight Performance of High Vacuum Friction Tester Loading Arm No. 4.

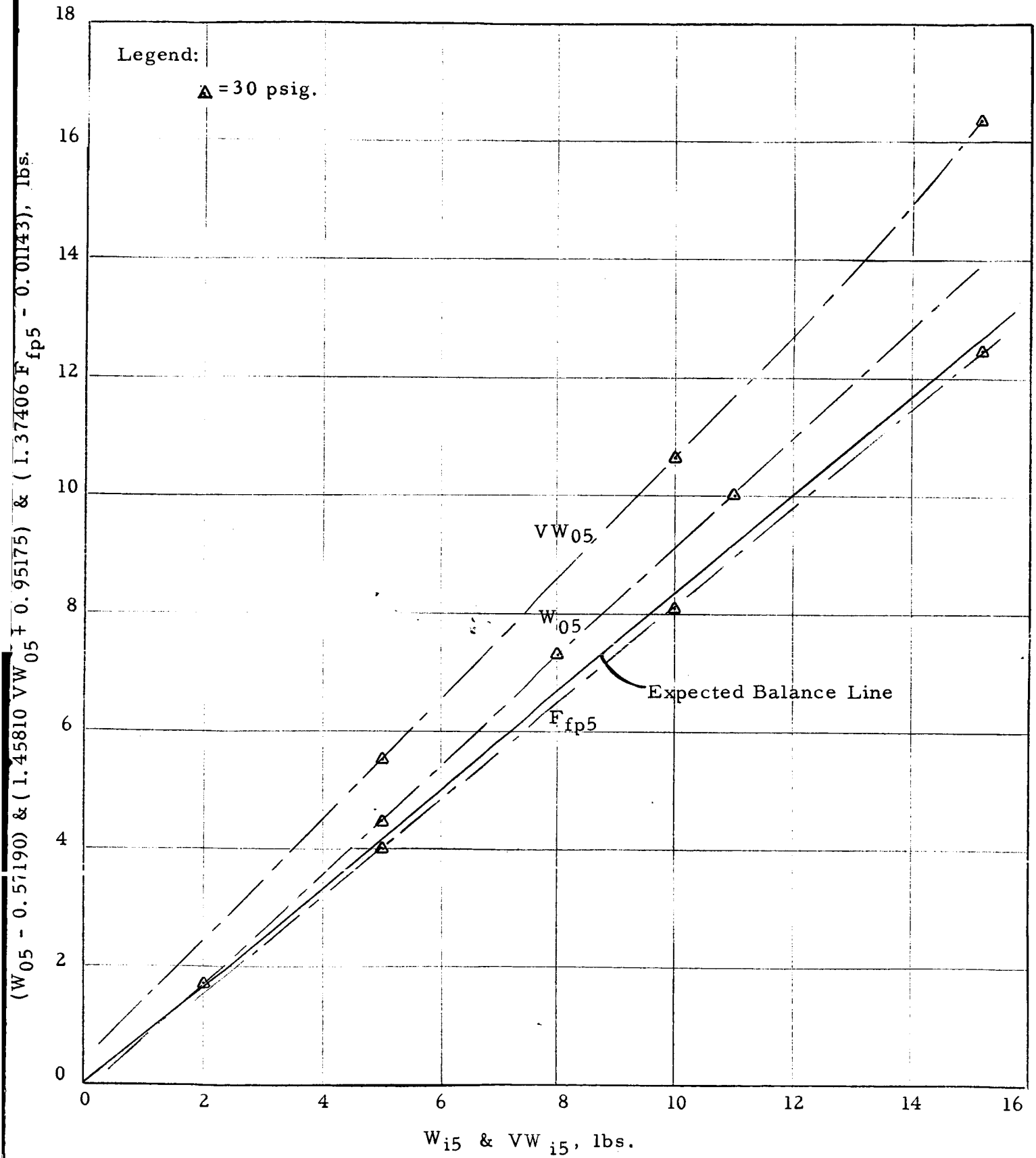

Figure 12. Tare-Weight Performance of Potassium Friction Tester Loading Arm No. 5.

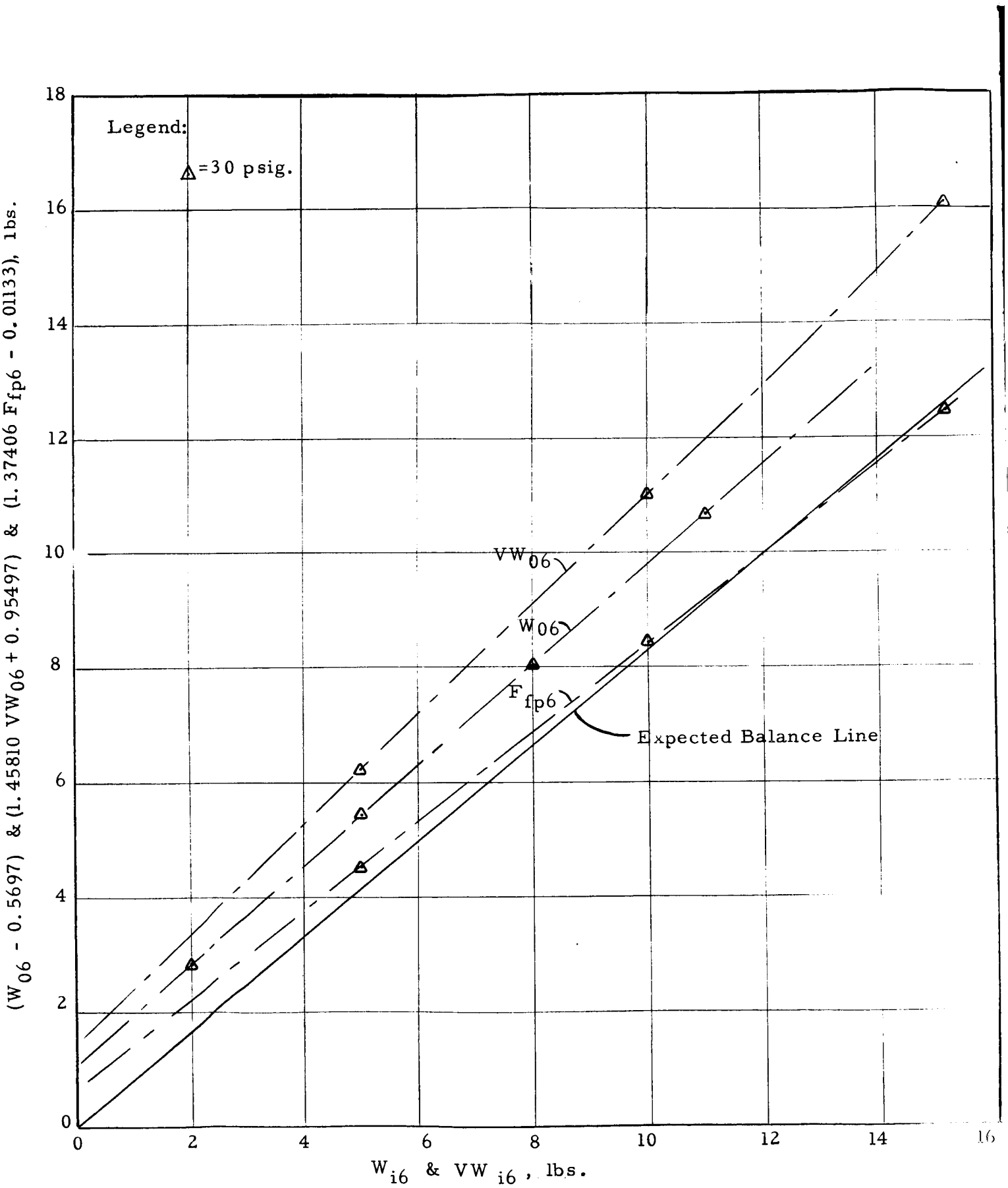

Figure 13. Tare-Weight Performance of Potassium Friction Tester Loading Arm No. 6.

where:

M_{to} = moment of the outer tray and weights

M_{p} = moment of the force pickup connector

M_{ss} = moment of the support shaft friction

M_{ao} = moment of the weight of the arms from the gimbal outward

M_{d} = moment of the dial indicator force

M_{ftc} = moment of the external thermocouple force

M_{g} = moment of the gimbal friction

M_{b} = moment of the bellows force

M_{ai} = moment of the weight of the arms from the gimbal inward

M_{wtc} = moment of the weight of the thermocouples

M_{ti} = moment of the inner tray and weights

M_{s} = moment of the weight of the stationary specimen and its set screw

M_{c} = moment of the compressive force between specimens

Appendix B describes the method for determining the moment equilibrium for loading arms 1, 2, and 4. It was the intention to use the derived equations (21), (25), and (29) relating the outer weights, W_o, and the compressive loads, C, for the duration of the test program to calculate the required dead-weight to be applied to the loading arm trays. However, it became apparent that the lack of reproducibility of the data precluded this plan.

Because of the tolerances of the holes by which the loading arm supports are attached to the flanges of the friction tester and due to variations in the locations of the bellows and flanges of the loading arms, each time a loading arm is assembled to the tester a different bellows force is induced. This change in bellows force cannot be predicted in advance and is sufficiently large, i.e., greater than a few percent of the applied weights, such that it will be necessary to tare out each loading arm before every test after the shaft, specimens, loading arms and gimbals had stabilized at the test temperature and test pressure. This would account for nearly every variable, including relative thermal expansion between the shaft and loading arms which has a small affect on the compression loading

A summation of the equations of the known moments that was made, as shown in Appendix C, in order to determine whether the unknown moments could be predicted is given in Table V and in Figures 8 thru 13 as the "Expected Balance

TABLE V. SUMMARY OF EQUATIONS OF EXPECTED BALANCE LINES FOR THE LOADING ARMS IN THE FRICTION AND WEAR TESTERS

	Balance Line Equations	Balance Line Equations Normalized to Slope of W_i
Loading Arm No. 1 (HVFT)	$W_{o1} = 0.86756\ W_{i1} + 0.57647$	$W_{o1} - 0.57647 = 0.86576\ W_{i1}$
	$VW_{o1} = 0.59498\ VW_{i1} - 0.65214$	$1.45810\ VW_{o1} + 0.95809 = 0.86756\ VW_{i1}$
	$F_{fp1} = 0.63138\ VW_{i1} + 0.00858$	$1.37406\ F_{fp1} - 0.01179 = 0.86756\ VW_{i1}$
Loading Arm No. 2 (HVFT)	$W_{o2} = 0.86756\ W_{i2} + 0.55025$	$W_{o2} - 0.55025 = 0.86756\ W_{i2}$
	$VW_{o2} = 0.59498\ VW_{i2} - 0.66029$	$1.45810\ VW_{o2} + 0.96277 = 0.86756\ VW_{i2}$
	$F_{fp2} = 0.63138\ VW_{i2} + 0.00858$	$1.37406\ F_{fp2} - 0.01179 = 0.86756\ VW_{i2}$
Loading Arm No. 3 (HVFT)	$W_{o3} = 0.86756\ W_{i3} + 0.30740$	$W_{o3} - 0.30740 = 0.87656\ W_{i3}$
	$VW_{o3} = 0.59498\ VW_{i3} - 0.96740$	$1.45810\ VW_{o3} + 1.41057 = 0.86756\ VW_{i3}$
	$F_{fp3} = 0.63138\ VW_{i3} + 0.00858$	$1.37406\ F_{fp3} - 0.01179 = 0.86756\ VW_{i3}$
Loading Arm No. 4 (HVFT)	$W_{o4} = 0.86756\ W_{i4} + 0.56570$	$W_{o4} - 0.56570 = 0.86756\ W_{i4}$
	$VW_{o4} = 0.59498\ VW_{i4} - 0.65434$	$1.45810\ VW_{o4} + 0.95409 = 0.86756\ VW_{i4}$
	$F_{fp4} = 0.63138\ VW_{i4} + 0.00858$	$1.37406\ F_{fp4} - 0.01179 = 0.86756\ VW_{i4}$
Loading Arm No. 5 (KFT)	$W_{o5} = 0.83342\ W_{i5} + 0.57190$	$W_{o5} - 0.57190 = 0.83342\ W_{i5}$
	$VW_{o5} = 0.57157\ VW_{i5} - 0.65273$	$1.45810\ VW_{o5} + 0.95175 = 0.83342\ VW_{i5}$
	$F_{fp5} = 0.60653\ VW_{i5} + 0.00825$	$1.37406\ F_{fp5} - 0.01134 = 0.83342\ VW_{i5}$

TABLE V. (Cont'd)

	Balance Line Equations	Balance Line Equations Normalized to Slope of W_i
Loading Arm No. 6 (KFT)	$W_{06} = 0.83342\ W_{i6} + 0.56970$	$W_{06} - 0.56970 = 0.83342\ W_{i6}$
	$VW_{06} = 0.57157\ VW_{i6} - 0.65494$	$1.45810\ VW_{06} + 0.95497 = 0.83342\ VW_{i6}$
	$F_{fp6} = 0.60653\ VW_{i6} + 0.00825$	$1.37406\ F_{fp6} - 0.01134 = 0.83342\ VW_{i6}$

NOTE:

Vertical Tare Test

W_0 = outer balance weight excluding tray, etc.

W_i = inner test weight excluding tray, etc.

Vector Tare Test

VW_0 = outer balance weight excluding tray, etc.

VW_i = inner test weight excluding tray, etc.

F_{fp} = force pickup reading

Lines". The vertical tare test results of Table IV are plotted as the "W_o" lines. For clarity, only the lowest pressure points were plotted for loading arms numbers 1 thru 4 and only the highest pressure points were plotted for loading arms numbers 5 and 6.

It will be noted that, at times, the data points fall exactly on the expected balance point line, indicating that the bellows and other frictional forces are negligible (a desirable condition). Such a condition would be true when the center-lines of both the bellows and the loading arm coincide with the "balance stop" position of the loading arm center-line in the free state condition. Thus, although the bellows are stiff in a plane of parallel translation of its ends, the bellows produce no force because no deflection is require at the balance point. When the data points describe a line parallel to expected balance line, the indication is that in the fabrication of the loading arm the coincident center-line condition described above was not produced. Other data that fail to describe parallel lines or that fail to reproduce prior data indicate unacceptable accuracy of the system. This lack of reproducibility can be traced to the differences in the diameter and locations of the holes in the loading arm support and loading arm pads on the friction tester. However, the measured data lines remain nearly parallel to the expected balance lines under all test conditions. Since the tangent of the slope of the expected balance line is merely the ratio of the moment arms

$$\frac{\text{distance from gimbal to inner load}}{\text{distance from gimbal to outer load}},$$

consistent parallelism of the measured data lines indicates the absence of any significant purely linear measured forces. Therefore, if one could determine the degree to which the measured data lines are out of parallel by measuring the value of the functions f (W_o) when $W_i = 0$, the problem of reproducibility of data would largely be solved.

Vector Tare Weight Tests - The test setup for the vector loading tare-weight test is illustrated in Figure 14. The detailed procedure of performing the tests is similar to that of the vertical tare tests and also is given in Appendix A. The exceptions being noted. The summation of the known moment equations for vector loading, obtained as shown in Appendix C, is given in Table V and the method of calculation of the horizontal and vertical components of the vector tare test inner weight, VW, is shown in Appendix D.

Results of the vector tare tests are tabulated in Table VI. The outer weight (VWO) represents the dead weights in the outer loading arm tray at the balance points. The pickup force (F_{fp}) represents the load derived from the Sanborn trace and the calibration curve of the pickup being used when the balance weights are loaded in the tray. Both values are plotted in Figure 8 thru 13.

The purpose of the vector tare-weight tests was to impose simultaneous vertical and horizontal loads simulating the compressive load between the specimens and the friction load.

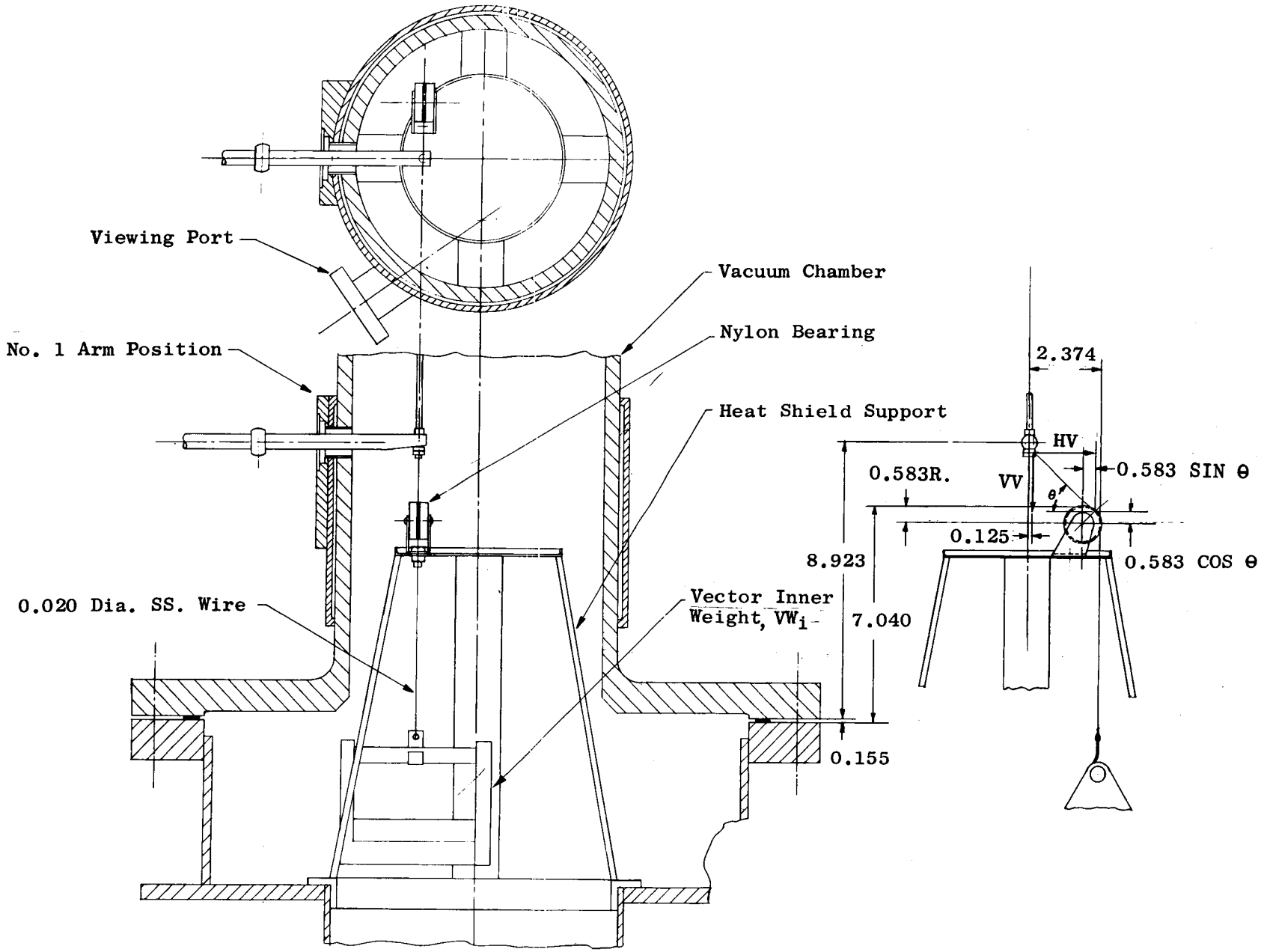

Figure 14. Vector Tare-Weight Assembly for the Calibration of the Loading Arms for the Friction and Wear Testers.

TABLE VI. VECTOR TARE TEST - UNCORRECTED MEASURED VALUES OF VW_o (OUTER WEIGHTS) VERSUS VW_i (INNER WEIGHTS) FOR THE LOADING ARMS OF THE FRICTION AND WEAR TESTERS

Loading Arm No.	Torr Pressure	VW_i, 5 lbs.		VW_i, 10 lbs.		VW_i, 15.6 lbs.	
		VW_o, lbs.	Ffp, lbs.	VW_o, lbs.	Ffp, lbs.	VW_o, lbs.	Ffp, lbs.
HVFT							
1*	Vac., 0.05 Torr	2.2552	1.15	5.2234	4.12	8.7115	8.40
	0 psig	2.2656	1.65	5.3750	4.18	8.7813	8.32
		2.1719	2.49	--	--	8.7813	8.31
	30 psig	2.3313	1.74	5.4313	4.40	8.9359	8.45
2	Vac., 0.05 Torr	3.9844	3.11	7.3865	6.44	11.0188	9.28
	0 psig	4.0344	3.30	7.3885	6.28	11.1344	9.60
		3.4531	--	--	--	10.3281	--
		2.8914	3.20	--	--	9.8750	9.62
		2.7620	3.08	--	--	10.0688	9.65
		2.7781	2.56	--	--	10.1063	9.68
		2.7952	2.82	--	--	--	--
		2.7644	3.00	--	--	--	--
		3.5719	4.17	--	--	--	--
	30 psig	3.9917	3.08	7.3375	6.16	11.1083	9.55
		3.4688	--	--	--	10.3250	--
		2.8063	--	--	--	9.8906	--
3	0 psig	3.6828	2.80	7.3297	5.73	11.2521	8.72
		2.4906	3.15	--	--	9.5750	9.62
	30 psig	3.6703	3.10	7.2656	5.93	11.1958	8.90
4	Vac., 0.05 Torr	--	--	--	--	10.5859	9.00
	0 psig	3.9417	3.14	7.2031	6.08	10.5239	9.10
		3.9328	3.27	--	--	9.5750	9.62
	30 psig	3.8771	3.08	7.1133	6.28	10.4453	9.16

TABLE VI. (Cont'd)

Loading Arm No.	Torr Pressure	VW_i, 5 lbs.		VW_i, 10 lbs		VW_i, 15.6 lbs.	
		VW_o, lbs.	F_{fp}, lbs.	VW_o, lbs.	F_{fp}, lbs.	VW_o, lbs.	F_{fp}, lbs.
KFT							
5	0 psig	3.2188	3.05	6.7542	6.05	10.6469	9.05
		3.0328	3.30	--	--	10.1169	9.74
	30 psig	3.1385	2.95	6.6667	5.90	10.5844	9.10
6	0 psig	3.7594	3.40	7.0354	6.23	10.5156	9.30
		3.1656	3.30	--	--	9.3031	9.91
	30 psig	3.6500	3.30	6.9365	6.13	10.3917	9.15

* Innert Weight, VW_i, for Loading Arm No. 1 is 15 Pounds.

VW_i = Inner Weight

VW_o = Outer Weight

F_{fp} = Pickup Force

The force pickups required calibration before beginning the vector tare tests. It was believed initially that the pickups could be calibrated with the loading center-line vertical. However, when the calibration made in the vertical position was checked with a calibration where the loading center-lines were horizontal, it was apparent that they did not verify each other with acceptable accuracy. Subsequently, the calibration curves made with the pickup in the horizontal position were used, since this is the position in which the force pickups will be during specimen testing. The method of calibration is described in Appendix A. Results are reproduced in Figures 15 thru 20.

The hysterisis loop that was obtained for these pickups (Wiancko Engineering Company, Pasadena, California, range 20 lb tension) was expected. The dip in the "decreasing load" curve between 4-5 lbs probably is associated with the removal of a 5 lb weight and the addition of two 4 lb weights; this same process is reversed on the "increasing load" curve without producing this effect. The "increasing load" leg will be used for the tests.

Bakeout Heating Checkout Test

The high vacuum friction tester was assembled as shown in Figure 21. No loading arms or rotating parts were included in the assembly and all ports were sealed with blank-off flanges. The viewing port was used as a thermocouple access port. To evaluate the bakeout capability of the system, five Pt vs Pt+10%Rh thermocouples (T1-T5) were tack-welded directly to the inner walls of the chamber and two chromel-alumel, Inconel-sheathed thermocouples (T6-T7) were inserted in wells located near the upper and lower main shaft bearing housing. Care was taken to tack weld the Pt vs Pt+10%Rh thermocouples between the heater cables which are located on the outer wall surface instead of directly opposite the heaters.

The chamber was evacuated to a pressure of 5×10^{-8} torr, given a preliminary bakeout and subsequently evacuated to a pressure of 2×10^{-9} torr. Heating of the tester was started by applying the full line voltage of 110 volts. However, the voltage was reduced to 88 volts when the temperature of the heater lead wires became excessive. It will be necessary to change the lead wires so that full voltage can be applied. The results of the test are tabulated in Table VII and plotted in Figure 22. Initially, no cooling or insulation was utilized for the purpose of obtaining a uniform temperature distribution. However, it soon became evident that insulation would be required to achieve an acceptable temperature distribution. "Fibrefax" insulation was applied over all the external surfaces of the vacuum chamber of the tester below the lower bearing and excluding the loading arm pads and the viewing port flange.

The conclusion from this test is that the bakeout heaters, as now installed and when insulated, appear to be adequate for bakeout purposes. However, an improvement in the temperature distribution of the chamber can be achieved by relocation of the heater elements and by changing the heater lead wires to permit

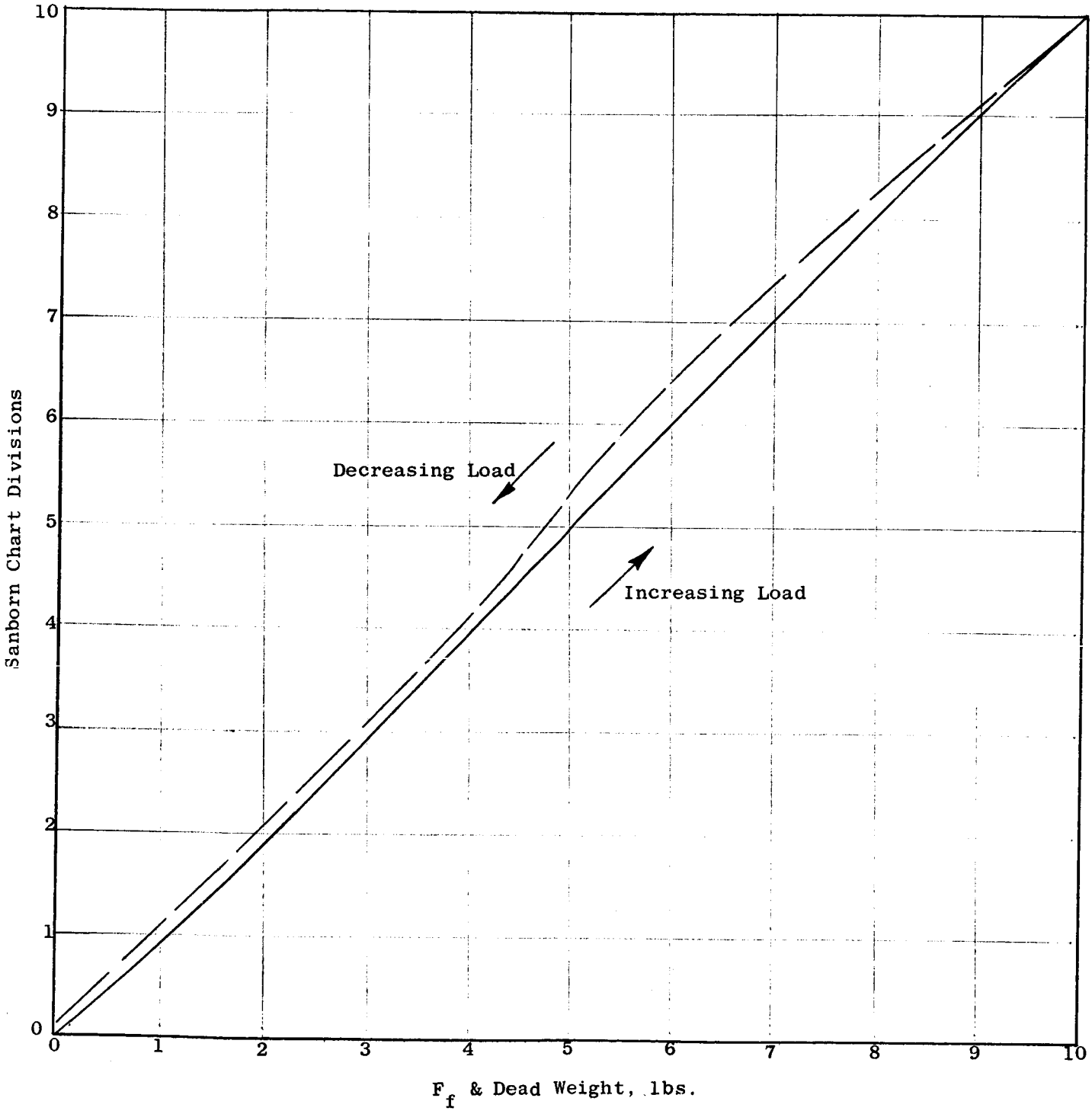

Figure 15. Calibration Curve For Force Pickup No. 101 (Loading Arm No. 1).

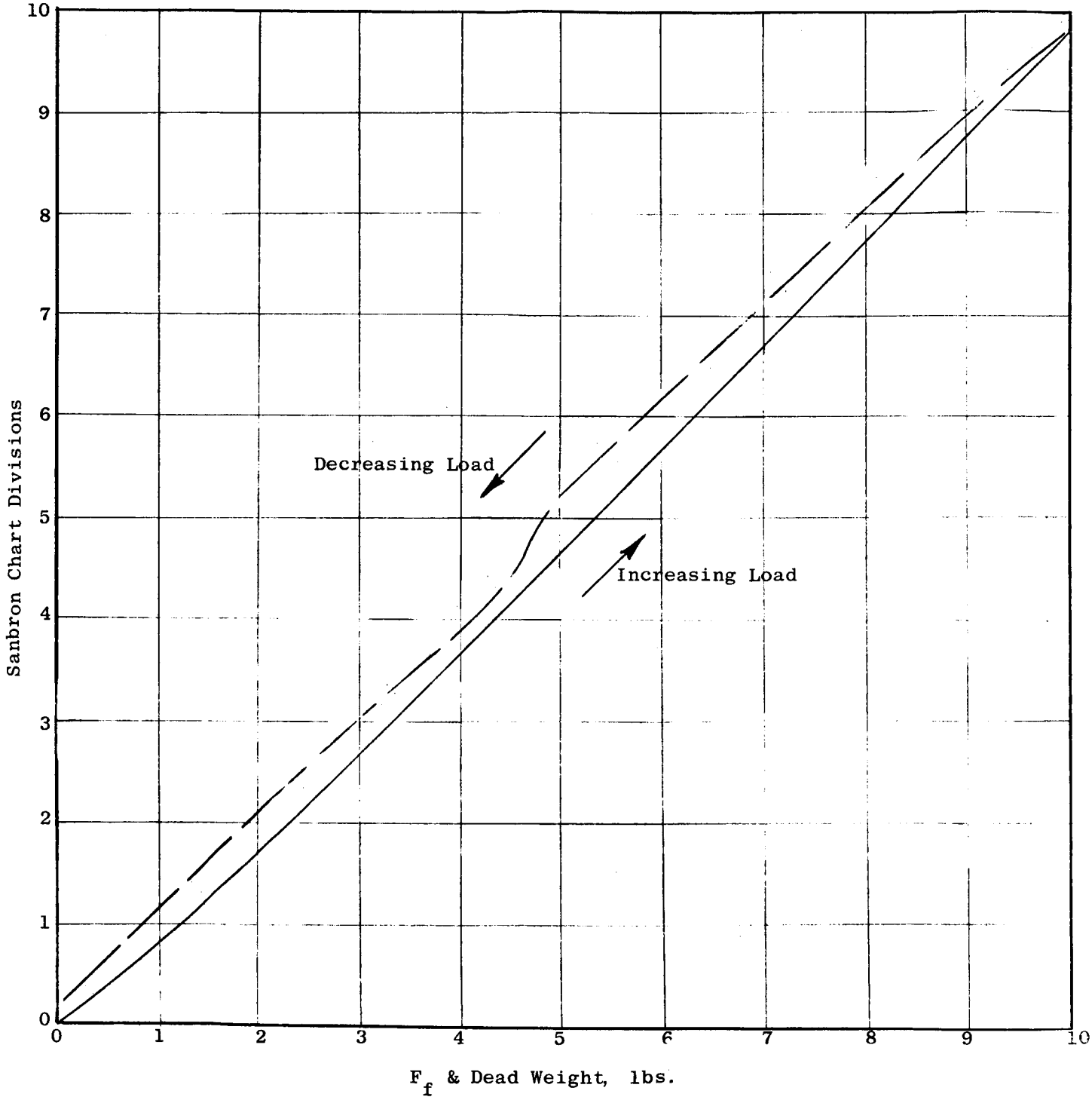

Figure 16. Calibration Curve For Force Pickup No. 102 (Loading Arm No. 2).

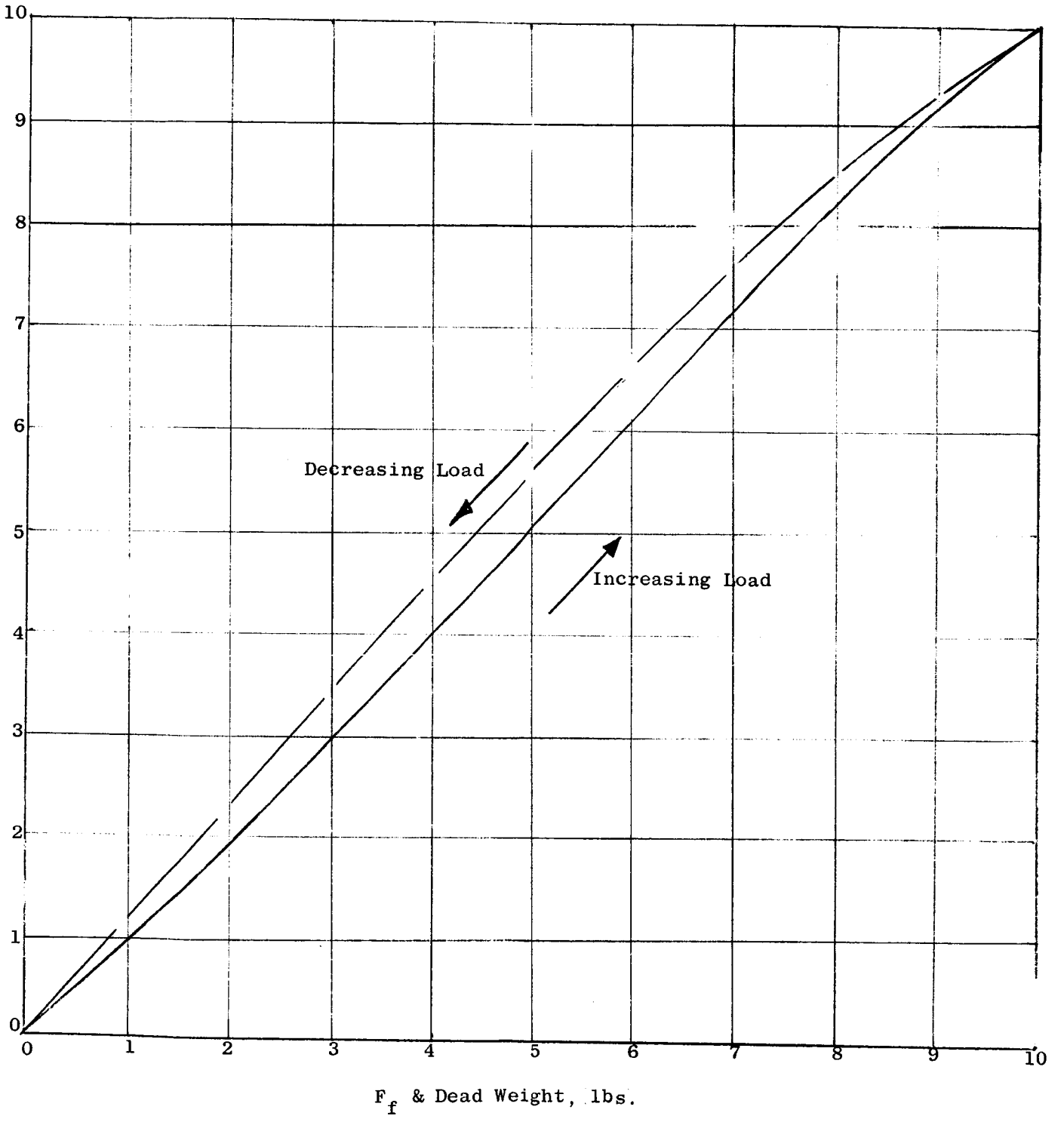

Figure 17. Calibration Curve For Force Pickup No. 103 (Loading Arm No. 3).

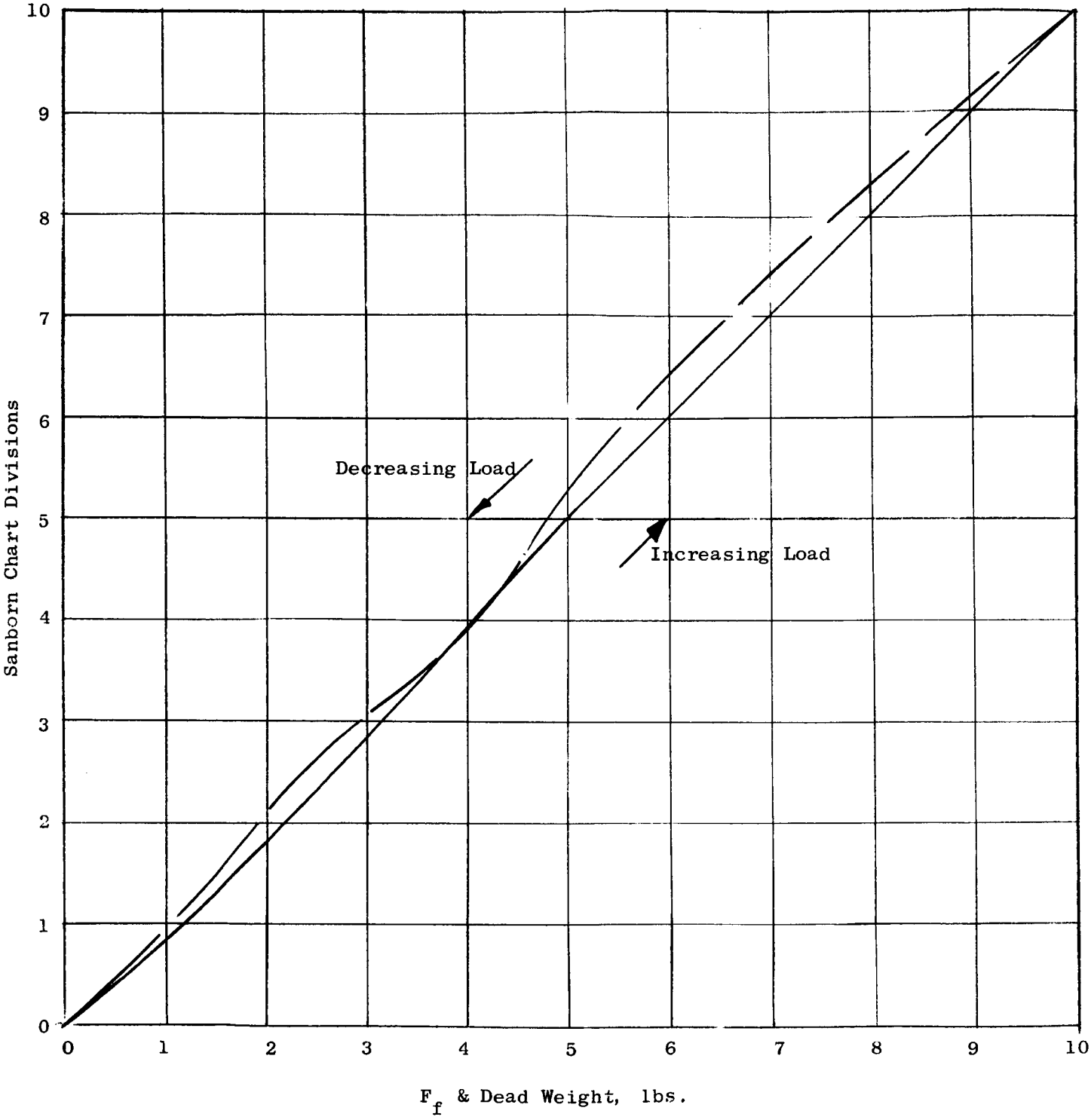

Figure 18. Calibration Curve For Force Pickup No. 104 (Loading Arm No. 4).

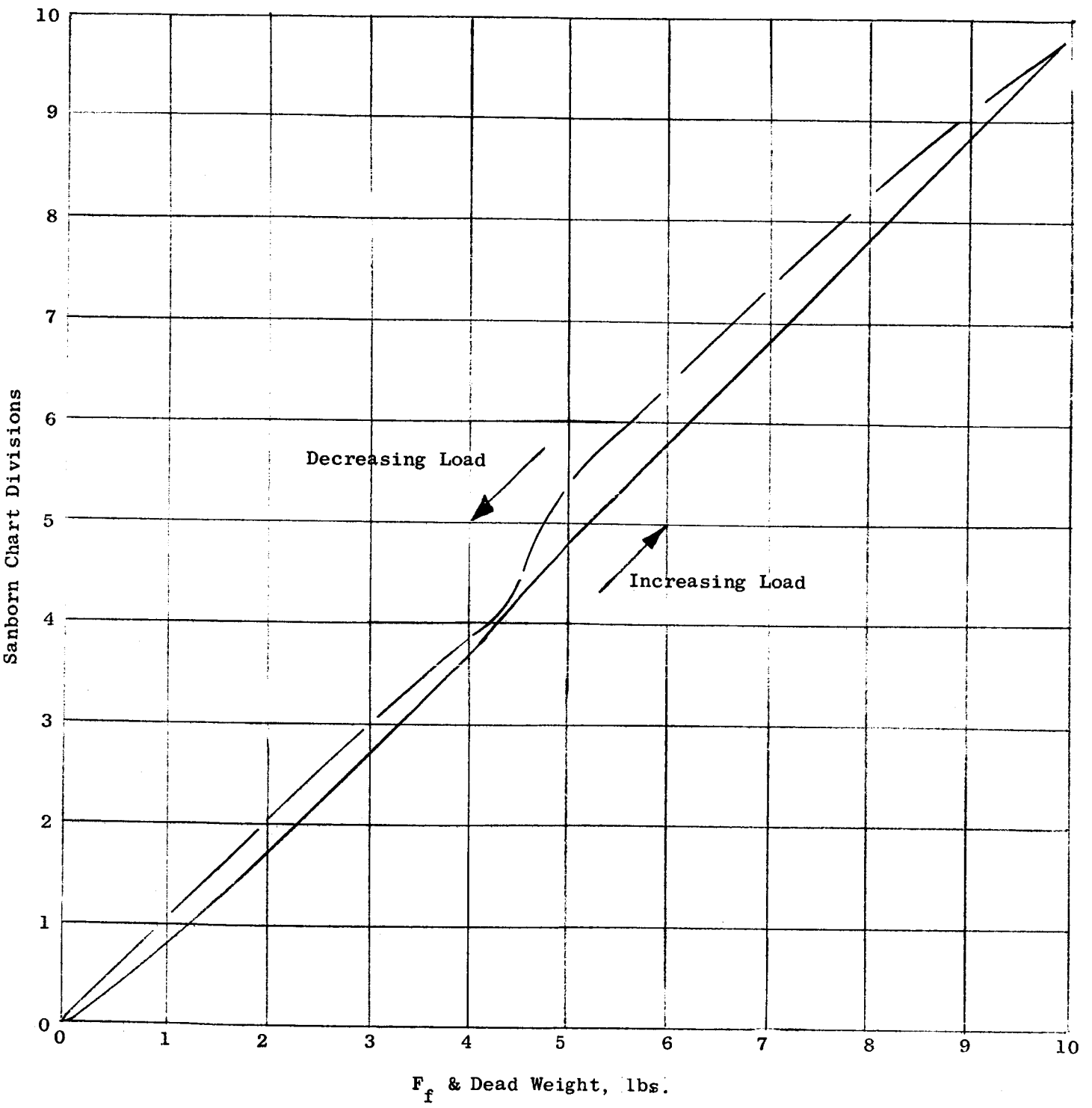

Figure 19. Calibration Curve for Force Pickup No. 105 (Loading Arm No. 5).

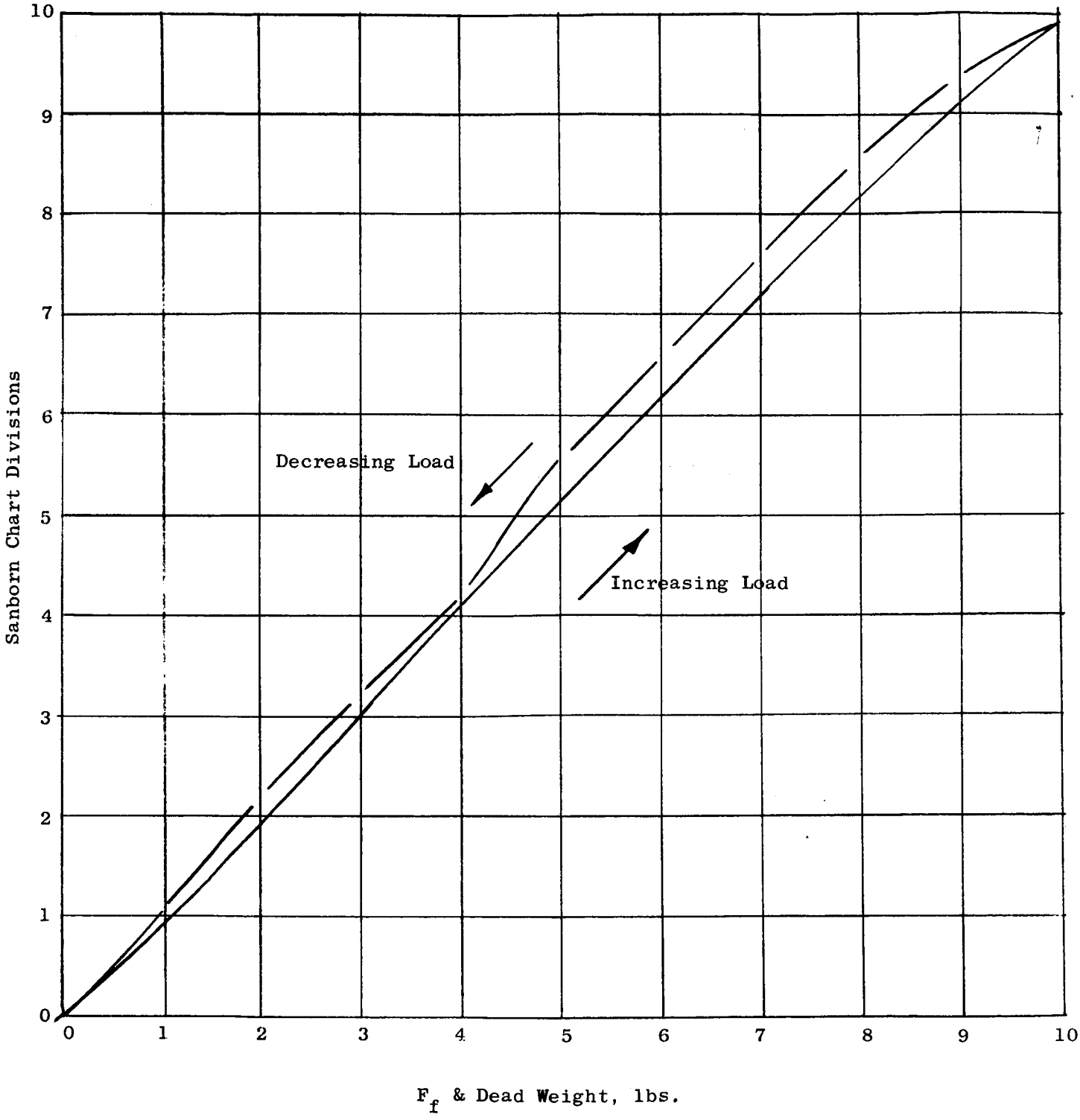

Figure 20. Calibration Curve For Force Pickup No. 106 (Loading Arm No. 6).

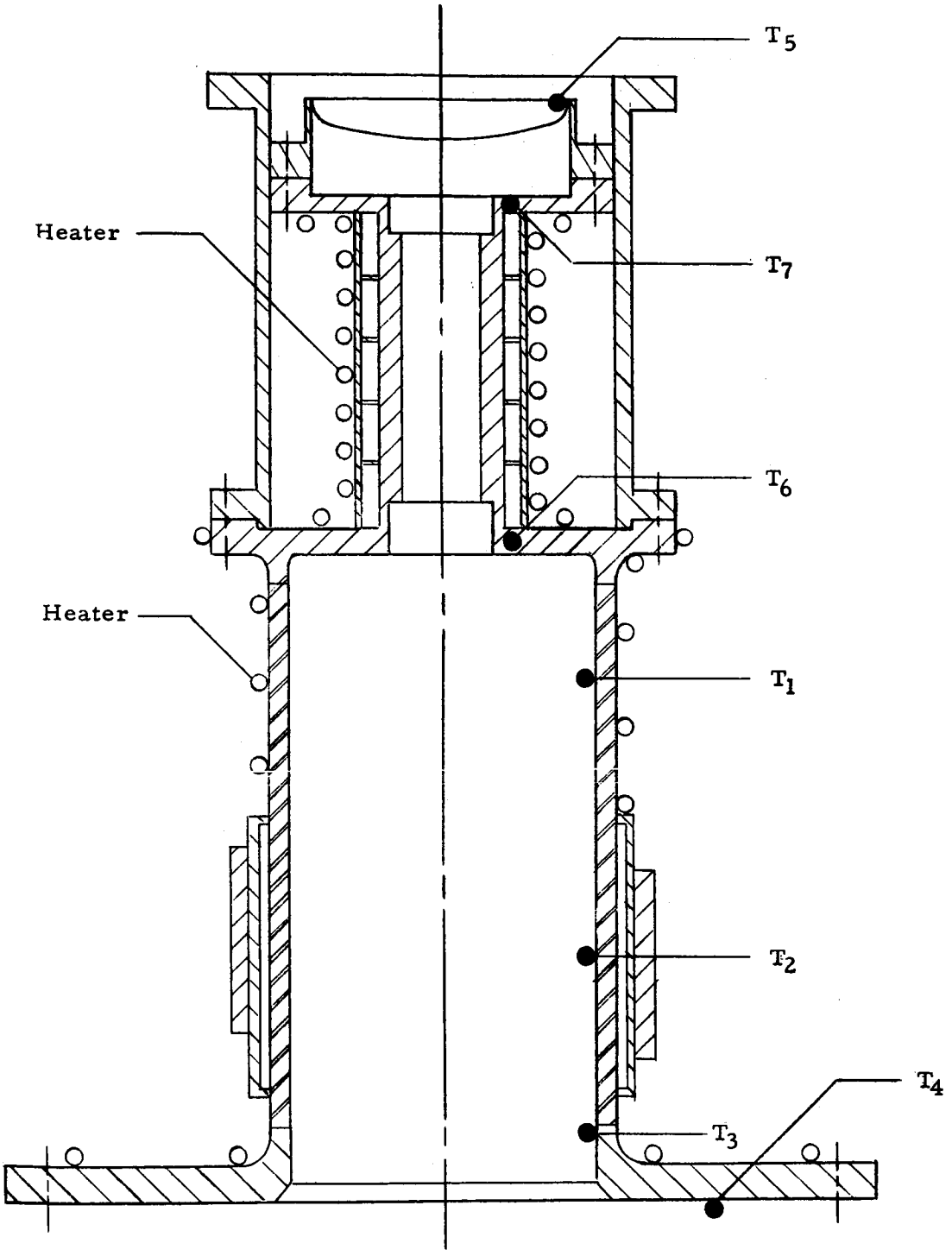

Figure 21. Thermocouple Location for Bakeout Heating Checkout Tests on High Vacuum Friction and Wear Tester.

TABLE VII. RESULTS OF BAKEOUT HEATING CHECKOUT TEST FOR HIGH VACUUM FRICTION AND WEAR TESTER

(Voltage Applied to External Bakeout Heaters, 88 Volts)

Elapsed Hours	Vacuum Torr	Temperature, °F							Remarks
		T_1	T_2	T_3	T_4	T_5	T_6	T_7	
0	8.5×10^{-9}	RT	RT	RT	RT	RT	RT	RT	Start Test
0.17	1×10^{-8}	125	80	100	100	100	212	220	
0.55	2×10^{-7}	240	125	130	130	190	Out	455	Replaced T_6
1.05	1.5×10^{-6}	335	185	170	160	260	560	630	
1.58	1.5×10^{-6}	395	240	205	200	295	620	580	20A Each Circuit
2.05	1.5×10^{-6}	420	270	225	215	310	645	602	
2.55	1.3×10^{-6}	440	295	250	230	310	660	610	
3.02	1.2×10^{-6}	455	305	260	240	315	664	612	
3.53	1.2×10^{-6}	460	320	275	255	315	665	612	
4.10	1.6×10^{-6}	470	330	300	305	460	665	626	Added Insulation - 3.80 - 4.30 Hours
4.60	1.8×10^{-6}	520	340	325	336	475	670	640	
5.07	3×10^{-6}	640	410	360	355	485	755	656	
5.60	4×10^{-6}	725	480	405	390	495	802	670	
6.03	4.1×10^{-6}	760	525	435	410	505	826	678	Power Off
47.00	2×10^{-7}	-	-	-	-	-	-	-	

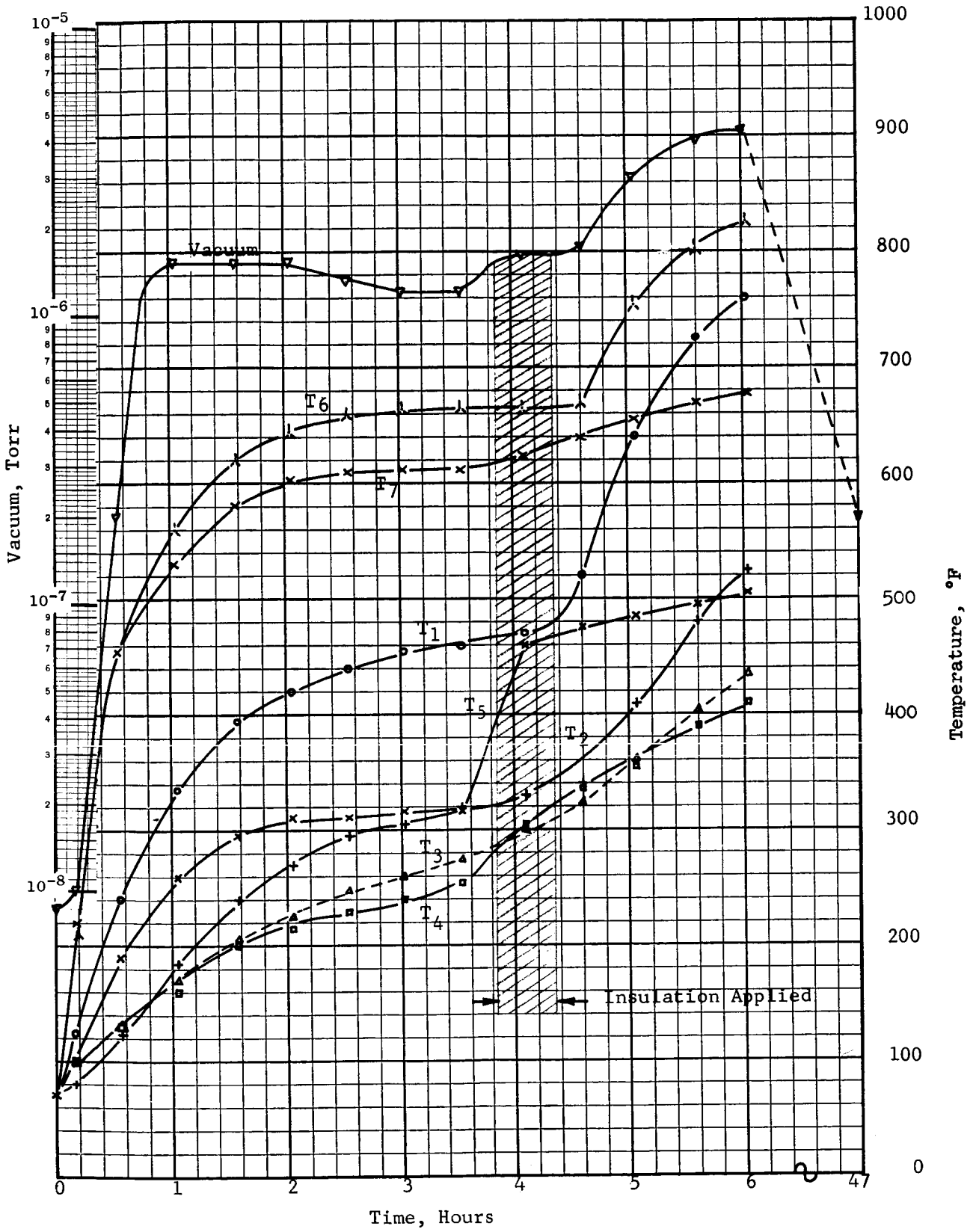

Figure 22. Change in Vacuum and Temperature with Time During Bakeout Heating Checkout Tests.

application of the full voltage. It should be noted that it will be necessary to apply cooling at the bearing locations when baking out the chamber.

Vacuum Checkout Test - After completion of the bakeout tests of the chamber, the getter-ion pump and base assembly were baked out and 75 hours after the power to the bakeout heaters was shut off, a vacuum of 6×10^{-10} torr was achieved. Ultimately a vacuum of 4.5×10^{-10} torr was reached. It is possible that the vacuum was lower, since the sensitivity of the gauge was reached. Data were tabulated in Table VIII and plotted in Figure 23.

Assembly Instructions - In order to minimize any possibility of error being made in the assembly of the high vacuum friction tester, the following assembly instructions have been written:

HVFT - A11	"High Vacuum Friction Tester SK-56131-250 - Subassembly of H28 Bearing Housing SK-56131-251"
HVFT - A12	"High Vacuum Friction Tester SK-56131-250 - Assembly of H44 Shaft (SK-56131-262G2) in H35 Vacuum Chamber (SK-56131-275)"
HVFT - A13	"High Vacuum Friction Tester SK-56131-250 - Subassembly of Loading Arms H64 Specimen Holder Assembly (119C2844)"

Engineering Drawings - A complete set of engineering drawings for the high vacuum friction tester has been red lined to show the present "as-built" condition. The modifications are being incorporated into the tracings and a final set of drawings will be issued when completed.

Friction and Wear in Liquid Potassium

Final Assembly - Approximately two weeks were required to complete the final assembly and conditional acceptance inspection (pending General Electric audit inspection) of the potassium friction and wear tester at the vendor's plant. During this time the General Electric project engineer was on-site to supervise all operations. Subsequently, the tester was shipped and currently is on hand at General Electric, Figure 24.

The rotating parts for the upper bearing housing, incorporating the bearings which will be used during the actual testing after balancing, were balanced to less than 0.300 gram-inch. The mating parts were marked to permit disassembly and reassembly and still maintain proper balance. The locations of significant points on the face of the magnet were measured, and the spacer bolts were set to provide 0.005-inch clearance between the magnet and diaphragm during shipment. The upper drive shaft was rotated by hand to assure ease of rotation. Final assembly of the upper bearing housing was completed without difficulty.

The main shaft was balanced to less than 0.300 gram-inch on a set of #7307 radial bearings which will be used for balancing purposes only. Angular-contact bearings #7207, the closest commercial bearings resembling the bearings to be

TABLE VIII. RESULTS OF VACUUM CHECKOUT CAPABILITY TEST FOR HIGH VACUUM FRICTION AND WEAR TESTER

Date	Time Hours	Elapsed Time Hours	Vacuum Torr	Remarks
3-4-65	2130	0	10^{-6}	Bakeout Started
3-5-65	0530	8	--	End Bakeout
	0800	10.5	2×10^{-8}	
	1630	19.0	6×10^{-9}	
3-6-65	0830	35.5	1.4×10^{-9}	
	1645	43.0	$< 1 \times 10^{-9}$	
3-8-65	0800	82.5	6×10^{-10}	
3-19-65	1500	353.5	4.5×10^{-10}	Opened Chamber

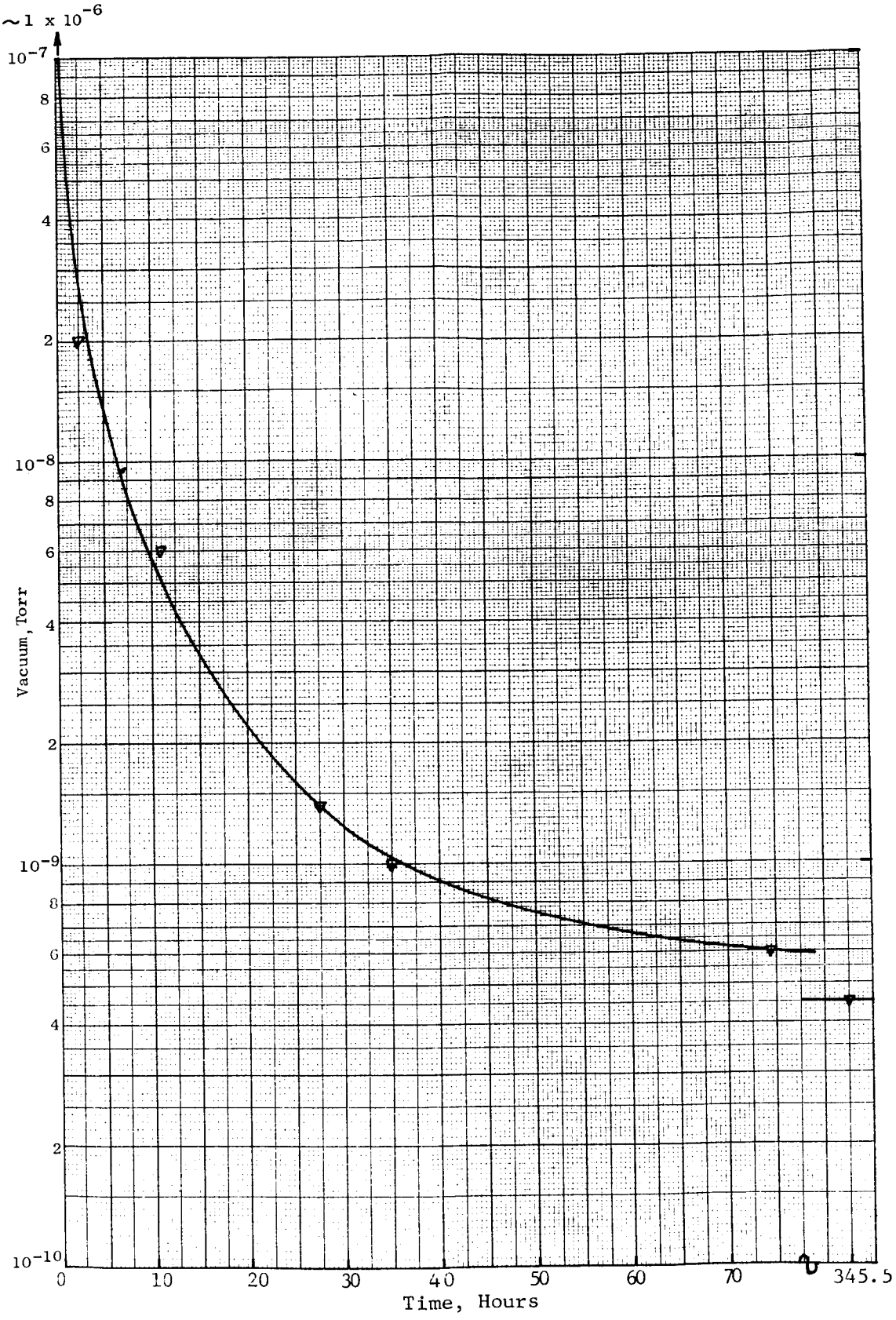

Figure 23. Ultimate Pressure Obtained in Vacuum Checkout Test for High Vacuum Friction and Wear Tester.

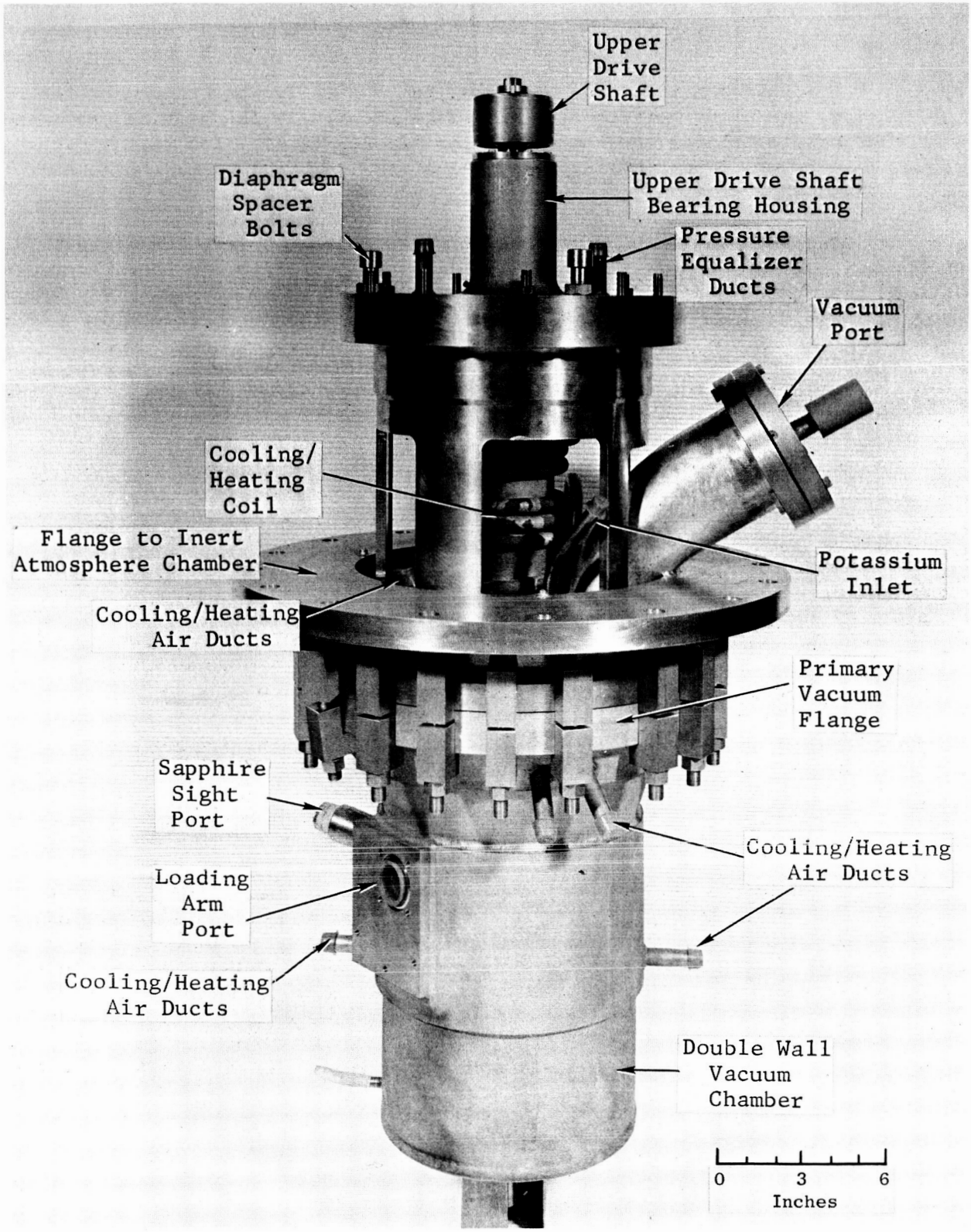

Figure 24. Liquid Potassium Friction and Wear Tester. (C65033007)

used in the actual testing, were too loose to be used for balancing and the circumferential and axial heat-transfer blockage grooves at the bearing seats made it impossible to balance the rotor on nylon blocks. Again, the mating parts were marked before disassembling after balancing so that they may be reassembled in proper balance.

Subsequently, the main bearing housing assembly was assembled without difficulty. A shim was machined to provide approximately 0.045-inch clearance between the magnet and the diaphragm during shipment. The two spare diaphragms were somewhat out of contour, and after inspection at General Electric, were rejected for rework. Also, it was apparent that a more accessible locking system should be devised for the rotating seal. Two loading arm assemblies were completed without difficulty. All spare parts for the tester, including one diaphragm which was reworked successfully, were received and are on hand.

The vacuum chamber and all the cooling chambers were helium leak checked at a sensitivity of 5×10^{-10} torr std cc air/sec and several small leaks were found in the vacuum chamber. No leaks were found after repair welding.

Sump Heater - The vendor has supplied three conductive, immersion heater elements for bench testing, Figure 25. These heaters consist of a swageable, high purity Al_2O_3 core*, Nichrome V No. 29 wire heating elements, nickel lead wires, a Cb-1Zr alloy sheath, a BN** end plug and BN*** powder packed between the Cb-1Zr alloy sheath and the elements. The BN powder, swageable Al_2O_3 core materials combinations represents a change in the heater design in that a high purity Al_2O_3 core material was substituted for a BN core. This change was necessary because of cracking of the BN core during the swaging operation. Radiographic examination of the swaged heaters with a BN core revealed the nichrome wires to be embedded in the cracks in the BN resulting in a non-uniform spacing between the wires and the Cb-1Zr alloy sheath. This condition would lead to non-uniform heating and probably burnout.

All of the BN powder that was used in the fabrication of the heaters was outgassed for one hour in a vacuum of 5×10^{-6} torr at General Electric and sealed under argon in polyethylene bags prior to being shipped to the vendor. A temperature of 2800°F was used to outgas the BN powder for two of the heaters and a temperature of 2200°F was used to outgas the BN for the third heater. Upon receipt of the fabricated heaters at General Electric, the BN end plugs were found to have been cracked. However, this condition was not expected to interfer with the bench tests or is it considered a serious problem with respect to the use of the heater in the friction tester.

---

* Saxonburg Ceramics, Saxonburg, Pa., Grade ST-61, >99.5% Al_2O_3; Analysis: MgO, 0.02%; SiO_2, 0.09%, Fe_2O_3, 0.06%; Cr_2O_3, 0.002%; TiO_2, 0.003%; CaO, 0.05%; C, 0.035%; S, 0.002%, B, < 10 ppm; Cd, < 8 ppm; Hf, < 80 ppm.

** Carborundum Electronics Div., Latrobe, Pa., Grade A, >97% BN; Typical Analysis: B_2O_3, 2.4%; Alkali Earth Oxides, 0.1%; Al_2O_3, 0.2%; SiO_2, 0.2%; C, 0.008%.

*** Carborundum Electronics Div., Latrobe, Pa., Grade HPC, >99.5% BN; Analysis Maximum: Cl, 0.01%; SO_4, 0.0005%; NH_3, 0.0005%; B_2O_3, 0.2%; Al, 0.1%; Si, 0.05%; Fe, 0.1%; Mg, 0.03%; Ca, 0.1%; Na, 0.1%; Cr, 0.1%; Mn, 0.005%; Ti, 0.1%.

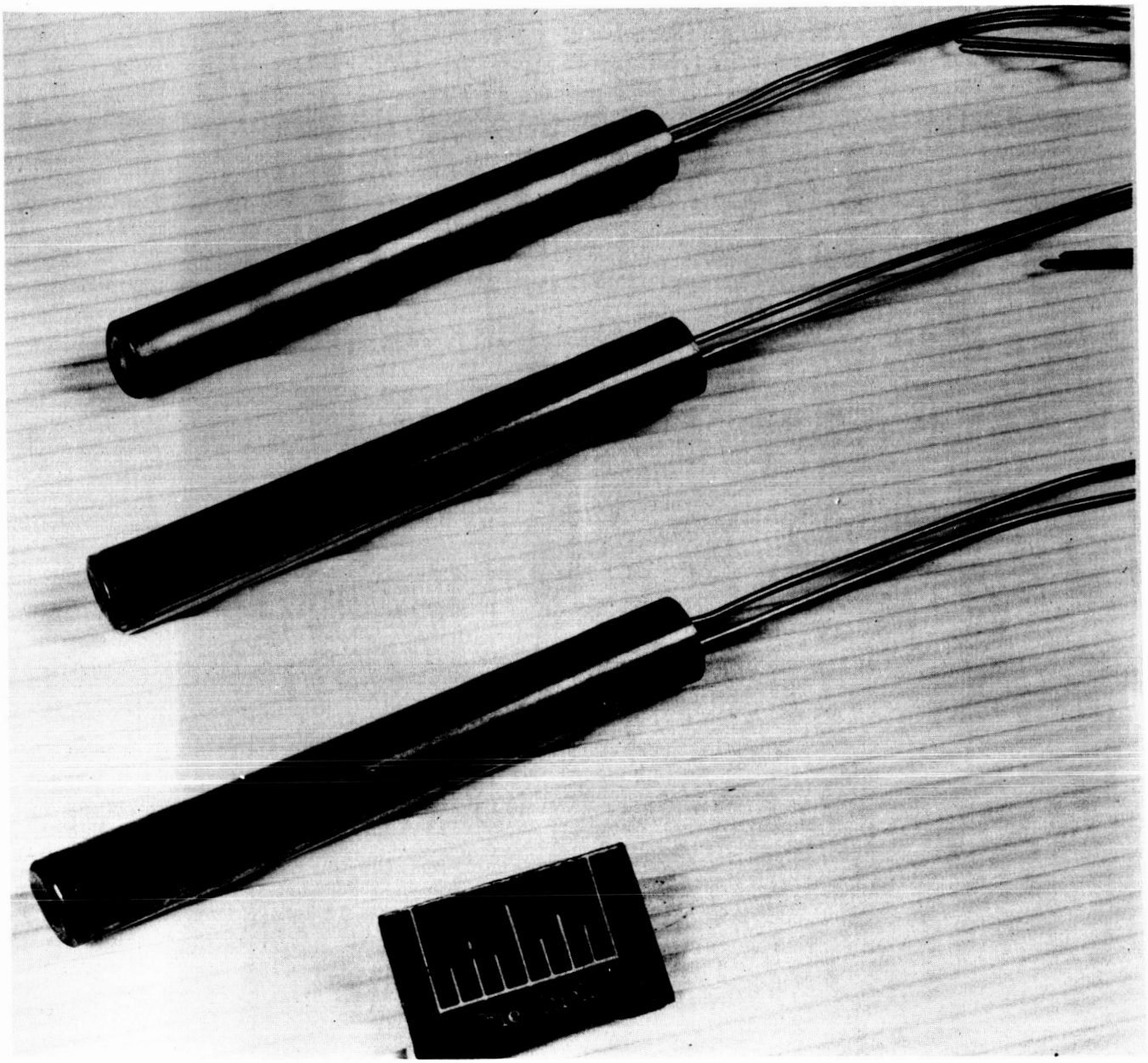

Figure 25. Cb-1Zr Alloy Sheathed Immersion Heaters for Potassium Friction and Wear Tester. (C650310112)

Radiographic examination of the heaters, Figure 26, revealed a uniform displacement of the BN between the heating elements and the Cb-1Zr alloy sheaths. Although the Nichrome wire appeared to be wound uniformly over most of the length of the Al_2O_3 core, the spacing of the wire was found to be uneven over the rest of the length (near the closed end). This can be seen in Figure 26. The vendor believes this condition can be corrected by making a smaller weld in the Cb-1Zr alloy end plug. Consequently, subsequent sets of Cb-1Zr alloy sheaths will be electron beam welded.

The outer surfaces of these heaters were cleaned by pickling in a 20%HF-20%HNO_3-60%H_2O acid solution, electrically connected in parallel and installed in a high-vacuum chamber. A Pt vs Pt+10%Rh thermocouple was spot welded to the surface of each heater prior to installation in the vacuum chamber, Figure 27. The chamber was evacuated to a pressure of 2×10^{-6} torr, given a bakeout and subsequently evacuated to a pressure of 6×10^{-8} torr. The heaters were heated gradually to the maximum planned service temperature of 1600°F as measured by the thermocouple attached to the heater surface, Figure 28. The total duration of the test was approximately 123 hours and at approximately 80 watts of electrical power each heater generated about 9 KW-hr. The test data are presented in Table IX. Because of the lack of means to cool the surface of the sheaths, this bench test did not permit the application of the full 1000 watts of power that is expected to be required to heat the potassium in the tester to 1600°F.

Electric resistance measurements were made at 500 volts (DC) across the insulation of the heaters before and after the 123-hour exposure at 1600°-1680°F in high vacuum and were found to be 1,000-10,000 megohms and 250,000 megohms, respectively. Results of resistance breakdown tests made after the 123-hour test exposure are given in Table X.

Two of the heaters were evaluated to determine the compatibility between the grade of BN powder used to fabricate the heaters and the Cb-1Zr alloy sheath and Nichrome heater wires. The BN used in one of the heaters (J3NX12A-No. 3) has been vacuum outgassed for one hour at 2800°F and the BN used in the other heater (J3NX12B-No. 2) had been vacuum outgassed for one hour at 2200°F. The Cb-1Zr alloy sheath and Nichrome wire were evaluated by means of metallographic examination and chemical analyses for oxygen, nitrogen and hydrogen; the Cb-1Zr alloy sheath also was chemically analyzed for boron. The locations of the various samples obtained for evaluation are shown in Figure 29. Samples for gas analysis of the Cb-1Zr alloy sheath were obtained by machining away the outer 0.030 inch of the wall leaving a solid 0.02 inch thick sample of the inner surface; the entire cross section of the nichrome wire was analyzed. Samples of the Cb-1Zr alloy sheath for spectrographic analysis of boron were obtained by milling two 0.010 inch thick layers from the inner surface. The Cb-1Zr alloy samples were cleaned by a light mechanical scrapping of the inner surface to remove discrete particles of BN that were imbedded in the wall followed by swabbing with alcohol; the Nichrome samples were cleaned by swabbing with alcohol.

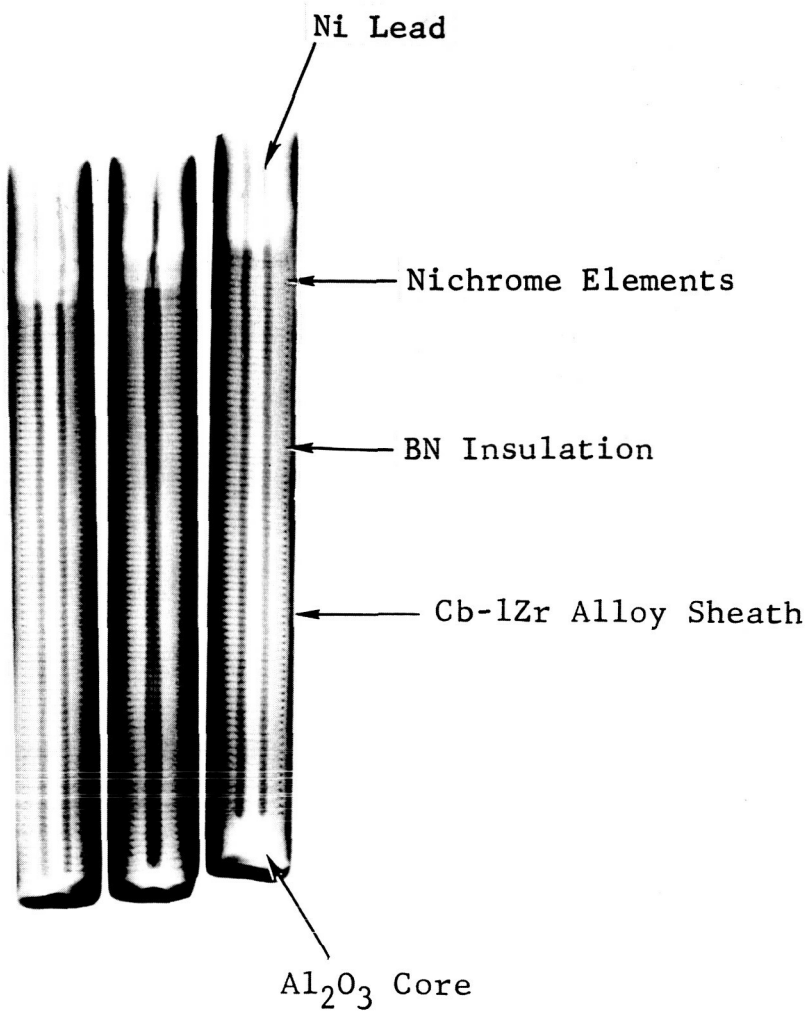

Figure 26. Radiograph (Positive) of Cb-1Zr Alloy Sheathed Immersion Heaters for Potassium Friction and Wear Tester.

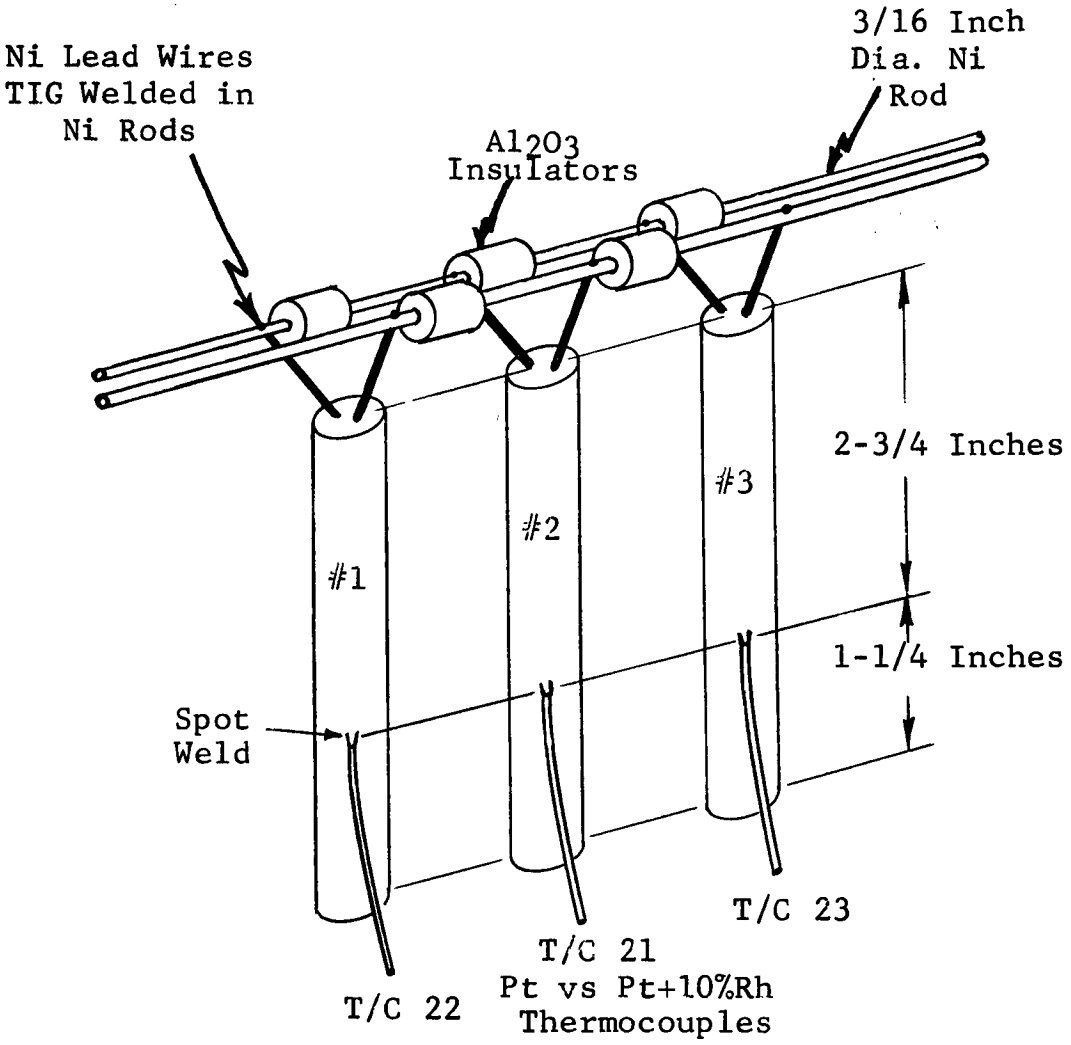

Figure 27. Test Set-Up for Conducting Compatibility Test of Cb-1Zr Alloy Sheathed Immersion Heaters in Vacuum.

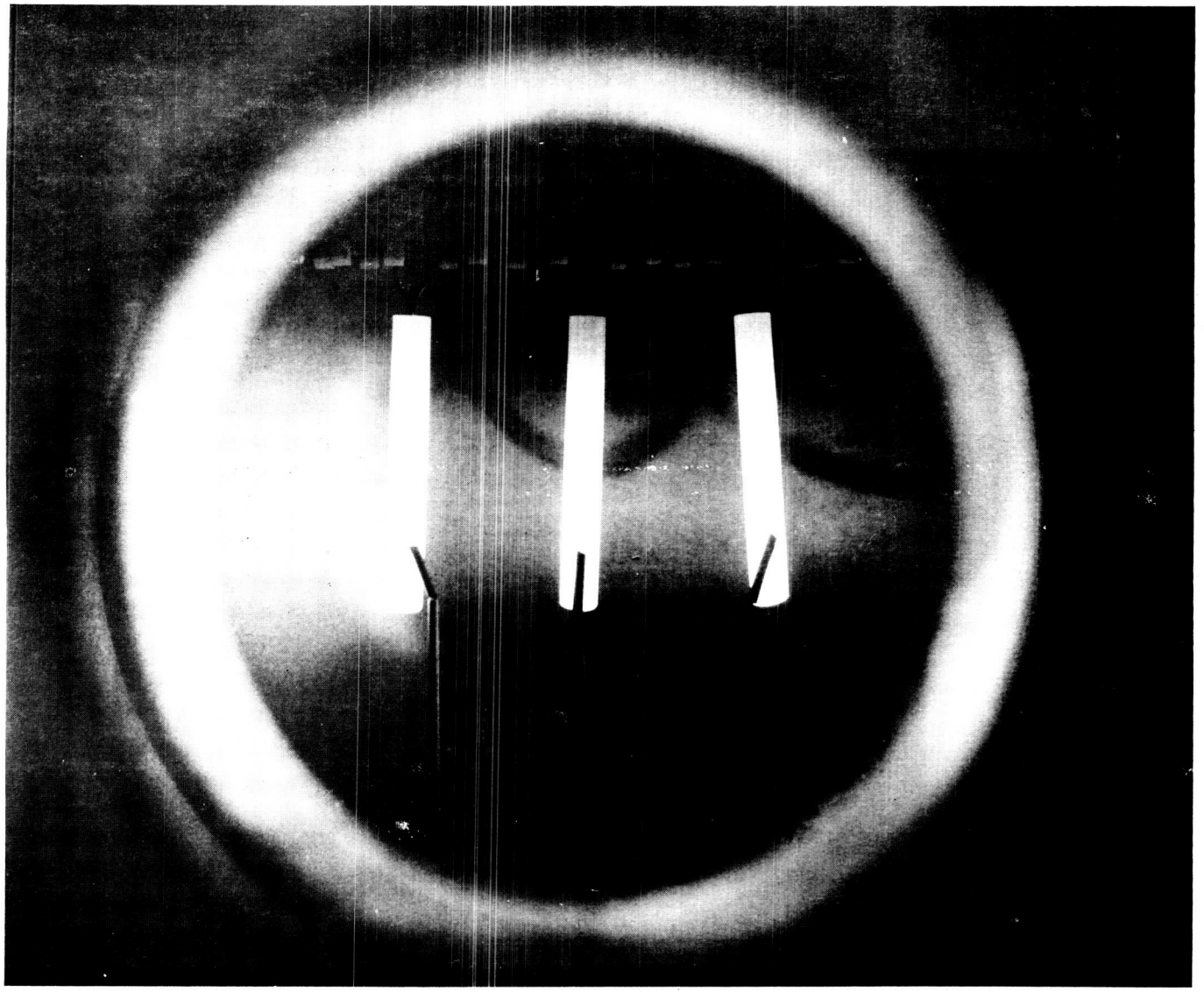

Figure 28. Photograph of Cb-1Zr Alloy Sheathed Immersion Heaters on Test in a Vacuum of 10^{-8} Torr at 1600° to 1680°F. Test Duration was 123 Hours. (CDC 3624)

TABLE IX. VACUUM CHECKOUT TEST OF Cb-1Zr ALLOY SHEATHED CONDUCTIVE IMMERSION HEATERS

S/N	Vendor Code	Core	Sheath Insulation	End Plug	BN Bakeout Temp., °F	Sheath
1,3	J3NX12A	Al_2O_3	BN	BN	2800	Cb-1Zr Alloy
2	J3NX12B	Al_2O_3	BN	BN	2200	Cb-1Zr Alloy

Test Date	Time Hours	Pressure Torr	A.C. Volts	Amps	Accumulated Time Hours	Temperature, °F #1	#2	#3	Remarks
3-17-65	1110	6.4×10^{-8}	11	1.0	0	110	110	110	Start
	1126	3.8×10^{-6}	11	1.0	0.27	300	300	300	
	1255	3.4×10^{-7}	--	0.4	1.25	290	280	280	
	1300	6.0×10^{-7}	11	1.0	1.83	325	315	315	
	1315	5.5×10^{-6}	15	1.2	2.08	560	540	530	
	1330	1.8×10^{-6}	15	1.2	2.34	660	630	620	
	1345	2.1×10^{-6}	20	1.6	2.58	840	810	805	
	1400	2.2×10^{-6}	25	1.9	2.84	1010	980	980	
	1410	1.6×10^{-6}	30	2.2	3.00	1140	1100	1110	
	1425	6.0×10^{-7}	35	2.7	3.25	1280	1230	1260	
	1435	5.0×10^{-7}	40	3.0	3.42	1380	1320	1350	
	1445	4.2×10^{-7}	45	3.4	3.60	1490	1430	1460	
	1455	3.6×10^{-7}	50	3.8	3.75	1590	1520	1550	
	1507	2.8×10^{-7}	53	4.0	3.95	1640	1560	1600	
	1520	2.2×10^{-7}	53	4.0	4.17	1640	1565	1600	
	1530	2.1×10^{-7}	55	4.2	4.32	1670	1595	1630	
	1545	1.8×10^{-7}	55	4.3	4.58	1670	1600	1630	
	1630	1.5×10^{-7}	55	4.25	5.33	1665	1600	1630	

TABLE IX (Cont'd)

Test Date	Date Hours	Pressure Torr	A.C. Volts	Amps	Accumulated Time Hours	Temperature, °F #1	#2	#3	Remarks
3-17-65	1700	1.4×10^{-7}	55	4.25	5.82	1660	1605	1630	
3-18-65	0800	5.5×10^{-8}	55	4.25	20.8	1640	1600	1620	
	1445	4.3×10^{-8}	55	4.2	25.9	1640	1600	1620	
3-19-65	0800	2.9×10^{-8}	55	4.2	45.0	1655	1610	1625	
	1600	2.7×10^{-8}	--	--	52.8	1650	1600	1625	
3-20-65	0800	2.4×10^{-8}	--	--	68.8	1660	1610	1620	
3-22-65	0630	1.8×10^{-8}	--	--	115.5	--	--	--	
	0900	1.8×10^{-8}	54.5	4.2	118.0	1665	1610	1625	
	1115	---	54	4.3	120.5	1680	1630	1610	
	1400	1.7×10^{-8}	54	4.2	123.0	1670	1625	1605	Power Off

Average Heater Energy Production $\approx \sum \frac{VI \quad t}{3 \times 60 \times 1000} \approx$ 9.230 KW-Hour.

TABLE X. RESISTANCE BREAKDOWN VOLTAGES FOR Cb-1Zr ALLOY SHEATHED IMMERSION HEATERS WITH BN AND Al_2O_3 INSULATION AFTER BEING EXPOSED TO HIGH VACUUM (10^{-8} TORR) FOR 123 HOURS AT 1600°-1680°F

Heater No.	DC Breakdown Voltage, KV	Remarks
J3NX12B-No. 2	3.4	Permanent Path Through Insulation
J3NX12A-No. 3	3.2	Arc-Over From Ni Lead to Cb-1Zr Alloy Sheath at Bottom of Heater

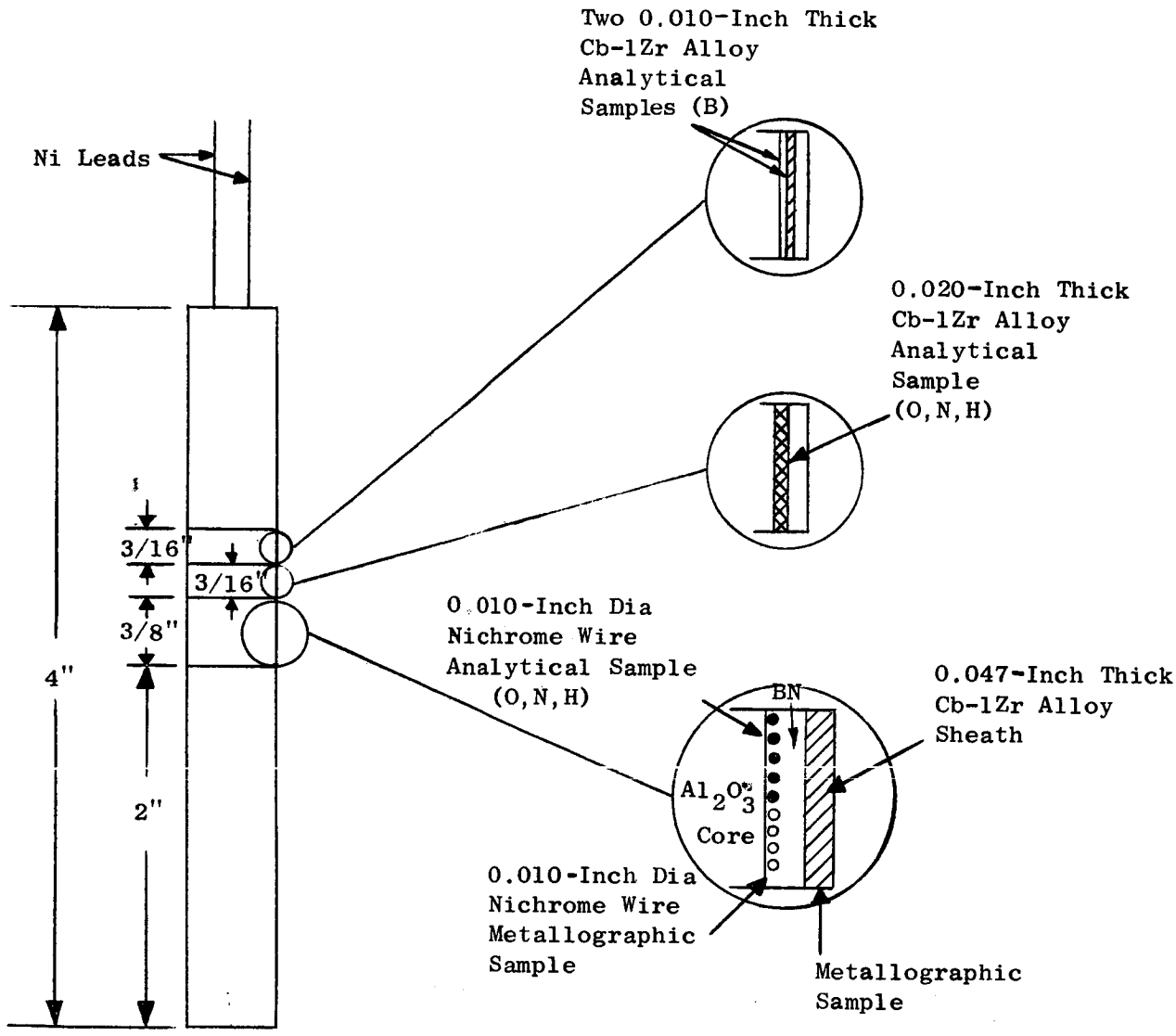

Figure 29. Location of Samples for Metallographic Examination and Chemical Analyses of Cb-1Zr Alloy Sheathed, BN/Al_2O_3 Insulated Immersion Heaters.

The results of the chemical analyses are presented in Table XI. The nitrogen content of the inner 0.020-inch layer of the Cb-1Zr sheaths increased 86 and 136 ppm with the smaller increase occuring in heater No. 3. This is attributed to the higher outgassing temperature (2800°F) of the BN powder used in the fabrication of heater No. 3 over that used for BN in heater No. 2. The data also suggest that the oxygen in the Cb-1Zr alloy was gettered by the outgassed BN. A heavy trace of boron was detected on the inner 0.010-inch layer of the Cb-1Zr alloy sample from both heaters. It is possible that small particles of BN which were imbedded in the Cb-1Zr alloy sheath were not removed in the cleaning of the sample resulting in an indicated pickup of nitrogen and boron by the Cb-1Zr alloy. Previous Cb-1Zr alloy BN compatibility bench tests using solid pieces of BN showed no pickup of nitrogen by the Cb-1Zr alloy in 100 hours at 1800°F[3]. No pretest gas analysis of the Nichrome V wire used in the fabrication of the heaters is available. However, a comparison of the post-test analyses with a typical analysis for Nichrome V wire in Table XI would indicate little or no pickup of nitrogen in the wire exposed to BN that had been vacuum outgassed at 2800°F and possibly several hundred ppm pickup of nitrogen in the wire that was exposed to BN that had been vacuum outgassed at 2200°F. A possibility of 100 to 200 ppm pickup in oxygen in the wire also exists with the larger increase being associated with the exposure to BN that was vacuum outgassed at the lower temperature (2200°F). However, since the BN appeared to getter oxygen from the Cb-1Zr alloy, the probable source of oxygen is the Al_2O_3 core on which the wire is wrapped.

Metallographic examination of the Cb-1Zr alloy sheath and Nichrome V wire after the 123 hour exposure to BN revealed no detectable changes in microstructure of either material, Figures 30 and 31. However, the cold-worked structure of the Cb-1Zr alloy sheath made examination by light microscopy extremely difficult. From Figure 30, it is obvious that the inner 3 to 5 mils of the as-received Cb-1Zr alloy tube was contaminated during processing; exposure to the 1600°F test temperature resulted in precipitation of ZrO_2 in the area near the surface. A high oxygen concentration near the surface also is evidenced from a comparison of the oxygen content of the inner 0.020-inch layer and the entire 0.047-inch thick cross section of the sheath, i.e., 353 ppm and 190 ppm, respectively. Microhardness traverses made across transverse sections of the as-received sheath and after the 123-hour exposure to BN show a slightly higher hardness near the inner surfaces of the sheaths. This is attributed to the high oxygen content near the surface. The slightly higher surface hardness observed in the Cb-1Zr alloy sheaths after the test exposure may be associated with the diffusion of a small amount of nitrogen into the surface, coherent precipitation of ZrO_2 and/or some work hardening resulting from the final swagging operation in the fabrication of the heater. It is interesting to note that the greater increase in hardness is associated with the lower vacuum outgassing temperature (2200°F) given the BN prior to fabrication of the heater.

TABLE XI. CHEMICAL ANALYSES OF Cb-1Zr ALLOY SHEATH AND NICHROME V WIRE FROM BN/Al_2O_3 INSULATED IMMERSION HEATERS AFTER A 123-HOUR EXPOSURE AT 1600°-1680°F IN HIGH VACUUM (10^{-8} TORR)

Sample Identity	Chemistry, ppm							
	Heater J3NX12B-No. 2[1]				Heater J3NX12A-No. 3[2]			
	O[3]	N[3]	H[3]	B[4]	O[3]	N[3]	H[3]	B[4]
Cb-1Zr[5] - Inner 0.020-Inch As-Received	353	57	7	---	353	57	7	---
Cb-1Zr - Inner 0.020-Inch After 120-Hour Exposure	326	193	10	---	216	143	5	---
Nichrome - 0.010-Inch Wire; Typical Analyses [6]	10-100	300-500	--	---	10-100	300-500	--	---
Nichrome - 0.010-Inch Wire After 123-Hour Exposure	223	711	6	---	183	423	12	---
Cb-1Zr - Inner 0.010-Inch Layer After 123-Hour Exposure	---	---	--	Heavy Trace	---	---	--	Heavy Trace
Cb-1Zr - Second 0.010-Inch Layer After 123-Hour Exposure	---	---	--	No Trace	---	---	--	No Trace

[1] BN Outgassed 1 Hour at 2200°F at 5×10^{-6} Torr Prior to Fabrication.

[2] BN Outgassed 1 Hour at 2800°F at 5×10^{-6} Torr Prior to Fabrication.

[3] By Vacuum Fusion Techniques.

[4] By Spectrographic Techniques.

[5] MCN 1081; Vendor's Bulk Analysis (0.047-Inch Thick Wall); O, 190 ppm; N, 70 ppm; H, 3 ppm, C, 80 ppm.

[6] Driver-Harris Company.

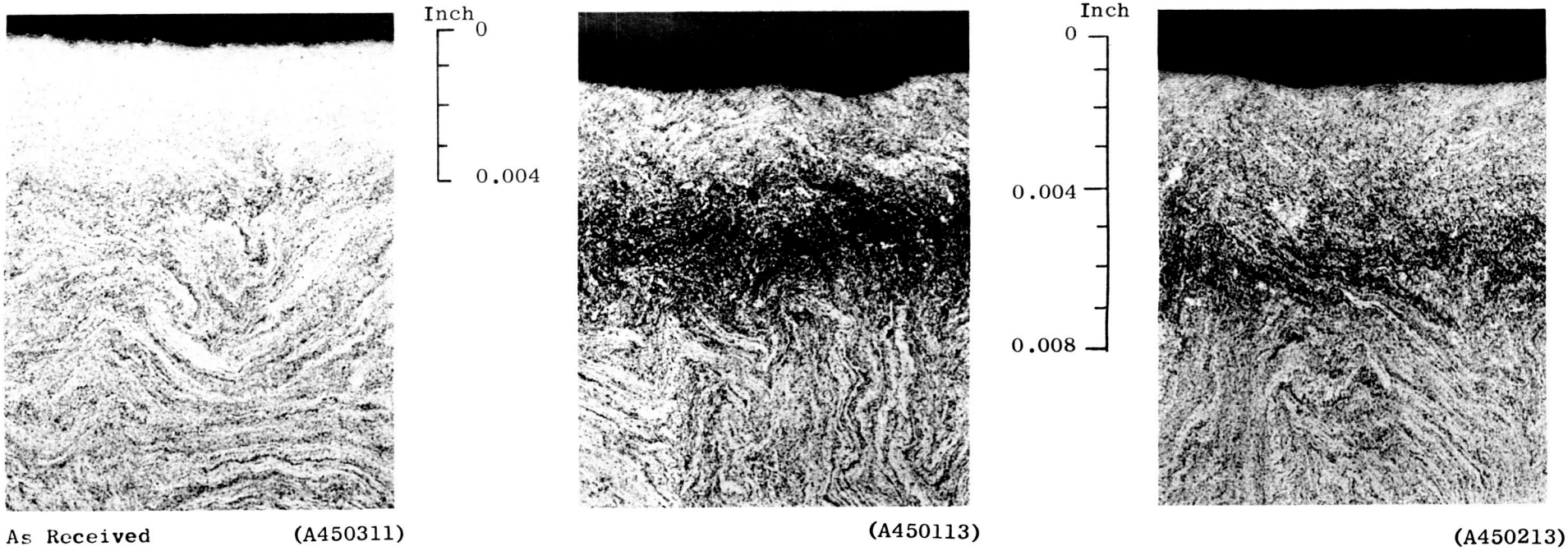

Figure 30. Microstructures of Cb-1Zr Alloy Sheaths from Immersion Heater J3NX12A-No. 3 (Center) Containing BN Insulation that had been Vacuum Outgassed for One Hour at 2800°F, and Immersion Heater J3NX12B-No. 2 (Right) Containing BN Insulation that had been Vacuum Outgassed for One Hour at 2200°F. The Heaters were Tested in a Vacuum (10^{-8} Torr) for 123 Hours with a Surface Temperature of 1600°F.

Etchant: 5%HF-30%HNO_3-50% Lactic

Mag: 250X

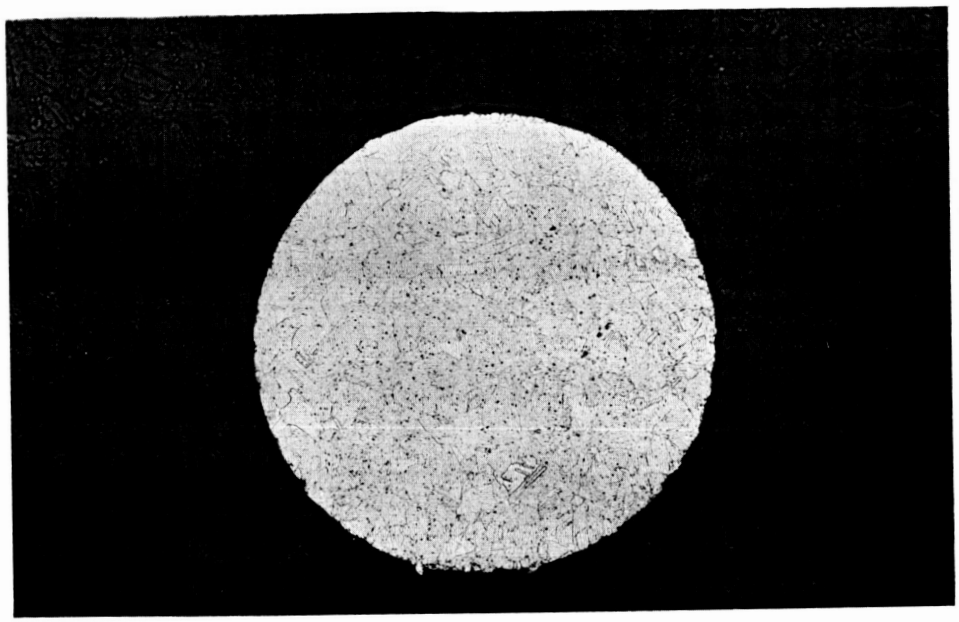

0 0.004
Inch

(L1373)

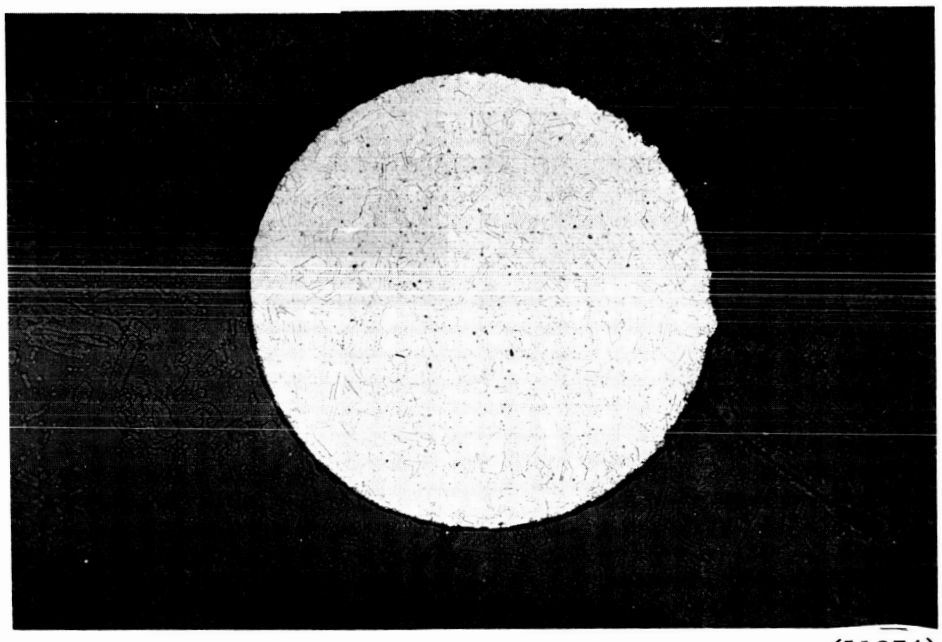

(L1374)

Figure 31. Microstructures of Nichrome V Heating Wires from Immersion Heater J3NX12A-No. 3 (Top) Containing BN Insulation that had been Vacuum Outgassed for One Hour at 2800°F, and Immersion Heater J3NX12B-No. 2 (Bottom) Containing BN Insulation that had been Vacuum Outgassed for One Hour at 2200°F. The Heaters were Tested in a Vacuum (10^{-8} Torr) for 123 Hours with a Surface Temperature of 1600°F.

Etchant: Marbles

Mag: 250X

Distance from Inner Surface, Inch	Hardness of Cb-1Zr Alloy Sheath, Knoop (100-Gram Load)		
	As-Received	After 123-Hour Exposure to BN at 1600°F	
		J3NX12A No. 3(1)	J3NX12B No. 2(2)
0.002	141	175	183
0.005	134	137	143
0.010	126	123	138
0.015	123	124	128
0.020	124	127	127

(1) BN Vacuum Outgassed 1 Hour at 2800°F at 5 x 10^{-6} Torr Prior to Fabrication.

(2) BN Vacuum Outgassed 1 Hour at 2200°F at 5 x 10^{-6} Torr Prior to Fabrication.

Based on the results obtained from the evaluation of the BN insulated heaters, the vendor was requested to proceed with the production of 14 additional heaters of the same design to be used in the fabrication of one immersion heater assembly for the potassium friction and wear tester. However, the vendor will continue to attempt to fabricate a Cb-1Zr alloy sheathed heater with a swageable, high purity Al_2O_3 core and high purity Al_2O_3* powder insulation between the Nichrome heating elements and the Cb-1Zr alloy sheath. Although, for reasons of superior compatibility with the Cb-1Zr alloy, the Al_2O_3 insulation is preferred over the BN insulation, the Al_2O_3 powders are harder than the BN powder and will be more difficult to compact without damaging the Nichrome V wires. If heaters with Al_2O_3 insulation are fabricated successfully, bench tests similar to those conducted with the BN insulated heaters will be conducted in high vacuum.

A Type 304SS mock-up of the sump heater assembly has been fabricated successfully and is shown in Figure 32. Although the heater has not been tested for power production, it has been tested for electrical continuity and helium leak-tested.

Test Facility

All electrical power and wiring for the control console for the high vacuum friction and wear tester have been completed. The inert gas environmental chamber for the liquid potassium friction and wear tester was received from the vendor after being leak checked according to procedures in MIL Std 271C; no leaks were found at a sensitivity of 5 x 10^{-10} std cc air/second. The chamber and other major components have been incorporated in the facility build-up and installed in the laboratory test areas as shown in Figure 33. An isometric

---

* Norton Company, Wooster, Mass., Grade Alumdum Type 38; Typical Analysis: Al_2O_3, 99.49%; SiO_2, 0.05%; Fe_2O_3, 0.10%; TiO_2, 0.01%; Na_2O, 0.35%.

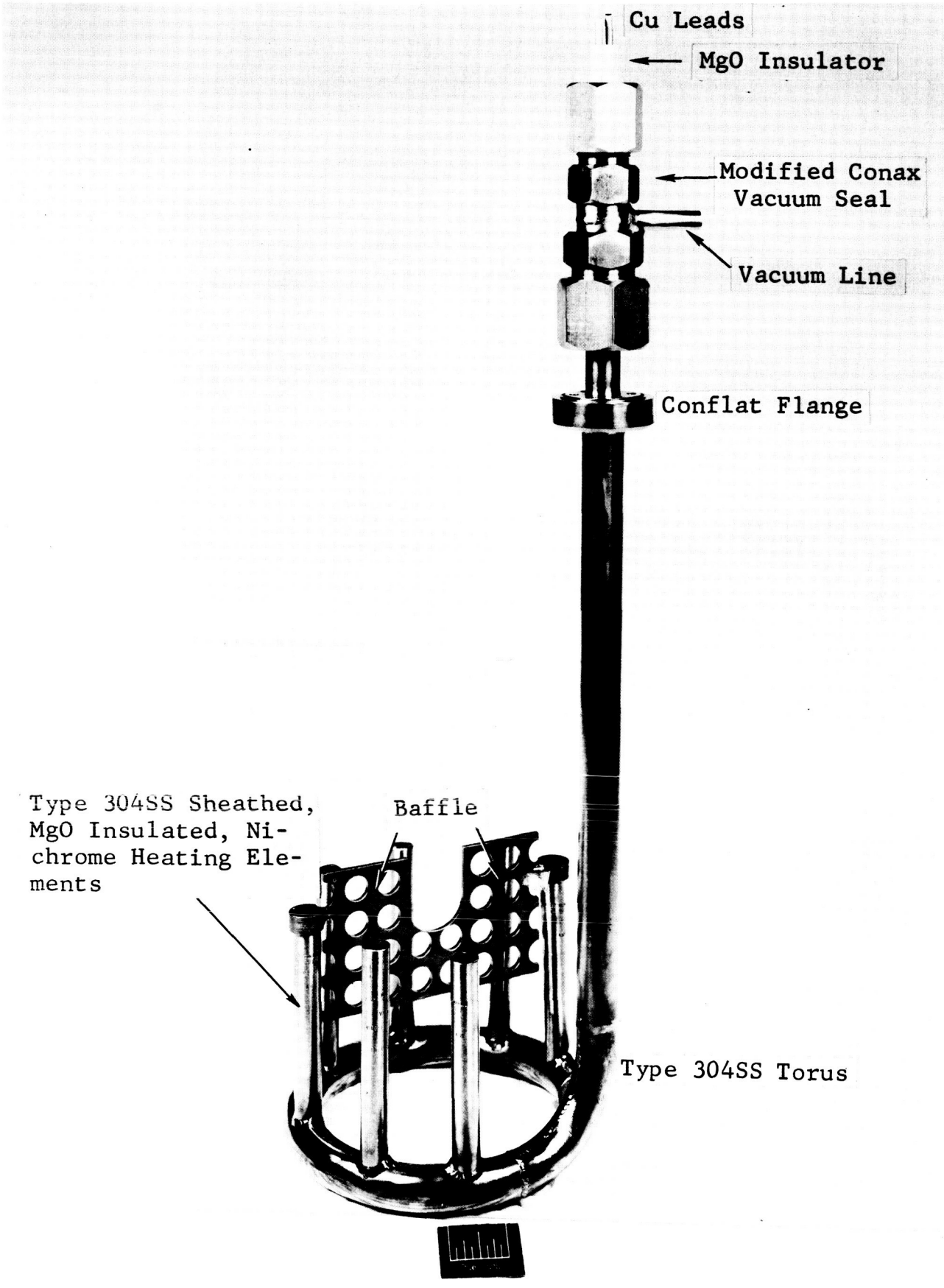

Figure 32. Type 304SS Mock-up of Conductive Immersion Heater Assembly for Potassium Friction and Wear Tester. (C650310114)

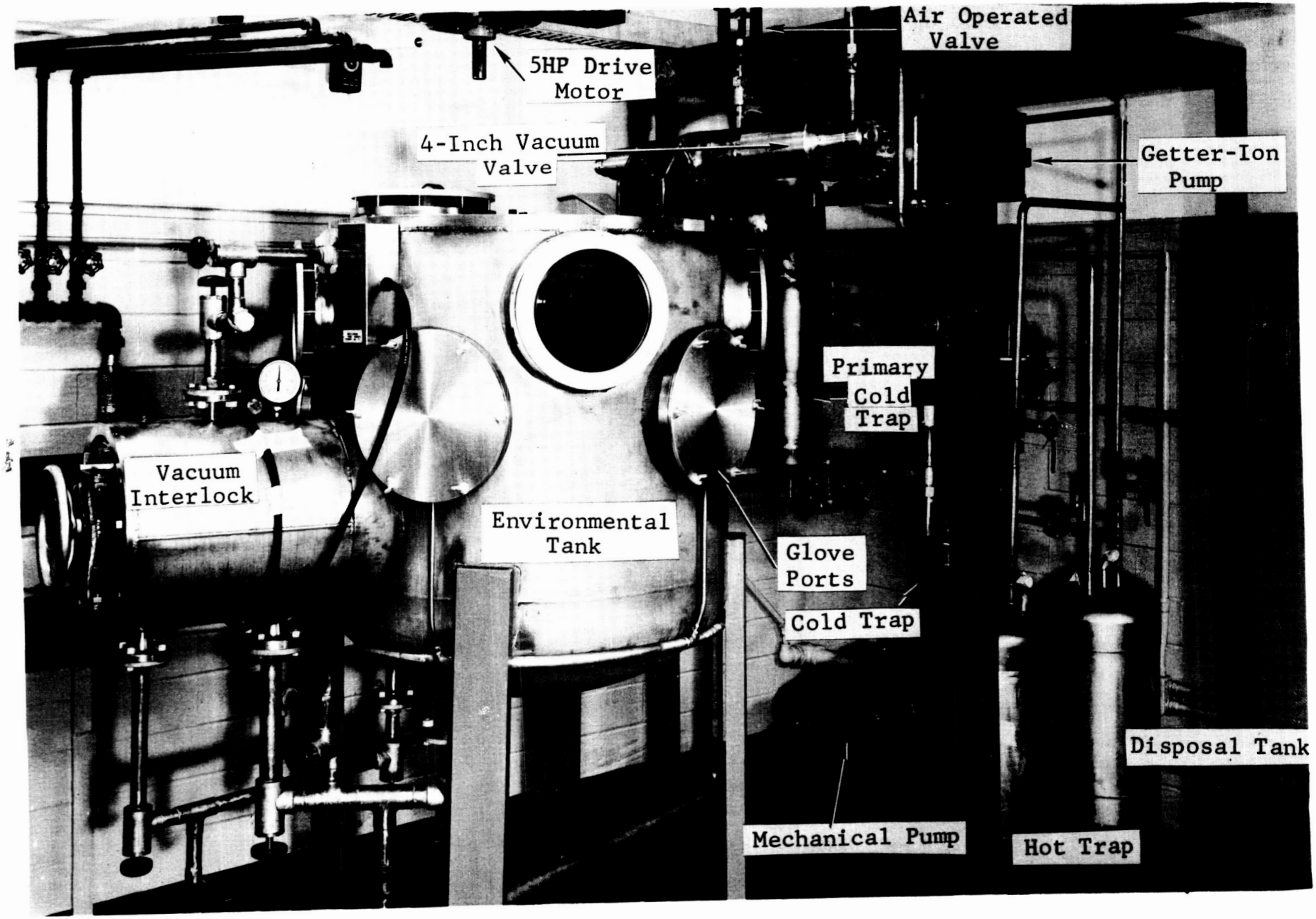

Figure 33. Test Facilities for Liquid Potassium Friction and Wear Tester. (C65030805)

drawing of the overall test facilities showing both the high vacuum and liquid potassium friction and wear testers is presented in Figure 34. The installation and checkout of the Omart liquid level gauge, installation of bakeout heaters and insulation for the hot trap, disposal tank, cold trap and transfer lines, and the installation of a number of valves are the major items that remain to be completed on the liquid potassium friction and wear test facility.

B. Potassium Wetting

The final drawings for the potassium wetting apparatus incorporating all the design revisions have been completed and a complete set of the revised drawings has been sent to the NASA Technical Manager on March 13, 1965. All components for the facility have been received, fabrication of all subassemblies has been completed and final assembly of the apparatus is nearing completion. Initial evacuation and checkout of the system will begin early in the report interim.

A drawing of the main test section including the specimen and potassium handling system is shown in Figure 35. The specimen is identical to those used in the dimensional stability tests, i.e., a rectangular configuration 1.00-inch long x 0.90-inch wide x 0.80-inch thick. The specimen is clamped in position within the chamber on a pedestal which is welded to the lower flange. A thermocouple well, welded to the lower flange and extending up into a blind hole in the specimen, terminates within 1/4 inch of the upper specimen surface. The internal location and close proximity of the thermocouple to the specimen surface will assure accurate temperature measurements.

A condenser plate of Cb-1Zr alloy is mounted directly above the specimen surface and can be cooled by the flow of fluid through the condenser cooling tube. The Cb-1Zr alloy condenser plate is brazed to the Type 316SS cooling tube, using Coast Metal 52 Special, to enhance heat transfer. To evaluate the integrity of the brazed joint, a trial Cb-1Zr alloy/Type 321SS brazed joint was heated eight times to 500°F and quenched in water without failure. The potassium inlet tube is attached to a bakeable, all metal valve by means of a special flange. The valve, in turn, is attached to the potassium reservoir. The inlet tube is so oriented that the stream of potassium vapor from the potassium reservoir impinges and condenses on the cooled condenser plate. The condensed potassium may be melted by flow of a hot fluid through the condenser cooling tube causing a droplet to form at the tip of the condenser plate and subsequently to fall to the surface of the specimen. The droplet may be observed through either of the two sapphire windows in the main test section. Contact angles between the specimen and the potassium drop will be measured with a telemicroscope (Gaertner Model M101AT) equipped with a protactor eyepiece. The relative orientation of the condenser assembly, the specimen mounted assembly with the specimen in position and the potassium inlet tube attached to the valve to the potassium reservoir can be seen in Figure 36.

The system will be evacuated by means of a 25 liter per second triode ion pump (GE Model 22TP202); the pressure will be measured with a Trigger Discharge Gauge (GE Model 22GT214) which is located on the main vacuum manifold. The

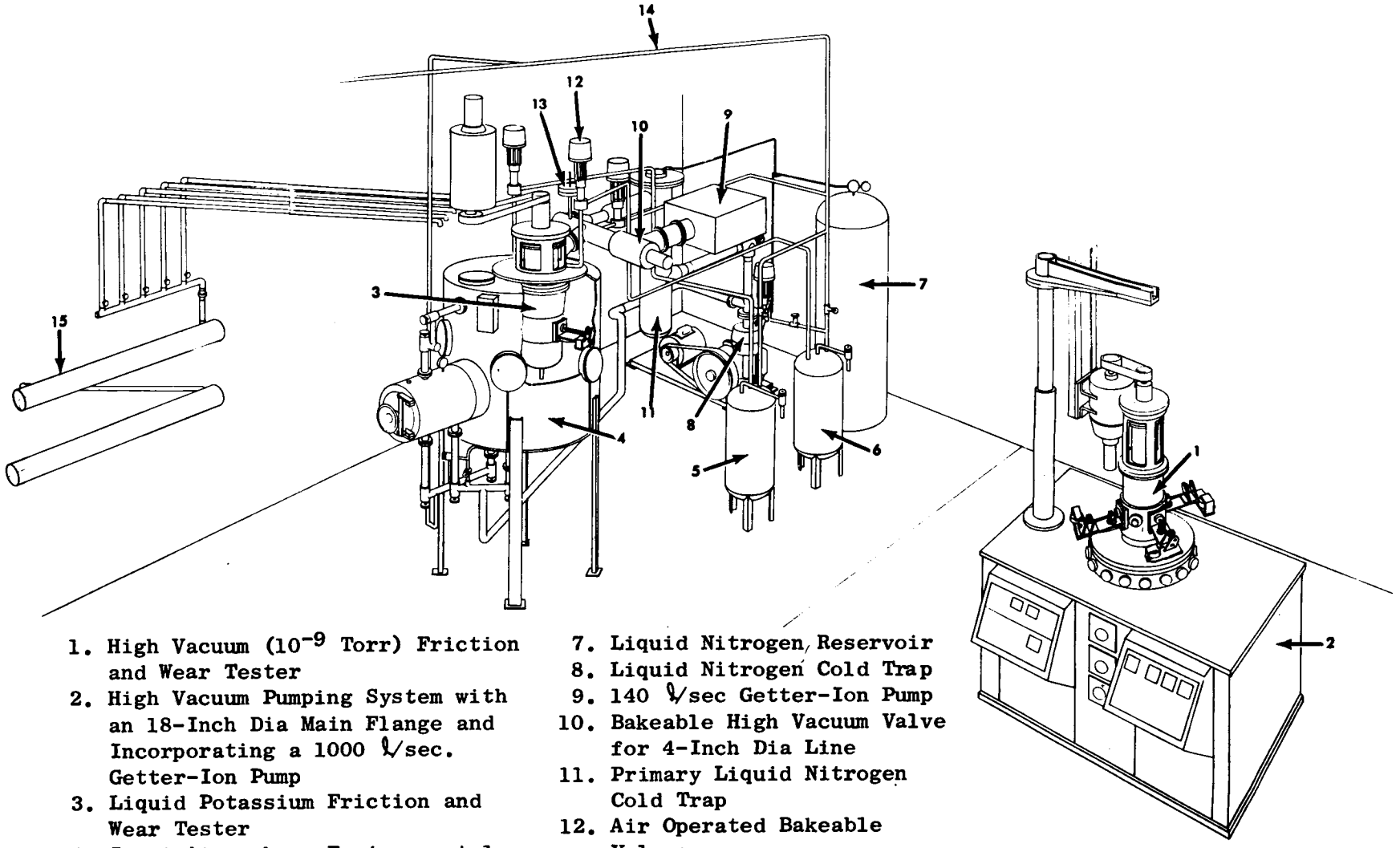

1. High Vacuum (10^{-9} Torr) Friction and Wear Tester
2. High Vacuum Pumping System with an 18-Inch Dia Main Flange and Incorporating a 1000 ℓ/sec. Getter-Ion Pump
3. Liquid Potassium Friction and Wear Tester
4. Inert Atmosphere Environmental Tank with Vacuum Interlock
5. Titanium-Lined, Zirconium-Gettered Type 316SS Hot Trap
6. Type 304SS Disposal Tank
7. Liquid Nitrogen Reservoir
8. Liquid Nitrogen Cold Trap
9. 140 ℓ/sec Getter-Ion Pump
10. Bakeable High Vacuum Valve for 4-Inch Dia Line
11. Primary Liquid Nitrogen Cold Trap
12. Air Operated Bakeable Valves
13. Taylor Pressure Gauge
14. High Purity Argon Line
15. Heating and Cooling Air Lines

Figure 34. Test Facilities for Conducting Friction and Wear Tests in High Vacuum and Liquid Potassium.

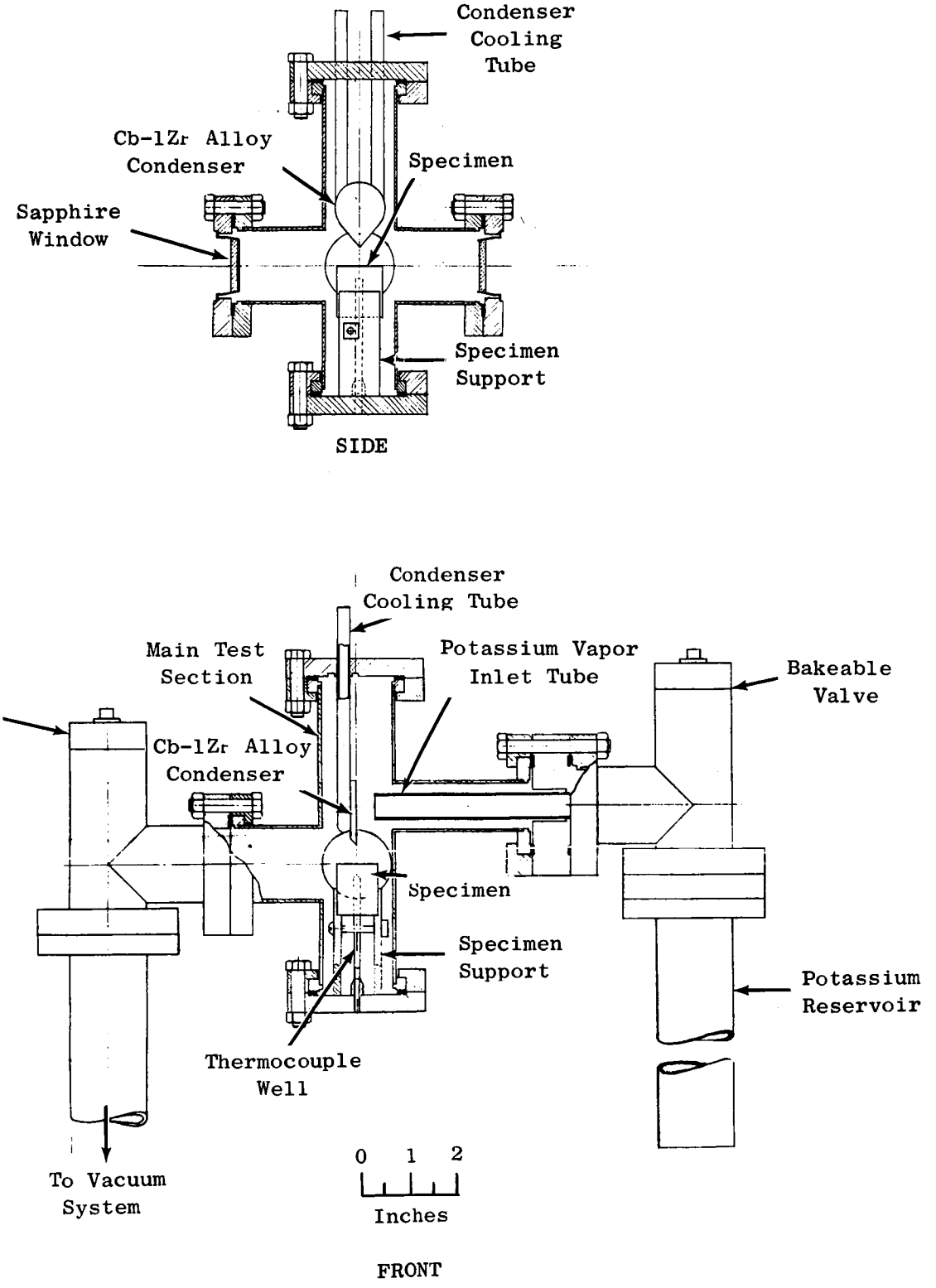

Figure 35. Main Test Section for Sessile Drop Wetting Test Facility.

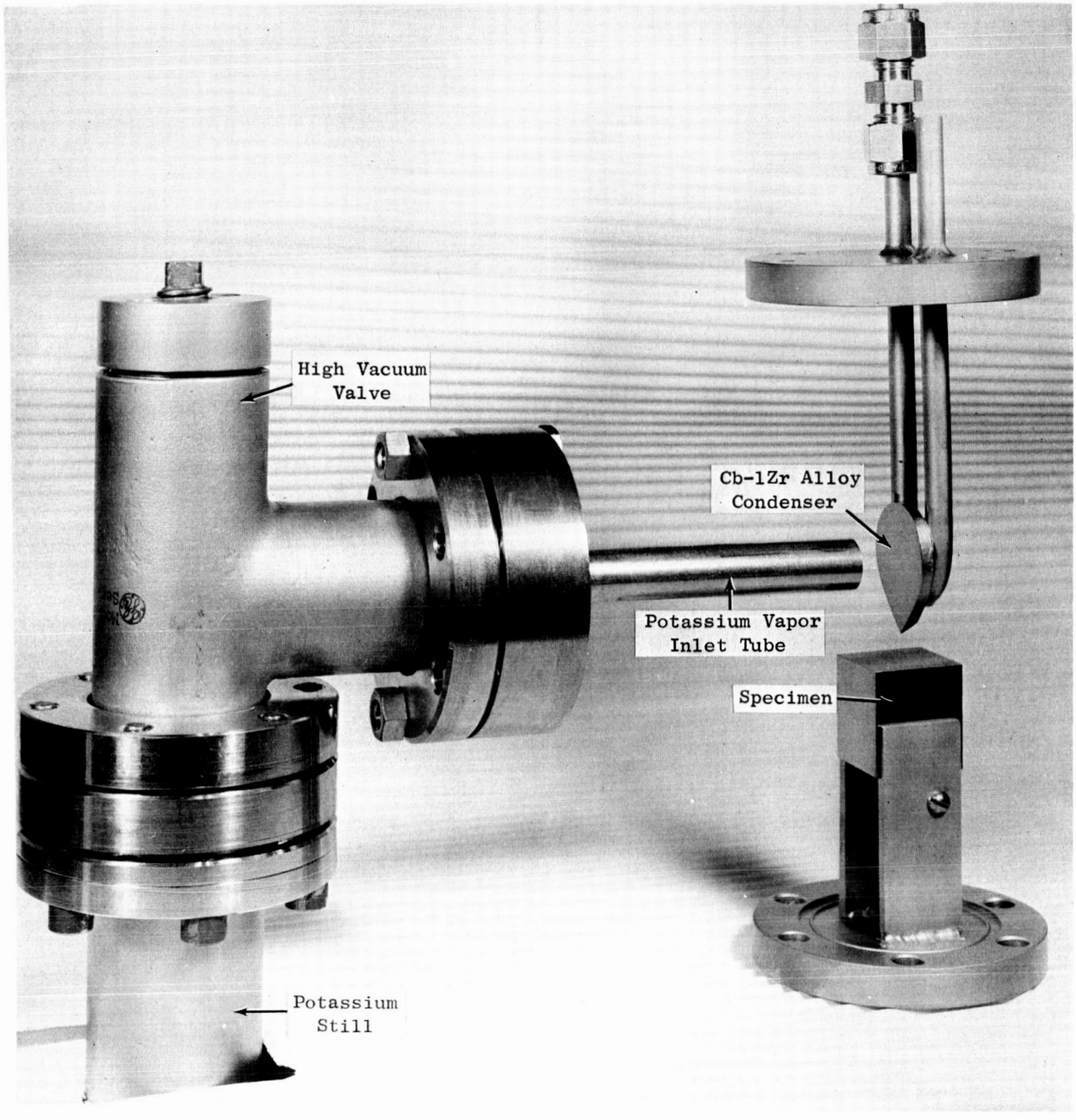

Figure 36. Relative Orientation of Condenser, Specimen and Potassium Inlet Tube Within the Main Test Section of the Sessile Drop Wetting Test Facility. (C65050525)

manifold is isolated from the rough pumping system by a bakeable valve. The rough pumping system consists of a cryogenic molecular sieve sorption pump, a thermocouple gauge and a vacuum release valve. A photograph of the partially assembled apparatus is shown in Figure 37.

The main test section and the two adjacent bakeable valves are enclosed in an oven capable of a maximum temperature of about 800°F. The oven will function as a source of heat both for bakeout purposes and to heat the specimen to the test temperature. Triple-pane windows are provided on each side of the oven opposite the sapphire windows in the test section. A view of the wetting apparatus with the oven and telemicroscope in position is shown in Figure 38.

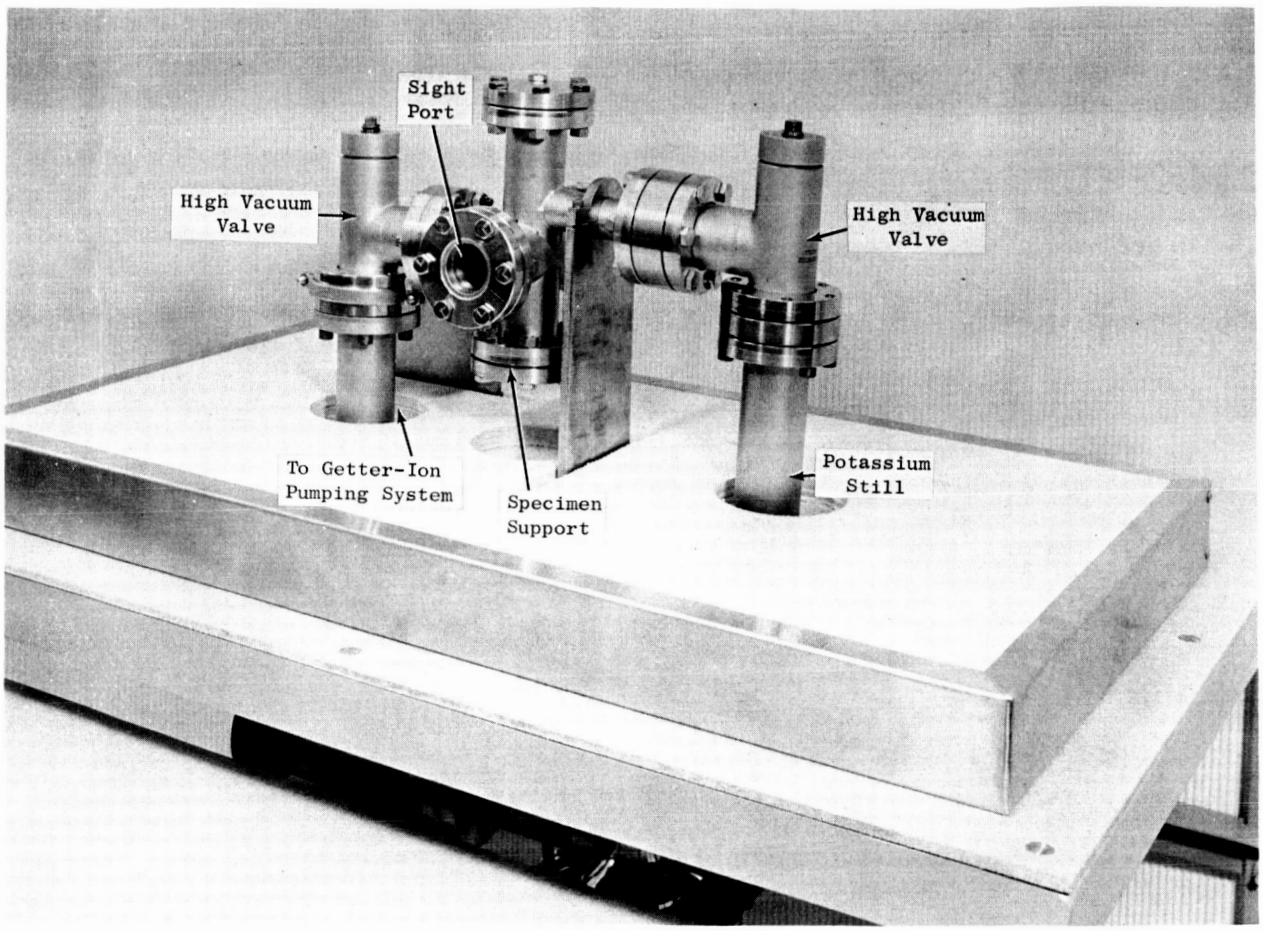

Figure 37. Partially Assembled Sessile Drop Wetting Test Facility. (C65042830)

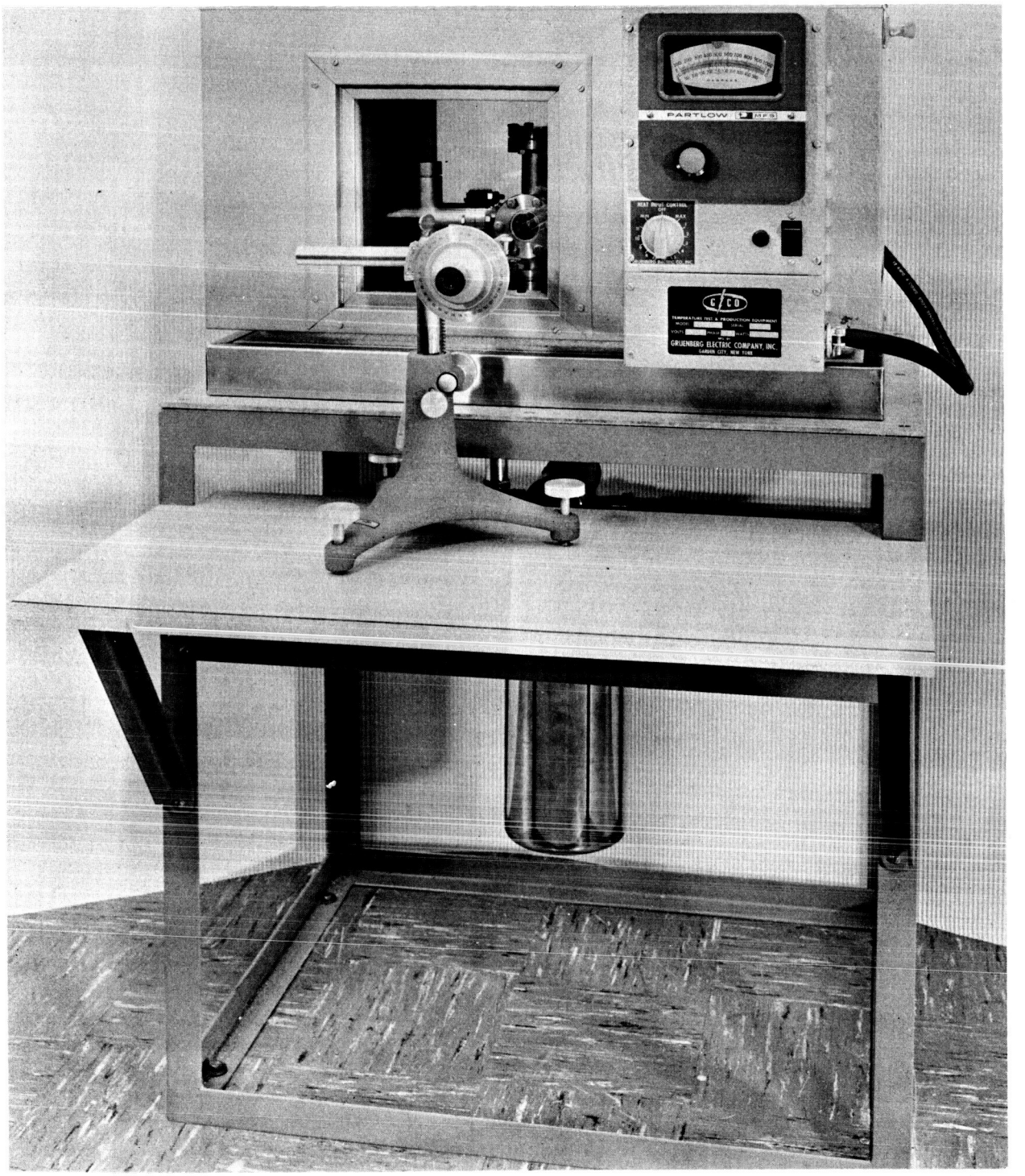

Figure 38. Sessile Drop Wetting Test Facility with Oven in Place. (C65042831)

V. TEST PROGRAM

A. Corrosion

All of the candidate bearing test specimens that were exposed to potassium for 1,000 hours at 1600°F in Cb-1Zr alloy capsules were sectioned, as shown in Figure 39, for metallographic examination and chemical analysis or x-ray diffraction analysis.

The chemical analyses of the Mo-TZM alloy, unalloyed tungsten, and Star J specimens tested at 1600°F for 1,000 hours have been completed and are shown in Table XII. A significant loss of carbon was observed in the Star J specimen located in the liquid region, i.e., 300 ppm. This loss of carbon in the specimen corresponds to a weight loss of 9.1 mg which is in good agreement with the measured weight loss of 9.2 mg. From these data, it is assumed that the weight loss observed in the Star J specimen (MCN 1047-A5) located in the liquid zone can be attributed to the loss in carbon. No significance is attached to the other slight variation in the chemical analyses observed in the specimens. It should be noted that no transport of nitrogen from the Star J specimens was observed as was expected to occur at 1600°F.

The Cb-1Zr alloy containment capsules from the 1600°F test have been sectioned, Figure 40, and a 0.020-inch thick specimen was removed from the ID of the liquid zone sample for oxygen, hydrogen, nitrogen and carbon analyses. The data are presented in Table XIII. With the exception of the capsules containing the Carboloy Grade 907 and 999 specimens, a visual examination of the ID of the capsules after sectioning revealed no changes in appearance. In the case of the former two capsules, a black discoloration was observed in the liquid regions of both capsules, Figures 41 and 42. The black discoloration observed was examined for the possibility of carbon and/or cobalt transfer from the specimens. X-ray fluorescence analyses of the capsule wall in the area in question did not detect the presence of cobalt. However, the capsules which contained the Carboloy 907, Carboloy 999, Grade 7178 and Star J specimens all showed a significant increase in carbon content. The specimens contained in these capsules all contain carbon in the form of WC or, in the case of Star J, as Cr_7C_3 or M_6C. Thermodynamically, these carbides are less stable than CbC and the transfer of carbon to the Cb-1Zr alloy capsule wall is not unexpected.

Atomic bonding in the refractory metal carbides is believed to be metallic in nature and since most of the monocarbides of the refractory metals have a cubic crystal structure and favorable atomic size differences, they generally form a complete series of solid solutions. Additions of other refractory metal monocarbides to WC, then, would tend to affect an increase in thermodynamic stability of the carbide body. This can be observed experimentally from the following data extracted from Table XIII.

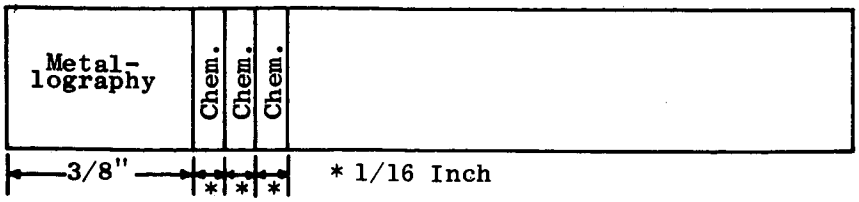

Mo-TZM Alloy and Unalloyed Tungsten

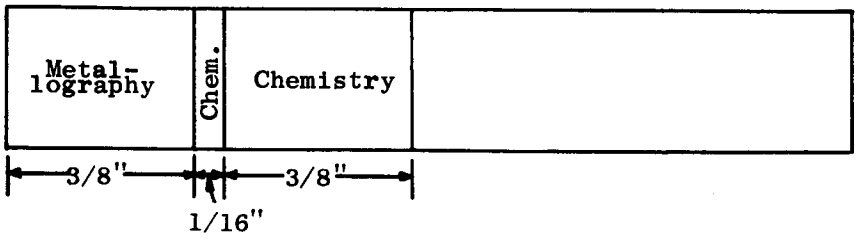

Star J

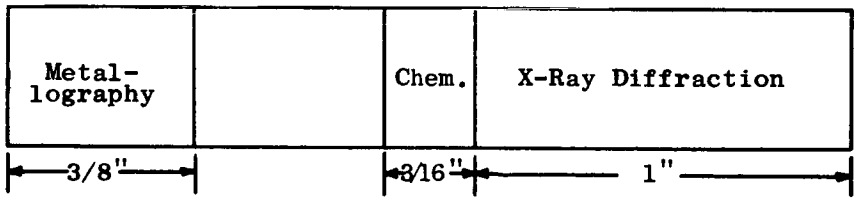

All Remaining Materials

Figure 39. Location of Samples Taken from Candidate Bearing Specimens Tested in Potassium for 1,000 Hours at 1600°F.

TABLE XII. CHEMICAL ANALYSES OF Mo-TZM ALLOY, UNALLOYED TUNGSTEN, AND STAR J SPECIMENS BEFORE AND AFTER EXPOSURE TO POTASSIUM FOR 1,000 HOURS AT 1600°F

Capsule No.	Material	Specimen No.	Specimen Location	Chemical Analyses[1], ppm			
				C	O	N	H
BIC-14	Mo-TZM Alloy	MCN-1037-A3	Liquid Zone	190-220	9-13	4-4	1-1
		MCN-1037-A4	Vapor Zone	220-280	13-27	4-5	1-1
		MCN-1037-A16	As-Received	180-230	9-22	1-5	1-3
BIC-27	Unalloyed Tungsten	MCN-1038-A3	Liquid Zone	20-30	4-12	1-1	1-1
		MCN-1038-A4	Vapor Zone	60-80	14-15	1-1	1-1
		MCN-1038-A16	As-Received	40-70	8-13	2-2	1-1
BIC-40	Star J	MCN-1047-A5	Liquid Zone	2.52-2.54[2]	92-103	757-764	5-5
		MCN-1047-A6	Vapor Zone	2.57-2.58[2]	68-93	720-744	3-5
		MCN-1047-A6	As-Received	2.57-2.58[2]	117-119	727-733	3-4

(1) All Analyses in Duplicate; Gas Analyses by Vacuum Fusion Techniques; Carbon Analyses by Combustion Conductometric.

(2) In Percent.

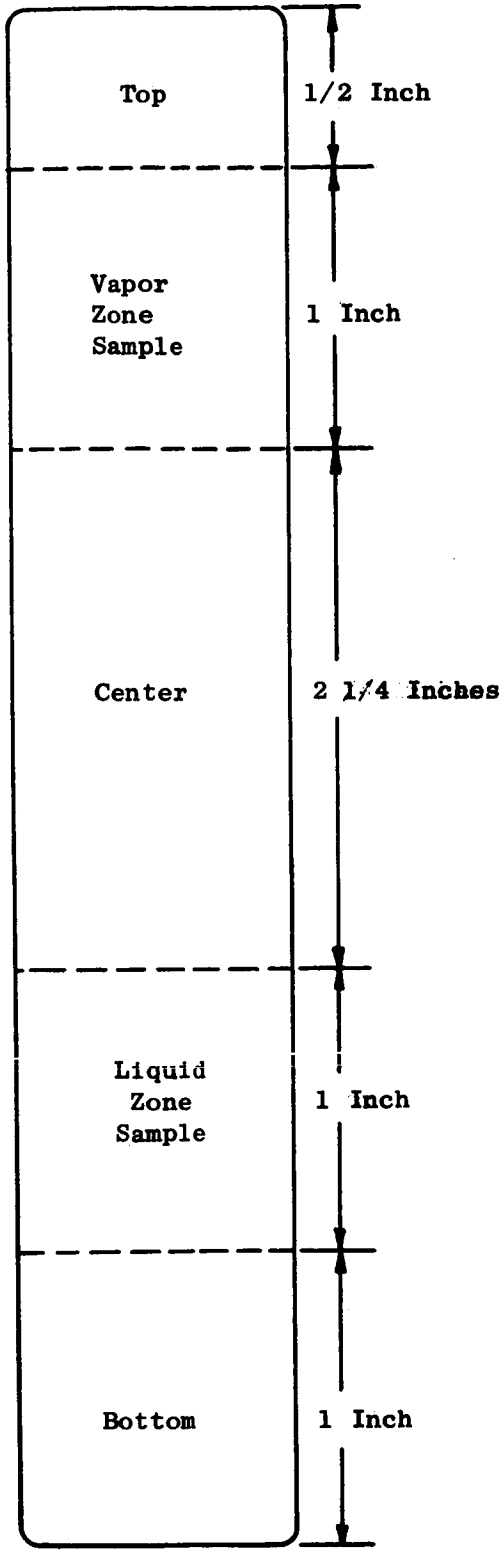

Figure 40. Location of Samples Taken from Cb-1Zr Alloy Containment Capsules Tested for 1,000 Hours at 1600°F.

TABLE XIII. CHEMICAL ANALYSES OF Cb-1Zr ALLOY CAPSULES CONTAINING CANDIDATE JOURNAL BEARING MATERIAL TEST SPECIMENS AND EXPOSED TO POTASSIUM FOR 1,000 HOURS AT 1600°F

Candidate Bearing Material	Capsule No.	Lab No.	Chemical Analyses,[1] ppm C	O	N	H
Carboloy 999	BIC-10	1777	390/390	317/328	108/108	7/8
Carboloy 907	BIC-9	1776	190/200	284/309	81/81	8/4
Grade 7178	BIC-34	1783	110/50/130	275/268	74/63	8/5
TiC+10%Cb	BIC-31	1782	10/80	342/350	100/105	2/5
TiC+10%Mo	BIC-47	1788	40/40	315/318	59/58	1/<1
TiC+5%W	BIC-46	1787	30/20	253/250	65/55	1/1
TiC	BIC-37	1784	60/40	286/321	86/89	3/3
K601	BIC-43	1786	50/20	263/262	81/63	2/1
Lucalox	BIC-20	1779	10/10	351/288	87/70	11/6
Zircoa 1027	BIC-23	1780	50/50	322/332	91/94	<1/3
Tungsten	BIC-27	1781	60/20	262/261	78/95	2/3
Mo-TZM	BIC-14	1778	50/60	247/282	97/100	10/5
Star J	BIC-40	1785	290/240	282/282	86/92	2/2
TiB_2	BIC-48	1789	60/10	359/320	94/83	6/<1
Control (1005-7)	--	1790	50/30	275/300	77/77	1/<1
Control (1005-4)	--	1791	50/70	370/394	90/89	6/1
As-Received (Bulk[2])	--	--	40	184	95	1

[1] Analyses of Inner 0.020-Inch Thick Layer of Cb-1Zr Alloy Capsule in Liquid Zone. Gas Analyses by Vacuum Fusion Techniques; Carbon Analyses by Combustion Conductometric.

[2] 0.080-Inch Thick Wall.

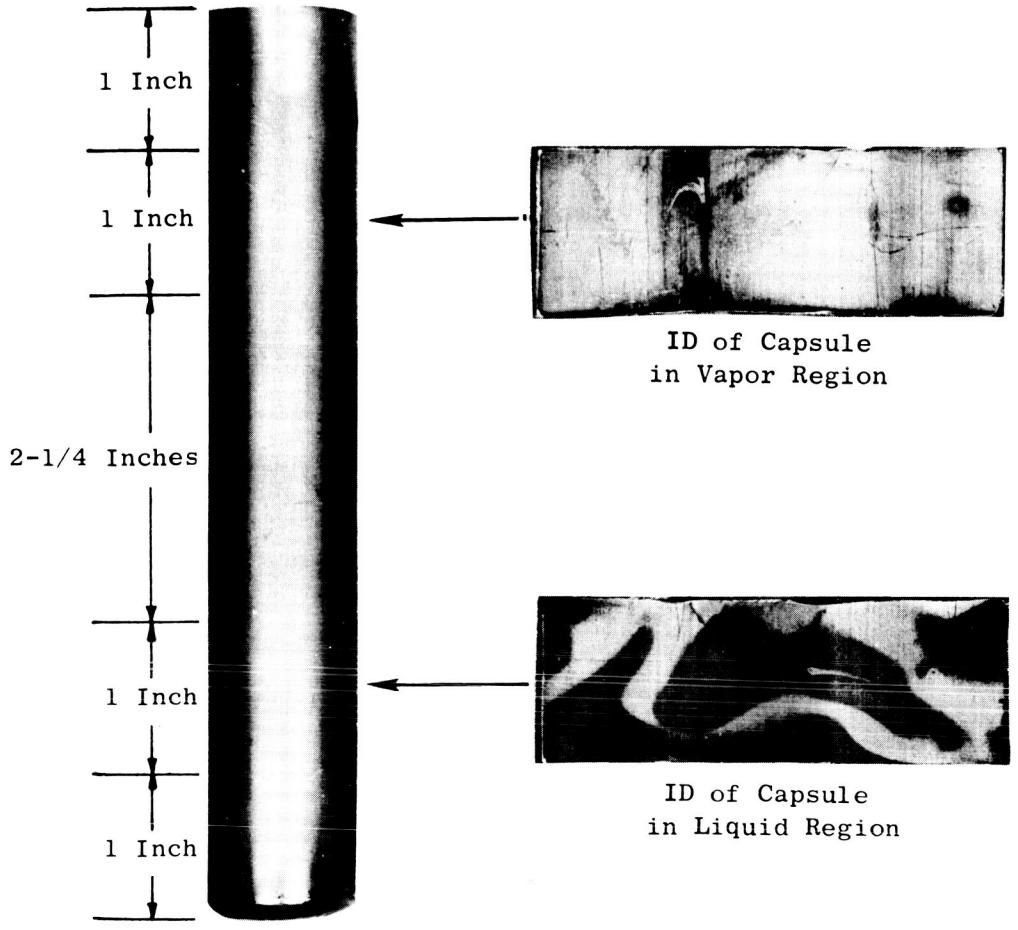

Figure 41. Sections Removed from Cb-1Zr Alloy Isothermal Corrosion Capsule Which Contained Carboloy 907 Test Specimens. The Capsule was Exposed to Potassium for 1,000 Hours at 1600°F.

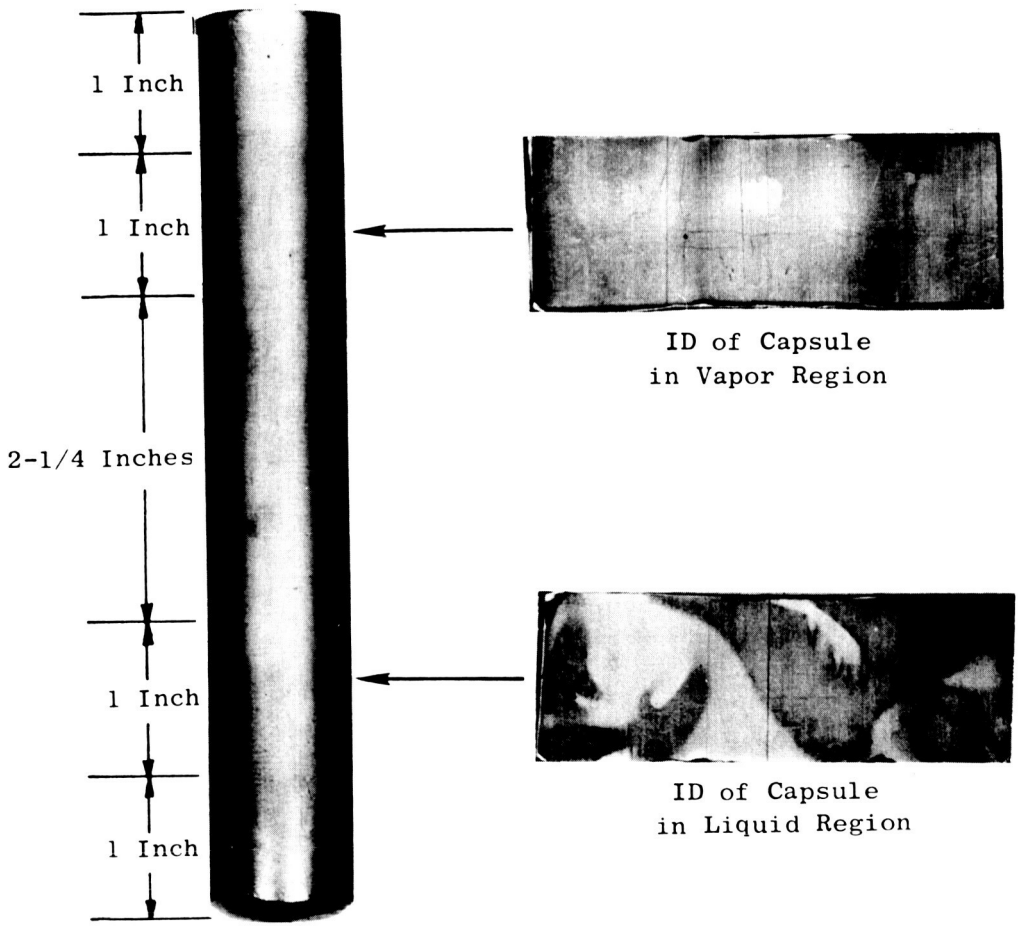

Figure 42. Sections Removed from Cb-1Zr Alloy Isothermal Corrosion Capsule Which Contained Carboloy 999 Test Specimens. The Capsule was Exposed to Potassium for 1,000 Hours at 1600°F.

Material	Composition	Carbon Analyses[1] of Inner 0.020 Inch Layer of Cb-1Zr Alloy Wall After 1,000-Hr. Exposure to Potassium at 1600°F, ppm
Carboloy 999	97%WC, 3%Co	390
Carboloy 907	74%WC, 20%Ta, 6%Co	195
Grade 7178	---	120
K601	84.5%W, 10%Ta, 5.5%C	35
Cb-1Zr Alloy Control	---	50

[1] Average of Two Analyses

The excellent stability of the complex carbide in K601 is attributed to the proprietary form in which the powder additions are added to the powder blend prior to compaction and vacuum sintering.

No significant changes in oxygen, nitrogen or hydrogen were observed in the inner surface of the Cb-1Zr alloy capsule, attesting to the high purity of the potassium.

Metallographic preparation of the test specimens tested at 1600°F has been completed and evaluation is underway.

Twenty-four isothermal corrosion capsules have been opened under argon, the potassium drained and the specimens cleaned by vacuum distillation in the manner described in Quarterly Progress Report No. 7.[2] Twelve of the capsules had been tested for 1,000 hours at 1200°F and twelve had been tested for 1,000 hours at 800°F. The capsules contained the following specimens in the liquid and vapor regions:

Star J	TiC+10%Cb
Unalloyed Tungsten	TiC
Mo-TZM	Carboloy 999
Zircoa 1027	Carboloy 907
Lucalox	Grade 7178
TiC+5%W	K601

The weight and dimensional measurements of the specimens tested at 1200°F were obtained and are reported in Table XIV along with the pre-test data and the observed changes. The data were evaluated in the same manner as were the test specimens tested at 1600°F [2]. Major differences in the results of the 1200°F test in comparison with the results of the 1600°F test can be summarized as follows:

1. A slight growth was observed in the Carboloy 999 and Carboloy 907 specimens tested at 1200°F in contrast to a negative change in dimensions for the specimens tested at 1600°F. Although a weight loss was observed for all the Carboloy specimens, the changes in weight were significantly less than those reported for the specimens tested at 1600°F.

2. Significantly smaller increases in dimensions and weight were observed for the Zircoa 1027 material.

3. No surface reactions occurred between the Lucalox specimens and potassium as was the case for the specimens tested at 1600°F. Also negligible changes in dimensions and weight were observed.

4. Positive weight changes were recorded for Star J and K601 in contrast to negative changes of similar specimens tested at 1600°F.

5. From the weight change data, it is believed that little, if any, carbon was transferred from Carboloy 999, Carboloy 907, and Star J specimens.

All other changes in dimensions and weights of the test specimens tested at 1200°F were the same or less in magnitude as observed for those specimens tested at 1600°F. Again, Mo-TZM, tungsten, TiC and the refractory metal bonded TiC specimens proved to have excellent stability in potassium.

The specimens tested at 1200°F have been sectioned for metallographic examination in the same manner as were the specimens tested at 1600°F and metallographic preparation is underway.

B. Hot Hardness

The unalloyed tungsten specimen, MCN 1038-D-1, that had exhibited a deviation in hardness values between the heating and cooling cycles in the initial hot hardness test[2] was given a recrystallization treatment of two hours at 2200°F in a vacuum of 10^{-6} torr. Initially, it was thought that the spread in hardness values between the heating and cooling curves might be due to differences in homogeniety in the amount of strain hardening imparted to the 0.750 inch diameter tungsten rod during processing and that the recrystallization anneal would minimize differences in hardness throughout the cross section of the specimen. Subsequently, the heat treated specimen was subjected to the

Table XIV. DIMENSIONAL AND WEIGHT CHANGES OF SPECIMENS EXPOSED IN POTASSIUM FOR 1,000 HOURS AT 1200°F

Specimen Identity			Specimen Length, Inches				Specimen Width$_1$, Inches				Specimen Width$_2$, Inches				Specimen Weight in Grams			
Material	MCN No.	Specimen Location	Before Test	After Test	Dimensional Change Inches x 10^{-3}	Dimensional Change Percent	Before Test	After Test	Dimensional Change Inches x 10^{-3}	Dimensional Change Percent	Before Test	After Test	Dimensional Change Inches x 10^{-3}	Dimensional Change Percent	Before Test	After Test	Weight Change Milligrams	Weight Change Mg/Cm^2
Carboloy Grade 999 Capsule # BIC-12	1035-A5	Liquid	2.00266	2.00294	+0.28	+0.014	0.25186	0.25198	+0.12	+0.048	0.25208	0.25209	+0.01	+0.004	31.6222	31.6214	-0.8	-0.058
	1035-A6	Vapor	2.00270	2.00300	+0.30	+0.015	0.25146	0.25149	+0.03	+0.012	0.25139	0.25145	+0.06	+0.024	31.5302	31.5304	+0.2	+0.014
Carboloy Grade 907 Capsule # BIC-7	1036-A1	Liquid	2.00268	2.00326	+0.58	+0.029	0.25191	0.25195	+0.04	+0.016	0.25164	0.25167	+0.03	+0.012	30.4888	30.4875	-1.3	-0.094
	1036-A2	Vapor	2.00251	2.00320	+0.69	+0.034	0.25168	0.25173	+0.05	+0.020	0.25184	0.25188	+0.04	+0.016	30.4945	30.4943	-0.2	-0.014
Mo-TZM[1] Capsule # BIC-15	1037-A5	Liquid	1.99998	1.99985	-0.13	-0.007	0.24782	0.24766	-0.16	-0.065	0.24782	0.24780	-0.02	-0.008	20.3882	20.3879	-0.3	-0.021
	1037-A6	Vapor	2.00077	2.00067	-0.10	-0.005	0.24937	0.25928	-0.09	-0.036	0.24817	0.24817	0.00	0.000	20.5550	20.5549	-0.1	-0.007
Unalloyed Tungsten[2] Capsule # BIC-26	1038-A7	Liquid	2.00088	2.00091	+0.03	+0.002	0.25061	0.25076	+0.15	+0.060	0.25008	0.25004	-0.04	-0.016	39.5088	39.5090	+0.2	+0.014
	1038-A8	Vapor	2.00153	2.00119	-0.34	-0.017	0.25007	0.25009	+0.02	+0.008	0.25047	0.25050	+0.03	+0.012	39.4991	39.4989	-0.2	-0.014
Lucalox Capsule # BIC-28	1039-A7	Liquid	2.00323	2.00328	+0.05	+0.003	0.25007	0.25011	+0.04	+0.016	0.25018	0.25023	+0.05	+0.020	8.1509	8.1509	0.0	0.000
	1039-A8	Vapor	2.00318	2.00321	+0.03	+0.001	0.25010	0.25011	+0.01	+0.004	0.25019	0.25019	0.00	0.000	8.1456	8.1461	+0.5	+0.036
Zircoa 1027 Capsule # BIC-24	1040-A5	Liquid	1.99881	1.99944	+0.63	+0.032	0.25105	0.25113	+0.08	+0.032	0.25218	0.25227	+0.09	+0.040	11.8687	11.8782	+9.5	+0.693
	1040-A6	Vapor	1.99909	2.00008	+0.99	+0.050	0.24901	0.24925	+0.24	+0.096	0.25189	0.25239	+0.50	+0.197	11.7665	11.7789	+12.4	+0.904
K601 Capsule # BIC-42	1041-A3	Liquid	2.00157	2.00168	+0.11	+0.006	0.25255	0.25272	+0.22	+0.087	0.25171	0.25195	+0.24	+0.096	32.9253	32.9255	+0.2	+0.014
	1041-A4	Vapor	2.00147	2.00155	+0.08	+0.004	0.25161	0.25184	+0.23	+0.092	0.25232	0.25253	+0.21	+0.083	32.9125	32.9129	+0.4	+0.029
TiC Capsule # BIC-36	1042-A3	Liquid	2.00084	2.00080	-0.04	-0.002	0.25022	0.25020	-0.02	-0.008	0.25029	0.25027	-0.02	-0.008	10.1589	10.1584	-0.5	-0.036
	1042-A4	Vapor	2.00076	2.00086	+0.10	+0.005	0.25035	0.25038	+0.03	+0.012	0.25050	0.25052	+0.02	+0.008	10.1639	10.1635	-0.4	-0.029
TiC+5%W Capsule # BIC-45	1043-A3	Liquid	2.00190	2.00207	+0.17	+0.008	0.25203	0.25214	+0.06	+0.024	0.25168	0.25184	+0.16	+0.064	10.6868	10.6858	-1.0	-0.072
	1043-A4	Vapor	2.00118	2.00131	+0.13	+0.006	0.25197	0.25204	+0.07	+0.028	0.25173	0.25190	+0.17	+0.063	10.6758	10.6750	-0.8	-0.058
TiC+10%Cb Capsule # BIC-30	1045-A3	Liquid	2.00033	2.00033	0.00	0.000	0.25216	0.25219	+0.03	+0.012	0.25240	0.25241	+0.01	+0.004	10.8080	10.8072	-0.8	-0.058
	1045-A4	Vapor	2.00041	2.00039	-0.02	-0.001	0.25223	0.25220	-0.03	-0.012	0.25154	0.25152	-0.02	-0.008	10.7921	10.7912	-0.9	-0.065
Grade 7178 Capsule # BIC-33	1046-A3	Liquid	2.00279	2.00280	+0.01	+0.001	0.25102	0.25117	+0.15	+0.060	0.24972	0.24992	+0.20	+0.080	29.4987	29.4978	-0.9	-0.065
	1046-A4	Vapor	2.00274	2.00294	+0.20	+0.010	0.25138	0.25159	+0.21	+0.084	0.25153	0.25173	+0.20	+0.080	29.6736	29.6729	-0.7	-0.051
Star J[3] Capsule # BIC-39	1047-A3	Liquid	2.00118	2.00093	-0.75	-0.037	0.25221	0.25235	+0.14	+0.056	0.25206	0.25222	+0.16	+0.064	18.1816	18.1829	+1.3	+0.094
	1047-A4	Vapor	2.00135	2.00121	-0.14	-0.007	0.25219	0.25237	+0.18	+0.071	0.25208	0.25224	+0.16	+0.064	18.1845	18.1846	+0.1	+0.007

[1]Stress Relieved 1/2 Hour at 2250°F.
[2]Stress Relieved 1 Hour at 2000°F.
[3]As Cast.

hot hardness test cycle and the resultant data, presented in Table XV and Figure 43, showed a spread in hardness, i.e., 75 Kg/mm^2 at approximately 600°F, between the heating and cooling cycles that was similar to the data obtained in the initial test on the stress-relieved specimen, i.e., 120 Kg/mm^2 at approximately 400°F. A room temperature hardness traverse from the edge to the center of the samples after the recrystallization treatment indicated the hardness to be within a range of 378 to 444 Kg/mm^2. Although the spread in hardness values measured in the room temperature traverse also was quite high, i.e., 66 Kg/mm^2, the fact that the cooling curve consistently was lower than the heating curve was disconcerting.

Since the specimen temperature is measured by a thermocouple located on the bottom surface opposite the surface where the impressions are made, a check test was conducted to determine whether the deviation in hardness between the heating and cooling cycles was due to a possible temperature differential between the two surfaces. A 0.020-inch diameter hole was drilled into a TiC specimen parallel to and approximately 0.032 inch below the top surface. A Pt vs Pt+10%Rh thermocouple (0.005-inch diameter wires) was inserted into the hole and the specimen was subjected to the typical hot hardness heating and cooling cycle. The data, presented in Table XVI, show that the top surface temperature was consistently higher during the heating cycle (maximum difference + 38°F at 600°F) and lower during the cooling cycle (maximum difference -47°F at approximately 1000°F) and suggest that if a deviation in hardness does exist, the hardness obtained upon cooling should be higher than the hardness obtained on heating rather than lower as was obtained with the unalloyed tungsten specimen. It is suggested that the interactions between one or more interstitial element(s) and dislocations in the tungsten at the lower temperatures are responsible for the hysteresis effect observed in the heating and cooling curves of the hardness data. Conceivably, interstitial elements locked at dislocation sites at the lower temperatures are free to move at the higher test temperatures and upon cooling reprecipitate at the dislocation sites. Hysteresis in this process could lead to the observed hardness behavior.

The initial hot hardness data presented for 10 of the 14 candidate materials in quarterly report No. 7[2] showed a considerable amount of general scatter, which is attributed, at least in part, to the light 100-gram load employed in those tests. This particular load had been selected, based on prior experience, to minimize the possibility of cracks developing around the impressions and still realize an impression of sufficient size to facilitate its measurement. However, in many of the materials tested, the extremely high hardness or the non-metallic matte-like surface finish (Lucalox, TiB_2) made accurate measurements quite difficult. Subsequently, a decision was made to increase the test load to 150 grams and test a second specimen of each of the 14 materials. These data are presented in Tables XIX thru XXXIV and Figures 44 thru 59.

To establish the effect of the 150-gram load on hardness values in comparison to values obtained with a 100-gram load, a room temperature hardness traverse was carried out on one of the candidate materials (the recrystallized tungsten specimen, MCN 1038-D-1). The data are shown in Table XVII, and it

TABLE XV. HOT HARDNESS DATA FOR UNALLOYED ARC CAST TUNGSTEN

Specimen Identity - MCN 1038-D-1

Specimen Condition - Recrystallized 2200°F/2 Hours

Test No./Run No. 1/4

Date - December 18, 1964

Indenter - 136° Diamond Pyramid (Vickers)

Load - 100 Grams

Holding Time - 15 Seconds

Time Minutes	Vacuum Torr	Temp. °F	Hardness Kg/mm^2
-	--	RT	396(1)
0	8.0×10^{-6}	RT	435(2)
5	1.0×10^{-5}	120	453
14	2.5×10^{-5}	206	421
24	6.0×10^{-5}	314	324
34	9.0×10^{-5}	429	234
43	8.5×10^{-5}	521	243
54	6.2×10^{-5}	599	234
68	3.0×10^{-5}	703	214
83	2.2×10^{-5}	822	Sticking-Overload
93	1.6×10^{-5}	983	
120	1.4×10^{-5}	1163	
126	1.4×10^{-5}	1218	170
133	1.2×10^{-5}	1384	153
159	1.2×10^{-5}	1484	152
182	2.6×10^{-5}	1647	157
185	2.0×10^{-5}	1663	144
	Power Off		
193	2.0×10^{-5}	1632	156
203	9.5×10^{-6}	1232	153
220	7.0×10^{-6}	1000	160
268	4.0×10^{-6}	607	160
295	3.0×10^{-6}	505	195
335	2.0×10^{-6}	397	231

TABLE XV. (Cont'd)

(1) Room Temperature Hardness of the Specimen on a Kentron Tester Using a Vickers Diamond Pyramid, a 100-Gram Load and a 15-Second Hold.

	396 Kg/mm^2
	396 Kg/mm^2
	396 Kg/mm^2
Average	396 Kg/mm^2

(2) Room Temperature Hardness of the Specimen on the Hot Hardness Tester Using a Vickers Diamond Pyramid, a 100-Gram Load and a 15-Second Hold.

	431 Kg/mm^2
	426 Kg/mm^2
	442 Kg/mm^2
	442 Kg/mm^2
Average	435 Kg/mm^2

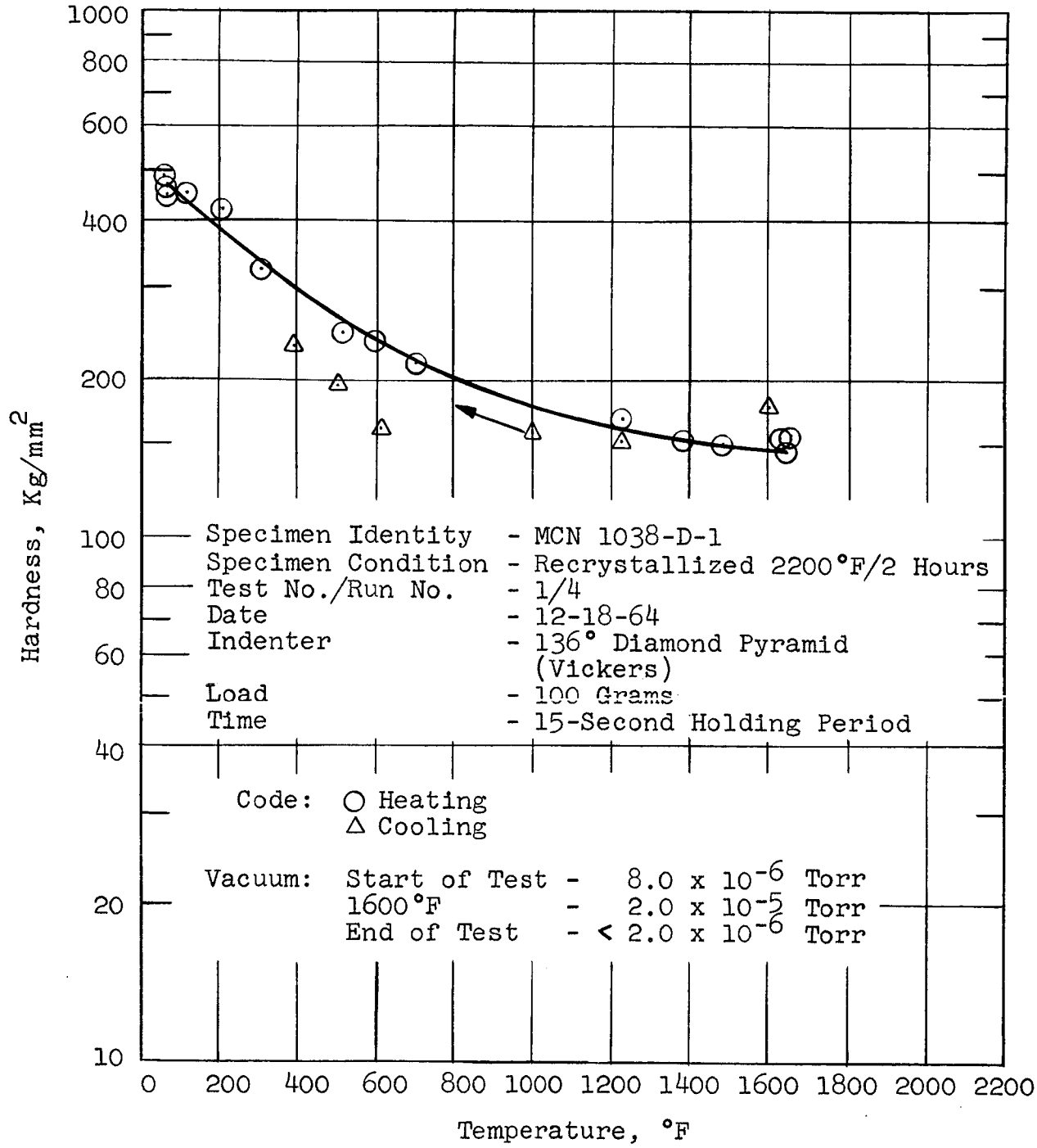

Figure 43. Hardness of Unalloyed Arc Cast Tungsten as a Function of Temperature.

TABLE XVI. TEMPERATURE DIFFERENTIAL BETWEEN THE TOP AND BOTTOM SURFACES OF A HOT HARDNESS SPECIMEN

Material: TiC

Specimen Identity: MCN 1042-D-2

Date: March 2, 1965

Time Minutes	Vacuum Torr	Temperature of Bottom Surface T.C. 1, °F(1)	Temperature of Top Surface T.C. 2, °F(2)	Temperature Difference (T.C. 2 - T.C. 1) °F
0	1.5×10^{-5}	77	78	+ 1
6	2.0×10^{-5}	129	139	+10
16	5.0×10^{-4}	219	241	+22
27	9.0×10^{-5}	363	380	+17
35	1.0×10^{-4}	460	474	+14
41	1.2×10^{-4}	530	555	+25
50	1.2×10^{-4}	601	639	+38
62	7.6×10^{-5}	682	719	+37
73	6.0×10^{-5}	797	818	+21
82	6.0×10^{-5}	890	912	+22
93	5.5×10^{-5}	945	972	+27
100	6.0×10^{-5}	1044	1069	+25
114	5.5×10^{-5}	1194	1202	+ 8
127	4.6×10^{-5}	1289	1293	+ 4
137	4.6×10^{-5}	1357	1355	- 2
153	5.0×10^{-5}	1449	1453	+ 4
174	7.0×10^{-5}	1605	1597	- 8
186	---	1613	1605	- 8
190	6.8×10^{-5}	1628	1621	- 7
200		Power Off		
205	3.2×10^{-5}	1374	1337	-37
209	3.0×10^{-5}	1237	1210	-27
214	2.4×10^{-5}	1124	1093	-31
222	2.0×10^{-5}	1017	970	-47
242	1.6×10^{-5}	784	764	-20
264	1.4×10^{-5}	642	625	-17
280	1.4×10^{-5}	569	548	-21
295	1.2×10^{-5}	518	496	-22
310	1.2×10^{-5}	471	448	-23
32	1.0×10^{-5}	398	375	-23

TABLE XVI. (Cont'd)

(1) Control Thermocouple (Pt vs Pt+10%Rh) Used in all Hot Hardness Tests. Embedded in Anvil Upon Which Hot Hardness Specimen is Seated. Bead of Thermocouple is in Contact with Bottom of Specimen.

(2) Test Thermocouple (Pt vs Pt+10%Rh) Placed Inside a 0.020-Inch Diameter Hole Drilled Parallel to and Approximately 0.032 Inch Below the Top Surface.

TABLE XVII. ROOM TEMPERATURE HARDNESS TRAVERSE OF UNALLOYED ARC CAST TUNGSTEN

Specimen Identity - MCN 1038-D-1

Specimen Condition - Recrystallized 2200°F/2 Hours

Test No./Run No. - 1/7

Date - March 18, 1965

Indenter - 136° Diamond Pyramid - #2006 (Vickers)

Load - 150 Grams

Holding Time - 15 Seconds

Location of Impression	Hardness Kg/mm^2
0.042 inch from edge	420
0.047 inch from edge	420
0.052 inch from edge	408
0.062 inch from edge	412
0.072 inch from edge	400
0.087 inch from edge	408
0.102 inch from edge	400
0.122 inch from edge	408
0.152 inch from edge	416
0.177 inch from edge	424
0.202 inch from edge	408
0.227 inch from edge	420
0.232 inch from edge	408
0.237 inch from edge	421
Average	411
Spread	400 - 424

is apparent that the 150-gram load is effective in reducing the scatter in the hardness data over that obtained with the 100-gram load (400-424 Kg/mm^2 vs 378-444 Kg/mm^2).

Prior to initiation of the second series of tests, a new Vickers indentor (#2006) was mounted in the hot hardness tester and a room temperature check test was carried out on the recrystallized tungsten specimen to establish any variation in hardness values between a Kentron tester and the hot hardness tester. These data are presented in Table XVIII and, as can be seen, indicated that the hot hardness tester produced readings approximately 5% higher than the measured values produced by the Kentron instrument at the same location on the specimen.

The initial hot hardness test employing the heavier load was performed on the recrystallized tungsten specimen MCN 1038-D-1. The data shown in Table XIX and Figure 44 indicate slightly lower hardness values are obtained at the higher temperatures on the heating cycle with the 150-gram load than obtained with the 100-gram load. Although difficulty with the vacuum system during the cooling cycle interrupted the taking of hardness impressions, the few points obtained on the cooling cycle at the lower temperatures (200° to 400°F) again were lower than the values obtained on the heating cycle similar to that observed with the 100-gram load and further substantiating the existance of a hysteresis effect. The hot hardness data for the Mo-TZM alloy, Table XX and Figure 45, that were obtained with the 150 gram load also were more uniform and exhibited slightly lower hardness values at the higher test temperatures.

Two additional tests were conducted with the Mo-TZM alloy, utilizing another specimen, MCN 1037-D-1, and a 150-gram load, to check the reproducibility of the hot hardness tester. These tests were conducted at two week intervals and as can be seen from the data in Tables XXI and XXII and Figures 46 and 47, the agreement in the hardness data for all three tests is excellent indicating good reproducibility for the instrument.

The hot hardness curve for the TiC material, Table XXIII and Figure 48, was quite similar to the first curve. However, minute cracking was observed around the majority of the room temperature hardness impressions.

The hardness data for the Carboloy Grades 907 and 999, Tables XXIV and XXV and Figures 49 and 50, are more uniform for both the heating and cooling cycles at the higher load. The hardness levels were essentially the same for both materials under either load.

The data for the TiB_2 material, Table XXVI and Figure 51, showed considerable scatter in both the heating and cooling cycles. This is believed to be due to the porous condition of the material; extremely fine porosity was noted in penetrant inspection and metallographic examination of test specimens used in other phases of the program. Also, the resultant matte-like surface finish made accurate measurements of the hardness impressions most difficult. Because of the latter surface finish condition, data could not be

TABLE XVIII. COMPARISON OF HARDNESS VALUES BETWEEN A KENTRON TESTER AND THE GE HOT HARDNESS TESTER

Material - Unalloyed Arc Cast Tungsten

Specimen Identity - MCN 1038-D-1

Specimen Condition - Recrystallized 2200°F/2 Hours

Test No./Run No. - 1/6

Date - March 18, 1965

Indenter - 316° Diamond Pyramid - #2006 (Vickers)

Load - 150 Grams

Holding Time - 15 Seconds

Instrument	Impression No.		Hardness Kg/mm^2
Kentron Tester	1		426
	2		428
	3		430
		Average	428
Hot Hardness Tester	1		446
	2		451
	3		451
		Average	449

TABLE XIX. HOT HARDNESS DATA FOR UNALLOYED ARC CAST TUNGSTEN

Specimen Identity - MCN 1038-D-1

Specimen Condition - Recrystallized 2200°F/2 Hours

Test No./Run No. - 1/8

Date - March 19, 1965

Indenter - 136° Diamond Pyramid - #2006 (Vickers)

Load - 150 Grams

Holding Time - 15 Seconds

Time Minutes	Vacuum Torr	Temp. °F	Hardness Kg/mm^2
--	--	RT	428(1)
0	2.0×10^{-5}	RT	414(2)
6	3.0×10^{-5}	117	433
13	3.5×10^{-5}	209	442
22	6.2×10^{-5}	323	392
32	1.2×10^{-4}	458	290
46	2.0×10^{-4}	752	184
53	1.2×10^{-4}	830	165
60	5.0×10^{-4}	862	194
75	4.8×10^{-5}	981	162
86	4.6×10^{-5}	1111	158
100	4.0×10^{-5}	1210	156
114	5.0×10^{-5}	1396	148
	Vacuum Leak - 70 Microns		
127	6.0×10^{-5}	1504	128
	Power Off		
300	8.0×10^{-5}	367	268
--	6.5×10^{-5}	348	281
--	---	320	281
--	---	200	375

TABLE XIX. (Cont'd)

(1) Room Temperature Hardness of the Specimen on a Kentron Tester Using a Vickers Diamond Pyramid, a 150-Gram Load and a 15-Second Hold.

(2) Room Temperature Hardness of the Specimen on the Hot Hardness Tester Using a Vickers Diamond Pyramid (#2006), a 150-Gram Load and a 15-Second Hold.

	399 Kg/mm^2
	415 Kg/mm^2
	428 Kg/mm^2
Average	414 Kg/mm^2

(3) Room Temperature Hardness of the Specimen After the Test Cycle on a Kentron Tester Using a Vickers Diamond Pyramid, a 150-Gram Load and a 15-Second Hold.

	468 Kg/mm^2
	453 Kg/mm^2
	477 Kg/mm^2
Average	460 Kg/mm^2

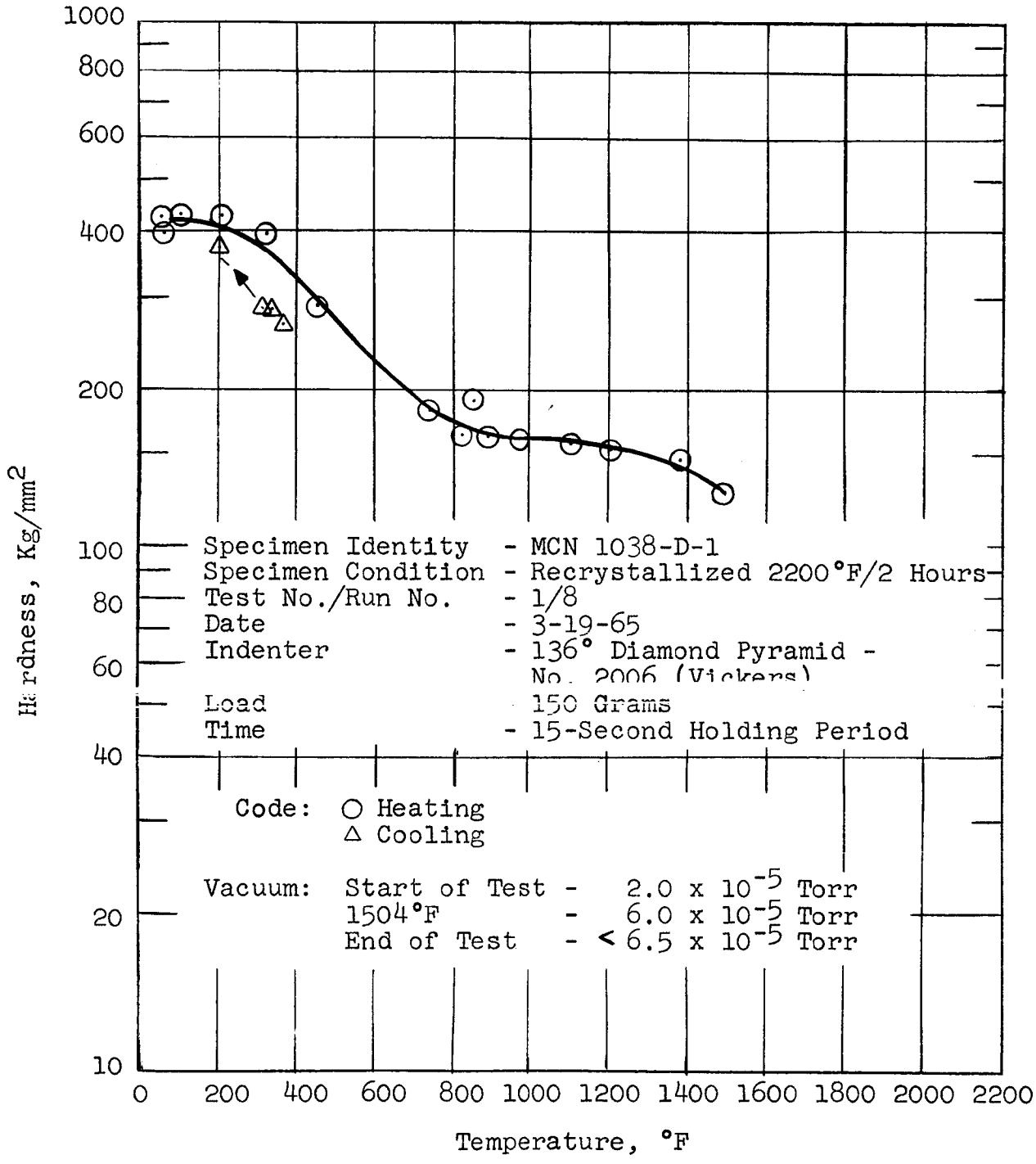

Figure 44. Hardness of Unalloyed Arc Cast Tungsten as a Function of Temperature.

TABLE XX. HOT HARDNESS DATA FOR Mo-TZM ALLOY

Specimen Identity - MCN 1037-D-2

Specimen Condition - Stress-Relieved 2250°F/1/2 Hour

Test No./Run No. - 17/1

Date - March 20, 1965

Indenter - 136° Diamond Pyramid - #2006 (Vickers)

Load - 150 Grams

Holding Time - 15 Seconds

Time Minutes	Vacuum Torr	Temp. °F	Hardness Kg/mm^2
--	--	RT	295(1)
0	2.5×10^{-5}	RT	262(2)
6	2.5×10^{-5}	122	272
15	3.0×10^{-5}	206	266
25	4.5×10^{-5}	301	243
37	5.0×10^{-5}	427	220
47	1.0×10^{-4}	553	212
60	3.5×10^{-5}	592	220
73	3.0×10^{-5}	746	213
90	2.5×10^{-5}	884	201
101	2.0×10^{-5}	1065	208
110	2.0×10^{-5}	1111	199
120	2.5×10^{-5}	1244	196
125	3.0×10^{-5}	1346	192
142	---	1484	191
145	5.0×10^{-5}	1551	189
162	1.8×10^{-5}	1220	186
174	1.4×10^{-5}	1055	196
185	---	1019	192
212	Power Off	860	214
230	8.0×10^{-6}	701	214
279	6.0×10^{-6}	513	235
320	5.0×10^{-6}	402	228
360	5.0×10^{-6}	345	250
400	4.0×10^{-6}	285	255
-	4.0×10^{-6}	250	258
3-22-65	3.0×10^{-3}	RT	309(3)
3-22-65	---	RT	306(4)

TABLE XX. (Cont'd)

(1) Room Temperature Hardness of the Specimen on a Kentron Tester Using a Vickers Diamond Pyramid, a 150-Gram Load and a 15-Second Hold.

(2) Room Temperature Hardness of the Specimen on the Hot Hardness Tester Using a Vickers Diamond Pyramid (#2006), a 150-Gram Load and a 15-Second Hold.

	218 Kg/mm^2
	284 Kg/mm^2
	284 Kg/mm^2
Average	262 Kg/mm^2

(3) Room Temperature Hardness of the Specimen, After the Test Cycle, on the Hot Hardness Tester Using a Vickers Diamond Pyramid (#2006), a 150-Gram Load and a 15-Second Hold.

	307 Kg/mm^2
	311 Kg/mm^2
	307 Kg/mm^2
Average	309 Kg/mm^2

(4) Room Temperature Hardness of the Specimen, After the Test Cycle, on a Kentron Tester Using a Vickers Diamond Pyramid, a 150-Gram Load and a 15-Second Hold.

	311 Kg/mm^2
	306 Kg/mm^2
	302 Kg/mm^2
Average	306 Kg/mm^2

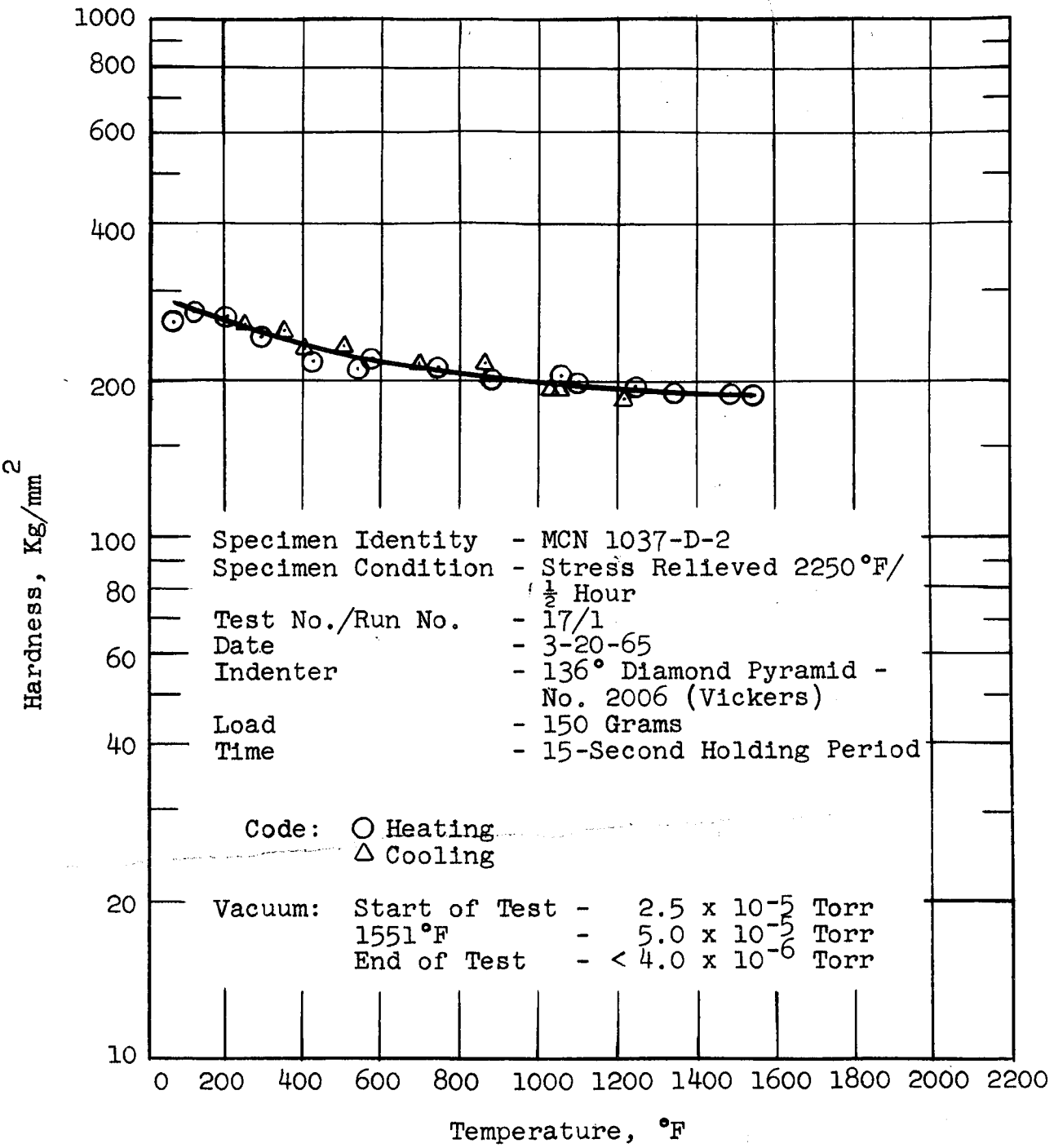

Figure 45. Hardness of Mo-TZM Alloy as a Function of Temperature.

TABLE XXI. HOT HARDNESS DATA FOR Mo-TZM ALLOY

Specimen Identity - MCN 1037-D-1

Specimen Condition - Stress-Relieved 2250°F/1/2 Hour

Test No./Run No. - 2/2

Date - April 14, 1965

Indenter - 136° Diamond Pyramid - #2006 (Vickers)

Load - 150 Grams

Holding Time - 15 Seconds

Time Minutes	Vacuum Torr	Temp. °F	Hardness Kg/mm^2
--	---	RT	325(1)
0	5×10^{-3}	RT	301(2)
13	2.6×10^{-5}	206	297
22	5.0×10^{-5}	301	253
31	8.6×10^{-5}	400	234
43	1.2×10^{-4}	509	231
55	6.8×10^{-5}	604	221
68	3.8×10^{-5}	700	218
80	2.8×10^{-5}	814	209
91	2.4×10^{-5}	926	215
98	2.2×10^{-5}	1008	203
108	1.6×10^{-5}	1106	198
118	1.4×10^{-5}	1200	200
137	1.2×10^{-5}	1313	196
160	1.2×10^{-5}	1404	200
172	1.0×10^{-5}	1504	196
183	1.0×10^{-5}	1404	210
198	1.0×10^{-5}	1304	207
208	8.0×10^{-6}	1211	209
215	7.0×10^{-6}	1088	215
222	6.5×10^{-6}	974	229
240	5.6×10^{-6}	858	231
268 Power Off	5.0×10^{-6}	682	243
293	4.0×10^{-6}	569	247
317	4.0×10^{-6}	495	261
360	3.0×10^{-6}	395	267
490	3.0×10^{-6}	238	285
675	3.0×10^{-6}	136	285
--	3.0×10^{-6}	136	297
--	---	RT	319(3)

TABLE XXI. (Cont'd)

(1) Room Temperature Hardness of the Specimen on a Kentron Tester Using a Vickers Diamond Pyramid, a 150-Gram Load and 15-Second Hold.

	328 Kg/mm^2
	326 Kg/mm^2
	326 Kg/mm^2
Average	325 Kg/mm^2

(2) Room Temperature Hardness of the Specimen on the Hot Hardness Tester Using a Vickers Diamond Pyramid (#2006), a 150-Gram Load and a 15-Second Hold.

	329 Kg/mm^2
	276 Kg/mm^2
	299 Kg/mm^2
Average	301 Kg/mm^2

(3) Room Temperature Hardness of the Specimen, After the Test Cycle, on a Kentron Tester Using a Vickers Diamond Pyramid, a 150-Gram Load and a 15-Second Hold.

	320 Kg/mm^2
	318 Kg/mm^2
	318 Kg/mm^2
Average	319 Kg/mm^2

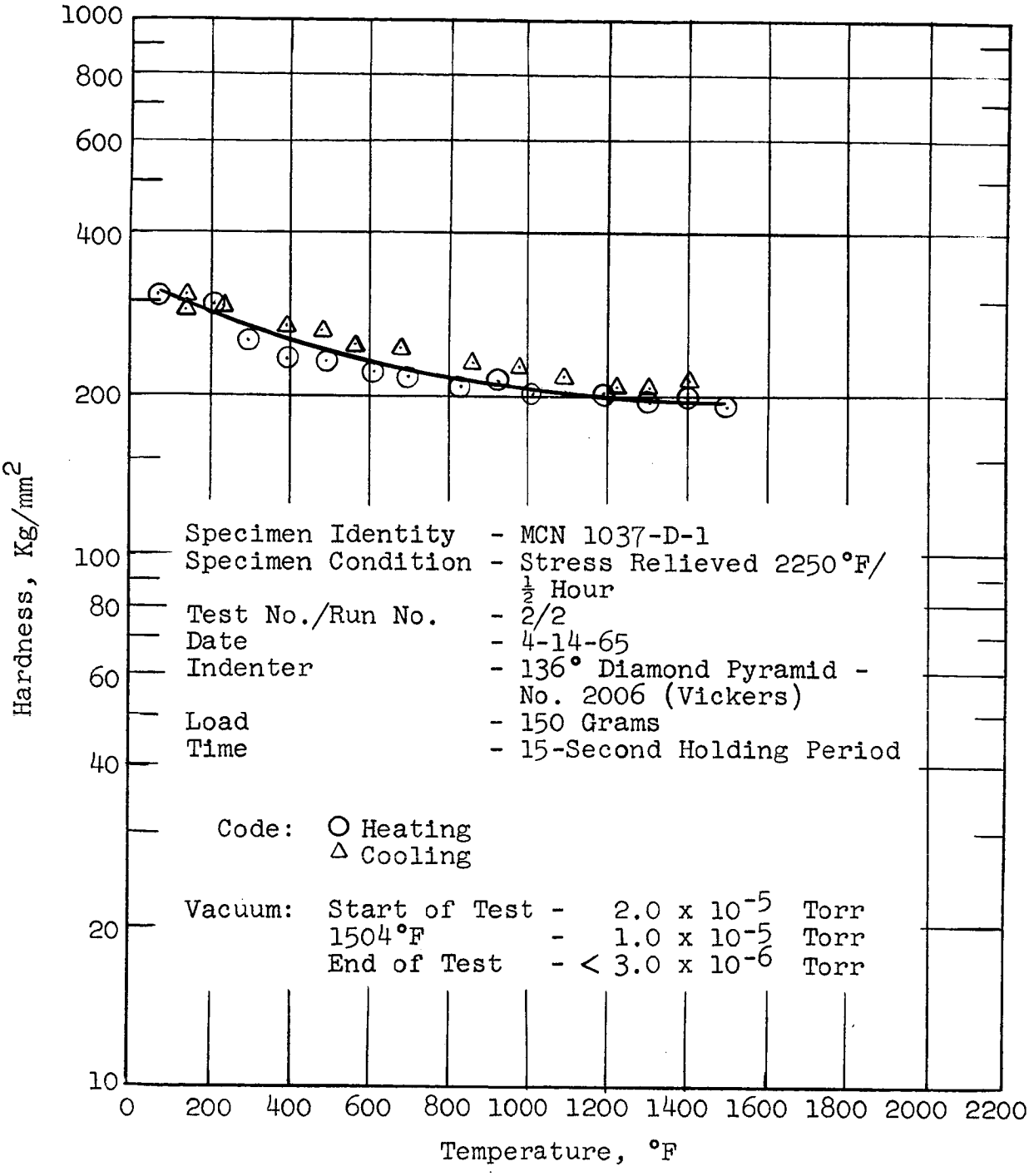

Figure 46. Hardness of Mo-TZM Alloy as a Function of Temperature.

TABLE XXII. HOT HARDNESS DATA FOR Mo-TZM ALLOY

Specimen Identity - MCN 1037-D-1

Specimen Condition - Stress-Relieved 2250°F/1/2 Hour

Test No./Run No. - 2/4
Date - April 27, 1965

Indenter - 136° Diamond Pyramid - #2006 (Vickers)

Load - 150 Grams

Holding Time - 15 Seconds

Time Minutes	Vacuum Torr	Temp. °F	Hardness Kg/mm^2
-	---	RT	319(1)
0	2.0×10^{-5}	RT	291(2)
3	2.6×10^{-5}	103	315
13	3.6×10^{-5}	200	290
25	6.0×10^{-5}	300	282
33	6.8×10^{-5}	400	269
45	9.4×10^{-5}	505	253
58	7.0×10^{-5}	608	241
70	4.5×10^{-5}	700	237
79	4.4×10^{-5}	800	226
88	4.0×10^{-5}	904	221
96	3.4×10^{-5}	1000	209
124	2.2×10^{-5}	1234	209
130	2.2×10^{-5}	1307	204
140	2.3×10^{-5}	1400	204
150	2.8×10^{-5}	1500	198
162	2.6×10^{-5}	1600	199
	Power Off		
171	2.0×10^{-5}	1484	203
177	1.6×10^{-5}	1400	204
184	1.4×10^{-5}	1300	215
193	1.2×10^{-5}	1183	207
208	1.0×10^{-6}	1063	221
217	7.0×10^{-6}	979	219
240	8.0×10^{-6}	800	219
256	6.5×10^{-6}	700	233
4-28-65	3.0×10^{-3}	RT	307(3)
4-28-65	---	RT	319(4)

TABLE XXII. (Cont'd)

(1) Room Temperature Hardness of the Specimen on a Kentron Tester Using a Vickers Diamond Pyramid, a 150-Gram Load and 15-Second Hold.

	320 Kg/mm^2
	318 Kg/mm^2
	318 Kg/mm^2
Average	319 Kg/mm^2

(2) Room Temperature Hardness of the Specimen on the Hot Hardness Tester Using a Vickers Diamond Pyramid (#2006), a 150-Gram Load and a 15-Second Hold.

	290 Kg/mm^2
	292 Kg/mm^2
Average	291 Kg/mm^2

(3) Room Temperature Hardness of the Specimen, After the Test Cycle, on the Hot Hardness Tester Using a Vickers Diamond Pyramid (#2006), a 150-Gram Load and a 15-Second Hold.

(4) Room Temperature Hardness of the Specimen, After the Test Cycle, on a Kentron Tester Using a Vickers Diamond Pyramid, a 150-Gram Load and a 15-Second Hold.

	320 Kg/mm^2
	318 Kg/mm^2
	318 Kg/mm^2
Average	319 Kg/mm^2

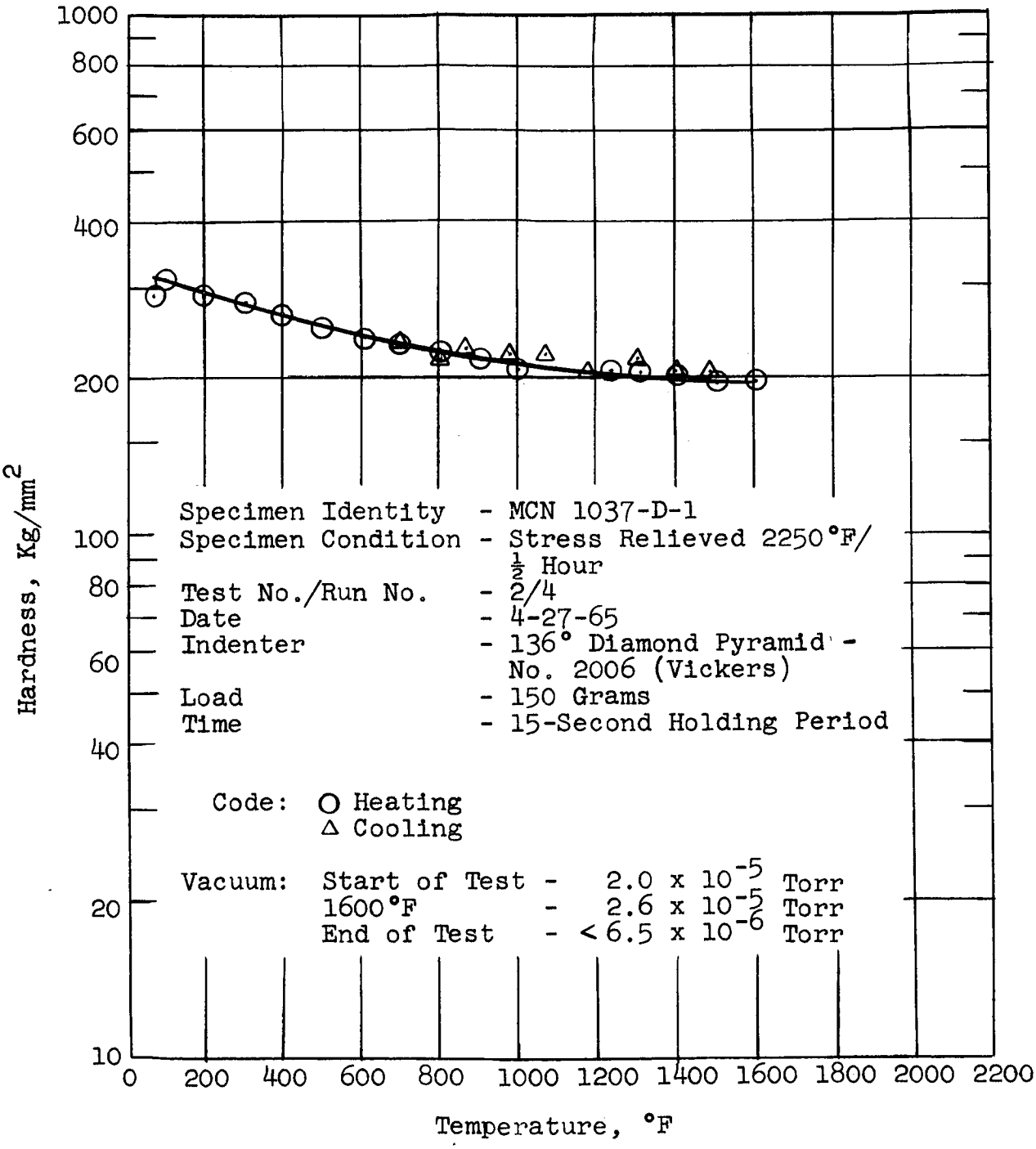

Figure 47. Hardness of Mo-TZM Alloy as a Function of Temperature.

TABLE XXIII. HOT HARDNESS DATA FOR TiC

Specimen Identity - MCN 1042-D-3

Test No./Run No. - 18/1

Date - March 22, 1965

Indenter - 136° Diamond Pyramid - #2006 (Vickers)

Load - 150 Grams

Holding Time - 15 Seconds

Time Minutes	Vacuum Torr	Temp. °F	Hardness Kg/mm^2
-	---	RT	2210(1)
0	3.5×10^{-5}	RT	2620(2)
5	2.8×10^{-5}	128	2718
13	4.0×10^{-5}	209	2585
25	8.0×10^{-5}	314	2650
33	1.2×10^{-4}	422	2190
47	1.5×10^{-4}	537	1840
57	1.0×10^{-4}	604	1696
73	6.0×10^{-5}	704	1599
90	4.0×10^{-5}	838	1260
97	4.0×10^{-5}	906	1218
118	3.0×10^{-5}	1197	865
135	2.8×10^{-5}	1214	764
152	2.4×10^{-5}	1304	679
159	2.4×10^{-5}	1404	654
175	---	1504	601
183	2.4×10^{-5}	1404	663
191	2.0×10^{-5}	1396	734
201	1.8×10^{-5}	1192	807
214	1.6×10^{-5}	1095	735
234	1.5×10^{-5}	963	1004
253	1.5×10^{-5}	892	1158
260	Power Off		
290	1.2×10^{-5}	729	1730
300	1.2×10^{-5}	600	1568
340	1.4×10^{-5}	489	2004
480	1.4×10^{-5}	278	2404
-	---	200	2585
3-23-65	---	RT	2655(3)
3-23-65	---	RT	3247(4)

TABLE XXIII. (Cont'd)

(1) Room Temperature Hardness of the Specimen on a Kentron Tester Using a Vickers Diamond Pyramid, a 150-Gram Load and a 15-Second Hold.

(2) Room Temperature Hardness of the Specimen on the Hot Hardness Tester Using a Vickers Diamond Pyramid (#2006), a 150-Gram Load and a 15-Second Hold.

	2718 Kg/mm^2
	2522 Kg/mm^2
Average	2620 Kg/mm^2

(3) Room Temperature Hardness of the Specimen, After the Test Cycle, on the Hot Hardness Tester Using a Vickers Diamond Pyramid (#2006), a 150-Gram Load and a 15-Second Hold.

	2788 Kg/mm^2
	2522 Kg/mm^2
Average	2655 Kg/mm^2

(4) Room Temperature Hardness of the Specimen, After the Test Cycle, on a Kentron Tester Using a Vickers Diamond Pyramid, a 150-Gram Load and a 15-Second Hold.

	3420 Kg/mm^2
	3130 Kg/mm^2
	3190 Kg/mm^2
Average	3247 Kg/mm^2

NOTE: Small Cracks were Observed Around all Room Temperature Hardness Impressions.

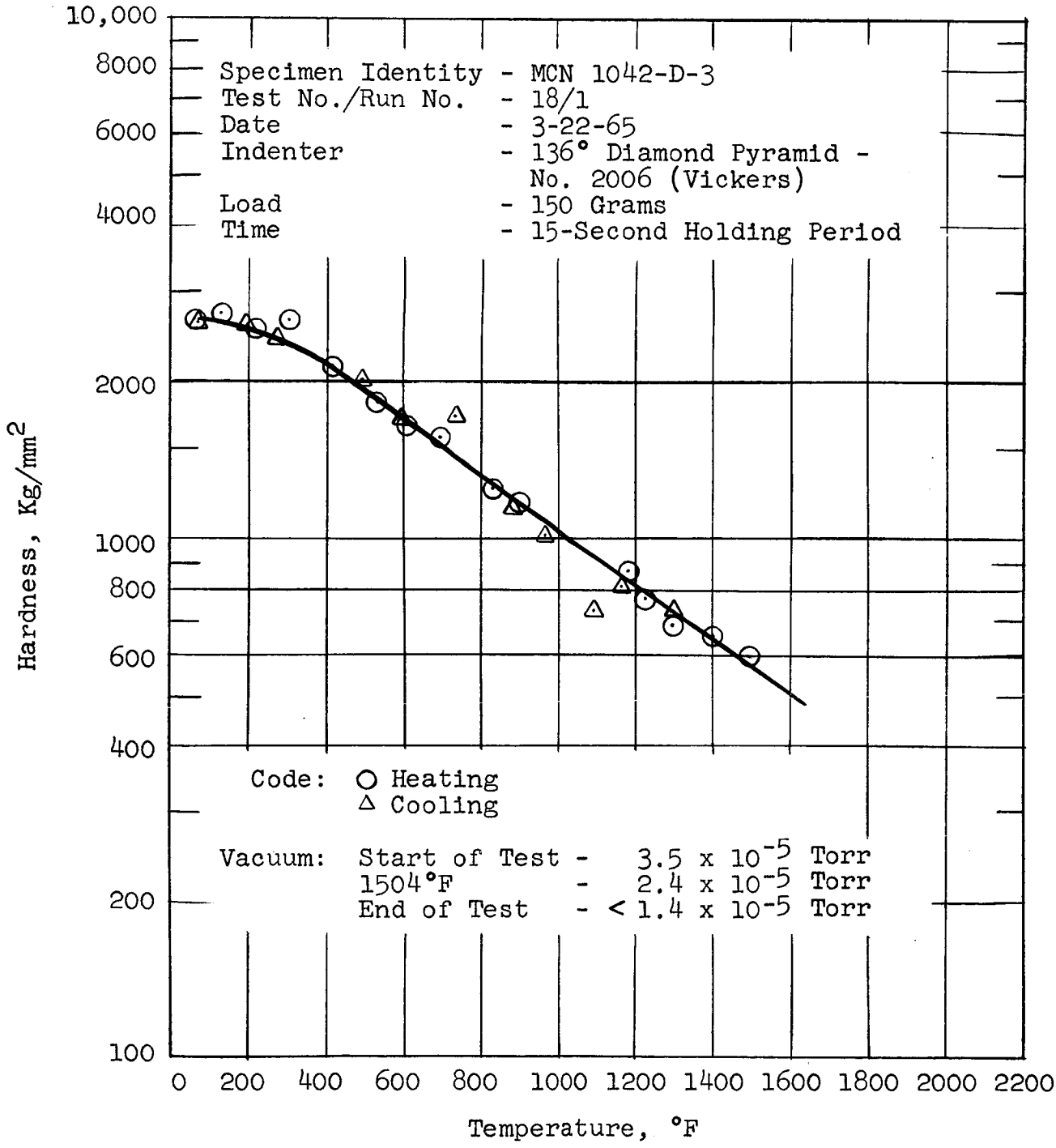

Figure 48. Hardness of TiC as a Function of Temperature.

TABLE XXIV. HOT HARDNESS DATA FOR CARBOLOY 907

Specimen Identity - MCN 1036-D-2

Test No./Run No. - 19/1

Date - March 23, 1965

Indenter - 136° Diamond Pyramid - #2006 (Vickers)

Load - 150 Grams

Holding Time - 15 Seconds

Time Minutes	Vacuum Torr	Temp. °F	Hardness Kg/mm^2
--	--	RT	1500(1)
0	8.0×10^{-6}	RT	1739(2)
5	1.8×10^{-5}	120	1840
14	2.0×10^{-5}	200	1802
26	4.6×10^{-5}	321	1630
34	8.0×10^{-5}	412	1630
45	9.2×10^{-5}	515	1481
58	6.2×10^{-5}	612	1481
73	3.6×10^{-5}	710	1305
86	3.6×10^{-5}	840	1402
94	3.2×10^{-5}	959	1282
100	2.6×10^{-5}	1011	1239
116	2.0×10^{-5}	1201	1019
132	1.6×10^{-5}	1321	917
154	1.6×10^{-5}	1404	807
170	2.6×10^{-5}	1504	697
188	1.2×10^{-5}	1388	785
195	1.0×10^{-6}	1304	878
210	9.0×10^{-6}	1173	1121
230	8.0×10^{-6}	1065	1178
245	Power Off		
280	5.6×10^{-6}	729	1218
320	4.0×10^{-6}	470	1509
--	4.0×10^{-6}	358	1568
420	3.0×10^{-6}	343	1481
--	3.0×10^{-6}	307	1538
3-24-65	--	RT	1821(3)
3-24-65	--	RT	1700(4)

TABLE XXIV. (Cont'd)

(1) Room Temperature Hardness of the Specimen on a Kentron Tester Using a Vickers Diamond Pyramid, a 150-Gram Load and a 15-Second Hold.

1500 Kg/mm^2

(2) Room Temperature Hardness of the Specimen on the Hot Hardness Tester Using a Vickers Diamond Pyramid (#2006), a 150-Gram Load and a 15-Second Hold.

	1662 Kg/mm^2
	1730 Kg/mm^2
	1696 Kg/mm^2
	1840 Kg/mm^2
	1766 Kg/mm^2
Average	1739 Kg/mm^2

(3) Room Temperature Hardness of the Specimen, After the Test Cycle, on the Hot Hardness Tester Using a Vickers Diamond Pyramid (#2006), a 150-Gram Load and a 15-Second Hold.

	1802 Kg/mm^2
	1840 Kg/mm^2
Average	1821 Kg/mm^2

(4) Room Temperature Hardness of the Specimen, After the Test Cycle, on a Kentron Tester Using a Vickers Diamond Pyramid, a 150-Gram Load and a 15-Second Hold.

	1840 Kg/mm^2
	1780 Kg/mm^2
	1480 Kg/mm^2
Average	1700 Kg/mm^2

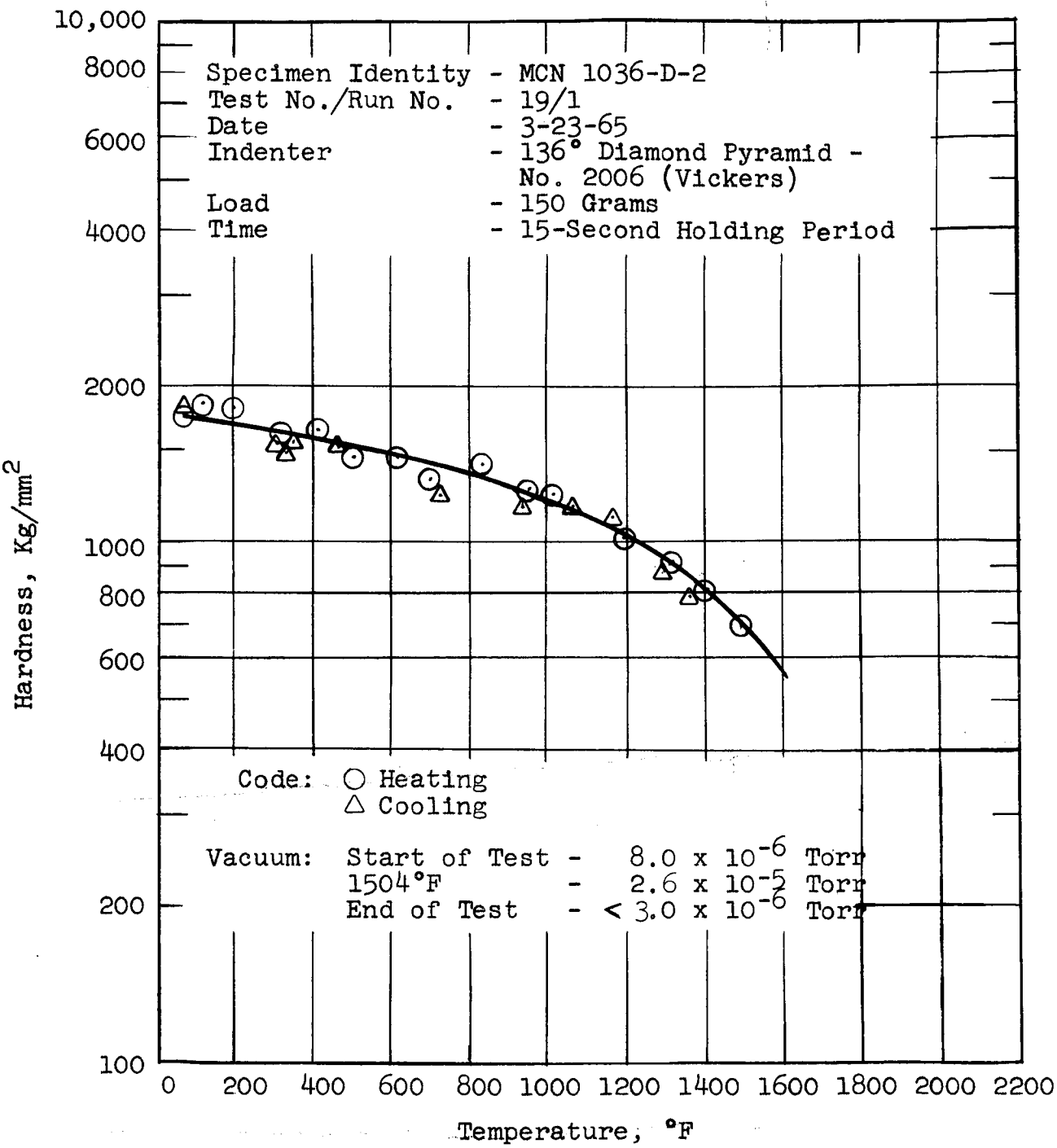

Figure 49. Hardness of Carboloy 907 as a Function of Temperature.

TABLE XXV. HOT HARDNESS DATA FOR CARBOLOY 999

Specimen Identity - MCN 1035-D-2

Test No./Run No. - 23/1

Date - April 16, 1965

Indenter - 136° Diamond Pyramid - #2006 (Vickers)

Load - 150 Grams

Holding Time - 15 Seconds

Time Minutes	Vacuum Torr	Temp. °F	Hardness Kg/mm^2
--	--	RT	2085(1)
0	9.0×10^{-6}	59	2617(2)
4	1.0×10^{-5}	105	2141
15	3.0×10^{-5}	250	2293
24	6.5×10^{-5}	352	1802
31	9.0×10^{-5}	421	2094
42	9.8×10^{-5}	525	1730
52	7.0×10^{-5}	597	1840
67	3.5×10^{-5}	718	1663
77	3.0×10^{-5}	812	1481
92	2.0×10^{-5}	955	1402
100	1.8×10^{-5}	1033	1402
108	1.6×10^{-5}	1148	1239
116	1.5×10^{-5}	1209	1121
129	1.2×10^{-5}	1304	1085
143	1.4×10^{-5}	1404	1068
160	2.0×10^{-5}	1535	917
172	1.0×10^{-5}	1408	904
180	8.5×10^{-6}	1304	1103
191	7.0×10^{-6}	1204	1178
206	6.0×10^{-6}	1035	1305
227	5.0×10^{-6}	877	1509
245 Power Off	4.5×10^{-6}	761	1802
272	4.0×10^{-6}	618	1802
314	3.0×10^{-6}	478	2004
363	3.0×10^{-6}	400	2004
495	--	250	1961
645	--	150	2347
4-17-65	5.0×10^{-3}	RT	2320(3)
4-17-65	--	RT	2447(4)

TABLE XXV. (Cont'd)

(1) Room Temperature Hardness of the Specimen on a Kentron Tester Using a Vickers Diamond Pyramid, a 150-Gram Load and a 15-Second Hold.

	2031 Kg/mm^2
	1965 Kg/mm^2
	2258 Kg/mm^2
Average	2085 Kg/mm^2

(2) Room Temperature Hardness of the Specimen on the Hot Hardness Tester Using a Vickers Diamond Pyramid (#2006), a 150-Gram Load and 15-Second Hold.

	3097 Kg/mm^2
	2462 Kg/mm^2
	2293 Kg/mm^2
Average	2617 Kg/mm^2

(3) Room Temperature Hardness of the Specimen, After the Test Cycle, on the Hot Hardness Tester Using a Vickers Diamond Pyramid (#2006), a 150-Gram Load and a 15-Second Hold.

	2293 Kg/mm^2
	2347 Kg/mm^2
Average	2320 Kg/mm^2

(4) Room Temperature Hardness of the Specimen, After the Test Cycle, on a Kentron Tester Using a Vickers Diamond Pyramid, a 150-Gram Load and a 15-Second Hold.

	2040 Kg/mm^2
	2650 Kg/mm^2
	2650 Kg/mm^2
Average	2447 Kg/mm^2

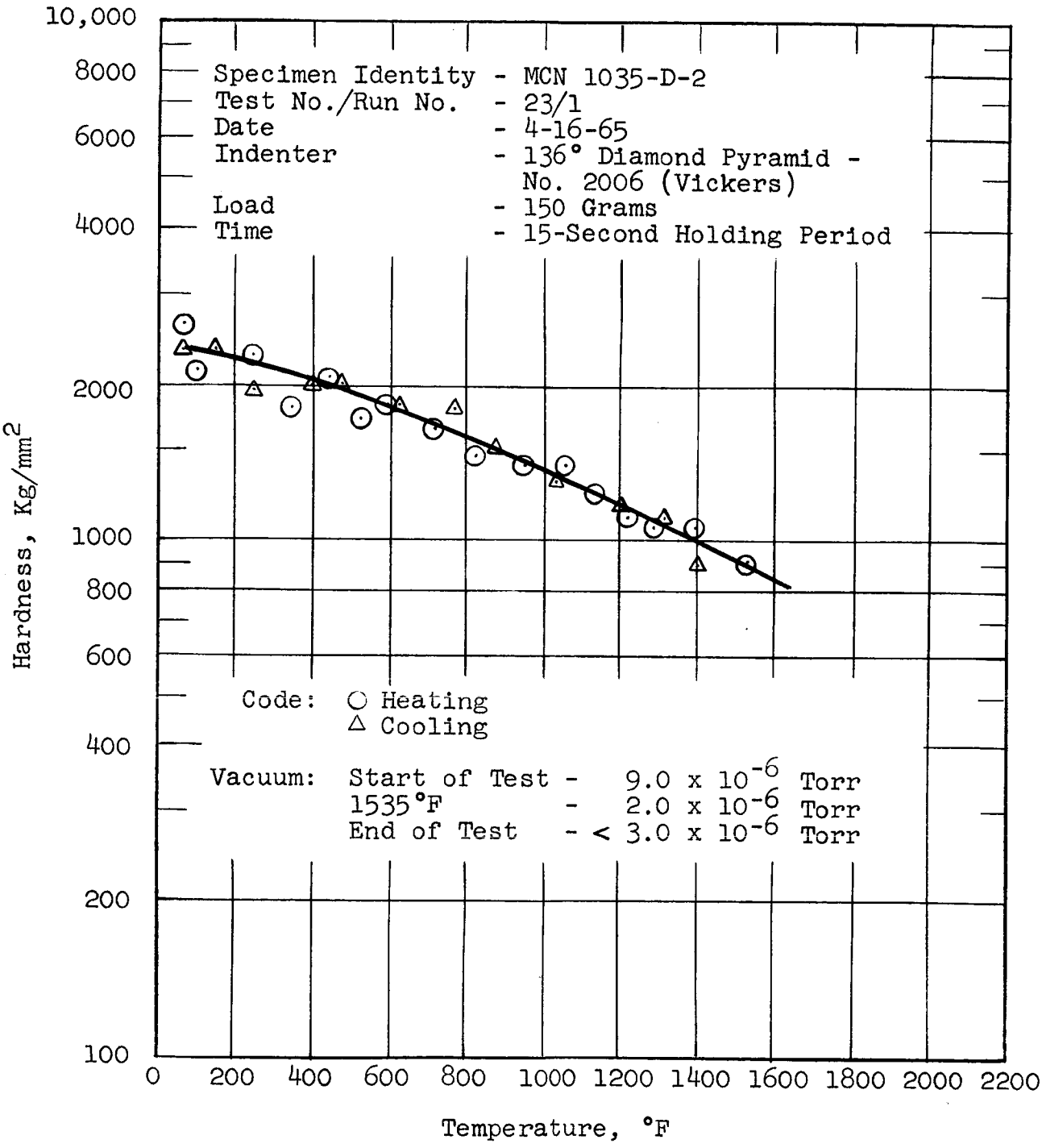

Figure 50. Hardness of Carboloy 999 as a Function of Temperature.

TABLE XXVI. HOT HARDNESS DATA FOR TiB_2

Specimen Identity - MCN 1048-D-2

Test No./Run No. - 26/1

Date - April 20, 1965

Indenter - 136° Diamond Pyramid - #2006 (Vickers)

Load - 150 Grams

Holding Time - 15 Seconds

Time Minutes	Vacuum Torr	Temp. °F	Hardness Kg/mm^2
--	--	RT	3210(1)
0	9.6×10^{-6}	RT	3241(2)
21	4.0×10^{-5}	307	3183
38	9.5×10^{-5}	500	2650(3)
47	7.5×10^{-5}	565	1840(3)
52	5.6×10^{-5}	600	1538(3)
66	3.0×10^{-5}	708	1630(3)
80	2.0×10^{-5}	799	1803
91	1.8×10^{-5}	900	1305(3)
104	1.2×10^{-5}	1050	973
110	1.0×10^{-5}	1100	1085
119	1.0×10^{-5}	1210	890
126	1.0×10^{-5}	1307	904
139	1.0×10^{-5}	1375	973
151	1.2×10^{-5}	1500	917
161	2.4×10^{-5}	1600	1019
172	1.0×10^{-5}	1434	931
180	8.0×10^{-6}	1400	1068
198	6.0×10^{-6}	1237	1599
201	5.5×10^{-6}	1087	1305
210	5.0×10^{-6}	987	1282
226 Power Off	4.5×10^{-6}	851	1103(3)
240	4.0×10^{-6}	758	2190
260	3.5×10^{-6}	641	1481
287	3.0×10^{-6}	533	2004
319	2.5×10^{-6}	452	1428
374	2.0×10^{-6}	345	3364(3)
420	2.0×10^{-6}	292	2293
4-21-65	--	RT	2360(4)

TABLE XXVI. (Cont'd)

(1) Room Temperature Hardness of the Specimen on a Kentron Tester Using a Vickers Diamond Pyramid, a 150-Gram Load and 15-Second Hold.

	2940 Kg/mm^2
	3120 Kg/mm^2
	3570 Kg/mm^2
Average	3210 Kg/mm^2

(2) Room Temperature Hardness of the Specimen on the Hot Hardness Tester Using a Vickers Diamond Pyramid (#2006), a 150-Gram Load and a 15-Second Hold.

	3562 Kg/mm^2
	3893 Kg/mm^2
	3668 Kg/mm^2
	1840 Kg/mm^2
Average	3241 Kg/mm^2

(3) Small Cracks were Observed Around Hardness Impression.

(4) Room Temperature Hardness of the Specimen, After the Test Cycle, on a Kentron Tester Using a Vickers Diamond Pyramid, a 150-Gram Load and a 15-Second Hold.

	2450 Kg/mm^2
	2400 Kg/mm^2
	2230 Kg/mm^2
Average	2360 Kg/mm^2

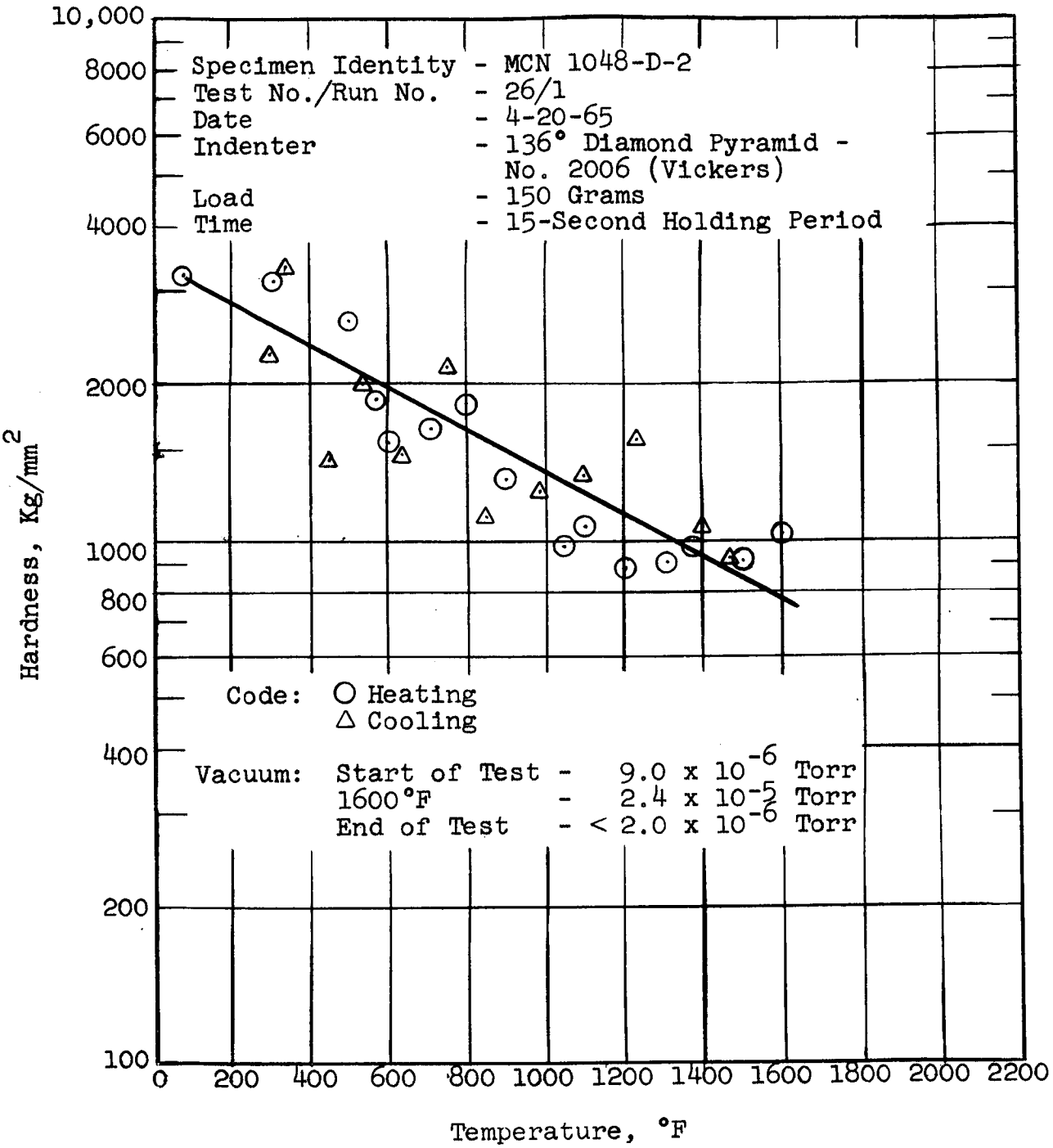

Figure 51. Hardness of TiB_2 as a Function of Temperature.

obtained with the 100-gram load and, therefore, no comparison in hardness could be made between the two test loads. For similar reasons no comparison in hardness could be made for the Lucalox or the TiC+10%Mo materials as a function of test load. The data obtained for these materials with a 150-gram load are presented in Tables XXVII and XXVIII and Figures 52 and 53.

The hardness data for the Zircoa 1027 material under the 150-gram load, Table XXIX, Figure 54, indicated a slightly higher overall hardness level than that obtained under the 100-gram load and a similar lower hardness on the cooling cycle. The latter may be associated with the transformation of the monoclinic structure.

The K601 material showed slightly less scatter and a similar hardness level as that obtained in the initial test at the lighter load, Table XXX and Figure 55.

The hardness of the TiC+5%W material is shown in Table XXXI and Figure 56, and is approximately the same level as that produced by the 100-gram load. As in the case of the TiC material, cracking was observed around the room temperature impressions.

A slightly lower hardness was exhibited by the TiC+10%Cb material at the higher testing load, Table XXXII, Figure 57. This was especially evident in the 1200° to 1600°F range. Again, as with the TiC and TiC+5%W materials cracking was evident in the room temperature impressions. It should be noted that no cracking was observed around the room temperature impressions made in the TiC+10%Mo material.

Considerably less scatter in the hardness data was obtained on the same specimen of Grade 7178 material using the 150-gram load as was obtained with the 100-gram load, Table XXXIII and Figure 58.

The scatter in the hardness data for the Star J alloy, presented in Table XXXIV and Figure 59, is due to the existance of a multiphase structure of varying hardnesses and the inability to pre-select the location of each hardness impression. Post-test examination of the impressions at a magnification of 370X revealed that only one impression was completely within the carbide phase; the other impressions either were entirely within the matrix phase or were partially within two or more phases. Although the data suggest a possible softening trend above 1200°F, i.e., change in slope of the hardness curve, additional data points are required to conclusively establish this fact. A change in slope of the hardness curve was not observed in the data obtained with a 100-gram load[2] and from a knowledge of the composition, a sharp break in the hardness curve at 1200°F would not be expected with this alloy.

A summary of the hardness values for each material at temperatures of 400°, 800°, 1200° and 1600°F, obtained under the 100-gram and 150-gram testing loads, is presented in Table XXXV.

C. Compression

Room temperature compression tests have been completed on duplicate specimens of thirteen candidate bearing materials. Depending on the type of material that was being tested, a strain rate of 0.005 inch/inch/minute was maintained

TABLE XXVII. HOT HARDNESS DATA FOR LUCALOX

Specimen Identity - MCN 1039-D-2

Test No./Run No. - 28/1

Date - April 22, 1965

Indenter - 136° Diamond Pyramid - #2006 (Vickers)

Load - 150 Grams

Holding Time - 15 Seconds

Time Minutes	Vacuum Torr	Temp. °F	Hardness Kg/mm^2
--	--	RT	2140(1)
0	8.0×10^{-6}	RT	2573(2)
4	9.8×10^{-6}	114	2585
10	1.8×10^{-5}	200	3015
20	4.0×10^{-5}	316	2788
26	8.6×10^{-5}	405	2585
36	1.2×10^{-4}	509	2048
48	7.0×10^{-5}	602	1879
66	3.0×10^{-5}	720	2004
78	2.2×10^{-5}	819	1630
88	2.0×10^{-5}	925	1305
99	1.4×10^{-5}	1037	1305(3)
107	1.2×10^{-5}	1106	1328(3)
117	1.0×10^{-5}	1204	1178(3)
126	1.0×10^{-5}	1307	1282(3)
141	1.0×10^{-5}	1400	988
152	1.2×10^{-5}	1484	973
168	2.2×10^{-5}	1600	744(3)
177	1.0×10^{-5}	1484	917(3)
187	8.0×10^{-6}	1362	1085(3)
195	7.0×10^{-6}	1265	1019(3)
200	6.5×10^{-6}	1190	1019(3)
210	6.0×10^{-6}	1055	1376
221 Power Off	5.0×10^{-6}	943	1376(3)
248	4.0×10^{-6}	733	1481(3)
277	3.4×10^{-6}	581	1802(3)
305	3.0×10^{-6}	490	1879
354	2.0×10^{-6}	380	2861
390	2.0×10^{-6}	323	3015
4-23-65	--	RT	3099(4)
--	--	RT	2340(5)

TABLE XXVII. (Cont'd)

(1) Room Temperature Hardness of the Specimen on a Kentron Tester Using a Vickers Diamond Pyramid, a 150-Gram Load and a 15-Second Hold.

	2175 Kg/mm^2
	2175 Kg/mm^2
	2070 Kg/mm^2
Average	2140 Kg/mm^2

(2) Room Temperature Hardness of the Specimen on the Hot Hardness Tester Using a Vickers Diamond Pyramid (#2006), a 150-Gram Load and a 15-Second Hold.

	2141 Kg/mm^2
	2718 Kg/mm^2
	2861 Kg/mm^2
Average	2573 Kg/mm^2

(3) Small Cracks were Observed Around Hardness Impressions.

(4) Room Temperature Hardness of the Specimen, After the Test Cycle, on the Hot Hardness Tester Using a Vickers Diamond Pyramid (#2006), a 150-Gram Load and 15-Second Hold.

	3015 Kg/mm^2
	3015 Kg/mm^2
	3183 Kg/mm^2
Average	3099 Kg/mm^2

(5) Room Temperature Hardness of the Specimen, After the Test Cycle, on a Kentron Tester Using a Vickers Diamond Pyramid, a 150-Gram Load and a 15-Second Hold.

	2350 Kg/mm^2
	2350 Kg/mm^2
	2320 Kg/mm^2
Average	2340 Kg/mm^2

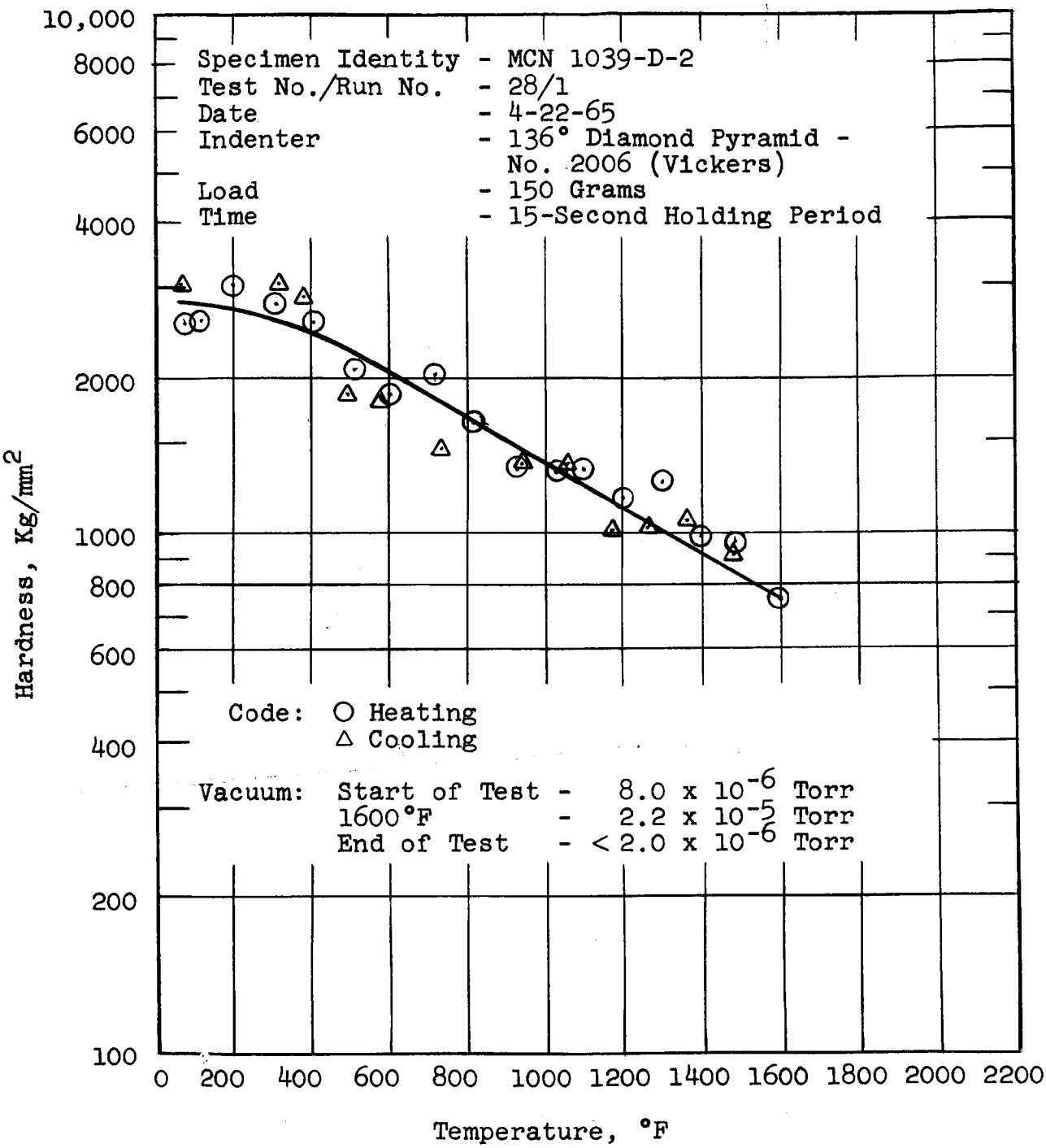

Figure 52. Hardness of Lucalox as a Function of Temperature.

TABLE XXVIII. HOT HARDNESS DATA FOR TiC+10%Mo

Specimen Identity - MCN 1044-D-3

Test No./Run No. - 27/1

Date - April 21, 1965

Indenter - 136° Diamond Pyramid - #2006 (Vickers)

Load - 150 Grams

Holding Time - 15 Seconds

Time Minutes	Vacuum Torr	Temp. °F	Hardness Kg/mm^2
--	--	RT	2512(1,2)
0	9.5×10^{-6}	RT	4239(2,3)
4	1.0×10^{-6}	123	3778
11	2.0×10^{-5}	200	4014(2)
18	3.5×10^{-5}	300	3893
30	8.0×10^{-5}	424	3562(2)
39	9.0×10^{-5}	500	3461(2)
53	5.5×10^{-5}	602	2650
67	3.0×10^{-5}	700	2141
82	2.0×10^{-5}	812	1730
90	2.0×10^{-5}	906	1568
--	1.0×10^{-5}	1010	1376
105	1.0×10^{-5}	1100	1178
117	1.0×10^{-5}	1209	1068
128	9.5×10^{-6}	1307	1019
139	1.0×10^{-5}	1399	944
155	1.0×10^{-5}	1500	917
165	2.0×10^{-5}	1600	865
175	1.0×10^{-5}	1500	904
185	7.5×10^{-6}	1350	988
193	6.0×10^{-6}	1250	1004
209	5.0×10^{-6}	1143	1121
218	5.0×10^{-6}	1050	1158
225 Power Off	5.0×10^{-6}	950	1305
240	4.0×10^{-6}	830	1696
265	3.5×10^{-6}	710	1961
279	3.0×10^{-6}	594	2404
363	2.0×10^{-6}	380	3015
410	2.0×10^{-6}	315	3272
542	--	200	3183
--	--	RT	3413(4)
--	--	RT	2857(5)

TABLE XXVIII. (Cont'd)

(1) Room Temperature Hardness of the Specimen on a Kentron Tester Using a Vickers Diamond Pyramid, a 150-Gram Load and 15-Second Hold.

	2430 Kg/mm^2
	2475 Kg/mm^2
	2730 Kg/mm^2
Average	2512 Kg/mm^2

(2) Small Cracks were Observed Around Hardness Impressions.

(3) Room Temperature Hardness of the Specimen on the Hot Hardness Tester Using a Vickers Diamond Pyramid (#2006), a 150-Gram Load and 15-Second Hold.

	4412 Kg/mm^2
	4412 Kg/mm^2
	3893 Kg/mm^2
Average	4239 Kg/mm^2

(4) Room Temperature Hardness of the Specimen, After the Test Cycle, on the Hot Hardness Tester Using a Vickers Diamond Pyramid (#2006), a 150 Gram-Load, and a 15-Second Hold.

	3097 Kg/mm^2
	3778 Kg/mm^2
	3364 Kg/mm^2
Average	3413 Kg/mm^2

(5) Room Temperature Hardness of the Specimen, After the Test Cycle, on a Kentron Tester Using a Vickers Diamond Pyramid, a 150-Gram Load and a 15-Second Hold.

	2870 Kg/mm^2
	2940 Kg/mm^2
	2760 Kg/mm^2
Average	2857 Kg/mm^2

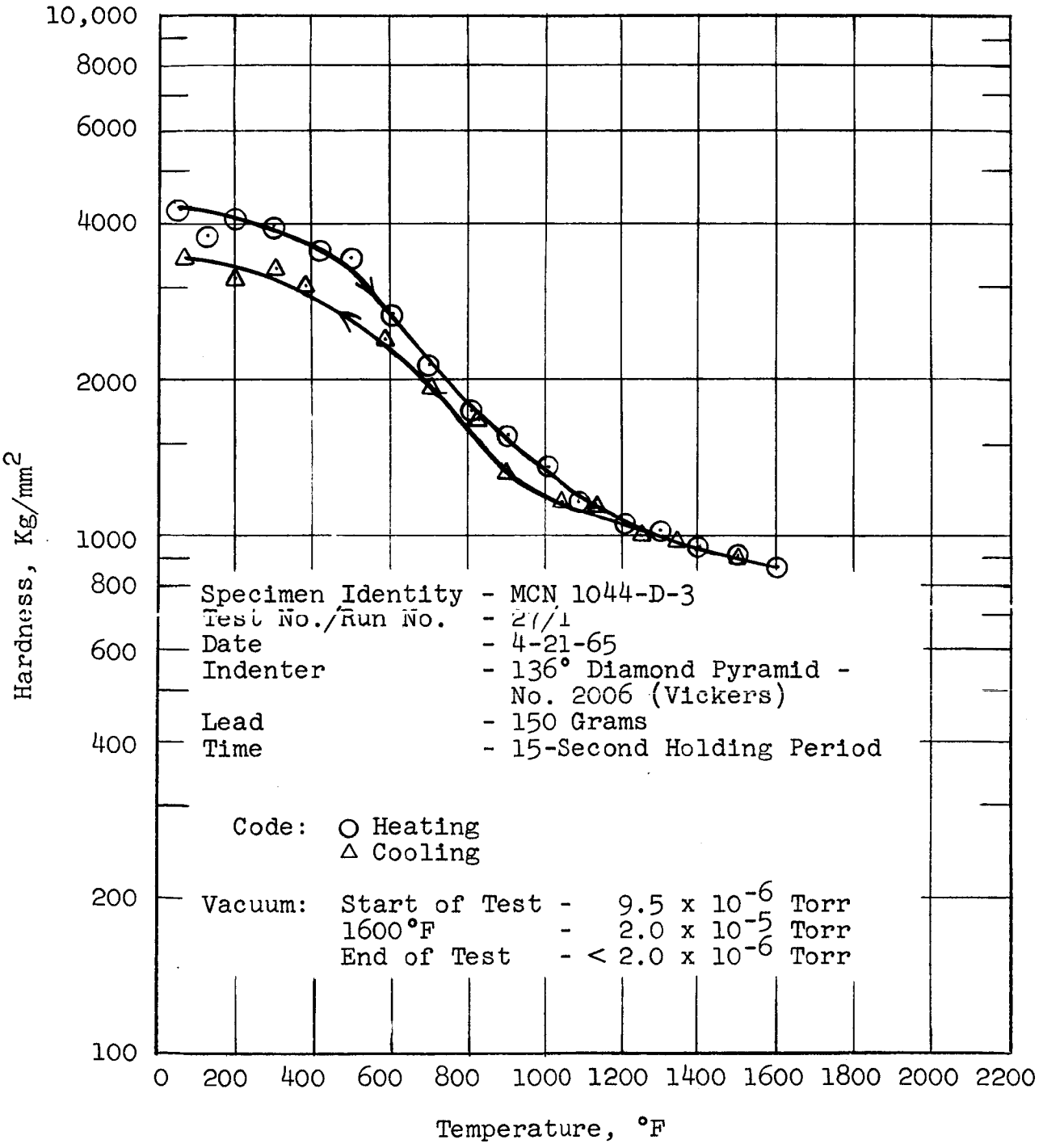

Figure 53. Hardness of TiC+10%Mo as a Function of Temperature.

TABLE XXIX. HOT HARDNESS DATA FOR ZIRCOA 1027

Specimen Identity - MCN 1040-D-1

Test No./Run No. - 29/1

Date - April 23, 1965

Indenter - 136° Diamond Pyramid - #2006 (Vickers)

Load - 150 Gram

Holding Time - 15 Seconds

Time Minutes	Vacuum Torr	Temp. °F	Hardness Kg/mm^2
--	--	RT	1155(1)
0	9.0×10^{-6}	RT	1328(2)
3	1.0×10^{-5}	103	1402
10	2.0×10^{-5}	201	1568
18	4.0×10^{-5}	306	1305
28	9.0×10^{-5}	420	1352
40	1.4×10^{-4}	533	1305
51	8.0×10^{-5}	604	1068
66	3.0×10^{-5}	708	1019
81	2.0×10^{-5}	833	853
90	1.8×10^{-5}	930	959
110	1.0×10^{-5}	1106	807
123	1.0×10^{-5}	1220	623
132	1.0×10^{-5}	1316	679
141	1.0×10^{-5}	1400	608
149	1.2×10^{-5}	1500	433
164	2.4×10^{-5}	1600	465
170	1.2×10^{-5}	1500	470
178	8.0×10^{-6}	1392	465
185	7.0×10^{-6}	1300	567
197	6.0×10^{-6}	1153	541
208	5.0×10^{-6}	1022	774
220	4.5×10^{-6}	900	754
239 Power Off	4.0×10^{-6}	791	890
254	3.5×10^{-6}	699	1019
Test Terminated Due to Fracture of Positioning Rod			
--	--	RT	1157(3)
--	--	RT	1233(4)

TABLE XXIX. (Cont'd)

(1) Room Temperature Hardness of the Specimen on a Kentron Tester Using a Vickers Diamond Pyramid, a 150-Gram Load and a 15-Second Hold.

	1188 Kg/mm^2
	1073 Kg/mm^2
	1205 Kg/mm^2
Average	1155 Kg/mm^2

(2) Room Temperature Hardness of the Specimen on the Hot Hardness Tester Using a Vickers Diamond Pyramid (#2006), a 150-Gram Load and a 15-Second Hold.

	1103 Kg/mm^2
	1454 Kg/mm^2
	1428 Kg/mm^2
Average	1328 Kg/mm^2

(3) Room Temperature Hardness of the Specimen, After the Test Cycle, on the Hot Hardness Tester Using a Vickers Diamond Pyramid (#2006), a 150-Gram Load and a 15-Second Hold.

	1178 Kg/mm^2
	1178 Kg/mm^2
	1198 Kg/mm^2
	1178 Kg/mm^2
	1052 Kg/mm^2
Average	1157 Kg/mm^2

(4) Room Temperature Hardness of the Specimen After the Test Cycle, on a Kentron Tester Using a Vickers Diamond Pyramid, a 150-Gram Load and a 15-Second Hold.

	1170 Kg/mm^2
	1320 Kg/mm^2
	1210 Kg/mm^2
Average	1233 Kg/mm^2

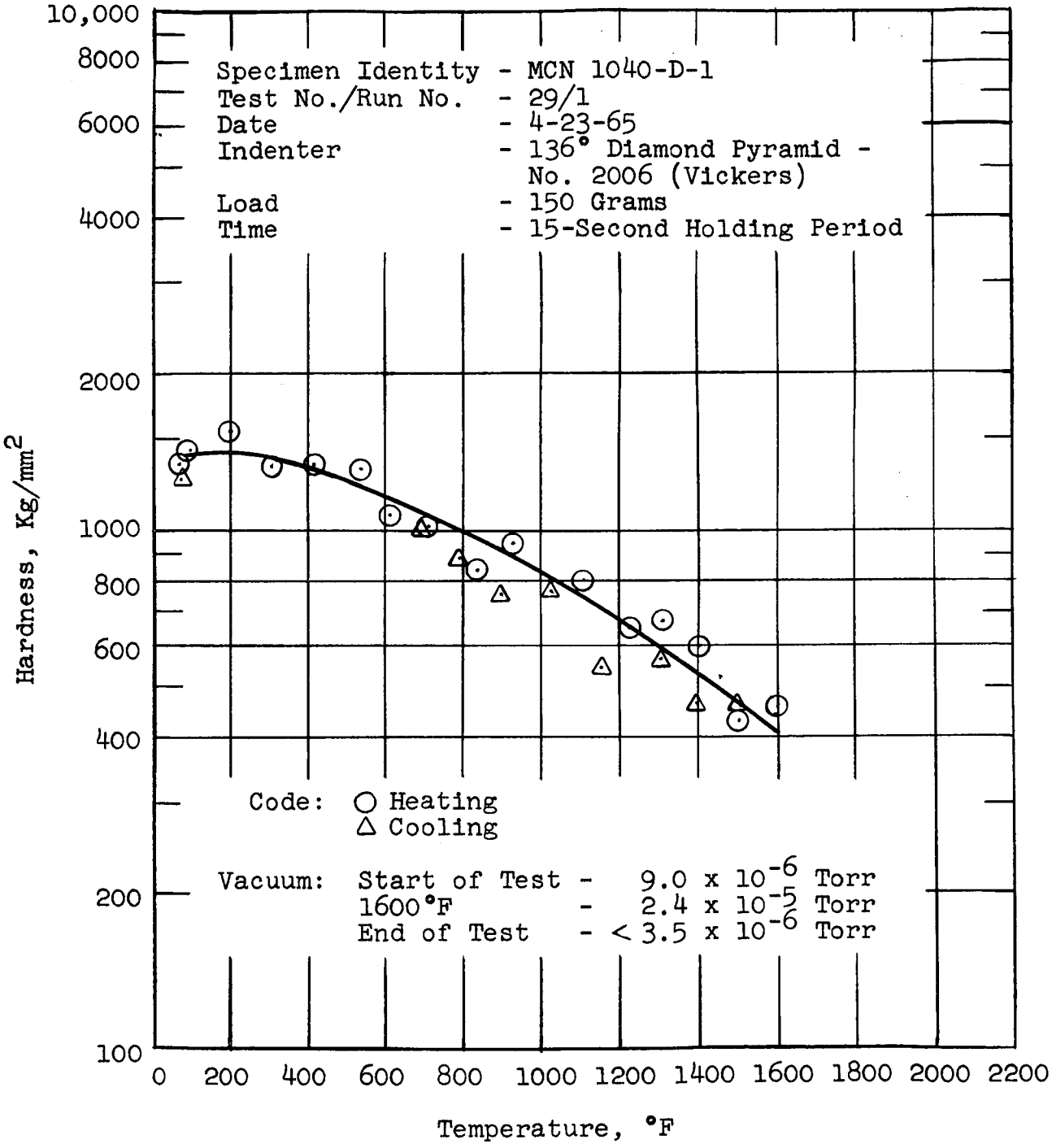

Figure 54. Hardness of Zircoa 1027 as a Function of Temperature.

TABLE XXX. HOT HARDNESS DATA FOR K-601

Specimen Identity - MCN 1041-D-1

Test No./Run No. - 25/1

Date - April 19, 1965

Indenter - 136° Diamond Pyramid - #2006 (Vickers)

Load - 150 Grams

Holding Time - 15 Seconds

Time Minutes	Vacuum Torr	Temp. °F	Hardness Kg/mm^2
--	--	RT	2344(1)
0	--	RT	1958(2)
4	9.0×10^{-6}	117	2094
11	3.0×10^{-5}	214	2293
21	4.5×10^{-5}	325	1802
32	9.5×10^{-5}	441	2094
43	1.3×10^{-4}	525	2048
53	7.5×10^{-5}	604	1599
67	4.5×10^{-5}	716	1730
82	3.0×10^{-5}	830	1879
90	2.5×10^{-5}	930	1599
109	1.8×10^{-5}	1105	1509
122	1.2×10^{-5}	1216	1282
132	1.2×10^{-5}	1400	1328
145	1.2×10^{-5}	1484	1239
160	1.6×10^{-5}	1600	1239
178	9.0×10^{-6}	1484	1121
193	7.0×10^{-6}	1342	1239
201	6.5×10^{-6}	1282	1328
207	6.5×10^{-6}	1078	1454
215	5.5×10^{-6}	984	1538
225 Power Off	5.0×10^{-6}	900	1599
243	4.5×10^{-6}	765	1599
265	4.0×10^{-6}	649	1663
285	3.0×10^{-6}	553	1879
335	2.5×10^{-6}	427	2004
390	2.2×10^{-6}	343	1961
520	1.0×10^{-6}	222	1766
578	2.0×10^{-6}	181	1961
7-20-65	--	RT	2158(3)
--	--	RT	1983(4)

TABLE XXX. (Cont'd)

(1) Room Temperature Hardness of the Specimen on a Kentron Tester Using a Vickers Diamond Pyramid, a 150-Gram Load and 15-Second Hold.

	2475 Kg/mm^2
	2340 Kg/mm^2
	2217 Kg/mm^2
Average	2344 Kg/mm^2

(2) Room Temperature Hardness of the Specimen on the Hot Hardness Tester Using a Vickers Diamond Pyramid (#2006), a 150-Gram Load and a 15-Second Hold.

	1724 Kg/mm^2
	1724 Kg/mm^2
	2141 Kg/mm^2
Average	1958 Kg/mm^2

(3) Room Temperature Hardness of the Specimen, After the Test Cycle, on the Hot Hardness Tester Using a Vickers Diamond Pyramid (#2006), a 150-Gram Load and a 15-Second Hold.

	1961 Kg/mm^2
	2094 Kg/mm^2
	2190 Kg/mm^2
	2190 Kg/mm^2
Average	2158 Kg/mm^2

(4) Room Temperature Hardness of the Specimen, After the Test Cycle, on a Kentron Tester Using a Vickers Diamond Pyramid, a 150-Gram Load and a 15-Second Hold.

	2040 Kg/mm^2
	2040 Kg/mm^2
	1870 Kg/mm^2
Average	1983 Kg/mm^2

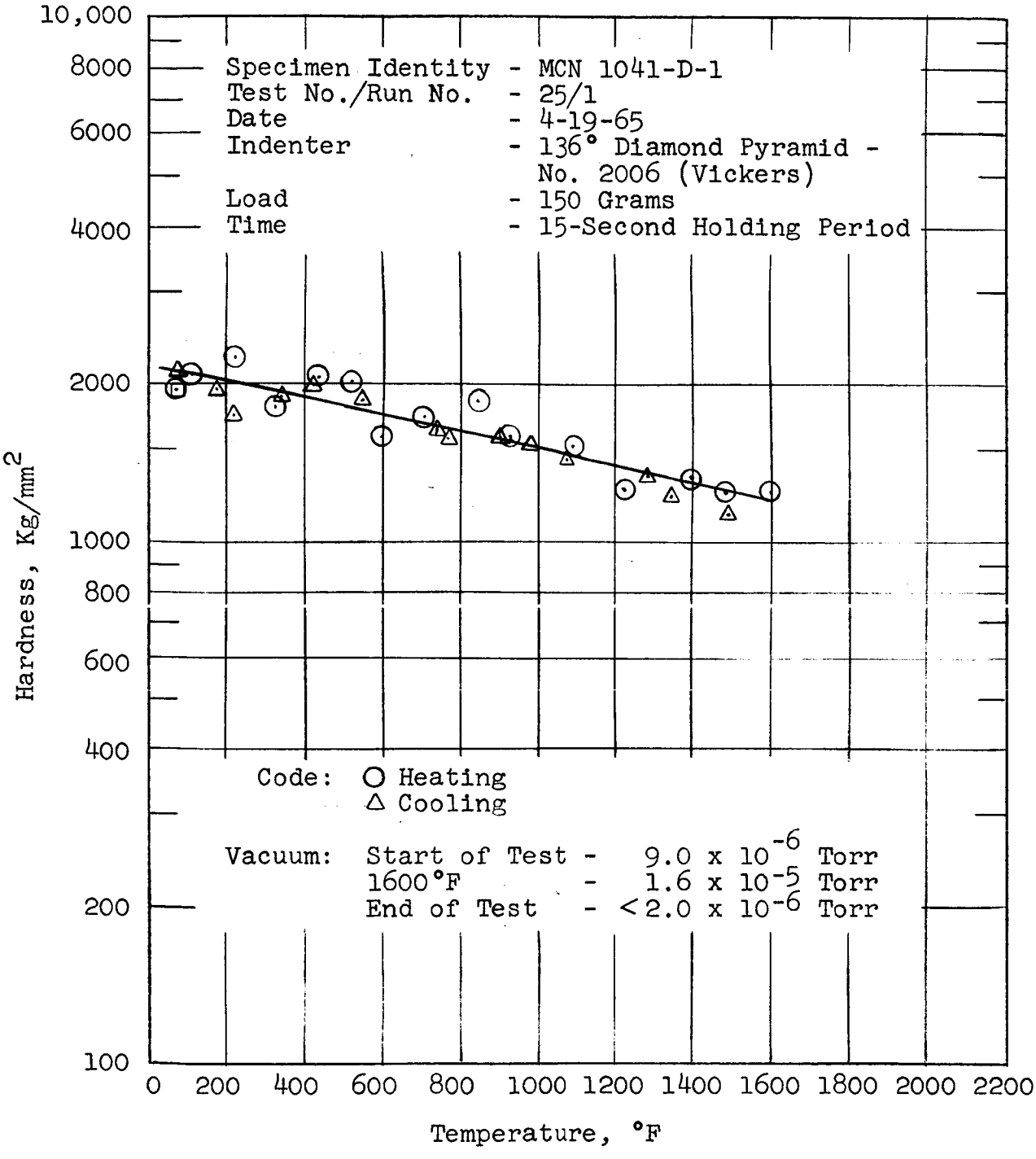

Figure 55. Hardness of K601 as a Function of Temperature.

TABLE XXXI. HOT HARDNESS DATA FOR TiC+5%W

Specimen Identity - MCN 1043-D-3

Test No./Run No. - 21/1

Date - April 14, 1965

Indenter - 136° Diamond Pyramid - #2006 (Vickers)

Load - 150 Grams

Holding Time - 15 Seconds

Time Minutes	Vacuum Torr	Temp. °F	Hardness Kg/mm^2
--	--	RT	2418(1)
0	6.0×10^{-6}	RT	2129(2,3)
4	6.0×10^{-6}	117	2293
13	1.8×10^{-5}	207	2048(3)
23	3.5×10^{-5}	303	2190
34	8.0×10^{-5}	406	1802
44	9.0×10^{-5}	503	1840
60	6.0×10^{-5}	633	1481
71	4.0×10^{-5}	706	1730
83	3.5×10^{-5}	801	988(3)
94	3.5×10^{-5}	948	1198
100	3.0×10^{-5}	1022	1068
117	1.8×10^{-5}	1133	1352
123	1.5×10^{-5}	1218	853
132	1.8×10^{-5}	1304	853
158	--	1404	853
178	2.2×10^{-5}	1511	853
191	1.0×10^{-5}	1396	807
199	8.0×10^{-6}	1304	807
201	8.8×10^{-6}	1204	818
227 Power Off	7.8×10^{-6}	947	1019
243	6.5×10^{-6}	800	1158
270	5.0×10^{-6}	653	1662
320	4.0×10^{-6}	478	1481
382	3.5×10^{-6}	361	1599
500	3.0×10^{-6}	230	2141
--	--	RT	2083(3,4)
--	--	RT	2277(5)

TABLE XXXI. (Cont'd)

(1) Room Temperature Hardness of the Specimen on a Kentron Tester Using a Vickers Diamond Pyramid, a 150-Gram Load and a 15-Second Hold.

	2447 Kg/mm^2
	2313 Kg/mm^2
	2495 Kg/mm^2
Average	2418 Kg/mm^2

(2) Room Temperature Hardness of the Specimen on the Hot Hardness Tester Using a Vickers Diamond Pyramid (#2006), a 150-Gram Load and a 15-Second Hold.

	2004 Kg/mm^2
	2048 Kg/mm^2
	2462 Kg/mm^2
	2004 Kg/mm^2
Average	2129 Kg/mm^2

(3) Small Cracks were Observed Around Hardness Impression.

(4) Room Temperature Hardness of the Specimen, After the Test Cycle, on the Hot Hardness Tester Using a Vickers Diamond Pyramid (#2006), a 150-Gram Load and a 15-Second Hold.

	2094 Kg/mm^2
	2347 Kg/mm^2
	1961 Kg/mm^2
	2094 Kg/mm^2
	1919 Kg/mm^2
Average	2083 Kg/mm^2

(5) Room Temperature Hardness of the Specimen, After the Test Cycle, on a Kentron Tester Using a Vickers Diamond Pyramid, a 150-Gram Load and 15-Second Hold.

	2450 Kg/mm^2
	2190 Kg/mm^2
	2190 Kg/mm^2
Average	2277 Kg/mm^2

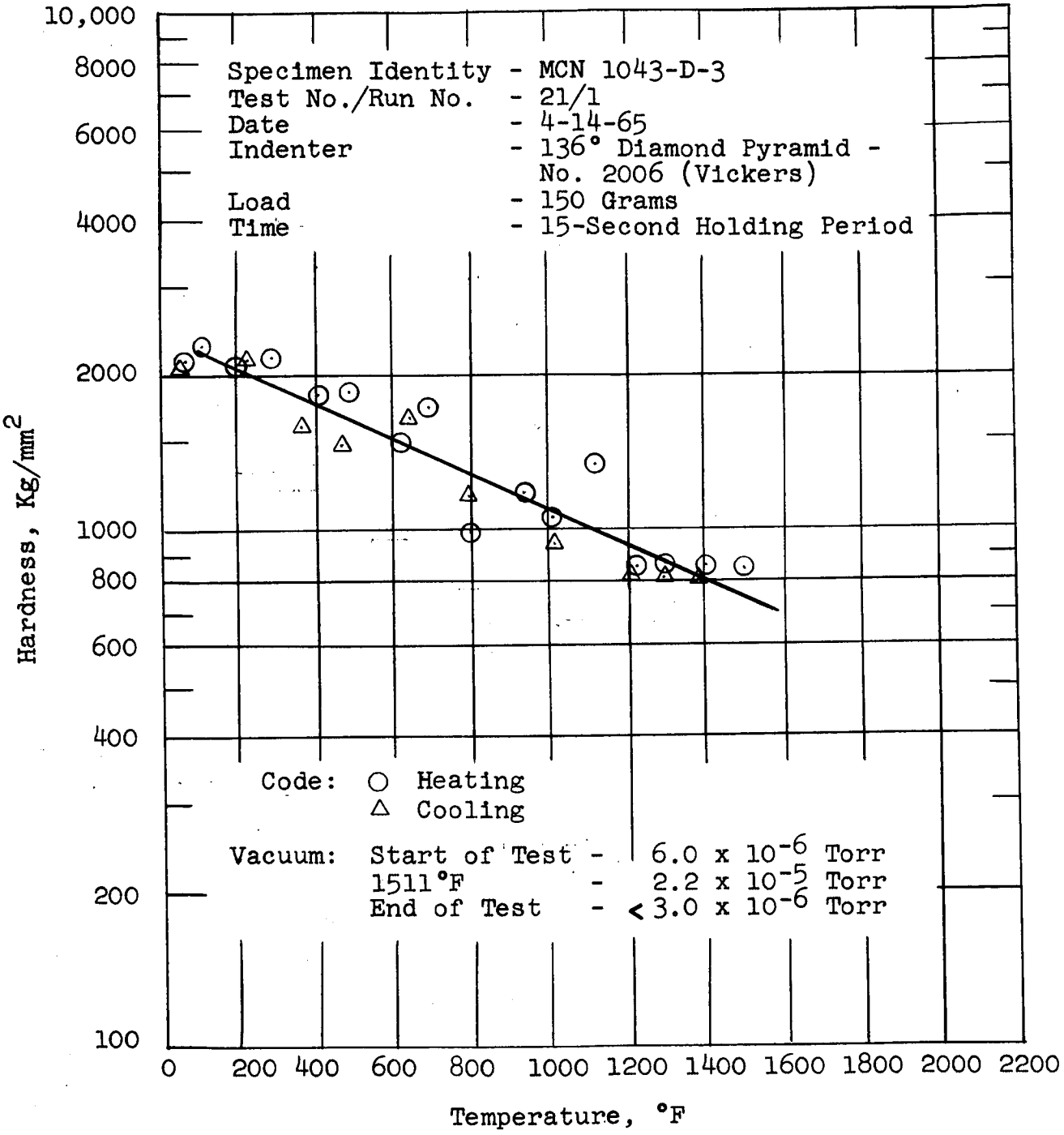

Figure 56. Hardness of TiC+5%W as a Function of Temperature.

TABLE XXXII. HOT HARDNESS DATA FOR TiC+10%Cb

Specimen Identity - MCN 1045-D-3

Test No./Run No. - 20/1

Date - March 24, 1965

Indenter - 136° Diamond Pyramid - #2006 (Vickers)

Load - 150 Grams

Holding Time - 15 Seconds

Time Minutes	Vacuum Torr	Temp. °F	Hardness Kg/mm^2
--	--	RT	2597(1)
0	2.0×10^{-5}	RT	2882(2)
5	9.0×10^{-6}	122	2585
17	2.8×10^{-5}	238	2650
22	3.0×10^{-5}	323	2094
31	8.0×10^{-5}	412	2190
40	9.6×10^{-5}	505	2048
55	5.8×10^{-5}	600	1879
80	5.0×10^{-5}	760	1402
85	2.0×10^{-5}	831	1139
96	2.0×10^{-5}	966	1004
101	2.0×10^{-5}	1021	890
109	1.0×10^{-5}	1111	796
122	1.0×10^{-5}	1207	734
126	1.2×10^{-5}	1262	715
136	1.2×10^{-5}	1321	706
146	1.6×10^{-5}	1421	608
160	1.6×10^{-5}	1511	567
178	9.6×10^{-6}	1330	890
199	7.4×10^{-6}	1290	734
205	6.8×10^{-6}	1134	878
237	5.2×10^{-6}	941	1158
253 Power Off	4.8×10^{-6}	810	1427
271	4.5×10^{-6}	666	1730
312	3.4×10^{-6}	529	1730
360	2.4×10^{-6}	410	1961
3-25-65	--	RT	2533(3)
--	--	RT	2327(4)

TABLE XXXII. (Cont'd)

(1) Room Temperature Hardness of the Specimen on a Kentron Tester Using a Vickers Diamond Pyramid, a 150-Gram Load and a 15-Second Hold.

	2700 Kg/mm^2
	2495 Kg/mm^2
	2597 Kg/mm^2
Average	2597 Kg/mm^2

(2) Room Temperature Hardness of the Specimen on the Hot Hardness Tester Using a Vicker Diamond Pyramid (#2006), a 150-Gram Load and a 15-Second Hold.

	3097 Kg/mm^2
	3461 Kg/mm^2
	2347 Kg/mm^2
	2788 Kg/mm^2
	2718 Kg/mm^2
Average	2882 Kg/mm^2

(3) Room Temperature Hardness of the Specimen, After the Test Cycle, on the Hot Hardness Tester Using a Vickers Diamond Pyramid (#2006), a 150-Gram Load and a 15-Second Hold.

	2462 Kg/mm^2
	2347 Kg/mm^2
	2141 Kg/mm^2
	3182 Kg/mm^2
Average	2533 Kg/mm^2

(4) Room Temperature Hardness of the Specimen, After the Test Cycle, on a Kentron Tester Using a Vickers Diamond Pyramid, a 150-Gram Load and a 15-Second Hold.

	2270 Kg/mm^2
	2260 Kg/mm^2
	2450 Kg/mm^2
Average	2327 Kg/mm^2

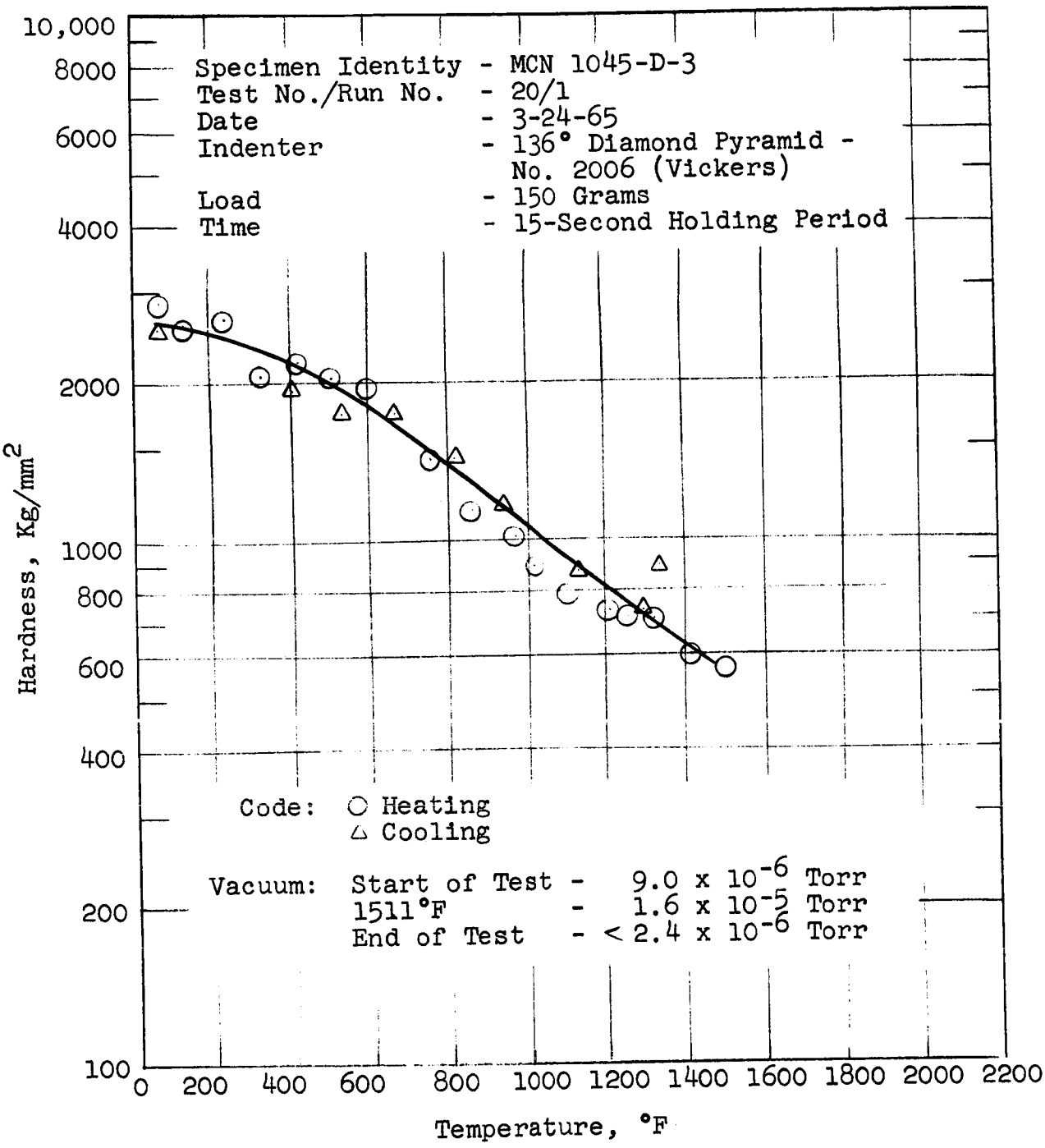

Figure 57. Hardness of TiC+10%Cb as a Function of Temperature.

TABLE XXXIII. HOT HARDNESS DATA FOR GRADE 7178

Specimen Identity - MCN 1046-D-1

Test No./Run No. - 7/2

Date - June 17, 1965

Indenter - 136° Diamond Pyramid - #2006 (Vickers)

Load - 150 Grams

Holding Time - 15 Seconds

Time Minutes	Vacuum Torr	Temp. °F	Hardness Kg/mm^2
--	--	RT	2850(1)
0	8.0×10^{-6}	RT	2380(2)
5	3.0×10^{-5}	100	2720
17	4.2×10^{-5}	207	2790
25	8.4×10^{-5}	306	2520
32	9.6×10^{-5}	420	2460
38	9.6×10^{-5}	505	2400
46	8.0×10^{-5}	600	2350
57	5.4×10^{-5}	693	2090
77	3.0×10^{-5}	836	2140
90	2.0×10^{-5}	907	2090
109	1.6×10^{-5}	1012	1920
133	1.6×10^{-5}	1190	2090
152	1.8×10^{-5}	1316	1600
171	1.4×10^{-5}	1384	1510
180	1.6×10^{-5}	1517	1430
192	2.0×10^{-5}	1600	1430
193	2.0×10^{-5}	1600	1330
206	1.0×10^{-5}	1484	1450
266 Power Off	5.0×10^{-6}	979	2090
335	2.5×10^{-6}	535	2290
387	2.5×10^{-6}	400	2400
408	2.5×10^{-6}	358	2787
430	2.5×10^{-6}	319	2400
467	2.0×10^{-6}	275	2350
6-18-65	--	RT	2830(3)

TABLE XXXIII. (Cont'd)

(1) Room Temperature Hardness of the Specimen on a Kentron Tester Using a Vickers Diamond Pyramid, a 150-Gram Load and 15-Second Hold.

	2940 Kg/mm^2
	2940 Kg/mm^2
	2520 Kg/mm^2
	3000 Kg/mm^2
Average	2850 Kg/mm^2

(2) Room Temperature Hardness of the Specimen on the Hot Hardness Tester Using a Vickers Diamond Pyramid (#2006), a 150-Gram Load and a 15-Second Hold.

	2460 Kg/mm^2
	2290 Kg/mm^2
	2190 Kg/mm^2
	2650 Kg/mm^2
	2290 Kg/mm^2
Average	2380 Kg/mm^2

(3) Room Temperature Hardness of the Specimen, After the Test Cycle, on the Hot Hardness Tester Using a Vickers Diamond Pyramid (#2006), a 150-Gram Load and a 15-Second Hold.

	2580 Kg/mm^2
	2790 Kg/mm^2
	2940 Kg/mm^2
	3010 Kg/mm^2
Average	2830 Kg/mm^2

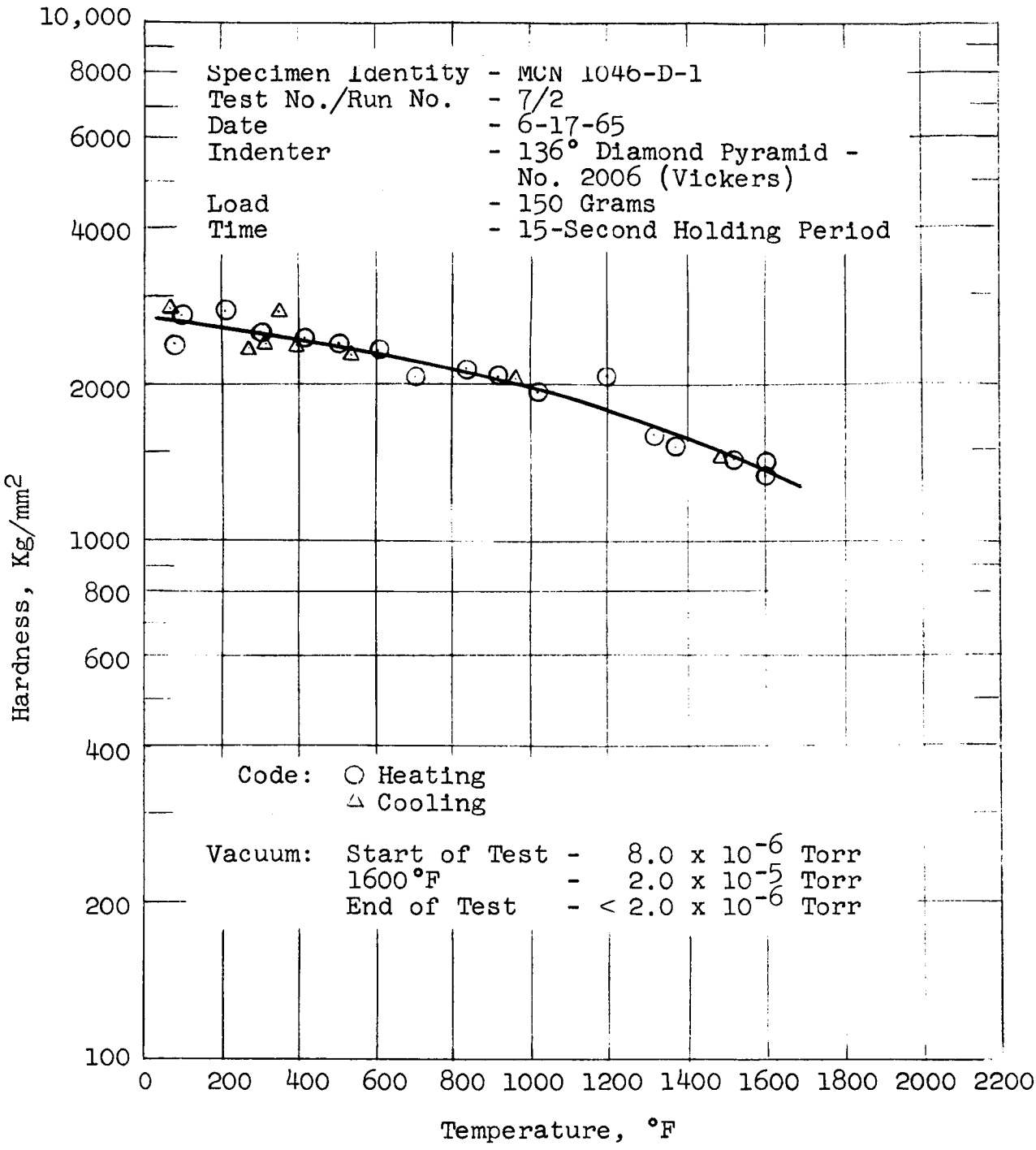

Figure 58. Hardness of Grade 7178 as a Function of Temperature.

TABLE XXXIV. HOT HARDNESS DATA FOR STAR J

Specimen Identity - MCN 1047-D-2

Condition - As-Cast

Test No./Run No. - 22/1

Date - April 15, 1965

Indenter - 136° Diamond Pyramid - #2006 (Vickers)

Load - 150 Grams

Holding Time - 15 Seconds

Time Minutes	Vacuum Torr	Temp. °F	Hardness Kg/mm^2
--	--	RT	775(1)
0	8.0×10^{-6}	RT	934(2)
4	1.4×10^{-5}	122	785
12	2.0×10^{-5}	200	944
24	4.0×10^{-5}	306	930
35	7.0×10^{-5}	414	744
45	8.4×10^{-5}	499	853
59	5.4×10^{-5}	601	744
71	3.6×10^{-5}	710	796
85	2.5×10^{-5}	856	724
90	2.4×10^{-5}	910	764
100	1.8×10^{-5}	1035	774
110	1.4×10^{-5}	1139	1376
120	1.2×10^{-5}	1225	841
132	1.0×10^{-5}	1313	706
156	1.0×10^{-5}	1388	608
170	--	1504	396
203	7.0×10^{-6}	1204	535
210	6.0×10^{-6}	1100	594
223	5.0×10^{-6}	979	764
240 Power Off	4.0×10^{-6}	851	646
252	4.0×10^{-6}	771	890
267	4.0×10^{-6}	685	764
286	3.5×10^{-6}	595	724
321	3.0×10^{-6}	490	638
364	2.5×10^{-6}	367	630
--	--	250	973
4-16-65	--	RT	937(3)
--	--	RT	794(4)

TABLE XXXIV. (Cont'd)

(1) Room Temperature Hardness of the Specimen on a Kentron Tester Using a Vickers Diamond Pyramid, a 150-Gram Load and a 15-Second Hold.

	808 Kg/mm^2
	718 Kg/mm^2
	799 Kg/mm^2
Average	775 Kg/mm^2

(2) Room Temperature Hardness of the Specimen on the Hot Hardness Tester Using a Vickers Diamond Pyramid (#2006), a 150-Gram Load and a 15-Second Hold.

	818 Kg/mm^2
	917 Kg/mm^2
	1068 Kg/mm^2
Average	934 Kg/mm^2

(3) Room Temperature Hardness of the Specimen, After the Test Cycle, on the Hot Hardness Tester Using a Vickers Diamond Pyramid (#2006), a 150-Gram Load and a 15-Second Hold.

	959 Kg/mm^2
	818 Kg/mm^2
	1035 Kg/mm^2
Average	937 Kg/mm^2

(4) Room Temperature Hardness of the Specimen, After the Test Cycle, on a Kentron Tester Using a Vickers Diamond Pyramid, a 150-Gram Load and a 15-Second Hold.

	836 Kg/mm^2
	765 Kg/mm^2
	782 Kg/mm^2
Average	794 Kg/mm^2

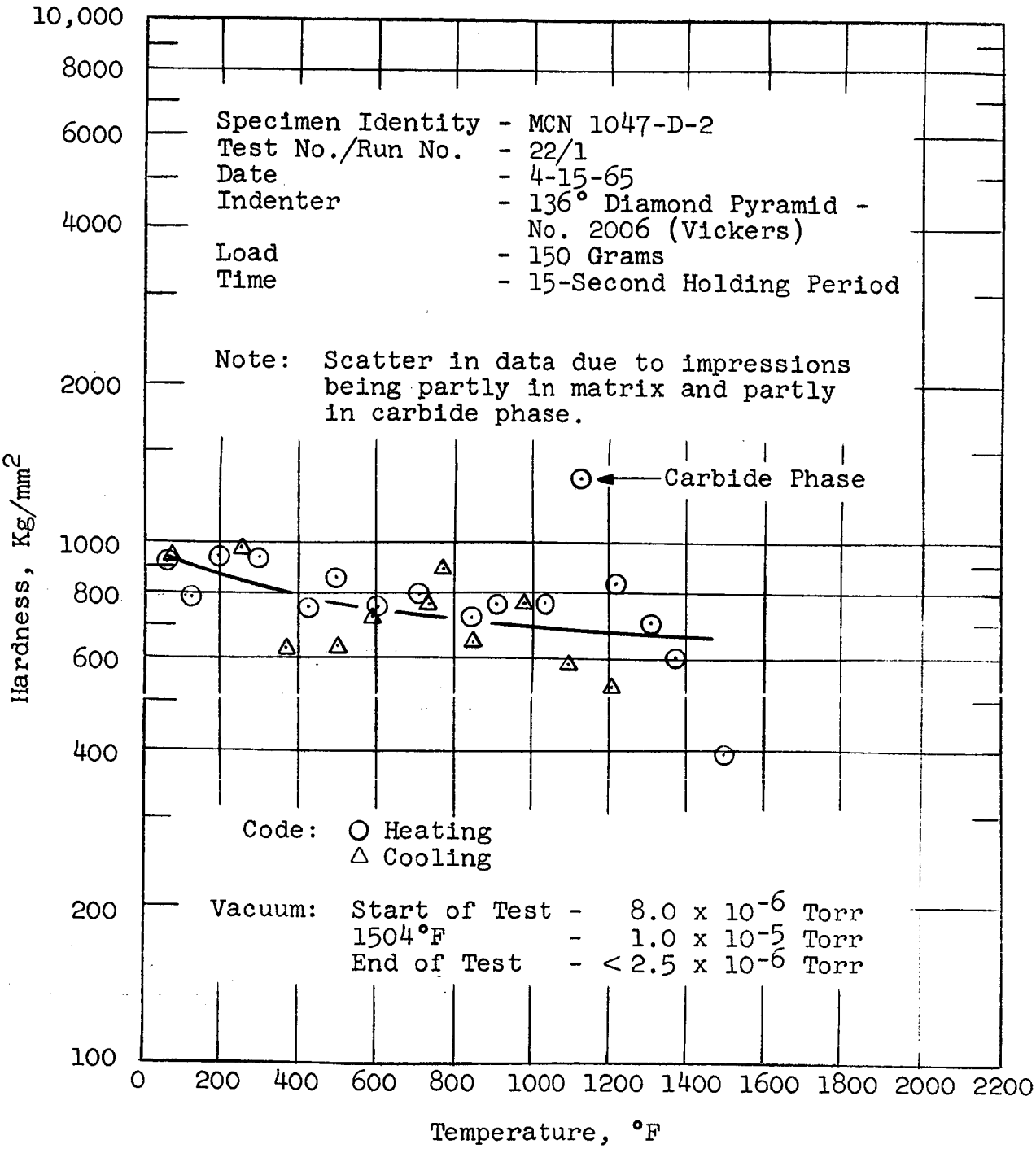

Figure 59. Hardness of Star J as a Function of Temperature.

TABLE XXXV. SUMMARY OF HOT HARDNESS DATA OF THE CANDIDATE BEARING MATERIALS

Material	Hardness, Kg/mm^2									
	RT		400°F		800°F		1200°F		1600°F	
	100 gm.	150 gm.	100 gm.	150 gm.	100 gm.	150 gm.	100 gm.	150 gm.	100 gm.	150 gm.
Mo-TZM (2250°F/1/2 Hr)	310	310	260	260	230	225	210	205	205	195
Tungsten (2000°F/1 Hr)										
Heating	400	-	300	-	180	-	145	-	140	-
Cooling	400	-	190	-	140	-	140	-	140	-
Tungsten (2200°F/2 Hr)										
Heating	430	420	290	330	200	175	165	155	150	120
Cooling	-	-	230	260	160	-	150	-	150	-
Star J (As-Cast)	800(1)/ 1700(2)	940(4)	650(1)/ 1100(2)	800(4)	560(1)/ 840(2)	720(4)	500(1)/ 680(2)	680(4)/ 1300(2)	480(1)/ 580(2)	-
Carboloy 907	1550	1750	1300	1600	1070	1370	890	1020	730	570
Carboloy 999	1700	2350	1400	2050	1200	1600	1080	1200	1000	860
K601	2200	2150	1900	1900	1600	1610	1320	1400	1100	1200
Grade 7178	2600	2650	2300	2450	1950	2150	1650	1800	1400	1380
TiC	2200	2650	2000	2200	1450	1300	920	820	530	500
TiC+5%W	2650	2300	1920	1750	1300	1300	890	940	600	700
TiC+10%Mo										
Heating	(3)	4200	(3)	3600	(3)	1800	(3)	1100	(3)	870
Cooling	-	3400	-	2900	-	1600	-	1060	-	870

TABLE XXXV. (Cont'd)

Material	RT		400°F		800°F		1200°F		1600°F	
	100 gm.	150 gm.	100 gm.	150 gm.	100 gm.	150 gm.	100 gm.	150 gm.	100 gm.	150 gm.
TiC+10%Cb	2200	2600	1950	2200	1400	1400	980	810	680	480
TiB_2	(3)	3200	(3)	2400	(3)	1650	(3)	1150	(3)	780
Lucalox	(3)	2800	(3)	2450	(3)	1680	(3)	1120	(3)	750
Zircoa 1027	1250	1400	1090	1300	860	1000	620	670	430	420

(1) Matrix.

(2) Carbide Phase.

(3) Unable to Read Impressions.

(4) Considerable Scatter in Data Due to Impressions Being Partly in Matrix and Carbide Phase.

through the 0.2% offset or until material fracture occurred. No attempt was made to control the strain rate beyond the 0.2% offset due to the difficulty in applying the load at a uniform rate as the specimen deformed plastically. The valve setting on the testing machine to achieve the 0.005 inch/inch/minute strain rate in the elastic region was left unchanged for the duration of the test. Further details of the testing procedures and calibration methods used for the LVDT/extensometer system and load cell are described in quarterly progress report No. 7[2]. Initially, both the load cell and the extensometer system were calibrated after every test. However, after numerous tests, it was found that the accuracy of the load and strain measurements was not impaired by the shock imparted to the load train upon fracture of the specimens and the recalibration was not necessary after every test. Subsequently, the load cell and the extensometer system were calibrated at the start of each testing day.

The data obtained are reported in Table XXXVI. From the data, it can be seen that the Carboloy 907, Carboloy 999 and Grade 7178 specimens did not fracture at the 115,000-pound load limit of the Baldwin testing machine. In the case of the Carboloy 907 material, a 115,000-pound load imposed an average stress of 607,500 psi on the test specimens. Possible additional testing of these materials at room temperature utilizing equipment of greater capacity will be delayed until the completion of the elevated temperature tests. Because of their good ductility, the Mo-TZM alloy specimens did not fracture in compression and the tests were terminated at a total strain of 5%.

Examination of the load-strain curves revealed the existence of an elastic limit for Carboloy 907, Carboloy 999 and Zircoa 1027 in addition to the metallic materials Mo-TZM alloy, tungsten and Star J alloy. Deviation from elastic behavior of the Carboloy and Zircoa 1027 materials is associated with grain boundary slip due to the presence of cobalt in the grain boundaries in the case of the Carboloy materials and weaker secondary phases, formed by the presence of stabilizing elements, in the case of the Zircoa 1027 material. Load-strain curves for Carboloy 907 and Zircoa 1027 are shown in Figures 60 and 61. Figure 62 illustrates the low elastic limit of Star J alloy with respect to the relatively high ultimate strength.

The TiB_2, TiC and the refractory metal bonded TiC materials all exhibited elastic behavior until fracture as exemplified by the load-strain curve for TiC in Figure 63. However, initial fracture occurred at a load below the ultimate strength for both specimens of TiB_2 and in one specimen of TiC+10%Cb and TiC+5%W as illustrated in the load-strain curve for TiC+10%Cb, Figure 64. Photographs of the tested specimens are shown in Figures 64 thru 74.

The values for the modulus of elasticity reported for the materials in Table XXXVI were calculated from the stress-strain relationship measured in the compression tests using an estimated effective gauge length. As discussed previously[2], it will be necessary to verify the assumptions used in estimating the effective gauge length of the specimens by measuring the actual strain that occurs in a specimen during testing by means of strain gauges attached to the specimen. For this purpose, four strain gauges (Type #C6121) have been attached to a Mo-TZM alloy specimen in the center of the reduced section at 90° intervals, two parallel

TABLE XXXVI. ROOM TEMPERATURE COMPRESSION PROPERTIES OF CANDIDATE BEARING MATERIALS

Material	Specimen Identity	0.02% Offset[1] psi	0.2% Offset[1] psi	Strength at 1% Total Strain, psi	Ultimate Strength psi	Modulus of Elasticity, psi x 10^6		Elastic Limit[1] psi
Grade 999	MCN 1035-G-1	422,300	---	----	> 608,000[2]	83.4[3]	88.8[4]	306,000
	MCN 1035-G-2	484,000	---	----	> 612,000[2]	79.8[3]	85.0[4]	367,000
Grade 907	MCN 1036-G-1	422,000	---	----	> 608,000[2]	75.1[3]	80.0[4]	296,000
	MCN 1036-G-2	438,000	---	---	> 607,000[2]	73.2[3]	78.0[4]	307,000
Mo-TZM, Arc Cast (2350°F/1 Hour)	MCN 1037-G-1	89,400	102,000	102,000	107,200[5]	39.1[3]	41.6[4]	73,300
	MCN 1037-G-2	86,000	104,200	104,300	111,000[5]	41.6[3]	44.3[4]	68,300
Tungsten, Arc Cast (2000°F/1 Hour)	MCN 1038-G-2	91,400	132,000	142,500	157,000	48.7[3]	51.8[4]	68,700
	MCN 1038-G-3	120,800	147,000	152,000	154,000	50.8[3]	54.1[4]	84,200
Lucalox	MCN 1039-G-1	---	---	---	360,700	52.3[3]	55.7[4]	---
	MCN 1039-G-3	---	---	---	325,000	51.3[3]	54.6 [4]	---
Zircoa 1027	MCN 1040-G-1	178,000[6]	220,000[6]	226,000	240,500	31.4[3]	33.4[4]	152,000[6]
	MNC 1040-G-5	114,000[6]	236,000[6]	240,000	265,800	30.8[3]	32.8[4]	89,200[6]
TiC	MCN 1042-G-5	---	---	---	420,000	58.0[3]	61.7[4]	---
	MCN 1042-G-6	---	---	---	365,000	57.4[3]	61.1 [4]	---
TiC+5%W	MCN 1043-G-8	---	---	---	424,000[8]	54.5 [3]	58.0 [4]	---
	MCN 1043-G-9[7]	---	---	---	394,000	65.2 [3]	69.4 [4]	---
TiC+10%Mo	MCN 1044-G-5	---	---	---	335,000	51.2[3]	54.5[4]	---
	MCN 1044-G-6[7]	---	---	---	304,000	55.0 [3]	58.5 [4]	---
TiC+10%Cb	MCN 1045-G-8[7]	---	---	---	321,000	57.8[3]	61.6[4]	---
	MCN 1045-G-9	---	---	---	376,000[9]	61.2 [3]	65.2 [4]	---

TABLE XXXVI (Cont'd)

Material	Specimen Identity	0.02% Offset[1] psi	0.2% Offset[1] psi	Strength at 1% Total Strain, psi	Ultimate Strength psi	Modulus of Elasticity, psi x 10^6		Elastic Limit[1] psi
Grade 7178	MCN 1046-G-4	---	---	---	> 605,000[2]	80.6[3]	85.7[4]	---
	MCN 1046-G-9	---	---	---	> 603,000[2]	77.2[3]	82.2[4]	---
Star J (As Cast)	MCN 1047-G-2	87,000	152,500	189,000	270,500	30.4[3]	32.4[4]	57,700
	MCN 1047-G-8	74,500	147,800	195,200	277,000	33.8[3]	36.0 [4]	52,800
TiB_2	MCN 1048-G-3	---	---	---	332,000[10]	69.5[3]	74.0[4]	---
	MCN 1048-G-10	---	---	---	363,000[11]	72.4[3]	77.1[4]	---

(1) Specimens were Tested at a Strain Rate of 0.005 In/In/Min. Through 0.2% Offset.

(2) Test Terminated at Load Limit of Baldwin Testing Machine (115,000 lbs).

(3) 1.0-Inch Measured Gauge Length.

(4) 1.065-Inch Estimated Effective Gauge Length.

(5) Test Terminated at 5% Total Strain.

(6) Specimens were Tested at a Strain Rate of 0.010 In/In/Min. Through 0.2% Offset.

(7) Specimen was Loaded to 75% of Ultimate Strength; the Load was Released and the Extensometer was Removed. Subsequently, the Specimen was Loaded to Failure.

(8) Specimen Cracked and Deviated from Straight Line Portion of Load-Strain Curve at a Stress of 358,000 psi.

(9) Specimen Cracked and Deviated from Straight Line Portion of Load-Strain Curve at a Stress of 324,000 psi.

(10) Specimen Cracked and Deviated from Straight Line Portion of Load-Strain Curve at a Stress of 229,000 psi.

(11) Specimen Cracked and Deviated from Straight Line Portion of Load-Strain Curve at a Stress of 311,000 psi.

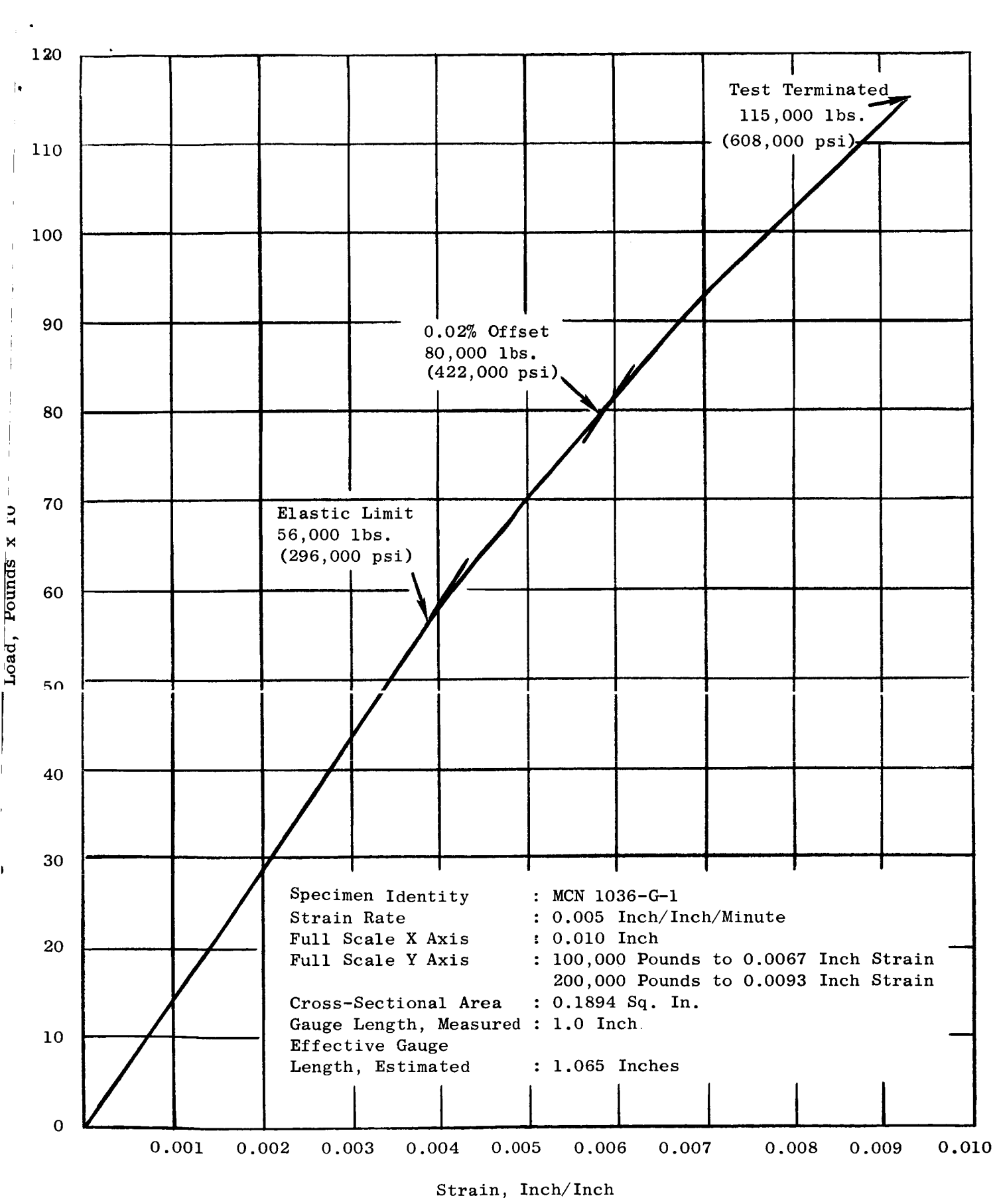

Figure 60. Room Temperature Load-Strain Curve for Carboloy 907 in Compression.

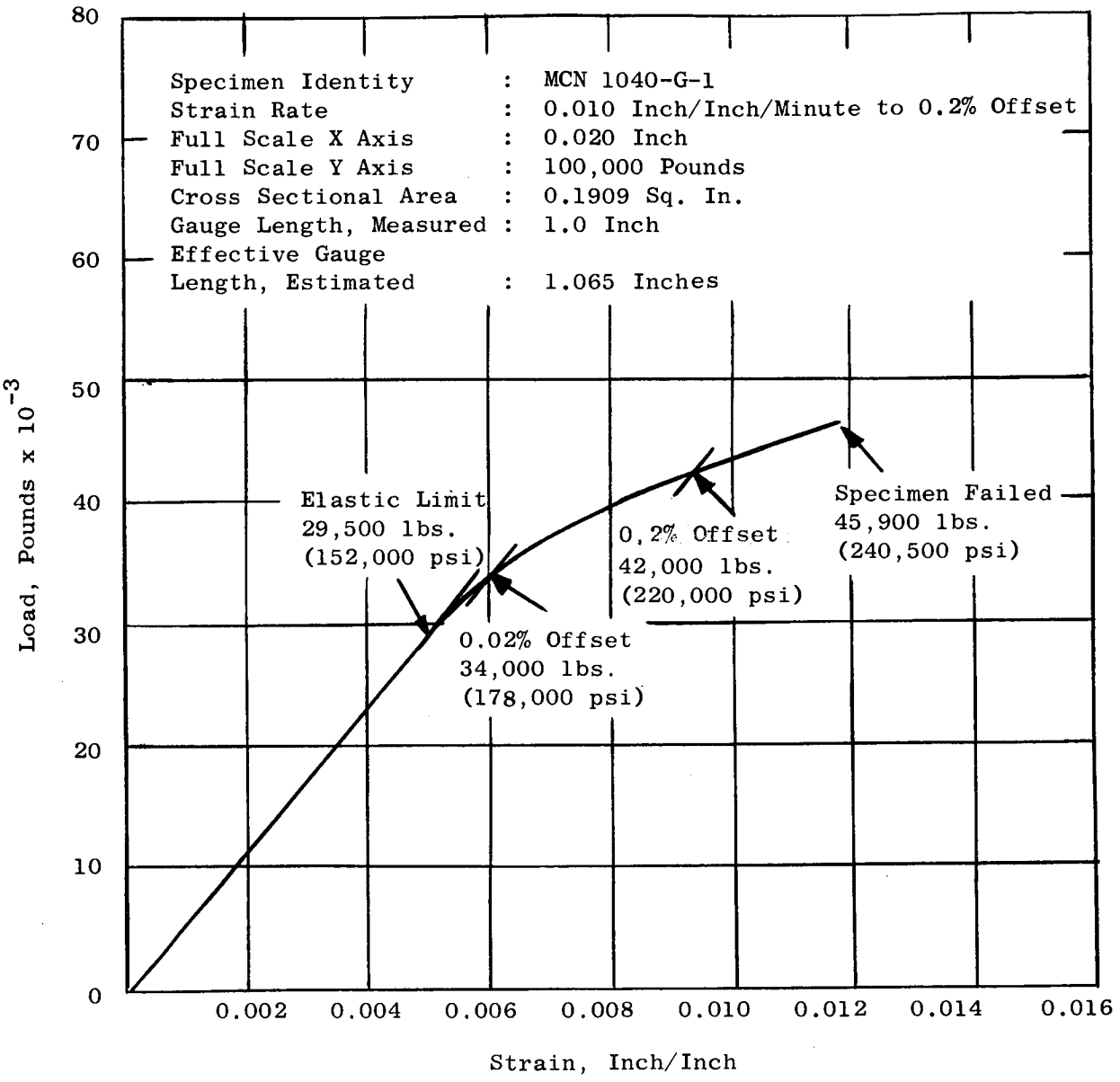

Figure 61. Room Temperature Load-Strain Curve for Zircoa 1027 in Compression.

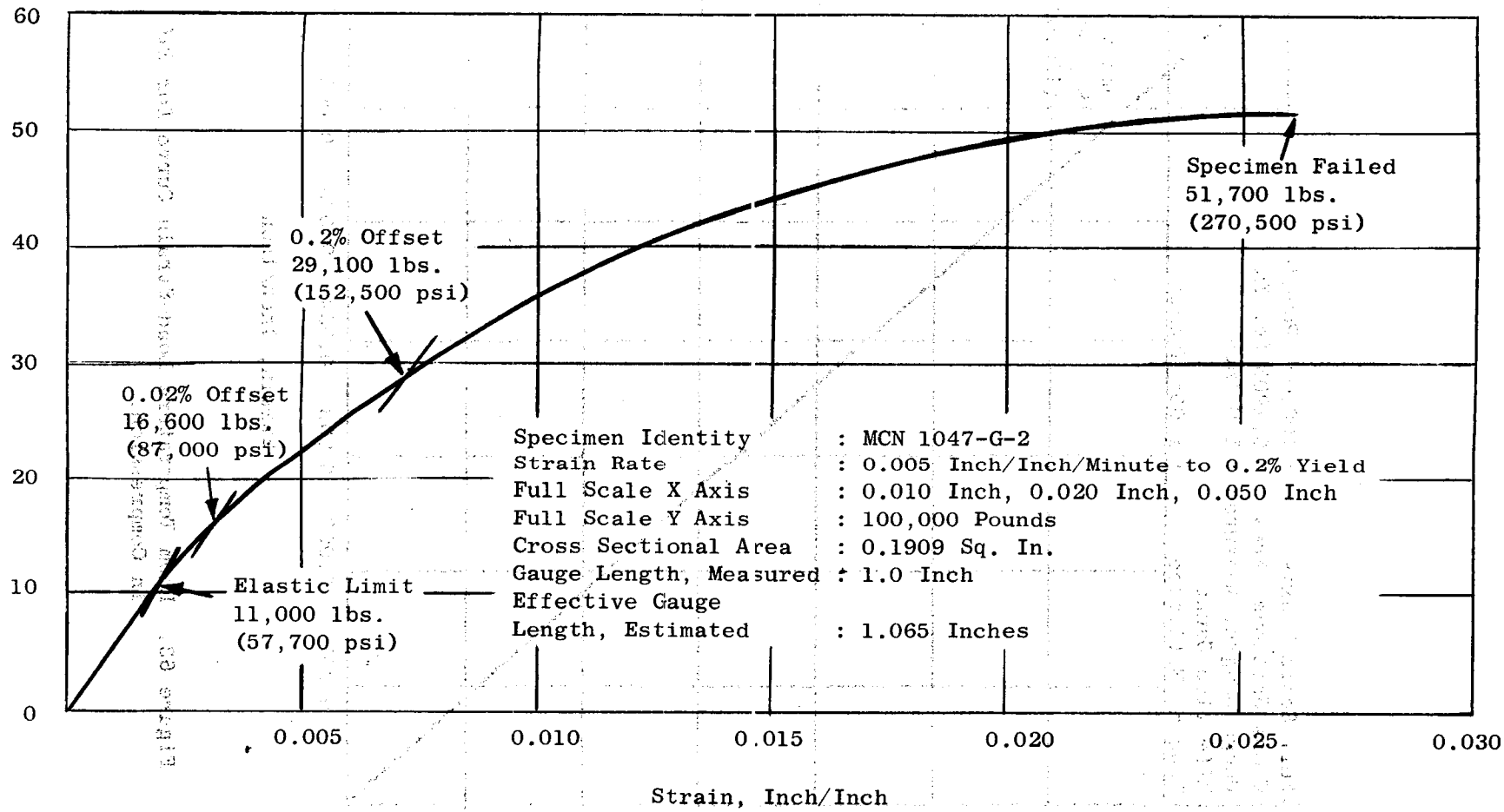

Figure 62. Room Temperature Load-Strain Curve for Star J in Compression.

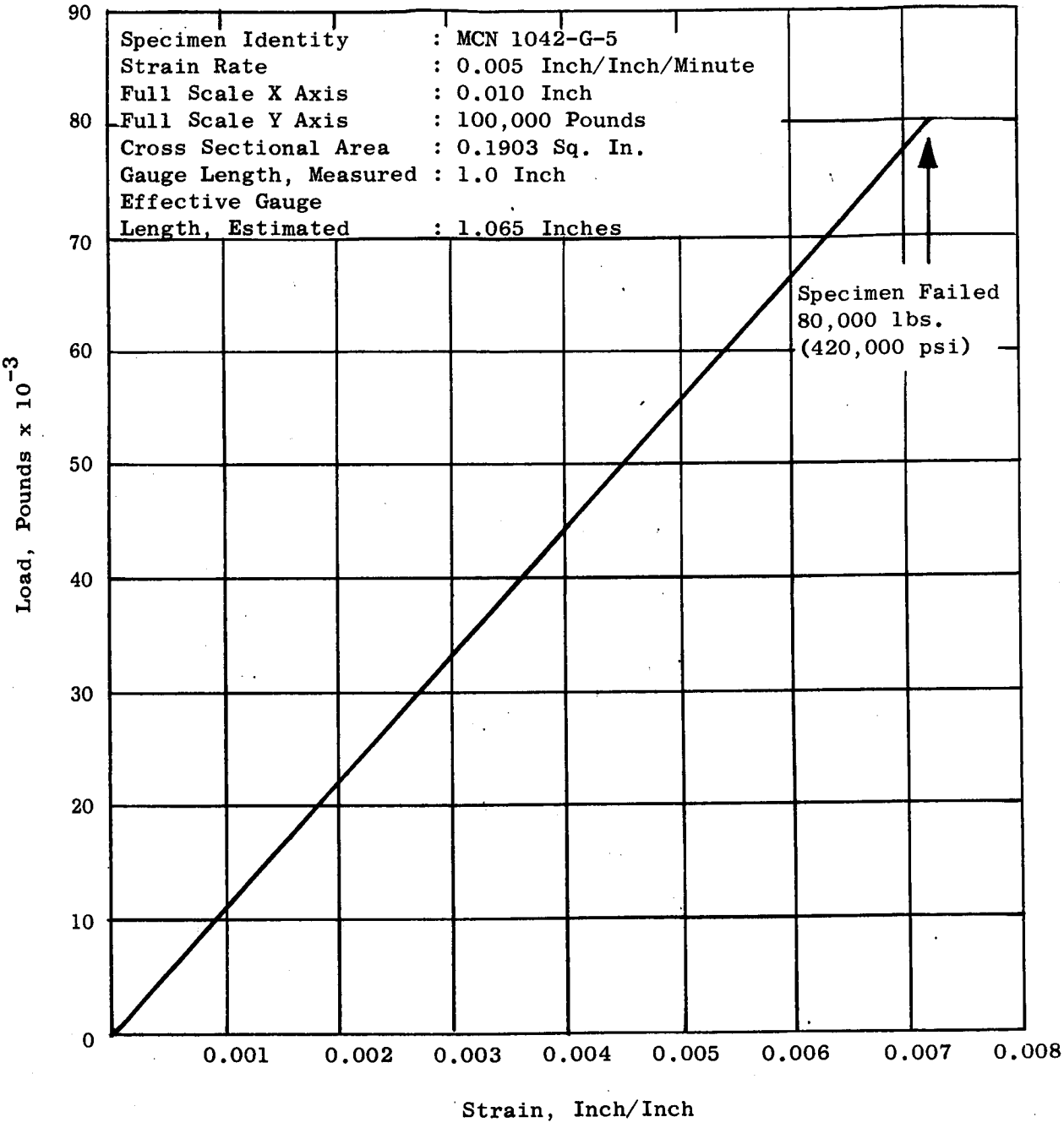

Figure 63. Room Temperature Load-Strain Curve for TiC in Compression.

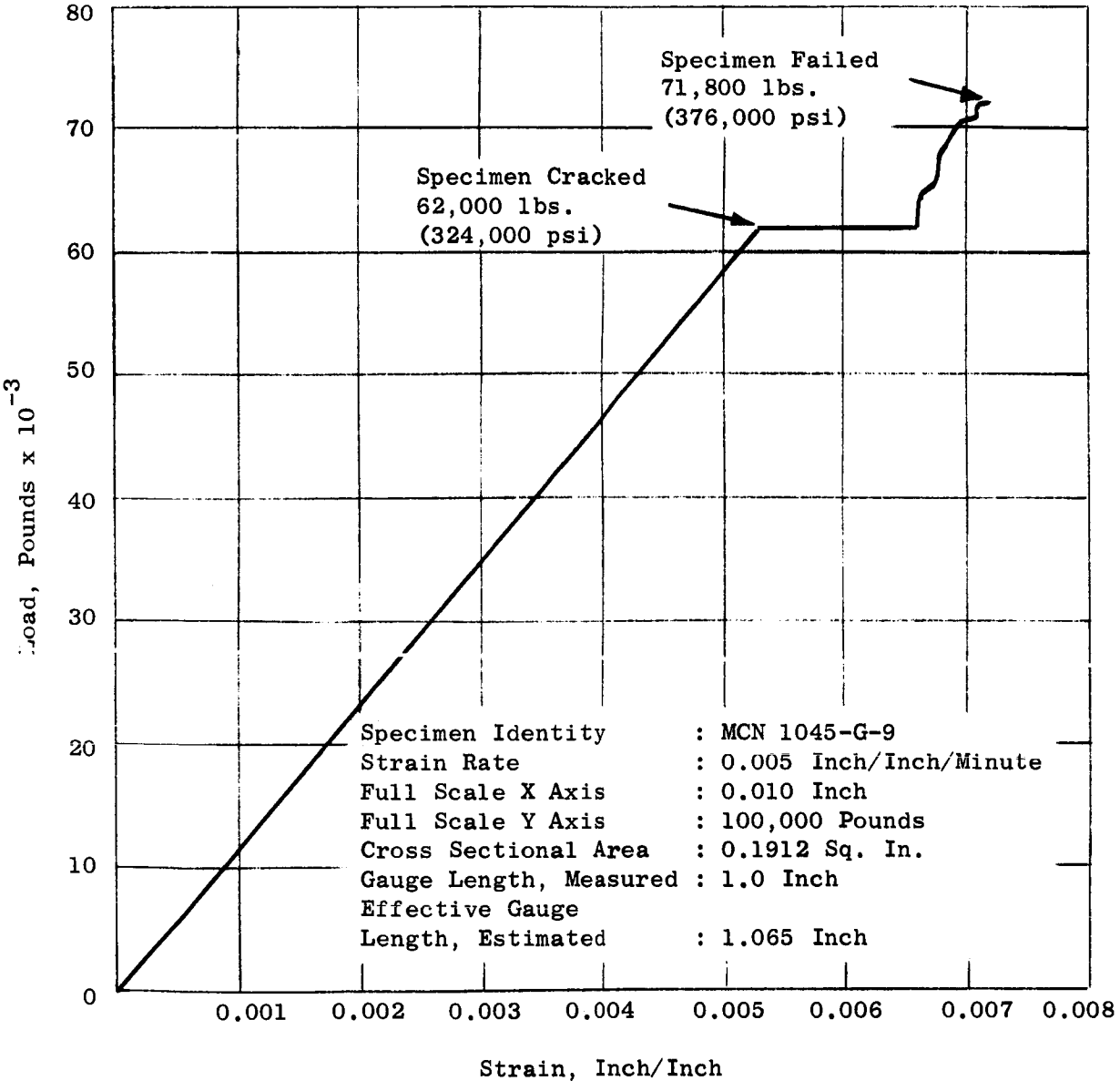

Figure 64. Room Temperature Load-Strain Curve for TiC+10%Cb in Compression.

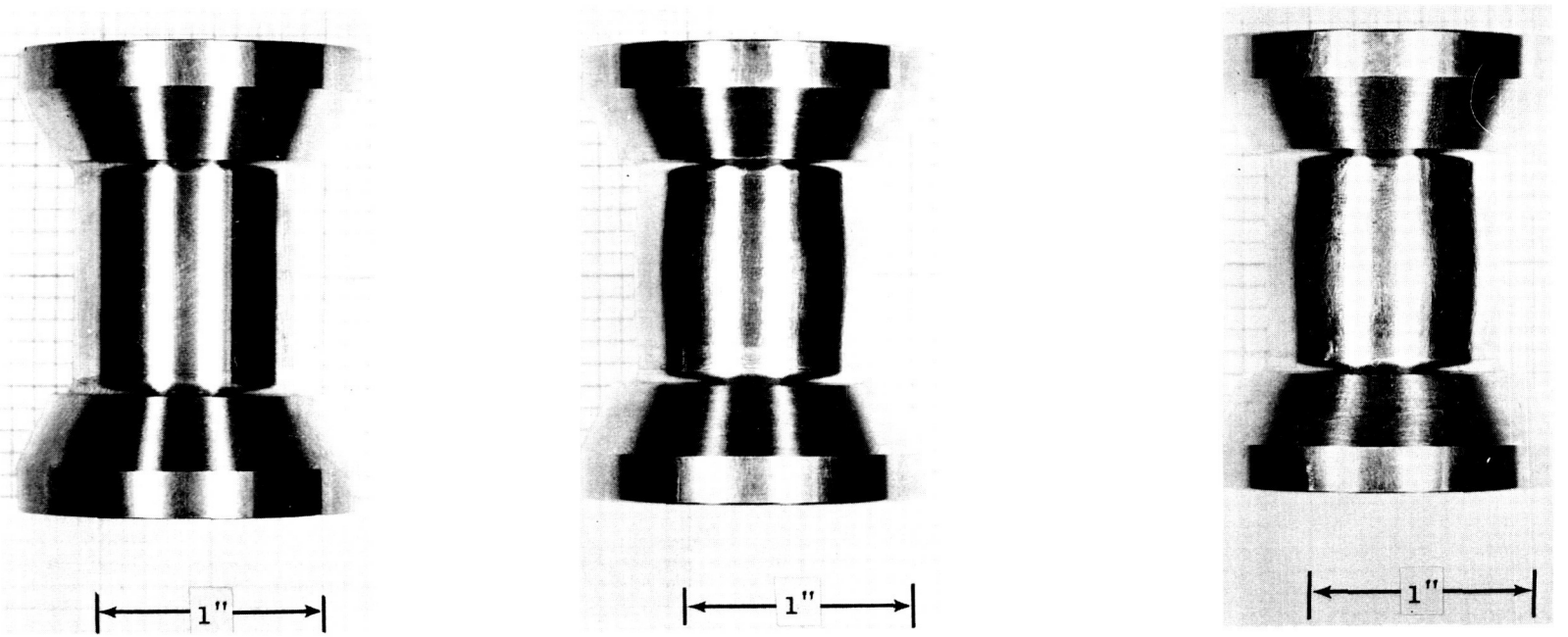

Figure 65. Photograph of Room Temperature Compression Specimens of Mo-TZM Alloy. Left, Before Test; Center, Specimen MCN 1037-G-1 After Test (C65062930); Right, Specimen MCN 1037-G-2 After Test (C65052933).

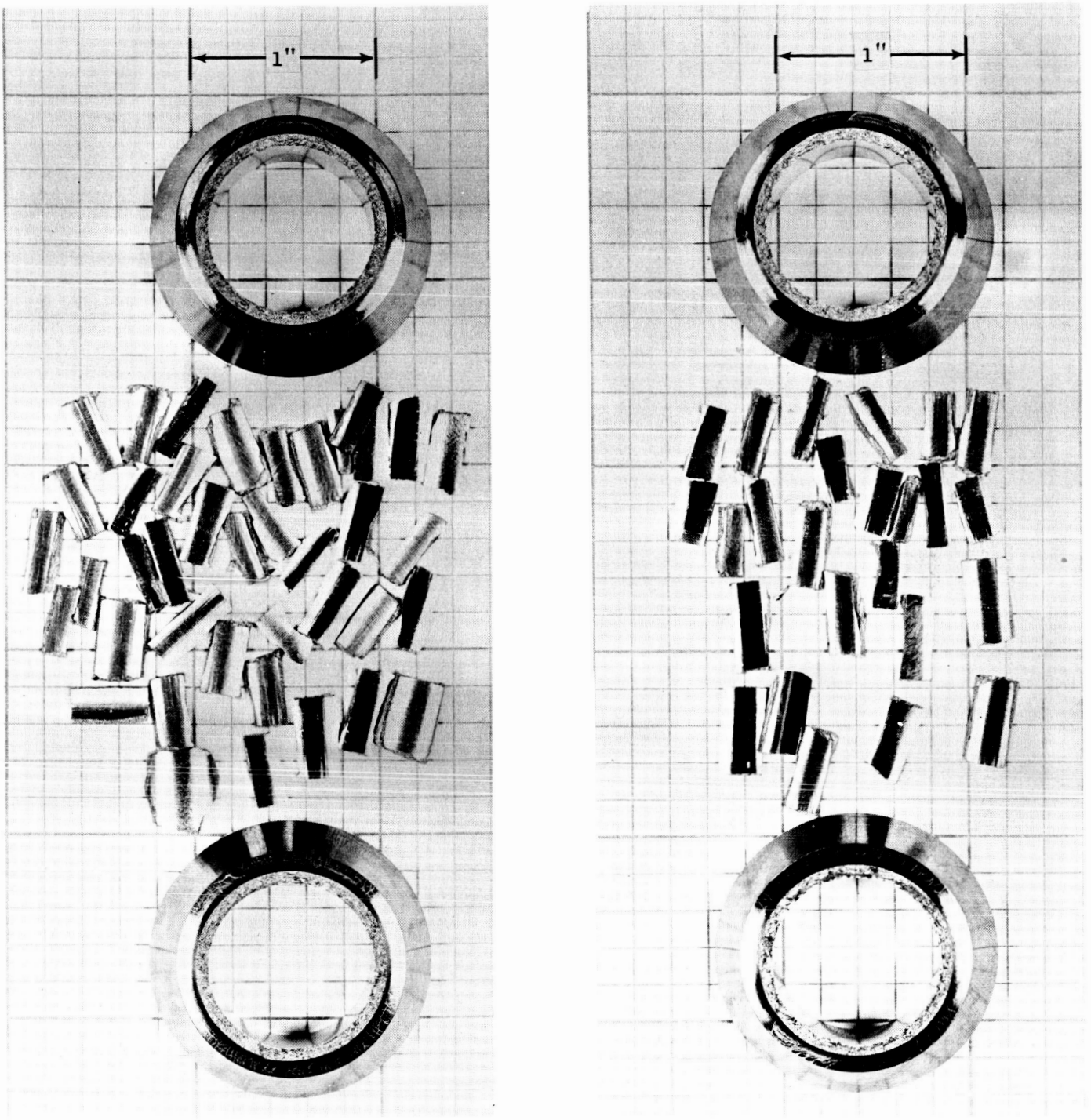

Figure 66. Photograph of Room Temperature Compression Specimens of Unalloyed Arc Cast Tungsten After Test. Left, Specimen MCN 1038-G-2 (C65052940); Right, Specimen MCN 1038-G-3 (C65052939).

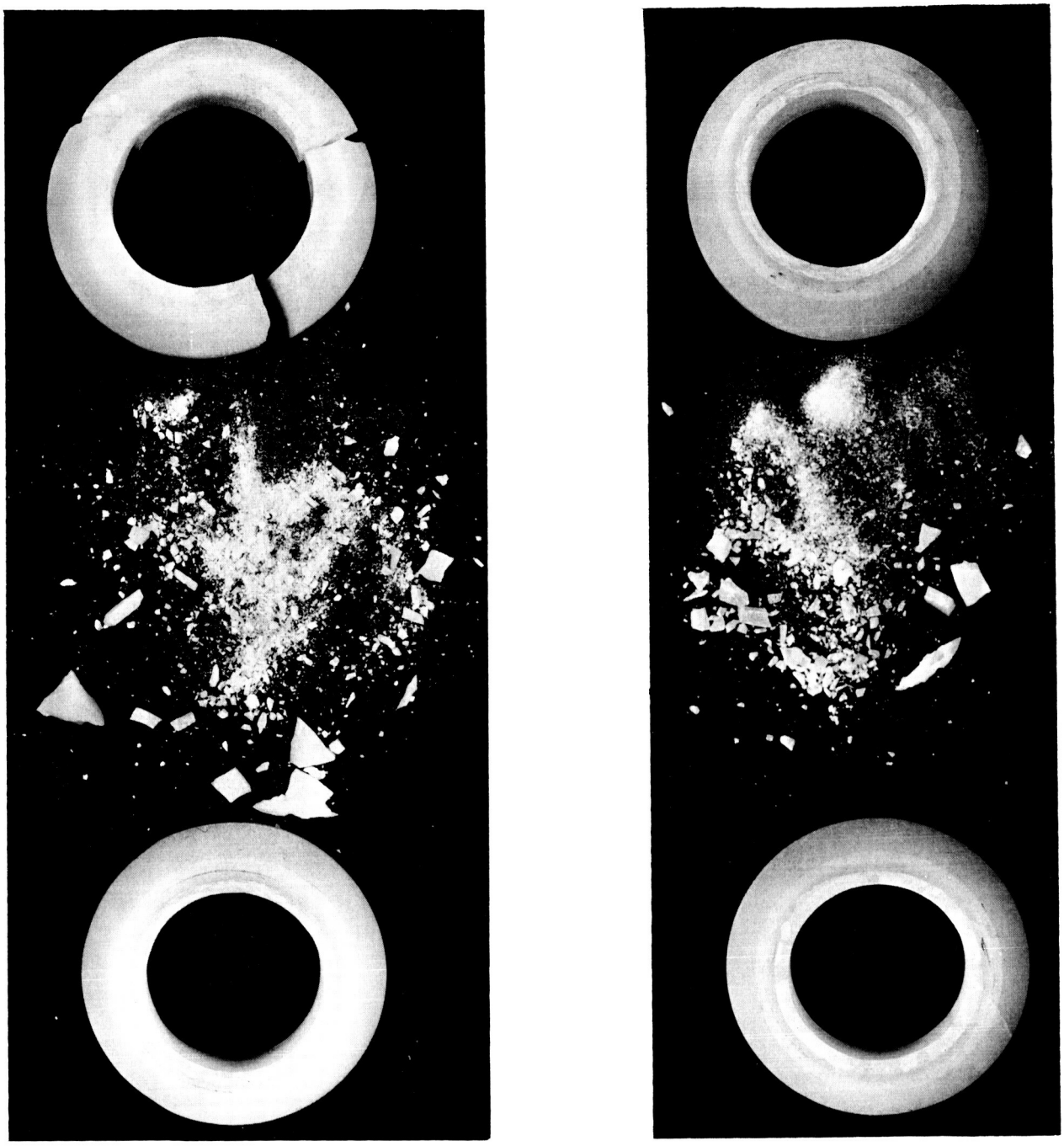

Figure 67. Photograph of Room Temperature Compression Specimens of Lucalox After Test. Left, Specimen MCN 1039-G-1 (C65052925); Right, Specimen MCN 1039-G-3 (C65052926).

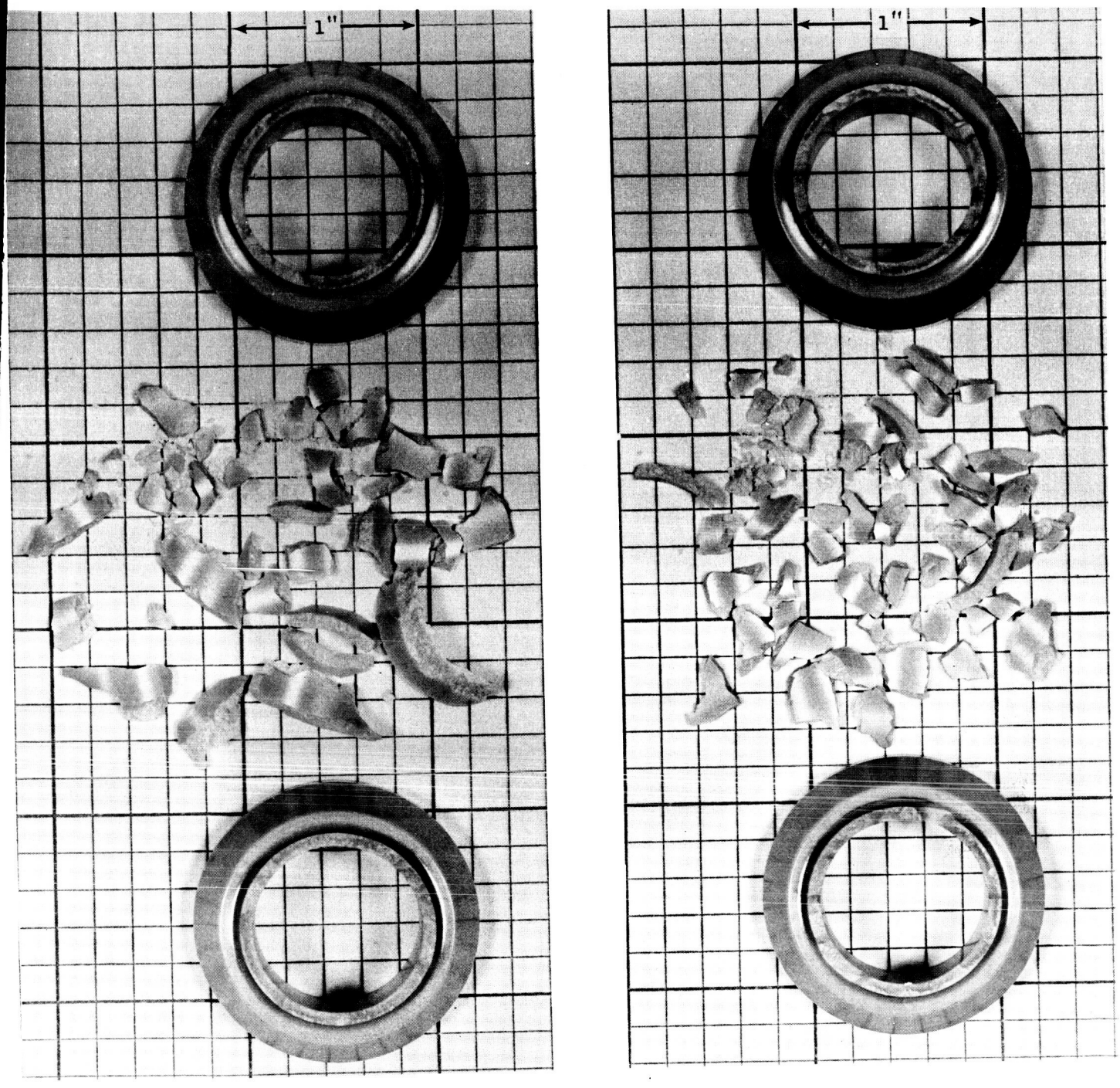

Figure 68. Photograph of Room Temperature Compression Specimens of Zircoa 1027 After Test. Left, Specimen MCN 1040-G-1 (C65052927); Right, Specimen MCN 1040-G-5 (C65062928).

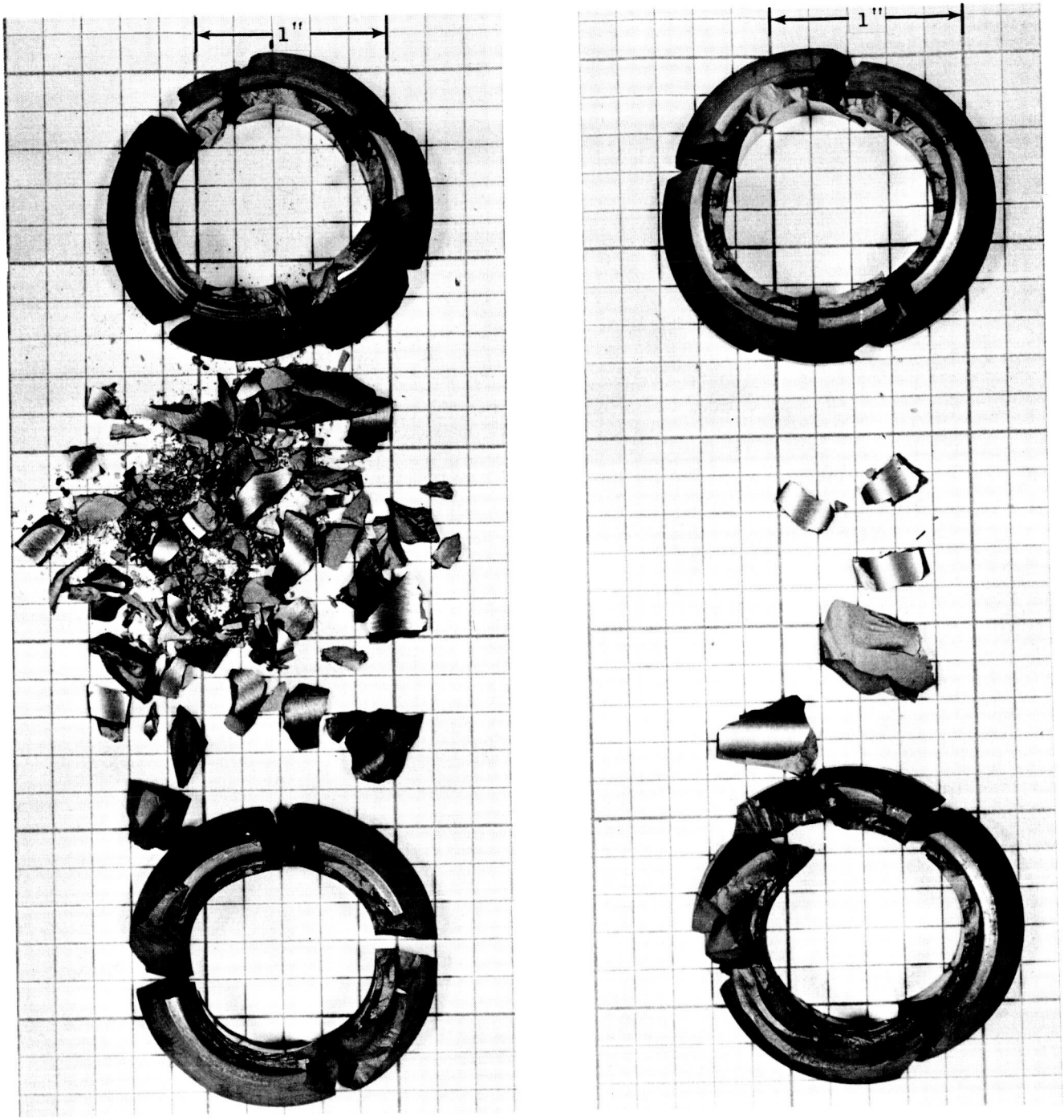

Figure 69. Photograph of Room Temperature Compression Specimens of TiC After Test. Left, Specimen MCN 1042-G-5 (C65062950); Right, Specimen MCN 1042-G-6 (C65052949).

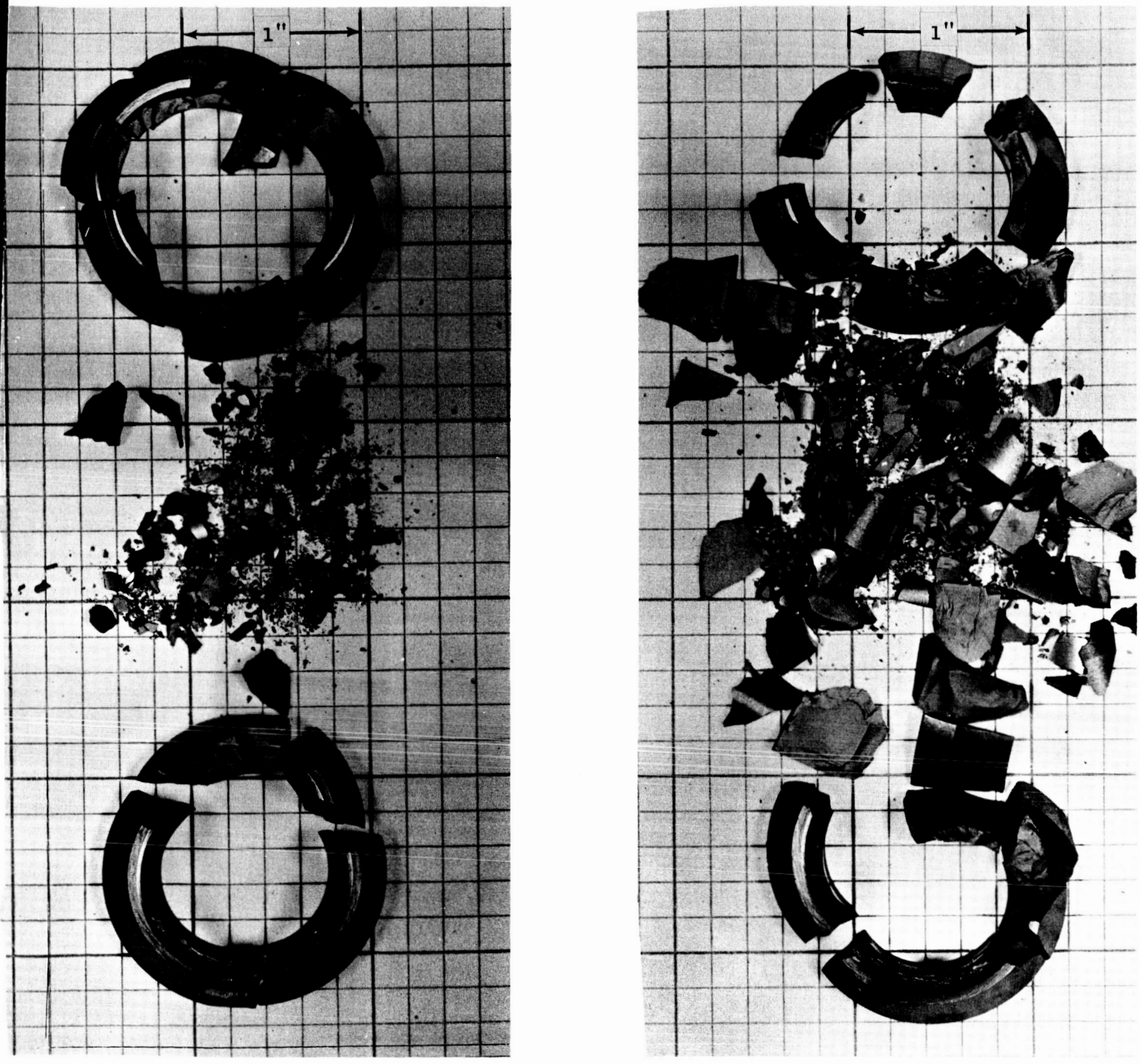

Figure 70. Photograph of Room Temperature Compression Specimens of TiC+5%W After Test. Left, Specimen MCN 1043-G-8 (C65062943); Right, Specimen MCN 1043-G-9 (C65062951).

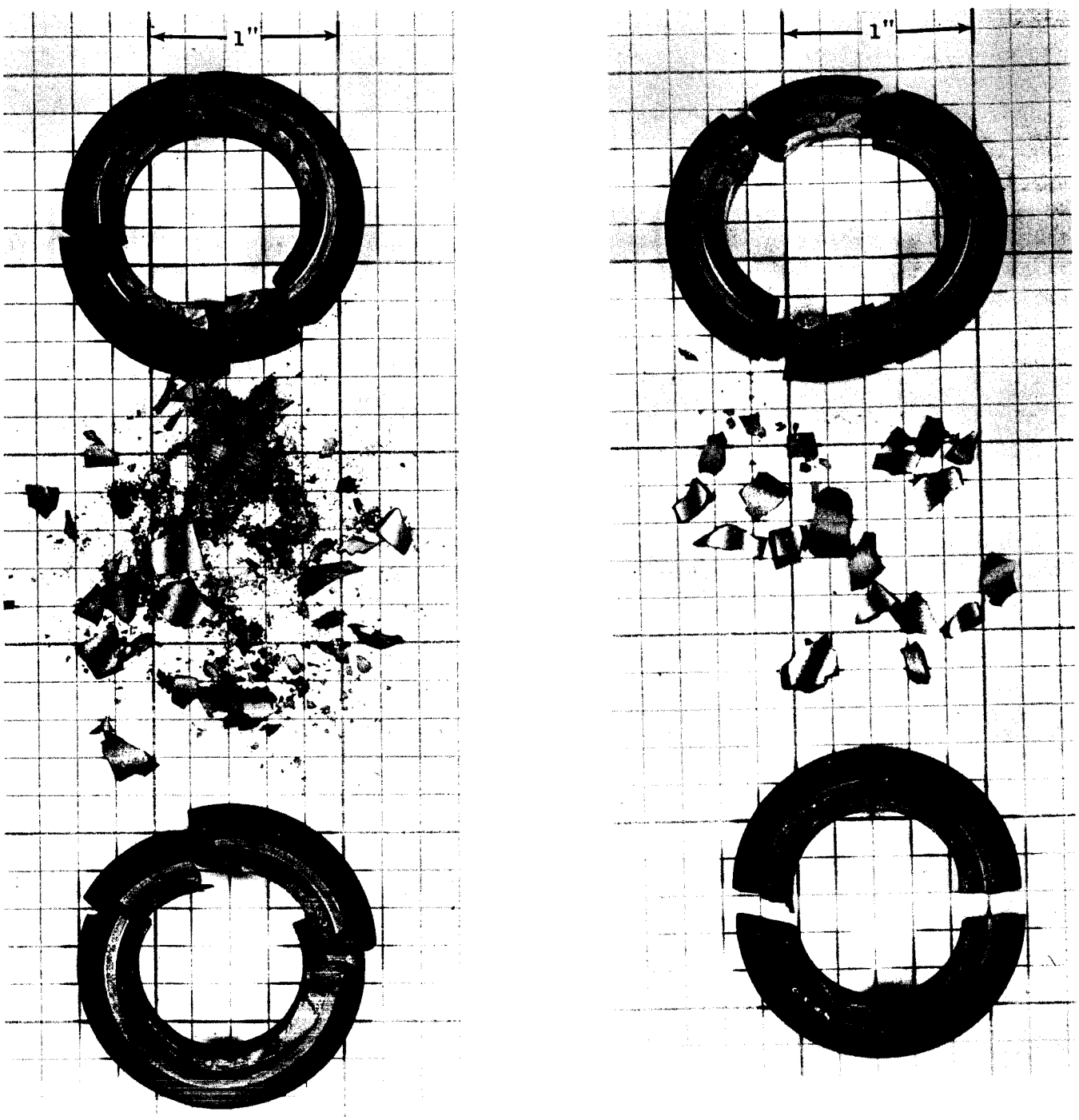

Figure 71. Photograph of Room Temperature Compression Specimens of TiC+10%Mo After Test. Left, Specimen MCN 1044-G-5 (C65062942); Right, Specimen MCN 1044-G-6 (C65062948).

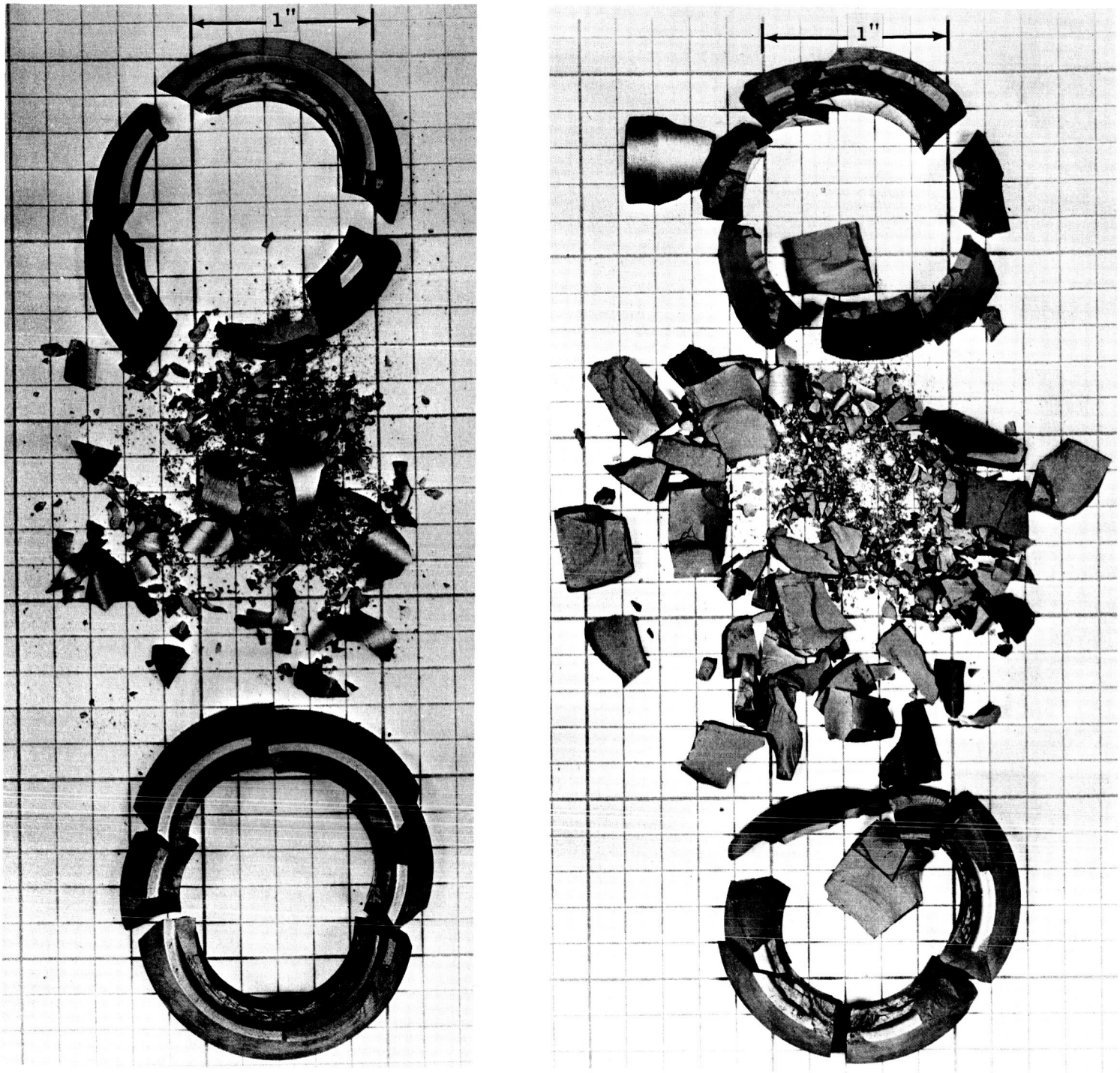

Figure 72. Photograph of Room Temperature Compression Specimens of TiC+10%Cb After Test. Left, Specimen MCN 1045-G-8 (C65062947); Right, Specimen MCN 1045-G-9 (C65062946).

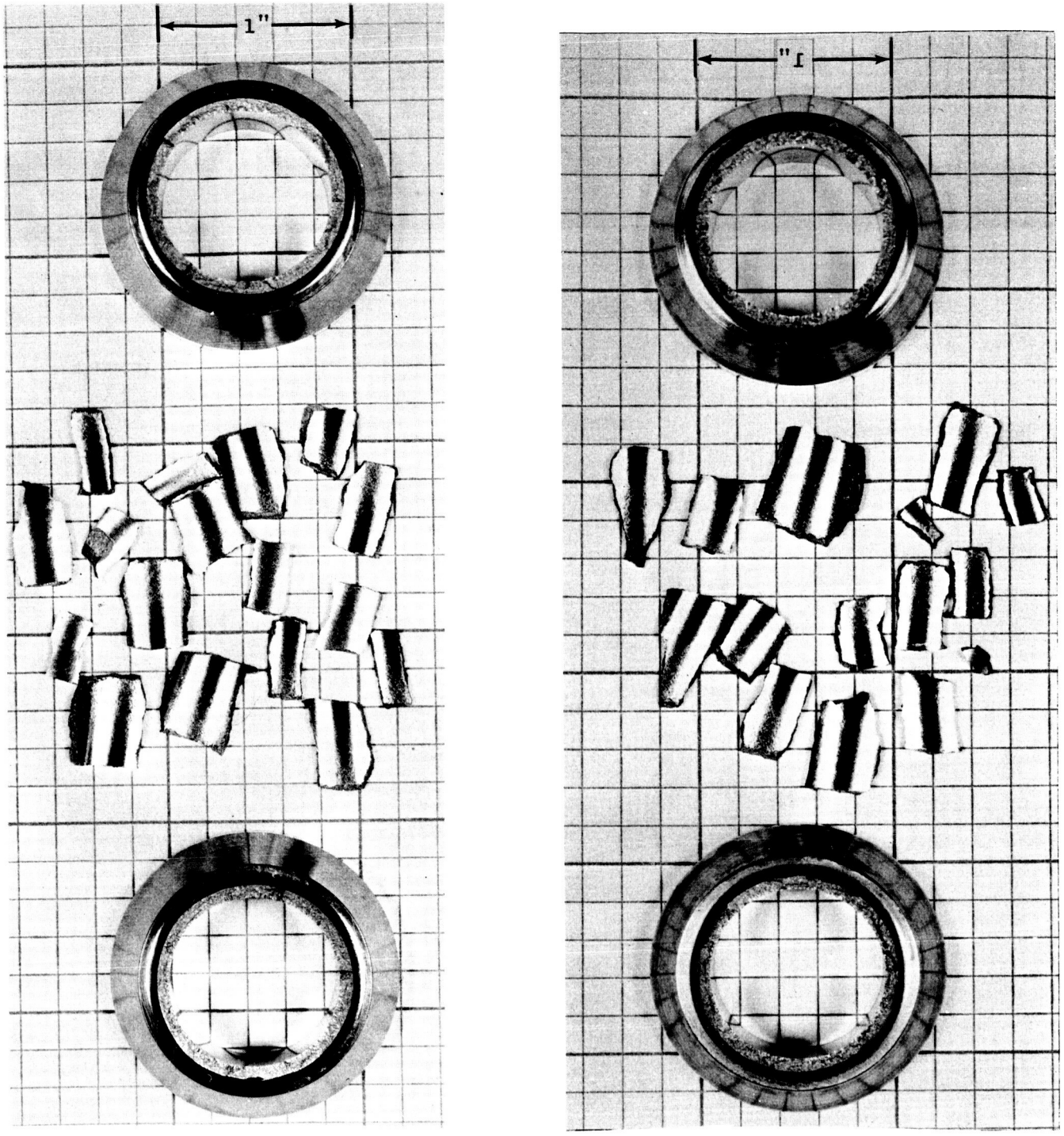

Figure 73. Photograph of Room Temperature Compression Specimens of Star J Alloy After Test. Left, Specimen MCN 1047-G-2 (C65062938); Right, Specimen MCN 1047-G-8 (C65062937).

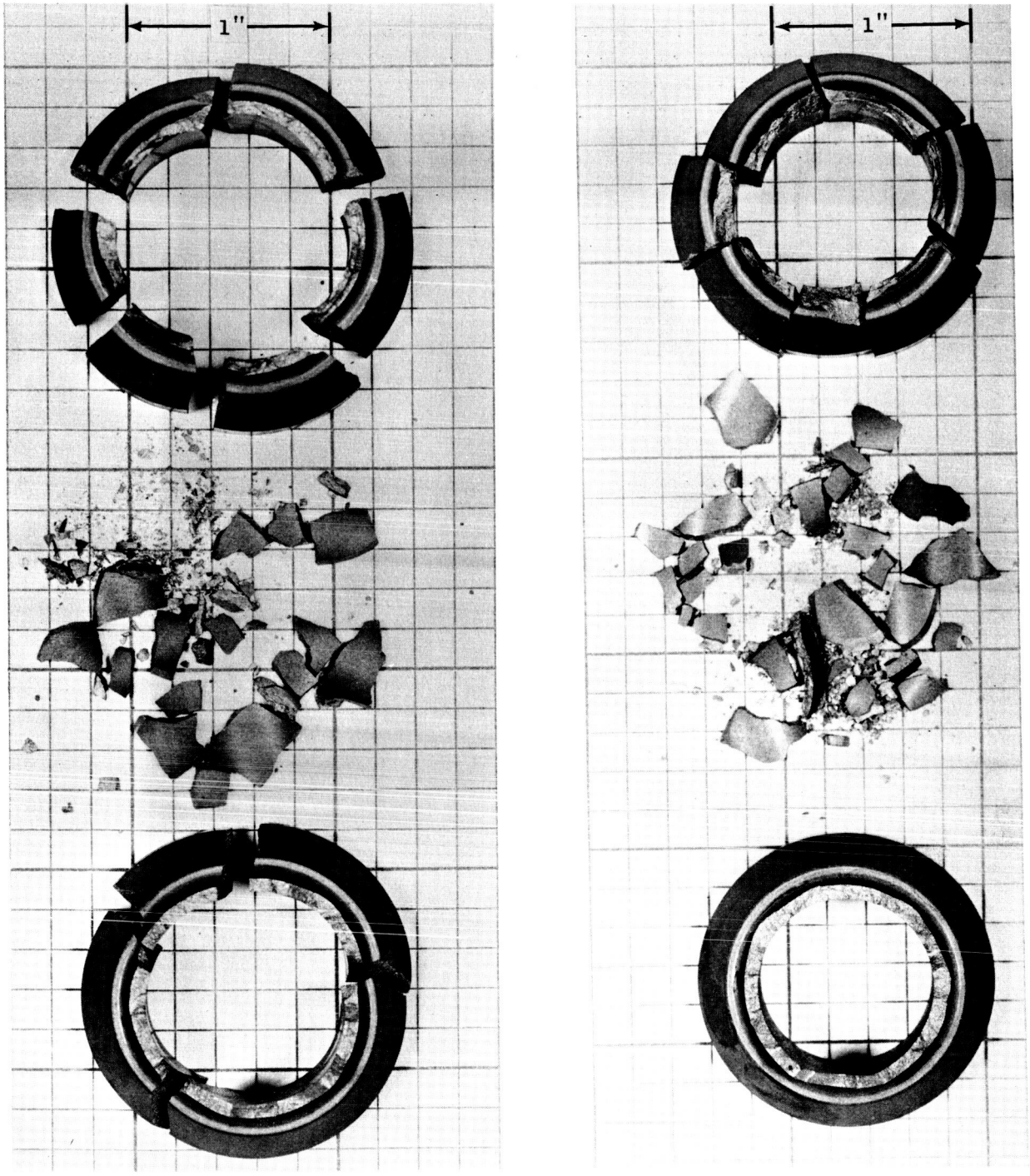

Figure 74. Photograph of Room Temperature Compression Specimens of TiB_2 After Test. Left, Specimen MCN 1048-G-3 (C65062945); Right, Specimen MCN 1048-G-10 (C65062941).

and two perpendicular to the long axis of the specimen. The data evolved from testing this specimen is expected to provide a correction factor to be used in determining the effective gauge length of all the compression test specimens. Corrected values for the moduli of elasticity presented in Table XXXVI will be reported in the next progress report.

VI. FUTURE PLANS

The summary which follows enumerates the steps to be pursued during the succeeding quarter to implement this study.

1. Procurement of all friction and wear test specimens will be completed.

2. Evaluation of the corrosion test specimens which were exposed to potassium for 1,000 hours at 1600°F will be completed and the evaluation of those specimens tested at 1200°F and 800°F will continue.

3. The isothermal corrosion testing of selected pairs of candidate bearing materials will be initiated at 800°, 1200° and 1600°F.

4. Friction and wear tests under high vacuum will be initiated.

5. The installation of the liquid potassium friction and wear test facility will be completed. Checkout tests of the tester will continue.

6. Assembly of the potassium wetting apparatus will be completed and the ultimate vacuum capability will be determined. Potassium will be introduced into the potassium reservoir in order to proceed with wetting measurements.

REFERENCES

1. "Materials for Potassium Lubricated Journal Bearings", Quarterly Progress Report No. 1, ctr. NAS 3-2534 (July 22, 1963), SPPS, MSD, General Electric Company; Report NASA-CR 54006.

2. "Materials for Potassium Lubricated Journal Bearings", Quarterly Progress Report No. 7, ctr. NAS 3-2534 (January 22, 1965), SPPS, MSD, General Electric Company; Report NASA-CR-54345.

3. "Materials for Potassium Lubricated Journal Bearings", Quarterly Progress Report No. 6, ctr. NAS 3-2534 (October 22, 1964), SPPS, MSD, General Electric Company; Report NASA-CR 54264.

4. Coffin, L.F, Jr., "Theory and Application of Sliding Contact of Metals in Sodium." Report KAPL-828, Knolls Atomic Power Laboratory, General Electric Company, October 1955.

5. Zeman, K.P, Young, W.R., and Coffin, L.F., Jr., "Friction and Wear of Refractory Compounds", Report 59GC-23, General Electric Company, May 1959.

6. AiResearch Manufacturing Company of Arizona, Quarterly Technical Progress Report for Period Ending September 30, 1965, SNAP 50/SPUR Contract AF33(615)-2280 DPSN: 5(6299-675A) 63409124, ADS-5152-R4, p 7.

APPENDICES

APPENDIX A

VERTICAL AND VECTOR TARE TEST PLAN FOR HIGH VACUUM FRICTION TESTER AND POTASSIUM FRICTION TESTER LOADING ARMS

APPENDIX A

VERTICAL AND VECTOR TARE TEST PLAN FOR HIGH VACUUM FRICTION TESTER AND POTASSIUM FRICTION TESTER LOADING ARMS

1. Assemble and lock the arm-stop mechanism in the HVFT with the stop centered inside pad No. 1.

2. Carefully weigh and record the weights of the force pickup connector (with set-screw and nut), exterior tray (with hooks, screws, etc.), inner button, eye, and inner tray.

3. Assemble loading arms No. 1, 2, 5, and 6 in the "tare test position" - force pickup connector and loading arm rotated 180° - and loading arms No. 3 and 4 in the "specimen test position". Lubricate all bearings with a suspension of 10% (by vol.) of MoS_2 (Molykote Type Z, The Alpha Corp., Greenwich, Conn.) in 90% (by vol.) Velocite #3 Spindle oil (Mobil Oil Co.). Shake well. Blow lubricant into bearings with pressurized air. Wipe off excess lubricant and clean the arm assembly with acetone and alcohol. Be sure the vacuum flange and interior portion of the loading arms are masked-off so that they do not come in contact with the lubricant.

(vertical only) 4a Clean the inside of the HVFT vacuum facility and the inner weight tray with acetone and alcohol. Set the tray inside the facility. Clean the inside of the HVFT with acetone and alcohol, including the arm holes and arm pads.

(vector only) 4b Secure the special nylon bearing to the heat shield support in the proper position, using an inspection table and vernier height gauge. Clean the heat shield and the inside of the HVFT vacuum facility with acetone and alcohol and place the heat shield inside the facility, aligning the proper reference marks and tapping securely into place.

(vector only) 5. Measure and record the height of the bottom of the bearing groove above the facility flange. Log all other measurements which define the relative locations of the bearing groove and the loading arm.

6. Clean and place a 1/4 inch diameter rubber O-ring on the facility flange.

7. Carefully set the HVFT on the facility flange with O-ring in place.

8. Clean three loading arm-hole blankoff flanges, the viewing port and four copper gaskets with acetone and alcohol and secure them to the HVFT.

9. Clean a copper gasket with acetone and alcohol and place on the loading arm to be tested.

10. Place the adaptor through the 1/8 inch diameter hole at the end of the loading arm.

11. Place the loading arm on the #1 pad and secure with the three support screws. The loading arm should be secured to the support with the locking sleeve and care should be taken to hold the support so that neither the sides of the loading arm hole nor the loading arm-stop are allowed to bend the arm. Tighten all three screws finger-tight before tightening with a wrench.

12. Secure the loading arm flange with four screws. If the screws will not assemble into the pad holes without rotation of the bellows, loosen the support screws and obtain a new position which does not require rotation.

13. Connect the force pickup cable and turn on the Sanborn recorder.

14. Draw a sketch of the assembly showing all components used, their weights and their moment arms. Record presence or absence of loading arm thermocouples.

15. With jo-blocks and a micrometer, measure the height of the loading arm centerline above the support on each side of the force pickup sleeve (support sleeve centering arm).

16. With jo-blocks and a micrometer, set the center-lines of the protrusion at each end of the force pickup the same height above the support as the loading arm center-line.

17. With the support sleeve still centering the loading arm, secure the nuts at each end of the force pickup and the force pickup height adjusting screws to a position which centers the force pickup vertically on the same center line as the loading arm and horizontally to a zero force reading on the force pickup. Use a jo-block to align the eye of the force pickup connector perpendicular to the support surface before the final adjustments are made and assure that the set screw hole in the force pickup sleeve was centered on the mark on the arm which is 5.625 inches from the gimbal center-line. Secure the set screw. Remove all jo-blocks.

(vertical only) 18. Remove the support centering sleeve and electrically adjust the Sanborn force pickup trace to chart zero.

(vertical only) 19. Clamp the second nylon bearing to the loading arm support, aligning the bottom of the bearing groove with the center-line of the set screw hole in the force pickup connector. Attach the eye to the set screw. Run a wire through the eye and bearing groove and attach the outer weight tray.

(vertical only)	20.	Apply loads of 1-10 lb. and record on the Sanborn recorder, then remove the eye, bearing, etc.
(vertical only)	21a	Raise the HVFT and attach the eye loosely to the button at the end of the loading arm. Attach the weight tray to the eye and place a dead weight Wi (20-lb. maximum) in the center of the tray. Stop all swinging of the tray. The support sleeve should be centering the outer end of the arm.
(vector only)	21b	Raise the HVFT and attach the eye (with wire and hook) loosely to the adaptor at the end of the loading arm. Lower the HVFT and hold the wire in the bearing groove. Set weight VWi in the hook.
	22a	Lower the HVFT onto the facility flange O-ring and secure with at least four equally-spaced bolts tightened to approximately 50 ft-lb.
(Vector only)	22b	Record the gap between the bottom of the HVFT flange and the top of the facility flange at each bolt location.
	23.	Impose the pressure at which the arm is to be calibrated.
	24.	Set the dial indicator on the arm at 2.375 inches out from the gimbal center-line.
	25.	Complete the arm sketch previously started.
	26.	Remove the support centering sleeve and apply loads in the outer weight tray until the balance point is found within 2 oz. With this information a piece of 0.07 inch division graph paper can be labelled: vertical axis - three zones 0 to - 0.008 inch arm deflection, each labelled for a different pressure; horizontal axis - balance weight minus 10 oz. to plus 10 oz. Record also: inner weight, Wi, arm number, date, and test personnel.
	27.	Load the weight tray with the balance weight minus 10 oz. Tap top of facility until deflection reading stabilizes. Set the zero point of the dial indicator under the pointer. Plot zero deflection at this weight (use 0 symbol).
	28.	Add four ounces, tap until reading stabilizes, and plot.
	29.	Repeat step 28 until a line with definitely decreased slope is established (four points minimum).
	30.	Draw two straight lines through the data points and log the weight at which they intersect.
	31.	Load the weight tray with balance weight minus 9 oz. (to nearest whole ounce), tap, and plot deflection with + symbol. Repeat steps 28 - 30 and log intersection weights.

32. Load the weight tray with balance weight minus 8 oz. (to nearest whole ounce), tap, and plot deflection with △ symbol. Repeat steps 28 - 30 and log intersection weights.

33. If the spread of intersection weights exceed 0.5 oz., take further readings until the spread is narrowed and the erroneous readings can be identified and discarded.

(vector only) 34. Compute the average intersection weight and apply to the weight tray (within nearest 1/16 oz.). Record force pickup reading on Sanborn recorder.

35. Without unbolting the HVFT from the facility or the arms from the pads, change to the next pressure(s) and repeat steps 27 - 34.

36. Without unbolting the arms from the pads, remove the facility flange bolts, raise the HVFT, and replace Wi with a new inner weight. Repeat steps 27 - 35 for all weights desired.

37. Remove all weights from the arm and replace centering sleeve.

CHECKLIST

VERTICAL OR VECTOR TARE TEST FOR HVFT OR KFT LOADING ARMS

APPLIED TO VERTICAL TARE TEST	APPLIED TO VECTOR TARE TEST	STEP NO.	OPERATION (circle X's as completed)
X	X	1	Locked arm-stop inside pad No. 1.
X	X	2	Recorded weights of all components.
X	X	3	Arms assembled in test position, lubricated & cleaned.
X		4a	Tray cleaned and set inside cleaned facility. HVFT cleaned inside.
	X	4b	Bearing assembled on cleaned heat shield support.
	X	4b	Heat shield support placed in cleaned facility.
	X	5	Measured bearing-to-flange height & recorded all pertinent dimensions.
X	X	6	Cleaned O-ring on facility flange.
X	X	7	HVFT set on O-ring.
X	X	8	Blankoff flanges and view-port cleaned and secured.
X	X	9	Cleaned copper gasket on loading arm to be tested.
X	X	10	Adaptor placed on end of loading arm.
X	X	11	Loading arm support secured to pad No. 1.
X	X	12	Arm flange secured without rotating bellows.
X	X	13	Force pickup cable connected.
X	X	13	Sanborn recorder turned on.
X	X	14	Arm assembly sketched.
X	X	15	Height of centered arm ℄ above support measured.
X	X	16	Force pickup set on arm ℄.
X	X	17	Force pickup secured at 0 turn on.
X	X	17	Eye of pickup connector ⊥ to support at 5.625 inches & secured.
	X	18	Support sleeve removed & Sanborn set to chart 0.
	X	19	Nylon bearing etc. attached to arm support.
	X	20	1-10 lb.weights recorded on Sanborn & bearing etc. removed.

CHECKLIST (Cont'd)

APPLIED TO VERTICAL TARE TEST	APPLIED TO VECTOR TARE TEST	STEP NO.	OPERATION (circle X's as completed)
X	X	21a	HVFT raised and eye loosely on adaptor.
X		21a	Weight tray & weights attached to centered arm.
	X	21b	Wire held in bearing groove & weights attached.
X	X	22a	HVFT secured to facility by 4 bolts at 50 ft-lb.
	X	22a	Gap between HVFT & facility recorded.
X	X	23	Test pressure set.
X	X	24	Dial indicator set at 2.375 inches from gimbal ℄.
X	X	25	Arm sketch completed.
X	X	26	Rough balance point found & graph set up.
X	X	27	Apply balance wt. -10 oz., -6 oz., -2 oz., +2 oz., +6 oz., & plot.
X	X	28	
X	X	29	
X	X	30	Log intersection weight.
X	X	31	Apply balance wt. -9 oz., -5 oz., -1 oz., + 3oz., +7 oz., & plot.
X	X	32	Apply balance wt. -8 oz., -4 oz., -0 oz., +4 oz., +8 oz., & plot.
X	X	33	Intersection weight spread does not exceed 0.5 oz.
	X	34	Sanborn recorded with average intersection weight (nearest 1/16 oz.).
X	X	35	Second test pressure set w/o moving HVFT or arms.
X	X	35	Steps 27 - 34 repeated.
X	X	36	HVFT raised & new Wi added.
X	X	36	Steps 27 - 35 repeated.
X	X	37	All weights removed from arm & centering sleeve replaced.

APPENDIX B

MOMENT EQUILIBRIUM CALCULATIONS

APPENDIX B

MOMENT EQUILIBRIUM CALCULATIONS

Equilibrium Under Specimen Testing Conditions for Loading Arm No. 1 - The weights W_o and W_i are the dead weights which were placed in the external and internal trays, respectively, uncorrected for the weights of the trays or associated equipment. The equations relating uncorrected values of W_o and W_i may be derived from the data in Table BI and Figures B1 and B2:

High Vacuum Friction Tester Arm No. 1; Vacuum Only; Uncorrected	$W_{o1} = 0.87684\ W_{i1} - 0.61934$	(1)
	$W_{i1} = 1.14045\ W_{o1} + 0.70633$	(2)
High Vacuum Friction Tester Arm No. 2; Vacuum Only; Uncorrected	$W_{o2} = 0.86034\ W_{i2} + 0.56629$	(3)
	$W_{i2} = 1.16232\ W_{o2} - 0.65822$	(4)
High Vacuum Friction Tester Arm No. 4; Vacuum Only; Uncorrected	$W_{o4} = 0.88791\ W_{i4} + 1.77988$	(5)
	$W_{i4} = 1.12624\ W_{o4} - 2.00457$	(6)

The values calculated from the above relationships should be rounded off after calculation.

The equilibrium equation for the calculation of M_{tol} of loading arm No. 1 follows (see Figure B3):

$$\Sigma M_{ss} = 0 \text{ (about support shaft)}$$

$$0.5\ W_{tol} + 0.5F_p + 0.5(0.85) + 0.5\ (3.64) + 0.5\ F_{ss} = 0.5\ (4.11) + 0.5\ (2.30) + 0.5\ (273.0) + 0.5\ W_{ol}$$

$$W_{tol} = 274.92 - F_p - F_{ss} + W_{ol} \quad \text{(grams)}$$

$$W_{tol} = 0.60608 - F_p - F_{ss} + W_{ol} \quad \text{(pounds)}$$

Separate F_p and F_{ss} when converting to moments, where the line of action is 5.625 inches from the gimbal:

ΣM_g (about gimbal) ↺+

$$M_{to} + M_p + M_{ss} = - 5.625\ W_{tol}$$

$$= - 5.625\ (0.60608 - F_p - F_{ss} + W_{ol})$$

$$= - 3.40920 + 5.625\ F_p + 5.625\ F_{ss} - 5.625\ W_{ol}$$

TABLE BI

UNCORRECTED MEASURED VALUES OF W_o (OUTER WEIGHTS) VERSUS W_i (INNER WEIGHTS) FOR HIGH VACUUM FRICTION TESTER LOADING ARMS

		Outer Weight, W_o, lbs						
Inner Weight, W_i, lbs →		1	2	3	5	8	11	15
Loading Arm No. 1	Vacuum 0.05 Torr	0.2575		2.0250	3.8297	6.2917		12.5333
	0 psig	0.3219		2.0156	3.8261	6.4615		12.6563
	15 psig	0.3489		2.1875	3.8125	6.5063		12.7094
Loading Arm No. 2	Vacuum 0.05 Torr		2.2711		4.8563	7.4844	10.1177	13.5323
	0 psig		2.2865		4.8833	7.4531	10.1112	13.5959
	15 psig		2.3115			7.4989		13.6198
Loading Arm No. 4	Vacuum 0.05 Torr		3.4958		6.2219	8.8913	11.5469	
	0 psig		3.5557		6.1677	8.8417	11.4530	
	15 psig		3.4500		6.1011			

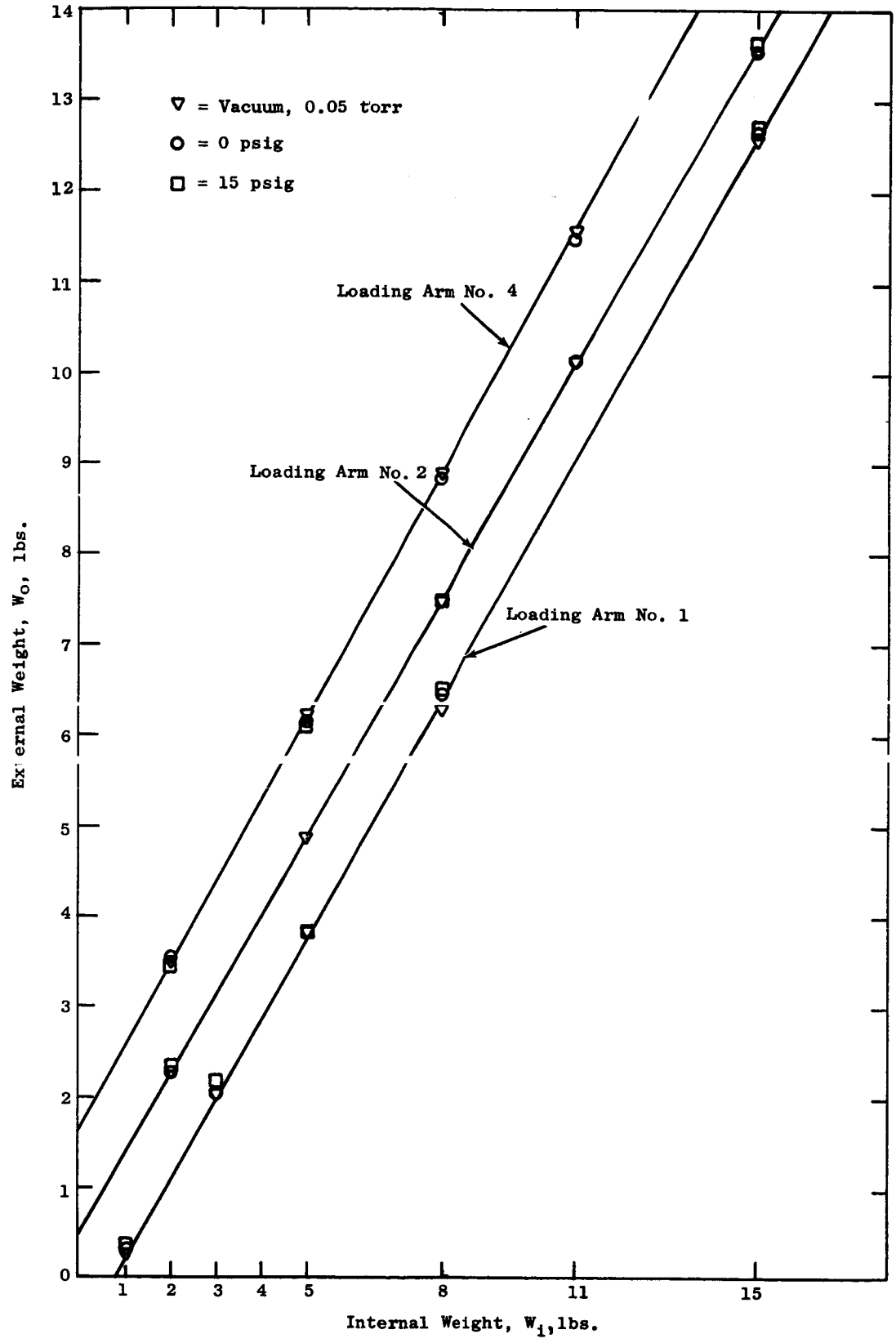

Figure B1. **Balance Point Curves for the Loading Arms of the High Vacuum Friction and Wear Tester.**

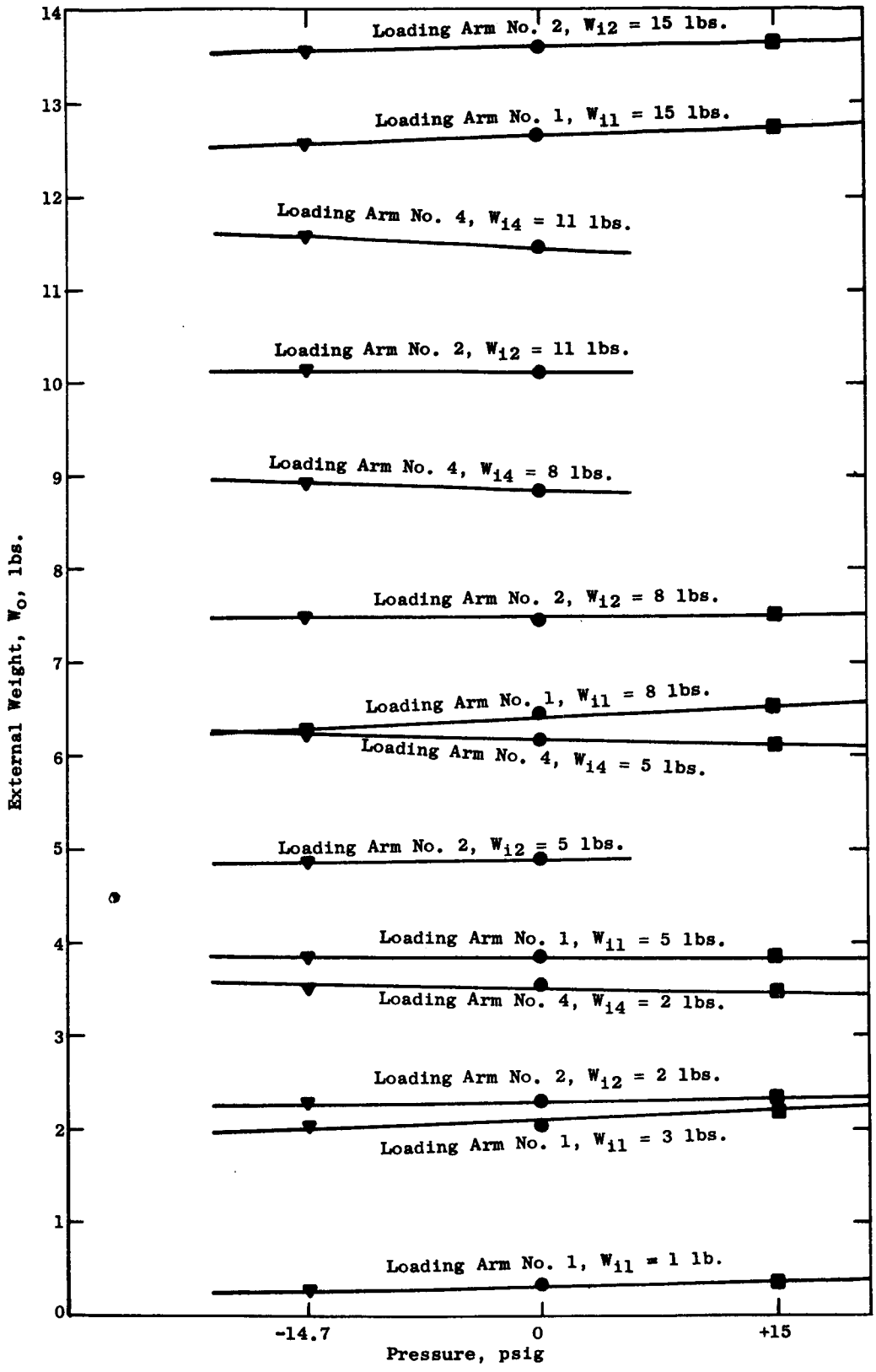

Figure B2. **Variation of Tare Weight with Pressure for High Vacuum Friction Tester Loading Arms.**

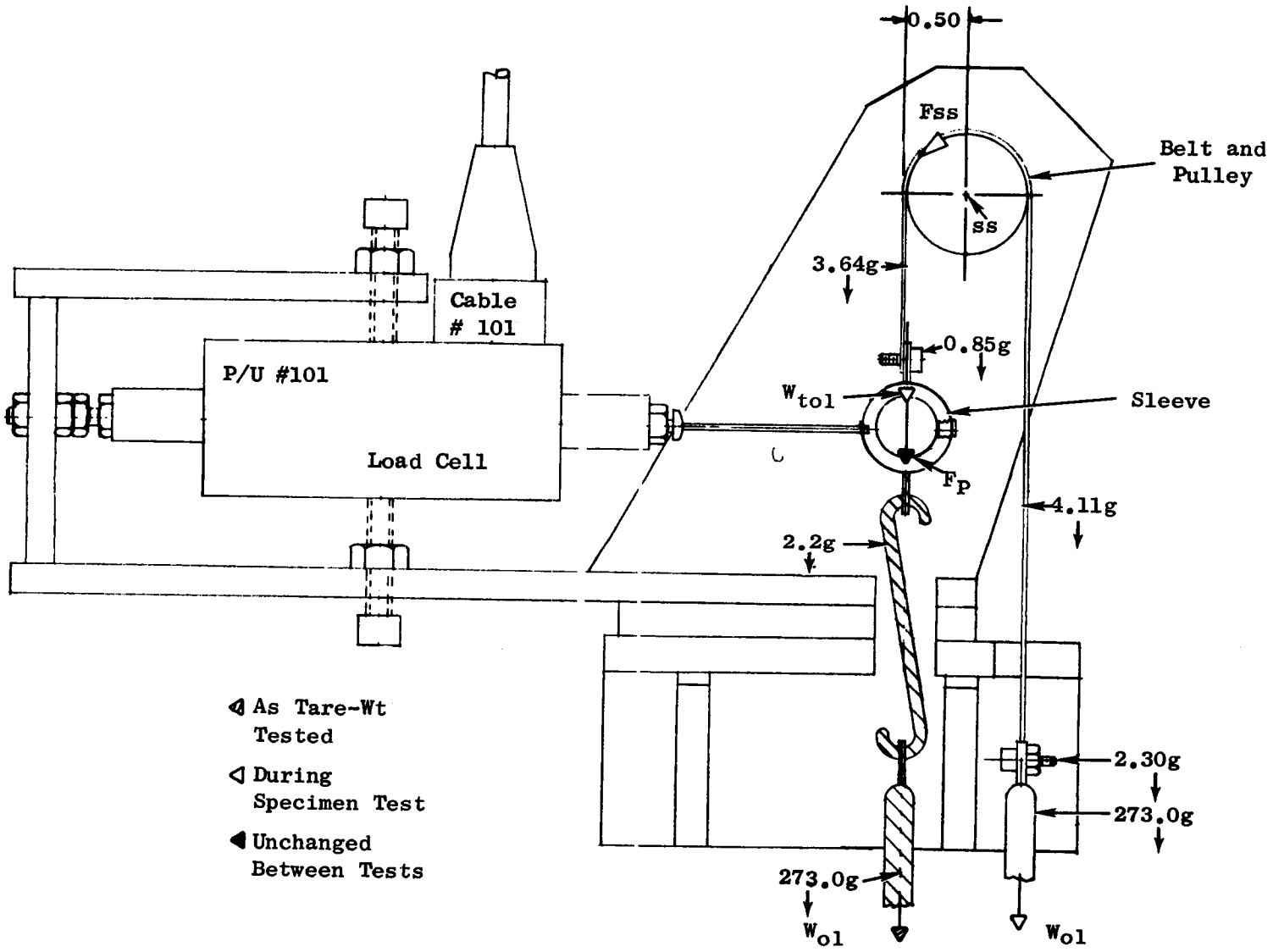

Figure B3. **Moments Used in the Equilibrium Equation for the Calculation of M_{tol} for Loading Arm No. 1 of the High Vacuum Friction and Wear Tester.**

Therefore:

$$M_{tol} = -3.40920 - 5.625\ W_{ol} \quad (8)$$

$$M_p = 5.625\ F_p \quad (9)$$

$$M_{ss} = 5.625\ F_{ss} \quad (10)$$

The line of action of the external forces transmitted to the loading arm by the thermocouples is 0.395 inch from the centerline of the gimbal. Therefore:

$$M_{ftc} = 0.395\ F_{tc}. \quad (11)$$

The measured length of the thermocouples from the gimbal was 4.59 inches and 4.49 inches; the 0.040-inch thermocouple wire weighed 0.12 g/m. Therefore:

$$W_{tc} = 0.12\ (4.59 + 4.49) = 1.0896g = 0.00222\ lb.$$

and the distance to the c.g. is:

$$X_{tc} = 0.25\ (4.59 + 4.49) = 2.270\ inches.$$

Therefore:

$$M_{wtc} = 2.270\ (0.00222) = 0.00504\ in\text{-}lb. \quad (12)$$

The weight of the stationary specimen and its stainless steel set screw is estimated for the present, using TZM density of 0.369 lb/in^3, as 0.00565 lbs. Its line of action is 4.880 inches from the gimbal. Therefore:

$$M_s = 4.880\ (0.00565) = 0.02757\ in\text{-}lb. \quad (13)$$

and

$$M_{cl} = 4.880\ C_l. \quad (14)$$

The equilibrium equation under specimen testing conditions can now be written (see Figure B4):

$$\Sigma M_g = 0 \text{ (about gimbal)}$$

$$-3.40920 - 5.625\ W_{ol} + 5.625\ F_p + 5.625\ F_{ss} + M_{ao} + 0 \quad (15)$$

$$+ 0.395\ F_{tc} + M_g = M_b + M_{ai} + 0.00504 + 0 + 0.02757 - 4.880\ C_l$$

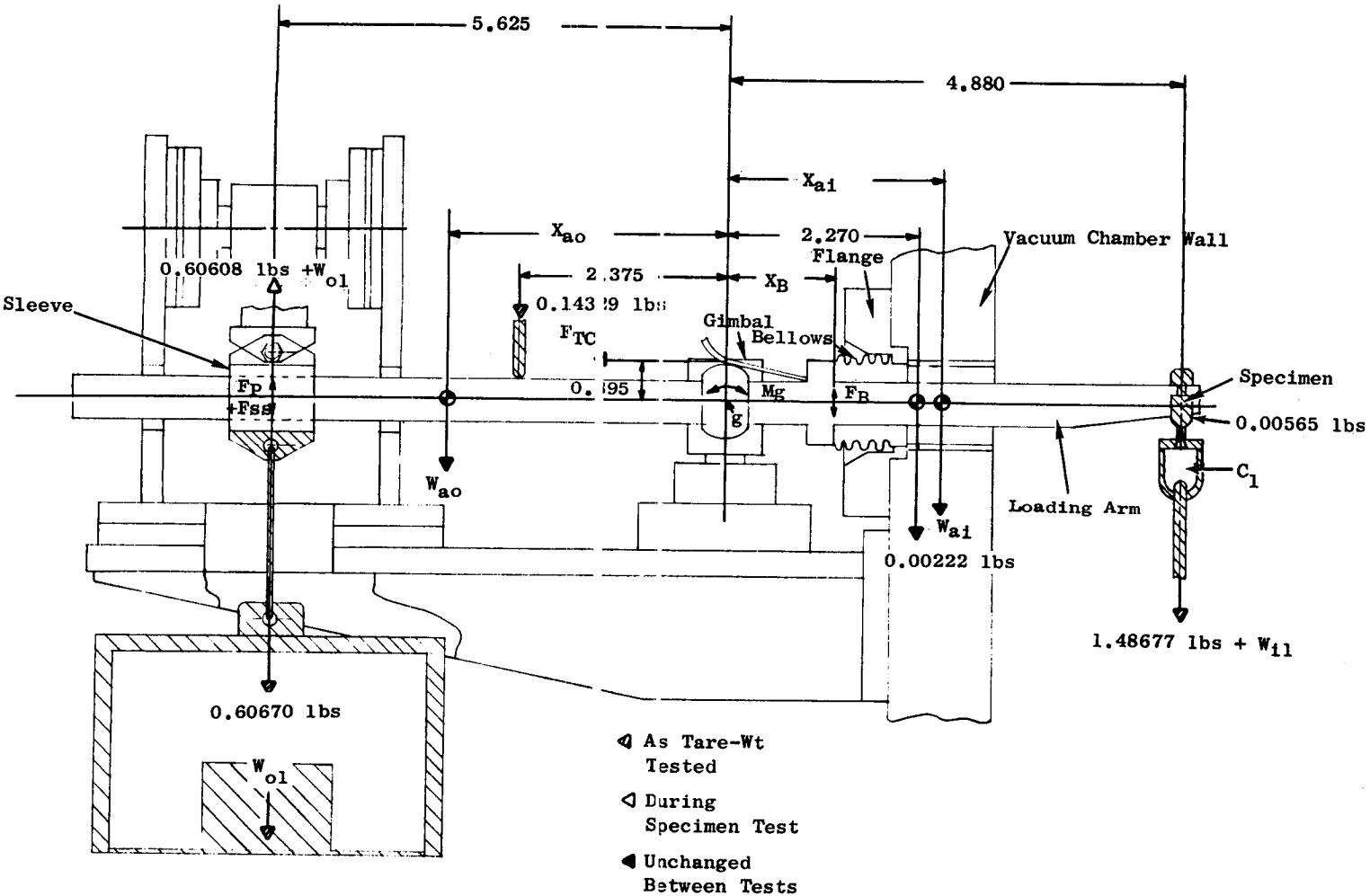

Figure B4. **Moments Used in Equilibrium Equation to Calculate M_{to} for Loading Arm No. 1 for the High Vacuum Friction and Wear Tester.**

Equilibrium Under Tare-Weight Testing Conditions for Loading Arm No. 1 - Since the weights hand directly under the arm (see Figure B4), the moment M_{to} of the outer tray and weights under tare-weight testing conditions is:

$\sum M_g$ (about gimbal)

$$M_{to} = 5.625\ (0.60670 + W_{ol})$$

$$M_{to} = 3.41269 + 5.625\ W_{ol}) \qquad (16)$$

The force of the dial indicator is proportional to its deflection, but measures 65 g = 0.14329 lb. at the usual balance point, and was located 2.375 inches from the gimbal. Therefore:

$$M_d = (2.374)\ (0.14329) = 0.34031 \text{ in-lb.} \qquad (17)$$

Since the line of action of the inner tray and weights of total weight 1.48677 lbs + W_{il} is 4.880 inches from the gimbal:

$$M_{ti} = 4.880\ (1.48677 + W_{il})$$

$$M_{ti} = 7.25544 + 4.880\ W_{il}. \qquad (18)$$

The equilibrium equation (19) under tare-weight testing conditions may now be substracted from the equilibrium equation (15) under specimen testing conditions to give the following Equation for C_l. Equations 19 and 15 are given in the supplement to Appendix B.

$$C_l = -0.01345 + 2.30532\ W_{ol} - 1.15266\ F_{ss} - W_{il}.$$

Substituting Equation (2) (vacuum, 0.05 torr),

$$-0.01345 + 2.30532\ W_{olv} - 1.15266\ F_{ss} - 1.14045\ W_{olv} - 0.70633 = C_{lv}$$

$$C_{lv} = 1.16487\ W_{olv} - 0.71978 - 1.15266\ F_{ss}\ (W_s \text{ assumed; vacuum only})$$

and

$$W_{olv} = 0.85846\ C_{lv} + 0.61790 + 0.98951\ F_{ss}\ (W_s \text{ assumed; vacuum only}).$$

Also, F_{ss} is a function of W_{olv} and would require a separate test to determine. Although this has not been done, it is estimated that F_{ss} will be of the order of a few grams, i.e., 5 grams (0.00903 lb.).

Check: when C_{lv} = 5 lbs.,

$$W_{oln} = 0.85846\ (5) + 0.61790 + 0.98951\ (0.00903)$$
$$= 4.91914, \text{ or } 4.92 \text{ lbs.}$$

If F_{ss} were ignored:

W_{o1v} = 4.91020 (4.91 lbs). The latter value for W_{o1v} is 0.2% low and it is thought that F_{ss} actually will be less than 5 g; therefore, it will be considered negligible.

Therefore:

High Vacuum Friction Tester Arm No. 1; Vacuum Only; W_s Assumed; F_{ss} Neglected	$C_{1v} = 1.16487\ W_{o1v} - 0.71978$	(20)
	$W_{o1v} = 0.85846\ C_{1v} + 0.61790$	(21)

Equilibrium Conditions for Loading Arm No. 2 - Because of the fragile nature of the sheathed thermocouples, they were omitted for the remaining loading arms and their moment was assumed to be the same as for loading arm No. 1 (see Equation 12). Also, using the weights of the belts and outer tray applicable to loading arm No. 2, the equations under specimen testing conditions (22) (see Supplement to Appendix B) and under tare-weight testing conditions (23) (see Supplement to Appendix B) are derived in a similar manner as for loading arm No. 1 (see Figures B5 and B6). From these equations, the equation for C_2 is obtained:

$$C_2 = 0.02669 + 2.30532\ W_{o2} - 1.15266\ F_{ss} - 0.08094\ F_{tc} - W_{t2}.$$

Substituting Equation (4) (vacuum conditions);

$$C_{2v} = 0.02669 + 2.30532\ W_{o2v} - 1.15266\ F_{ss} - 0.08094\ F_{tc} - 1.16232\ W_{o2v} + 0.65822$$

$$C_{2v} = 1.14300\ W_{o2v} + 0.68491 - 1.15266\ F_{ss} - 0.080904\ F_{tc}$$

$$W_{o2v} = 0.87489\ C_{2v} - 0.59922 + 1.00845\ F_{ss} - 0.07081\ F_{tc}.$$

Again it is estimated that 1.15266 F_{ss} may be considered negligible and that 0.08094 F_{tc} is even smaller, provided the thermocouple lead wires are properly supported, giving:

High Vacuum Friction Tester Arm No. 2; Vacuum Only; W_s Assumed; F_{ss} and F_{tc} Neglected	$C_{2v} = 1.14300\ W_{o2v} + 0.68491$	(24)
	$W_{o2v} = 0.87489\ C_{2v} - 0.59922$	(25)

Check: When C_{2v} = 5 lbs.,

$$W_{o2v} = 0.87489\ (5) - 0.59922$$
$$= 3.77523, \text{ or } 3.78 \text{ lbs.}$$

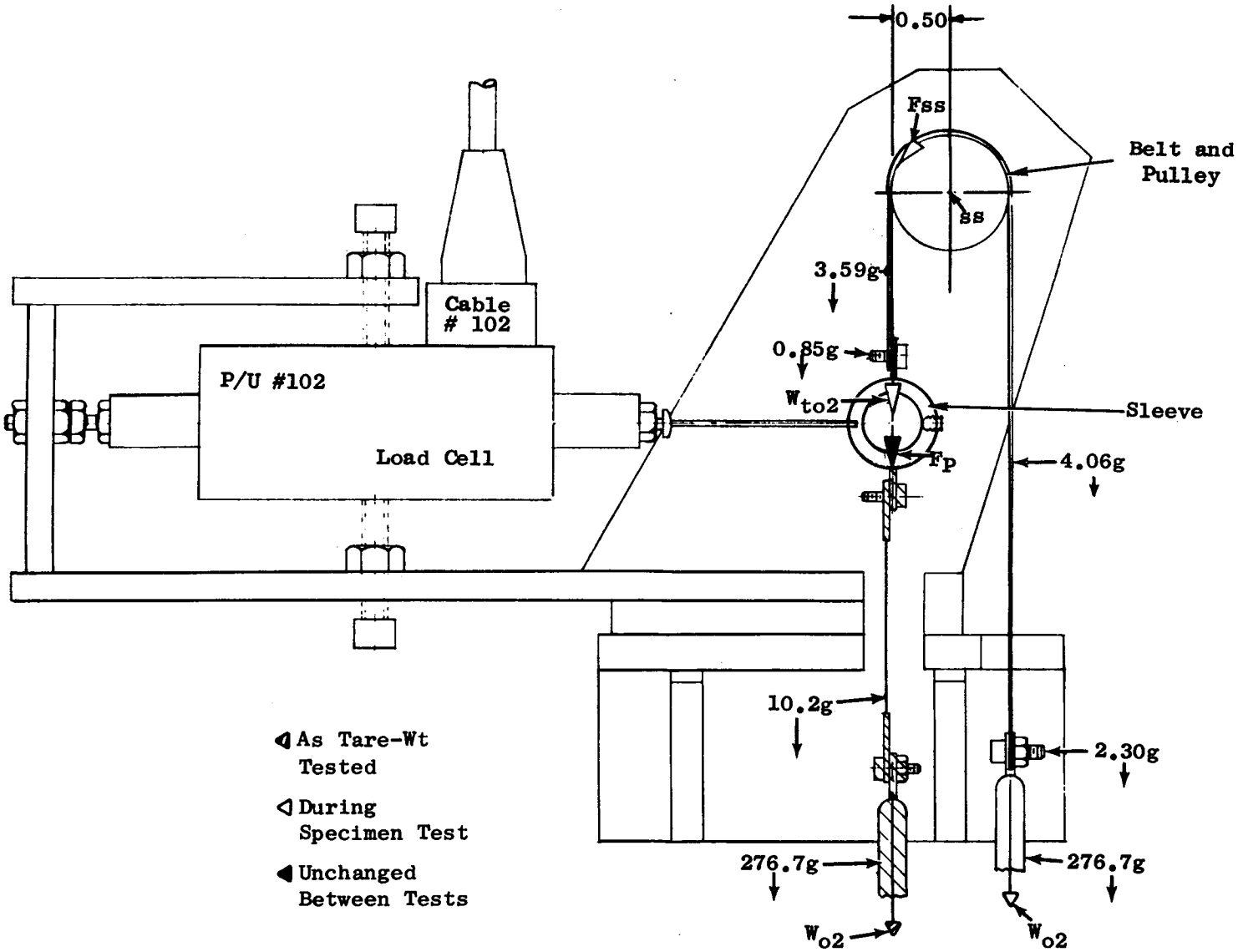

Figure B5. Moments Used in the Equilibrium Equation for the Calculation of M_{zo1} for Loading Arm No. 2 of the High Vacuum Friction and Wear Tester.

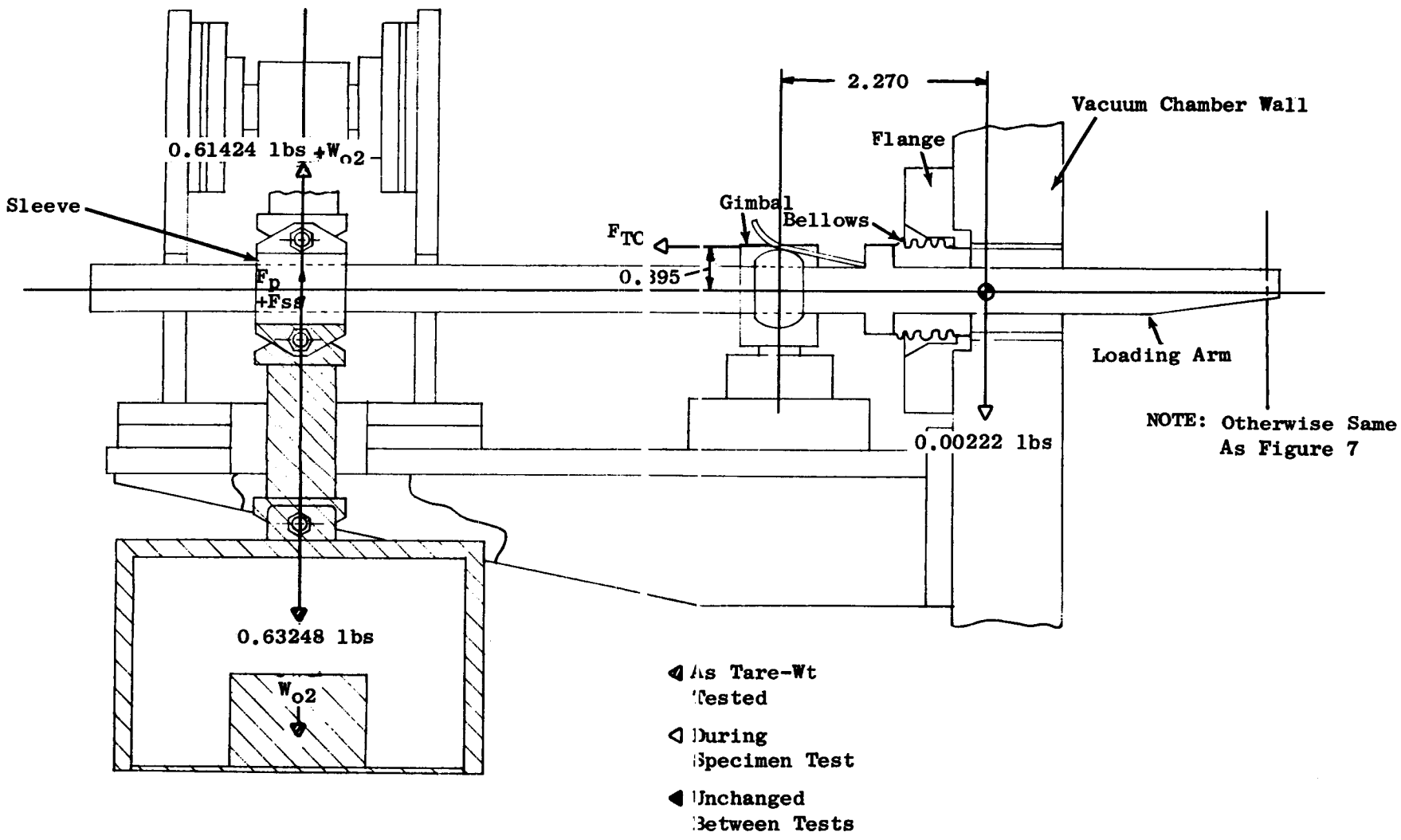

Figure B6. **Moments Used in Equilibrium Equation to Calculate M_{to} for Loading Arm No. 2 for the High Vacuum Friction and Wear Tester.**

Equilibrium Conditions for Loading Arm No. 4 - Loading arm No. 4 differs from loading arms No. 1 and No. 2 by the fact that it does not have a support shaft to change the direction of action of the outer weights, and in having the direction of the compressive load between specimens reversed. Again, loading arm No. 4 was tare-tested without thermocouples. Using the weight of the outer tray applicable to loading arm No. 4, the equations under specimen testing conditions (26) and under tare-weight testing conditions (27) (see Supplement to Appendix B) were derived, leading to the equation for C_4 (see Figure B7):

$$C_4 = 1.41035 + 0.08094\ F_{tc} + W_{i4}.$$

Substituting Equation (6) (vacuum only):

$$C_{4v} = 1.41035 + 0.08094\ F_{tc} + 1.12624\ W_{o4v} - 2.00457$$

$$C_{4v} = 1.12624\ W_{o4v} - 0.59422 + 0.08094\ F_{tc}$$

$$W_{o4v} = 0.88791\ C_4 \pm 0.52761 + 0.07186\ F_{tc}.$$

Again, it is estimated that $0.08094\ F_{tc}$ will be negligible, giving:

High Vacuum Friction Tester Arm No. 4; Vacuum Only; W_s Assumed; F_{tc} Neglected	$C_{4v} = 1.12624\ W_{o4v} - 0.59422$	(28)
	$W_{o4v} = 0.88791\ C_{4v} + 0.52761$	(29)

Check: When $C_{4v} = 5$ lbs.,

$$W_{o4v} = 0.88791\ (5) + 0.52761$$

$$= 4.96716, \text{ or } 4.97 \text{ lbs.}$$

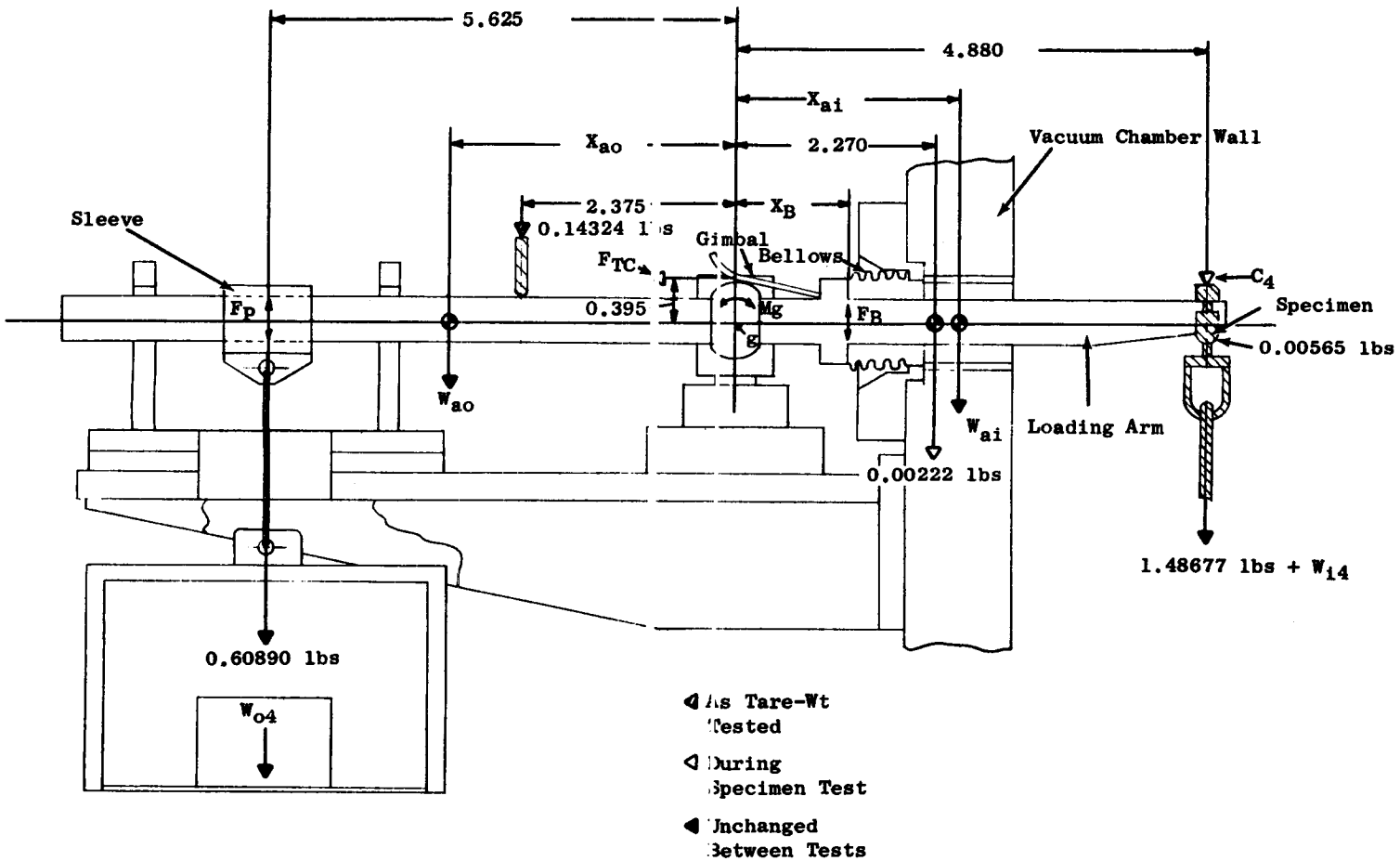

Figure B7. **Moments Used in Equilibrium Equation to Calculate M_{to} for Loading Arm No. 4 for the High Vacuum Friction and Wear Tester.**

$$-3.40920 - 5.625\,W_{o1} + 5.625\,F_p + 5.625\,F_{ss} + M_{ao} + 0 + 0.395\,F_{tc} + M_g = M_b + M_{ai} + 0.00504 + 0 + 0 + 0.02757 - 4.880\,C_1 \quad (15)$$

$$3.41269 + 5.625\,W_{o1} + 5.625\,F_p + 0 + M_{ao} + 0.34031 + 0.395\,F_{tc} + M_g = M_b + M_{ai} + 0.00504 + 7.25544 + 4.880\,W_{i1} + 0 + 0 \quad (19)$$

$$-6.82189 - 11.250\,W_{o1} + 0 + 5.625\,F_{ss} + 0 - 0.34031 + 0 + 0 = 0 + 0 + 0 - 7.25544 - 4.880\,W_{i1} + 0.02757 - 4.880\,C_1$$

$$0.06567 - 11.250\,W_{o1} + 5.625\,F_{ss} + 4.880\,W_{i1} = -4.880\,C_1$$

$$C_1 = -0.01345 + 2.30532\,W_{o1} - 1.15266\,F_{ss} - W_{i1}$$

$$-3.45510 - 5.625\,W_{o2} + 5.625\,F_p + 5.625\,F_{ss} + M_{ao} + 0 + 0.395\,F_{tc} + M_g = M_b + M_{ai} + 0.00504 + 0 + 0 + 0.02757 - 4.880\,C_2 \quad (22)$$

$$3.55770 + 5.625\,W_{o2} + 5.625\,F_p + 0 + M_{ao} + 0.34031 + 0 + M_g = M_b + M_{ai} + 0 + 7.25544 + 4.880\,W_{i2} + 0 + 0 \quad (23)$$

$$-7.01280 - 11.250\,W_{o2} + 0 + 5.625\,F_{ss} + 0 - 0.34031 + 0.395\,F_{tc} + 0 = 0 + 0 + 0.00504 - 7.25544 - 4.880\,W_{i2} + 0.02757 - 4.880\,C_2$$

$$-0.13028 - 11.250\,W_{o2} + 5.625\,F_{ss} + 0.395\,F_{tc} + 4.880\,W_{i2} = 4.880\,C_2$$

$$C_2 = 0.02669 + 2.30532\,W_{o2} - 1.15266\,F_{ss} - 0.0809\,F_{tc} - W_{i2}$$

$$3.55770 + 5.625\,W_{o4} + M_p + 0 + M_{ao} + 0 + 0.395\,F_{tc} + M_g = M_b + M_{ai} + 0.00504 + 0 + 0 + 0.02757 + 4.880\,C_4 \quad (26)$$

$$3.55770 + 5.625\,W_{o4} + M_p + 0 + M_{ao} + 0.34031 + 0 + M_g = M_b + M_{ai} + 0 + 7.25544 + 4.880\,W_{i4} + 0 + 0 \quad (27)$$

$$0 + 0 + 0 + 0 + 0 - 0.34031 + 0.395\,F_{tc} + 0 = 0 + 0 + 0.00504 - 7.25544 - 4.880\,W_{i4} + 0.02757 + 4.880\,C_4$$

$$6.88252 + 0.395\,F_{tc} + 4.880\,W_{i4} = 4.880\,C_4$$

$$C_4 = 1.41035 + 0.08094\,F_{tc} + W_{i4}$$

APPENDIX C

SAMPLE CALCULATIONS OF INNER AND OUTER TOTAL KNOW MOMENT SUMMATIONS

APPENDIX C

SAMPLE CALCULATION OF INNER AND OUTER TOTAL KNOWN MOMENT SUMMATIONS

I. Vertical Loading

Given: a) The outer balance weight W_{ol} and the tray and hanger weights of 0.65288 pound act at 5.625 inches out from the gimbal.

b) The dial indicator force of 0.14329 pound acts at 2.375 inches out from the gimbal.

c) The inner dial weight W_{il} and the tray and hanger weights of 1.48677 pound act at 4.880 inches in from the gimbal.

Therefore:

$$5.625\ (W_{ol} + 0.65288) + 2.375\ (0.14329) = 4.880\ (W_{il} + 1.48677)$$

$$5.625\ W_{ol} + 3.67245 + 0.34031 = 4.880\ W_{il} + 7.25544$$

$$5.625\ W_{ol} = 4.880\ W_{il} + 3.24268$$

$$\boxed{W_{ol} = 0.86755\ W_{il} + 0.57647} \qquad (1)$$

Equation 1 is the equation of the expected balance points, if the bellows and other miscellaneous frictional forces are zero. Any deviation from the above relationship would represent the effects of the bellows and frictional moments.

II. Vector Loading (Vertical Plane)

Given: a) The outer balance weight VW_{ol} and the tray and hanger weights of 0.60670 pound act at 5.625 inches out from the gimbal.

b) The dial indicator force of 0.14329 pound act at 2.375 inches out from the gimbal.

c) The vertical vector of the inner dead weight ($VV_1 = 0.68582\ VW_{il}$) and the vertical component of the hanger weights of 0.01735 pound act at 4.880 inches from the gimbal.

Therefore:

$$5.625\ (VW_{ol} + 0.60670) + 2.375\ (0.14329) = 4.880\ (0.68582\ VW_{il} + 0.01735)$$

$$5.625\ VW_{ol} + 3.41269 + 0.34031 = 3.34680\ VW_{il} + 0.08467$$

$$5.625\ VW_{ol} = 3.34680\ VW_{il} - 3.66833$$

$$\boxed{VW_{ol} = 0.59498\ VW_{il} - 0.65214} \qquad (2)$$

Equation 2 is the equation of the expected blanace points, if the bellows and other miscellaneous frictional forces were zero.

III. Vector Loading (Horizontal Plane)

Given: a) The force pickup force F_{fpl} acts at 5.625 inches out from the gimbal.

b) The horizontal vector of the inner dead weight ($HV_1 = 0.72777\ VW_{il}$) and the horizontal component hanger weights 0.00990 pound act at 4.880 inches in from the gimbal.

Therefore:

$$5.625\ F_{fpl} = 4.880\ (0.72777\ VW_{il} + 0.00990)$$

$$F_{fpl} = 0.86755\ (0.72777\ VW_{il} + 0.00990)$$

$$\boxed{F_{fpl} = 0.63138\ VW_{il} + 0.00859} \qquad (3)$$

Equation 3 is the equation of the expected balance points, if the bellows and other miscellaneous frictional forces were zero.

APPENDIX D

CALCULATION OF HORIZONTAL AND VERTICAL COMPONENTS OF THE VECTOR TARE TEST INNER WEIGHT VW_i

APPENDIX D

CALCULATION OF HORIZONTAL AND VERTICAL COMPONENTS OF THE VECTOR TARE TEST INNER WEIGHT VW_i

(Refer to Figure 14 "Assembly for Vector Tare Test" on page 35 of this report).

Vertical Leg V of Vector Triangle:

$$V = 8.923 + 0.155 - 0.250 - (7.040 - 0.583) - 0.583 \cos \theta$$

$$V = 2.371 - 0.583 \cos \theta$$

Horizontal Leg H of Vector Triangle:

$$H = 2.374 - 0.125 - 0.583 + 0.583 \sin \theta$$

$$H = 1.666 + 0.583 \sin \theta$$

$$\text{Tan } \theta = \frac{V}{H} = \frac{2.371 - 0.583 \cos \theta}{1.666 + 0.583 \sin \theta}$$

By Successive Iterations: $\theta = 43.30°$

$\cos \theta = 0.72777$

$\sin \theta = 0.68582$

$\tan \theta = 0.94235$

Then:

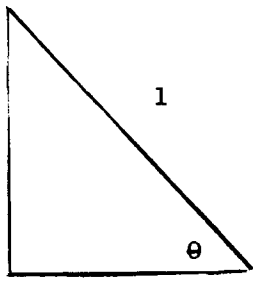

VV = 0.68582 VW_i (representing compressive force)

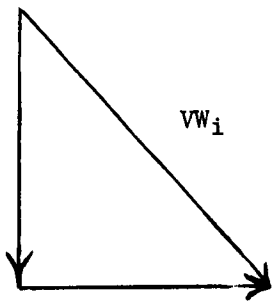

HV = 0.72777 VW_i (representing friction force)

DISTRIBUTION LIST
QUARTERLY AND FINAL PROGRESS REPORTS

Contract NAS3-2534

National Aeronautics and Space Administration
Washington, D.C. 20546
Attention: Arvin Smith (RNW)

National Aeronautics and Space Administration
Washington, D.C. 20546
Attention: James J. Lynch (RNP)

National Aeronautics and Space Administration
Washington, D.C. 20546
Attention: George C. Deutsch (RR)

National Aeronautics and Space Administration
Washington, D.C. 20546
Attention: Dr. Fred Schulman (RNP)

National Aeronautics and Space Administration
Scientific & Technical Information Facility
P.O. Box 33
College Park, Maryland 20740
Attention: Acquisitions Branch,
(SQT-34054)(2+repro)

National Aeronautics and Space Administration
Ames Research Center
Moffet Field, California 94035
Attention: Librarian

National Aeronautics and Space Administration
Goddard Space Flight Center
Greenbelt, Maryland 20771
Attention: Librarian

National Aeronautics and Space Administration
Langley Research Center
Hampton, Virginia 23365
Attention: Librarian

National Aeronautics and Space Administration
Manned Spacecraft Center
Houston, Texas 77001
Attention: Librarian

National Aeronautics and Space Administration
George C. Marshall Space Flight Center
Huntsville, Alabama 35812
Attention: Librarian

National Aeronautics and Space Administration
Jet Propulsion Laboratory
4800 Oak Grove Drive
Pasadena, California 99103
Attention: Librarian

National Aeronautics and Space Administration
Lewis Research Center
21000 Brookpark Road
Cleveland, Ohio 44135
Attention: Librarian M.S. 3-7

National Aeronautics and Space Administration
Lewis Research Center
21000 Brookpark Road
Cleveland, Ohio 44135
Attention: J. P. Joyce M.S. 500-309

National Aeronautics and Space Administration
Lewis Research Center
21000 Brookpark Road
Cleveland, Ohio 44135
Attention: Dr. B. Lubarsky M.S. 500-201

National Aeronautics and Space Administration
Lewis Research Center
21000 Brookpark Road
Cleveland, Ohio 44135
Attention: R. F. Mather M.S. 500-309

National Aeronautics and Space Administration
Lewis Research Center
21000 Brookpark Road
Cleveland, Ohio 44135
Attention: G. M. Ault M.S. 105-1

National Aeronautics and Space Administration
Lewis Research Center
21000 Brookpark Road
Cleveland, Ohio 44135
Attention: R. L. Davies M.S. 500-309 (2)

National Aeronautics and Space Administration
Lewis Research Center
21000 Brookpark Road
Cleveland, Ohio 44135
Attention: J. E. Dilley M.S. 500-309

National Aeronautics and Space Administration
Lewis Research Center
21000 Brookpark Road
Cleveland, Ohio 44135
Attention: J. J. Weber M.S. 3-19

National Aeronautics and Space Administration
Lewis Research Center
21000 Brookpark Road
Cleveland, Ohio
Attention: T. A. Moss M.S. 500-309

National Aeronautics and Space Administration
Lewis Research Center
21000 Brookpark Road
Cleveland, Ohio 44135
Attention: Thomas Strom M.S. 5-8

National Aeronautics and Space Administration
Lewis Research Center
21000 Brookpark Road
Cleveland, Ohio 44135
Attention: Dr. L. Rosenblum M.S. 106-1

National Aeronautics and Space Administration
Lewis Research Center
21000 Brookpark Road
Cleveland, Ohio 44135
Attention: Report Control Office M.S. 5-5

National Aeronautics and Space Administration
Lewis Research Center
21000 Brookpark Road
Cleveland, Ohio 44135
Attention: V. F. Hlavin M.S. 3-14
(Final Only)

National Aeronautics and Space Administration
Western Operations Office
150 Pico Boulevard
Santa Monica, California 90400
Attention: John Keeler

National Bureau of Standards
Washington, D.C. 20225
Attention: Librarian

Flight Vehicle Power Branch
Air Force Aero-Propulsion Lab
Wright-Patterson Air Force Base, Ohio
Attention: Charles Armbruster,
ASRPP-10

Flight Vehicle Power Branch
Air Force Aero-Propulsion Lab
Wright-Patterson Air Force Base, Ohio
Attention: John L. Mooris

Flight Vehicle Power Branch
Air Force Aero-Propulsion Lab
Wright-Patterson Air Force Base, Ohio
Attention: T. Cooper

Flight Vehicle Power Branch
Air Force Aero-Propulsion Lab
Wright-Patterson Air Force Base, Ohio
Attention: Librarian

Flight Vehicle Power Branch
Air Force Aero-Propulsion Lab
Wright-Patterson Air Force Base, Ohio
Attention: George E. Thompson,
APIP-1

Flight Vehicle Power Branch
Air Force Aero-Propulsion Lab
Wright-Patterson Air Force Base, Ohio
Attention: George Sherman, API

Flight Vehicle Power Branch
Air Force Aero-Propulsion Lab
Wright-Patterson Air Force Base, Ohio
Attention: George Glenn

Army Ordnance Frankford Arsenal
Bridesburg Station
Philadelphia, Pennsylvania 19137
Attention: Librarian

Bureau of Mines
Albany, Oregon
Attention: Librarian

Bureau of Ships
Department of the Navy
Washington, D.C. 20225
Attention: Librarian

Bureau of Weapons
Research & Engineering
Materials Division
Washington, D.C. 20225
Attention: Librarian

U.S. Atomic Energy Commission
Technical Reports Library
Washington, D.C. 20545
Attention: J. M. O'Leary (2)

U.S. Atomic Energy Commission
Germantown, Maryland 20767
Attention: K. E. Horton

U.S. Atomic Energy Commission
Germantown, Maryland 20767
Attention: H. Finger

U.S. Atomic Energy Commission
SNAP 50/SPUR Project Office
Germantown, Maryland 20767
Attention: H. Rochen

U.S. Atomic Energy Commission
SNAP 50/SPUR Project Office
Germantown, Maryland 20767
Attention: Col. Gordon Dicker

U.S. Atomic Energy Commission
Technical Information Service Extension
P.O. Box 62
Oak Ridge, Tennessee 27831 (3)

U.S. Atomic Energy Commission
Washington, D.C. 20545
Attention: M. J. Whitman

Office of Naval Research
Power Division
Washington, D.C. 20225
Attention: Librarian

U.S. Naval Research Laboratory
Washington, D.C. 20225
Attention: Librarian

Advanced Technology Laboratories
Division of American Standard
369 Whisman Road
Mountain View, California 94040-2
Attention: Librarian

Aerojet-General Corporation
P.O. Box 296
Azusa, California 91702
Attention: Librarian

Aerojet-General Corporation
P.O. Box 296
Azusa, California 91702
Attention: R. S. Carey

Aerojet-General Nucleonics
P.O. Box 77
San Ramon, California 94583
Attention: Librarian

AiResearch Manufacturing Company
Sky Harbor Airport
402 South 36th Street
Phoenix, Arizona 85034
Attention: Librarian

AiResearch Manufacturing Company
Sky Harbor Airport
402 South 36th Street
Phoenix, Arizona 85034
Attention: E. A. Kovacevich

AiResearch Manufacturing Company
Sky Harbor Airport
402 South 36th Street
Phoenix, Arizona 85034
Attention: John Dannan

AiResearch Manufacturing Company
9851-9951 Sepulveda Boulevard
Los Angeles, California 90045
Attention: Librarian

Argonne National Laboratory
9700 South Cross Avenue
Argonne, Illinois 60440
Attention: Librarian

Atomics International
8900 DeSoto Avenue
Canoga Park, California 91303
Attention: Librarian

Atomics International
8900 DeSoto Avenue
Canoga Park, California 91303
Attention: Harry Pearlman

AVCO
Research and Advanced Development Department
201 Lowell Street
Wilmington, Massachusetts 01800
Attention: Librarian

Babcock and Wilcox Company
Research Center
Alliance, Ohio 44601-2
Attention: Librarian

Battelle Memorial Institute
505 King Avenue
Columbus, Ohio 43201
Attention: Librarian

Battelle Memorial Institute
505 King Avenue
Columbus, Ohio 43201
Attention: E. M. Simmons

The Bendix Corporation
Research Laboratories Division
Southfield, Michigan 48200
Attention: Librarian

The Boeing Company
Seattle, Washington 98100
Attention: Librarian

Brookhaven National Laboratory
Upton, Long Island, New York 11973
Attention: Librarian

Carborundum Company
Niagara Falls, New York 14300
Attention: Librarian

Chance Vought Aircraft, Inc.
P.O. Box 5907
Dallas, Texas 75222
Attention: Librarian

Clevite Corporation
Mechanical Research Division
540 East 105th Street
Cleveland, Ohio 44108
Attention: N. C. Beerli

Climax Molybdenum Co., of Michigan
1600 Huron Parkway
Ann Arbor, Michigan 48105
Attention: Librarian

Climax Molybdenum Co., of Michigan
1600 Huron Parkway
Ann Arbor, Michigan 48105
Attention: Dr. M. Semchyshen

Convair Astronautics
5001 Kerrny Villa Road
San Diego, California 92111
Attention: Librarian

Curtiss-Wright Corporation
Research Division
Quehanna, Pennsylvania
Attention: Librarian

E. I. duPont deNemours and Co., Inc.
Lavoisier Library
Experimental Station
Wilmington, Delaware 19898
Attention: Librarian

E. I. duPont deNemours and Co., Inc.
Lavoisier Library
Experimental Station
Wilmington, Delaware 19898
Attention: H. Hix

Eitel McCullough, Incorporated
301 Industrial Way
San Carlos, California
Attention: Leonard Reed

Electro-Optical Systems, Inc.
Advanced Power Systems Division
Pasadena, California 91100
Attention: Librarian

Fansteel Metallurgical, Corp.
North Chicago, Illinois 60600
Attention: Librarian

Ford Motor Company
Aeronutronics
Newport Beach, California 92660
Attention: Librarian

General Atomic
John Jay Hopkins Laboratory
P.O. Box 608
San Diego, California 92112
Attention: Librarian

General Atomic
John Jay Hopkins Laboratory
P.O. Box 608
San Diego, California 92112
Attention: Dr. Ling Yang

General Electric Company
Atomic Power Equipment Division
P.O. Box 1131
San Jose, California

General Electric Company
Missile and Space Vehicle Department
3198 Chestnut Street
Philadelphia, Pennsylvania 19104
Attention: Librarian

General Electric Company
Vallecitos Atomic Lab.
Pleasanton, California 94566
Attention: Librarian

General Dynamics/Fort Worth
P.O. Box 748
Fort Worth, Texas 76100
Attention: Librarian

General Motors Corporation
Allison Division
Indianapolis, Indiana 46206
Attention: Librarian

Hamilton Standard
Division of United Aircraft Corporation
Windsor Locks, Connecticut
Attention: Librarian

Grumman Aircraft
Bethpage, New York
Attention: Librarian

Hughes Aircraft Company
Engineering Division
Culver City, California 90230-2
Attention: Librarian

IIT Research Institute
10 W. 35th Street
Chicago, Illinois 60616
Attention: Librarian

Kenmetal, Incorporated
Latrobe, Pennsylvania
Attention: Librarian

Lockheed Missiles and Space Division
Lockheed Aircraft Corporation
Sunnyvale, California
Attention: Librarian

Lockheed Missiles and Space Division
Lockheed Aircraft Corporation
Sunnyvale, California
Attention: John N. Cox

Lockheed Georgia Company
Division, Lockheed Aircraft Company
Marietta, Georgia
Attention: Librarian

Los Alamos Scientific Laboratory
University of California
Los Alamos, New Mexico
Attention: Librarian

Marquardt Aircraft Company
P.O. Box 2013
Van Nuys, California
Attention: Librarian

The Martin Company
Baltimore, Maryland 21203
Attention: Librarian

The Martin Company
Nuclear Division
P.O. Box 5042
Baltimore, Maryland 21220
Attention: Librarian

Martin Marietta Corporation
Metals Technology Laboratory
Wheeling, Illinois

Mechanical Technology, Inc.
968 Albany-Shaker Road
Latham, New York
Attention: Eli B. Arwas

Materials Research and Development
Manlabs, Incorporated
21 Erie Street
Cambridge, Massachusetts 02139

Materials Research Corporation
Orangeburg, New York
Attention: Librarian

McDonnell Aircraft
St. Louis, Missouri 63100
Attention: Librarian

MSA Research Corporation
Callery, Pennsylvania 16024
Attention: Librarian

North American Aviation, Inc.
Los Angeles Division
Los Angeles, California 90009
Attention: Librarian

Oak Ridge National Laboratory
Oak Ridge, Tennessee 37831
Attention: W. H. Cook

Oak Ridge National Laboratory
Oak Ridge, Tennessee 37831
Attention: W. O. Harms

Oak Ridge National Laboratory
Oak Ridge, Tennessee 37831
Attention: Dr. A. J. Miller

Oak Ridge National Laboratory
Oak Ridge, Tennessee 37831
Attention: J. H. DeVan

Pratt & Whitney Aircraft
400 Main Street
East Hartford, Connecticut 06108
Attention: Librarian

Republic Aviation Corporation
Farmingdale, Long Island, New York
Attention: Librarian

Rocketdyne
Canoga Park, California 91303
Attention: Librarian

Sintercast Division of Chromalloy Corp.
West Nyack, New York
Attention: Librarian

SKF Industries, Inc.
Philadelphia, Pennsylvania 19100
Attention: Librarian

Solar
2200 Pacific Highway
San Diego, California 92112
Attention: Librarian

Aouthwest Research Institute
8500 Culebra Road
San Antonio, Texas 78206

Superior Tube Company
Norristown, Pennsylvania
Attention: Mr. A. Bound

Sylvania Electrics Products, Inc.
Chem. & Metallurgical
Towanda, Pennsylvania
Attention: Librarian

The Timken Roller Bearing Co.
Canton, Ohio 44706
Attention: Librarian

TRW Inc.
Caldwell Research Center
23555 Euclid Avenue
Cleveland, Ohio 44117
Attention: Librarian

Union Carbide Corporation
Stellite Division
Kokomo, Indiana
Attention: Librarian

Union Carbide Nuclear Company
P.O. Box X
Oak Ridge, Tennessee 37831
Attention: X-10 Laboratory

Union Carbide Nuclear Company
P.O. Box X
Oak Ridge, Tennessee 37831
Attention: Records Department (2)

nion Carbide Metals
iagara Falls, New York 14300
ttention: Librarian

Jnited Aircraft Corporation
Pratt & Whitney Division
00 W. Main Street
Hartford, Connecticut 06108
Attention: W. H. Podolny

Jnited Nuclear Corporation
Five New Street
White Plains, New York 10600-5
Attention: Librarian

Union Carbide Corporation
Parma Research Center
P.O. Box 6115
Cleveland, Ohio 44101
Attention: Technical Information Services

Wah Chang Corporation
Albany, Oregon
Attention: Librarian

Westinghouse Electric Corporation
Astronuclear Laboratory
P.O. Box 10864
Pittsburgh, Pennsylvania 15236
Attention: Librarian

Westinghouse Electric Corporation
Astronuclear Laboratory
P.O. Box 10864
Pittsburgh, Pennsylvania 15236
Attention: R. T. Begley

Westinghouse Electric Corporation
Research & Development Center
Pittsburgh, Pennsylvania 15235
Attention: E. S. Bober

Westinghouse Electric Corporation
Materials Manufacturing Division
RD#2 Box 25
Blairsville, Pennsylvania
Attention: Librarian

Westinghouse Electric Corporation
Aerospace Electrical Division
Lima, Ohio
Attention: R. W. Briggs

Westinghouse Electric Corporation
Aerospace Electrical Division
Lima, Ohio
Attention: P. E. Kueser

Westinghouse Electric Corporation
Research & Development Center
Pittsburgh, Pennsylvania 15235
Attention: Librarian

Wyman-Gordon Company
North Grafton, Massachusetts
Attention: Librarian

Zirconium Corporation of America
Solon, Ohio
Attention: Librarian

Lawrence Radiation Laboratory
Livermore, California
Attention: Dr. James Hadley

Lawrence Radiation Laboratory
Livermore, California
Attention: Librarian

Allis Chalmers
Atomic Energy Division
Milwaukee, Wisconsin
Attention: Librarian

Allison-General Motors
Energy Conversion Division
Indianapolis, Indiana
Attention: Librarian

AMF Atomics
140 Greenwich Avenue
Greenwich, Connecticut
Attention: Librarian

American Machine and Foundry Company
Alexandria Division
1025 North Royal Street
Alexandria, Virginia
Attention: Librarian

Douglas Aircraft Company, Inc.
Missile and Space Systems Division
3000 Ocean Park Boulevard
Santa Monica, California
Attention: Librarian

National Research Corporation
402 Industrial Place
Newton, Massachusetts
Attention: Librarian

Varian Associates
Vacuum Products Division
611 Hansen Way
Palo Alto, California
Attention: J. Shields

Ultek Corporation
920 Commercial Street
Palo Alto, California
Attention: Librarian

Universal Cyclops Steel Corporation
Refractomet Division
Bridgeville, Pennsylvania
Attention: C. P. Mueller